



**HAL**  
open science

# Restoration of visual function by transplantation of optogenetically engineered photoreceptors

Marusa Lampic

► **To cite this version:**

Marusa Lampic. Restoration of visual function by transplantation of optogenetically engineered photoreceptors. Human health and pathology. Sorbonne Université, 2019. English. NNT : 2019SORUS233 . tel-02954123

**HAL Id: tel-02954123**

**<https://theses.hal.science/tel-02954123>**

Submitted on 30 Sep 2020

**HAL** is a multi-disciplinary open access archive for the deposit and dissemination of scientific research documents, whether they are published or not. The documents may come from teaching and research institutions in France or abroad, or from public or private research centers.

L'archive ouverte pluridisciplinaire **HAL**, est destinée au dépôt et à la diffusion de documents scientifiques de niveau recherche, publiés ou non, émanant des établissements d'enseignement et de recherche français ou étrangers, des laboratoires publics ou privés.

# Sorbonne Université

École doctorale Cerveau Cognition Comportement (ED158)

*Institut de la Vision*

## **Restoration of visual function by transplantation of optogenetically engineered photoreceptors**

Par **Maruša Lampič**

Thèse de doctorat de Neurosciences

Dirigée par **Jens Duebel and José-Alain Sahel**

Présentée et soutenue publiquement le 6 Septembre 2019

Devant un jury composé de :

**Pr. Christelle Monville**, Rapporteur

**Dr. Morgane Locker**, Rapporteur

**Pr. Rachel Sherrard**, Examineur

**Dr. Anselme Perrier**, Examineur

**Pr. José-Alain Sahel**, Directeur de thèse

**Dr. Deniz Dalkara**, Co-directeur de thèse



Except where otherwise noted, this work is licensed under  
<http://creativecommons.org/licenses/by-nc-nd/3.0/>

## Acknowledgements

I would like to thank:

- First Jens for accepting me into his team as the first joint member and for deciding to go through with this “crazy” project that seemed rather risky at first, but was such a perfect combination of everything I wished to work on. I think we now all agree it was worth the ride! Thank you for letting me free hands with taking research-related decisions, but at the same time letting me know that I can always come for help.
- Deniz for her generous help in the last year of my PhD, especially with the final phases of paper submission and revision, as well as with this manuscript. It was really a pleasure.
- Pr Sahel and Serge for running this amazing institute and all those who help them from “behind the scenes”.
- Other co-authors of the paper that was the result of this project – Marcela for handling the stem cell part, Laure for helping out with experiments, Antoine the SuperPatcher, our friends from Dresden, and others for their input.
- Members of our team, past and present – Abhishek, Antoine, Laure, Elric, Céline, Benjamin... and people who felt like they were members of our team because they always treated me so nicely, even when I didn’t feel like I deserved it – Mélissa, Romain and “the old IdV gang”...
- My office mates who I was always happy to see, in both “the old” and “the new” office.
- People working at the animal facility, all the friendly people producing viruses, Romain for being my “troubleshooting manual” when it came to MEA, Abhishek for helping me out more than he’ll ever know with so many things, Stéphane for his help with the microscopy-related issues (and for providing us coffee)...
- All the smiling kind faces of the IdV that I was bumping into daily, even if it was just for a “bonjour” or “bonne journée”.
- All the mice that paid the highest price in all this. This was not easy on me, I much prefer working on cell cultures, I swear!

- ♥ My “Parisian” friends from outside the lab – Shiri, Clarisse, Andrea, Francesco, Abhishek (well, you two guys – it was difficult to decide whether to put you in the “inside the lab” or “outside the lab” category)... And my friends from back home and those who moved from there around the world, who are irreplaceable and are always there for me despite the distance.
- ♥ Urban and Bor, who inevitably sometimes got the worst of me, although I am also trying to give them my best. A proverb in many languages says that “Two heads are better than one” (“Več glav več ve”). I therefore assume that growing two extra sets of brains in the course of my PhD had something to do with my success. While my son helped me with the more “practical” things - we did a lot of MEA together; my guess is that my soon-to-be-born daughter might grow up into more of a writing enthusiast. 😊
- ♥ My parents, my sister, my grandparents, who played the biggest part in making me who I am today. The absolute worst thing about living in Paris is that you don’t. I miss you every single day. Thank you for your love and constant support (even through the weirdest phases of my life 😊).
- Pottery, the beautiful hobby that I’ve discovered here in Paris and the beautiful people I met through it, my favourite coffee shops, my home jungle, the artists who’s tracks I’ve ever liked on Soundcloud, my bike, La coulée verte for being the best lunch spot, and Paris – for being difficult, but pretty.

## **Abstract**

A major challenge in treatment of retinal degenerative diseases with transplantation of replacement photoreceptors is the difficulty in inducing the grafted cells to grow and maintain light-sensitive outer segments in the host retina, which depends on proper interaction with the underlying retinal pigment epithelium (RPE). For an RPE-independent treatment approach, we introduced a hyperpolarizing microbial opsin into photoreceptor precursors from newborn mice, and transplanted them into blind mice lacking the photoreceptor layer. These optogenetically transformed photoreceptors were light responsive and their transplantation lead to the recovery of visual function, as shown by ganglion cell recordings and behavioral tests. Subsequently, we generated cone photoreceptors from human induced pluripotent stem cells (hiPSCs), expressing the chloride pump *Jaws*. After transplantation into blind mice, we observed light-driven responses at the photoreceptor and ganglion cell level. These results demonstrate that structural and functional retinal repair is possible by combining stem cell therapy and optogenetics.

## Résumé

Un défi majeur dans le traitement des maladies dégénératives de la rétine par transplantation de photorécepteurs de remplacement est la difficulté d'induire les cellules greffées à croître et à maintenir des segments externes sensibles à la lumière dans la rétine hôte, qui dépend d'une interaction adéquate avec l'épithélium pigmentaire rétinien (EPR) sous-jacent. Pour une approche de traitement indépendante de l'EPR, nous avons introduit une opsine microbienne hyperpolarisante dans les précurseurs de photorécepteurs provenant de souris nouveau-nées et les avons transplantés dans des souris aveugles dépourvues de la couche photoréceptrice. Ces photorécepteurs transformés optogénétiquement ont réagi à la lumière et leur transplantation a permis de rétablir la fonction visuelle, comme en témoignent les enregistrements des cellules ganglionnaires et les tests comportementaux. Par la suite, nous avons généré des photorécepteurs à cônes à partir de cellules souches humaines pluripotentes induites (hiPSCs), exprimant Jaws, un autre opsine hyperpolarisante. Après la transplantation chez des souris aveugles, nous avons observé des réponses à la lumière au niveau des photorécepteurs et des cellules ganglionnaires. Ces résultats démontrent que la réparation structurale et fonctionnelle de la rétine est possible en combinant la thérapie par cellules souches et l'optogénétique.

# Table of Contents

Acknowledgements.....	3
Abstract .....	5
Résumé.....	6
Table of contents.....	7
List of figures.....	10
List of tables.....	12
List of abbreviations.....	13
<b>INTRODUCTION</b>	<b>16</b>
1. THE RETINA AND THE PHOTORECEPTORS.....	17
1.1 The eye .....	17
1.2 The retina and its organization .....	18
1.3 Cell types of the neural retina.....	20
1.3.1 Photoreceptors.....	20
1.3.2 Bipolar cells.....	23
1.3.3 Horizontal cells .....	23
1.3.4 Amacrine cells.....	24
1.3.5 Retinal ganglion cells (RGCs) .....	24
1.4 How do we see? .....	25
1.4.1 Phototransduction cascade (in rods).....	25
1.4.2 Retinal circuitry and cortical processing.....	29
1.5 Retinal pigment epithelium (RPE) and its role in vision.....	31
2. OUTER RETINAL DYSTROPHIES .....	34
2.1 Inherited retinal diseases (IRDs) .....	34
2.1.1 Rod-dominated diseases .....	35
2.1.2 Cone-dominated diseases .....	36
2.1.3 Generalized photoreceptor diseases.....	37
2.2 Multifactorial retinal diseases.....	37
2.3 Animal models of retinal degeneration .....	38

3	THERAPEUTIC APPROACHES FOR TREATING PHOTORECEPTOR DEGENERATION .....	43
3.1	Pharmacotherapy.....	44
3.2	Gene replacement therapy .....	44
3.3	Gene editing .....	45
3.4	Neuroprotection.....	47
3.5	Optogenetics .....	49
3.6	Optopharmacology .....	49
3.7	Cell transplantation based treatments .....	50
3.8	Induced retinal regeneration .....	51
3.9	Visual prostheses.....	53
4	OPTOGENETICS.....	56
4.1	Microbial opsins .....	56
4.2	Vertebrate opsins.....	59
4.3	Choice of strategy – which retinal cells to target .....	61
4.4	Delivery of the optogene to the cells.....	63
5	CELL REPLACEMENT.....	64
5.1	RPE transplantation.....	64
5.2	Photoreceptor cell suspension transplantation.....	66
5.2.1	Donor-derived dissociated photoreceptor precursors .....	66
5.2.2	Dissociated pluripotent stem cell-derived photoreceptors .....	71
5.3	Retinal sheet transplantation.....	74
5.4	Cell-seeded scaffold transplantation .....	78
5.5	Issues with stem cell transplantation today .....	80
5.5.1	Cytoplasmic material exchange - paradigm shift in photoreceptor replacement therapy.....	80
5.5.2	Reaching proper PSC-derived photoreceptor differentiation and morphology <i>in vitro</i>	86
5.5.3	Orientation, cell morphology and synaptogenesis <i>in vivo</i> post-transplantation..	86
5.5.4	Immune response related concerns (and recent efforts to overcome them) .....	87

Restoration of visual function by transplantation of optogenetically engineered photoreceptors.....	93
Abstract.....	93
Introduction.....	94
Results.....	95
Discussion.....	99
Figures and figure legends.....	99
Materials and methods.....	114
Supplementary data.....	127

**DISCUSSION** **141**

Overcoming some of the present challenges of photoreceptor replacement therapy and optogenetics by combining the two.....	142
Evaluation of synaptogenesis and considering alternative mechanisms.....	146
The rationale behind the methods used to assess visual function improvement.....	153
The remaining challenges.....	154
Considerations for the future.....	158

**BIBLIOGRAPHY**.....161

# List of figures

## INTRODUCTION

### 1 THE RETINA AND THE PHOTORECEPTORS

Figure 1.1. The anatomy of the human eye with its main components.....	17
Figure 1.2. The layered structure of the retina with its main cell types. ....	19
Figure 1.3. A representation of retinal cell organization in the fovea (A) and a vertical section of monkey fovea (B).....	20
Figure 1.4. An illustration of rod and cone photoreceptors and their subcellular compartments.....	22
Figure 1.5. The diversity within the major neural cell types of the retina. ....	25
Figure 1.6. Phototransduction cascade and the visual cycle.....	29
Figure 1.7. The three rod pathways of the mammalian retina. ....	30
Figure 1.8. The summary of RPE functions.....	33

### 2 OUTER RETINAL DYSTROPHIES

Figure 2.1. Classification of the more important proteins associated with IRDs according to their localization in photoreceptors or RPE cells.....	35
Figure 2.2. Characterization of the two mouse models used in our study, <i>Cpfl1/Rho<sup>-/-</sup></i> (A) and <i>rd1</i> (B) mouse.....	41

### 3 THERAPEUTIC APPROACHES FOR TREATING PHOTORECEPTOR DEGENERATION

Figure 3.1. An overview of therapeutic approaches and their application based on photoreceptor degeneration progression.....	43
--	----

### 4 OPTOGENETICS

Figure 4.1. Mechanisms of action of ChR, an activating microbial opsin, and NpHR, an inhibitory microbial opsin. ....	57
Figure 4.2. A comparison of different optogenetic proteins used to restore visual responses in degenerated retinas.....	61

Figure 5.1. Subretinal transplantation via trans-scleral or trans-vitreous injections..... 68

Figure 5.2. Efforts to improve cell integration rates through CD73 marker enrichment (A-C), manipulation of host environment (D) and optimization of the injecting procedure for subretinal delivery. .... 70

Figure 5.3. Transplantation of PSC-derived retinal sheets. .... 78

Figure 5.4. A scaffold supporting photoreceptor cell polarisation, developed by Jung et al., 2018. .... 80

Figure 5.5. A summary of methods for distinguishing material transfer event from structural integration. .... 84

**RESULTS**

Figure 1. Transplanted photoreceptor precursors, expressing NpHR, integrate into the retina of blind mice..... 103

Figure 2. Transplanted NpHR-expressing photoreceptor precursors respond to light..... 105

Figure 3. NpHR-triggered responses from transplanted photoreceptors are transmitted to retinal ganglion cells (RGCs) and induce light avoidance behaviour in blind mice..... 107

Figure 4. Jaws-expressing photoreceptors, derived from hiPSCs, are sensitive to light..... 109

Figure 5. Transplanted photoreceptors, derived from hiPSCs, integrate into the retina of blind mice and display Jaws induced light responses that are transmitted to retinal ganglion cells (RGCs)..... 111

Figure 6. Schematic illustrating the three-fold challenge in photoreceptor cell replacement..... 113

Figure S1. NpHR expression in rod photoreceptors of donor mice..... 127

Figure S2. Transplanted NpHR-rod precursors are located in close apposition to the host INL and express the synaptic marker synaptophysin..... 128

Figure S3: Quantification of YFP <sup>+</sup> cells after transplantation of NpHR-rod precursors.....	129
Figure S4. NphR-expressing photoreceptor precursors transplanted into rd1 mouse respond to light.....	130
Figure S5. Halorhodopsin-triggered RGC responses in rd1 mice.....	131
Figure S6. Growth of the neuroepithelium in retinal organoids treated with FGF2 and the effect of Notch inhibition on retinal organoidogenesis and photoreceptor commitment.....	132
Figure S7. Physiological analysis of monolayer cultures derived from dissociated retinal organoids.....	134
Figure S8. Expression of human and photoreceptor markers in transplanted GFP <sup>+</sup> cells.....	135
Figure S9: Signal transduction from photoreceptors to the second order neurons in rd1 mouse transplanted with Jaws-photoreceptors.....	136
Figure S10. Jaws-triggered RGC responses in rd1 mice.....	137

## List of tables

Table S1. Media formulation.....	138
Table S2: List of TaqMan <sup>®</sup> Gene Expression ID Assays used for qRT-PCR.....	138
Table S3. List of primary antibodies used for immunostaining.....	138
Table S4. A list of all mice used to generate figures, with specified strain, experimental group, experiment type, and ages at the time of transplantation and at the time of experiment.....	138

## List of abbreviations

AAV	adeno-associated virus
AMD	age-related macular degeneration
AMPA	$\alpha$ -amino-3-hydroxy-5-methyl-4-isoxazolepropionic acid
BDNF	brain-derived neurotrophic factor
CD73	cluster of differentiation 73
cGMP	cyclic guanyl monophosphate
ChR	channelrhodopsin
CNTF	ciliary neurotrophic factor
Cpfl1	cone photoreceptor function loss 1
CRISPR/Cas9	clustered regularly interspaced short palindromic repeats/CRISPR-associated protein 9
CRX	cone-rod homeobox
DD	days of differentiation
ECM	extracellular matrix
EdU	5-ethynyl-2'-deoxyuridine
ERG	electroretinogram
ESC(s)	embryonic stem cell(s) –mESC(s) for mouse, hESC(s) for human
FACS	fluorescent activated cell sorting
FISH	Fluorescence <i>in situ</i> hybridization
GCL	retinal ganglion cell layer
GFAP	Glial fibrillary acidic protein
GFP	green fluorescent protein
GMP	good manufacturing practice
GNAT1	guanine nucleotide-binding protein G(t) subunit alpha-1
GPCR(s)	G-protein-coupled receptor(s)
GTP	guanosine-5'-triphosphate
HLA	human leukocyte antigen
HNA	human-nuclear antigen

HR	halorhodopsin
iGluR	ionotropic glutamate receptor
INL	inner nuclear layer
IPL	inner plexiform layer
iPSC(s)	induces pluripotent stem cell(s) – miPSC(s) for mouse, hiPSC(s) for human
IRD	Inherited retinal diseases
ipRGC(s)	intrinsically photosensitive retinal ganglion cell(s)
IS(s)	photoreceptor inner segment(s)
LCA	Leber congenital amaurosis
LGN	lateral geniculate nucleus
MACS	magnetic activated cell sorting
MEA	multi-electrode array
MERTK	tyrosine-protein kinase Mer
mGluR	metabotropic glutamate receptor
MHC	major histocompatibility complex
MMP2	matrix metalloprotease 2
NRL/Nrl	neural retina-specific leucine zipper
OLM	outer limiting membrane
ONL	outer nuclear layer
OPL	outer plexiform layer
OS(s)	photoreceptor outer segment(s)
NpHR	halorhodopsin isolated from <i>Natronomonas pharaonis</i>
P	postnatal day
PDE	phosphodiesterase
PLGA	poly-lactic-co-glycolic acid
PSC(s)	pluripotent stem cell(s)
PSTH	peristimulus time histograms
RCS	Royal College of Surgeons' rat
RdCVF	rod-derived cone viability factor
RGC(s)	retinal ganglion cell(s)

RHO/Rho	rhodopsin
RP	retinitis pigmentosa
RPE	retinal pigment epithelium
RPE65	retinal pigment epithelium-specific 65kDa
VEGF	vascular endothelial growth factor
YFP	yellow fluorescent protein

# INTRODUCTION

# 1 THE RETINA AND THE PHOTORECEPTORS

## 1.1 The eye

The eye collects light from the surrounding environment and focuses it through an adjustable lens to the back of the eye, to the retina, where the light signal is converted into electrical signals. This information is finally sent along the optic nerve to the visual cortex and other areas of the brain to form an image.

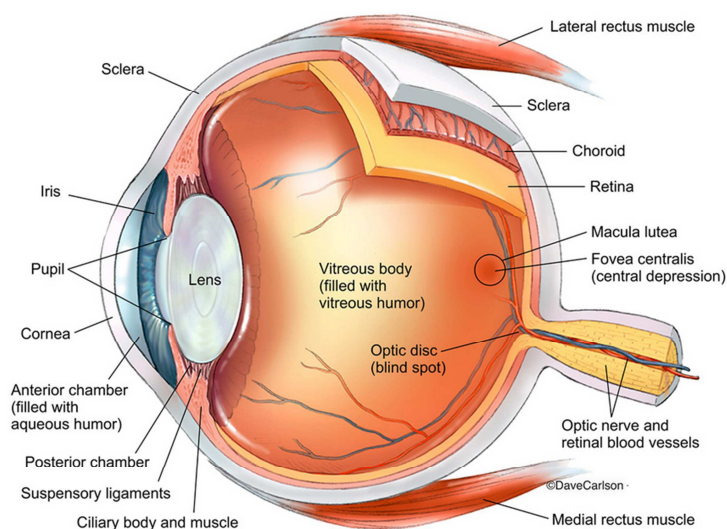


**Figure 1.1. The anatomy of the human eye with its main components.**

From Carlson Stock Art (Carlson Stock Art).

The outmost layer of the eye that appears white is called sclera. It gives the eye structural and mechanical support and contributes to the maintenance of the intraocular pressure. Light first passes through the cornea – the clear surface that covers the front of the eye. The cornea protects the eye from pathogens, UV rays, etc., but also acts as a lens, refracting the incoming light. The iris is a muscular ring, the coloured part of the eye that regulates the size of the pupil - the opening that controls the amount of light that enters the eye. Behind the pupil, we can find the lens. The shape of the lens can be modified with the help of the ligaments that connect the lens to the ciliary body and the ciliary muscle. This process is called accommodation and allows us to form a sharp image on the retina. After passing

through the vitreous humour, the transparent viscous fluid in the anterior part of the eye, the light finally hits the retina. The retina is a thin sheet of neural tissue at the back of the eye that converts the received light into electrical signals, further processes these signals and sends them through the optic nerve to the brain for visual perception. The central point for image focus (the visual axis) in humans is the fovea. Three pairs of extraocular muscles keep the eyeball in the orbital cavity and rotate the eyes to allow the image to be focused at all times on the fovea.

An illustration of the eye with its main components is shown in **Figure 1.1**.

## **1.2 The retina and its organization**

The retina is composed of two parts - neural retina and retinal pigment epithelium (RPE). The RPE is a pigmented monolayer of hexagonal cells located at the far back of the eye. RPE cells absorb the excess of light, contribute to the blood-retinal barrier and perform many tasks that are vital for the survival and function of the light-sensitive portion of the retina. The RPE and its importance for proper photoreceptor functioning is further discussed in Chapter 1.4.

The neural retina consists of three cellular layers and two synaptic layers connecting them. The outer nuclear layer (ONL) includes cell bodies of rod and cone photoreceptors and is positioned the outermost in the retina, at the far back of the eye, against the RPE and choroid – the vascular layer of the eye. The inner nuclear layer (INL) includes cell bodies of bipolar, horizontal, amacrine and Müller cells. Retinal ganglion cells (RGCs) and displaced amacrine cells form the most proximal nuclear layer, the retinal ganglion cell layer (GCL). The plexiform layers contain dendrites and synapses. The outer plexiform layer (OPL) connects photoreceptors to bipolar and horizontal cell dendrites. The inner plexiform layer (IPL) is where information is passed on from bipolar cells to amacrine cells and RGCs. This finally leads to the transmission of visual information to the brain via the optic nerve that is assembled of RGC axons. See **Figure 1.2** for a diagram showing the retinal layers and main cell types.

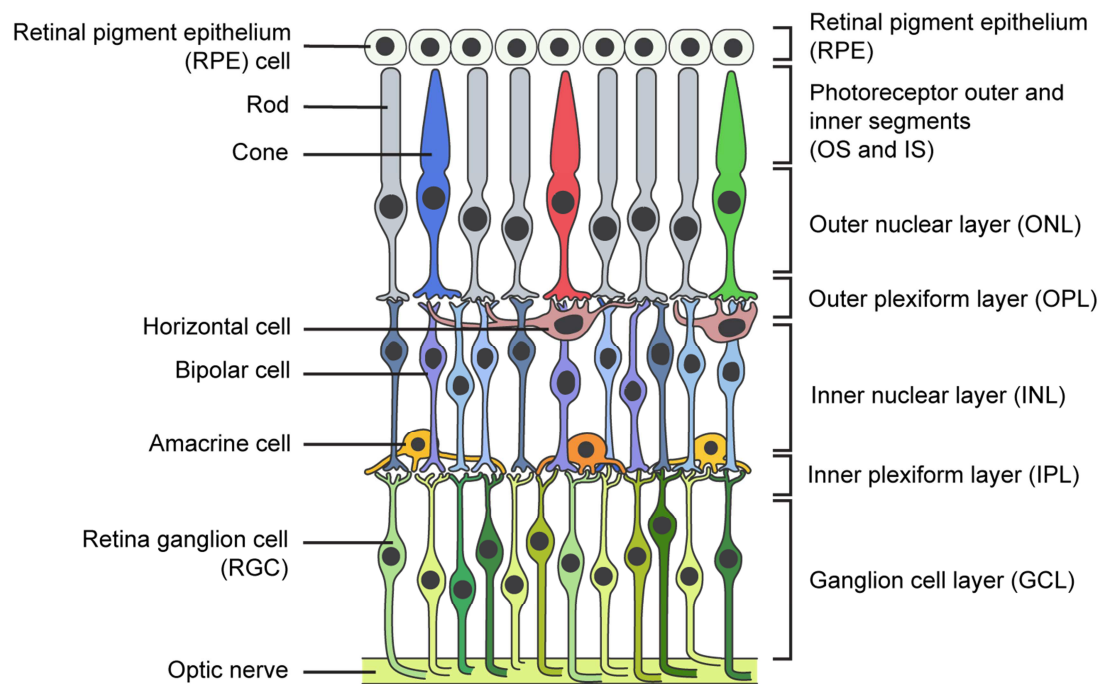


**Figure 1.2. The layered structure of the retina with its main cell types.**

Both limits of the retina are formed by Müller cells, the predominant radial glial cell type in the retina. The outer limiting membrane (OLM) forms a barrier between the subretinal space and the neural retina by adherens junctions between Müller cell apical end feet and the base of photoreceptor inner segments. Similarly, inner limiting membrane (ILM), separating the retina from the vitreous, is also made of Müller cell terminations and basement membrane constituents.

The two sources of blood supply to the mammalian retina are the choroidal blood vessels and the central retinal artery. The choroid capillary network supplies mainly photoreceptors through Bruch's membrane - the innermost layer of the choroid - and the RPE, while capillaries originating from the central retinal artery enter the eye with the optic nerve to supply the remainder of the retina.

An important particularity of primate eyes is the macula, or macula lutea, an oval-shaped yellow-pigmented area near the centre of the retina. This area is responsible for the central, high-resolution, colour vision. Within the centre of the macula lies the fovea, which is packed with cone photoreceptors and displays unusual lamination morphology. The cell bodies of INL and GCL are placed around the central 1mm of the fovea centralis, forming a foveal pit in the centre and a foveal slope in the surrounding, comprised of the displaced

cells. See **Figure 1.1.** for localization of the macula and fovea in the human eye, and **Figure 1.3.** for cell organization at the foveal site.

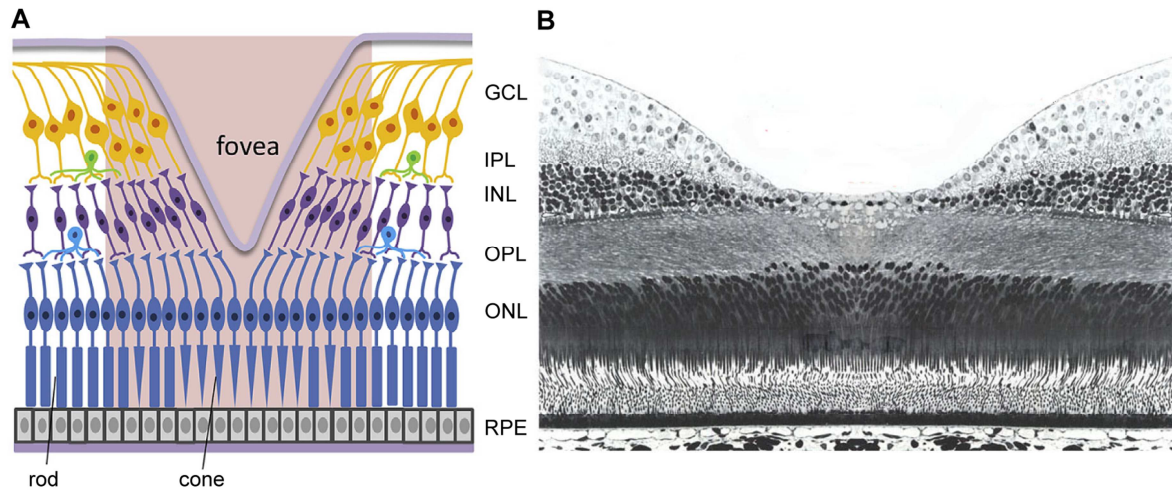


**Figure 1.3. A representation of retinal cell organization in the fovea (A) and a vertical section of monkey fovea (B).**

The centre of the fovea contains the highest density of cone photoreceptors in the retina. Retinal layers from OPL to GCL are laterally displaced, forming a pit. This organization allows high acuity vision. Adapted from Yue et al., 2016 and Hagerman and Jonson, 1991 (Hagerman and Johnson, 1991; Yue et al., 2016).

## 1.3 Cell types of the neural retina

### 1.3.1 Photoreceptors

There are two types of photoreceptors found in vertebrates, rods and cones. Rods mediate scotopic vision under dim light conditions; they can respond to single light quanta and are hundred-fold more sensitive than cones. Cones respond to bright light, permit colour perception and high resolution of visual images. Over 70% of retinal cells in mice and humans are photoreceptors. Rods outnumber cones by 30:1 in mice and 20:1 in humans (Carter-Dawson et al., 1978; Roorda and Williams, 1999). The human retina contains about 97 million rod cells, and 4,6 million cone cells (Curcio et al., 1990).

Both rods and cones have four distinct subcellular compartments: the outer segment, the inner segment, the nucleus, and the synaptic terminal. A representation is shown in **Figure 1.4**.

The photoreceptor **outer segment (OS)** contains all the components necessary for the capture of light and its conversion into electrical signals in a process known as phototransduction. Cones have a shorter conically shaped OS compared to thin cylindrically shaped rod OS. Dense stacks of discs derived from invaginations of the photoreceptor plasma membrane are found throughout the length of the OS, greatly increasing the probability of photon capture. Each disc incorporates several million opsin molecules, as well as other transduction components. Opsins are G-protein-coupled receptors (GPCRs) that are able to bind a retinal-based chromophore to form a light-sensitive photopigment.

Mammalian retina has only one type of rod visual pigment, rhodopsin, with peak spectral sensitivity at ~500 nm. In contrast, cones express several visual pigments, or opsins. Most mammals have two types of cone opsins allowing dichromatic vision – S opsin (blue-sensitive opsin) and M opsin (green-sensitive opsin). S opsin is most sensitive to light of short wavelengths (~419 nm), whereas M opsin sensitivity peaks in the medium-long wavelength region of the spectrum (~531 nm). Primates have developed a third type of cone expressing L-opsin (red-sensitive opsin), with peak spectral sensitivity at longer wavelengths (~558 nm) (Dartnall et al., 1983). In humans, the M- and L-cones form the big majority of cone population (about 93%) at a ratio of 1:1 to 1:2, whereas the S-cones make up for the remaining 7% of cones (Ahnelt, 1998). The three opsins in primates confer trichromatic colour vision, which is derived through neural computations that compare the rates of quantal catches by the three different classes of cones. While in primates each cone only expresses a single type of opsin, M and S opsins are actually co-expressed in the vast majority of cones in rodents, with the exception of about 3-5% of cones that purely express S opsin (Haverkamp et al., 2005). This means that rodents show two peaks of sensitivity in photopic conditions: one at ~510 nm due to cones expressing both M and S opsin, and one at ~360 nm, in the UV range, due to S opsin-expressing cones (Jacobs et al., 2004).

**The inner segment (IS)** houses all the protein synthesis and metabolic machinery required to assemble and transport opsin molecules to the OS. The visual proteins are transported via a connecting cilium. In addition to Golgi apparatus and endoplasmatic reticulum, it is

also packed with mitochondria, in order to meet the high demand for metabolic energy associated with phototransduction and OS renewal.

Cone **nuclei** are normally located near the OLM, whereas rod nuclei lie in the inner regions of the ONL. In addition, cone cell nuclei can be distinguished from rod nuclei by their characteristic irregularly shaped clumps of heterochromatin, compared to a single large clump in rods.

Photoreceptor **synaptic terminals** contain specialised structures termed synaptic ribbons that hold vesicles close to the site of neurotransmitter release (active zone). Rod synaptic terminal, the so called rod spherule, has a single active zone, a single ribbon and a single invagination with horizontal and bipolar cell processes. Cone pedicles in mammals contain 20 to 50 active zones and invaginations where second order neurons contact the release sites. Each cone pedicle makes up to 500 contacts, although the number of postsynaptic cells is smaller since each one receives multiple contacts (Wassle, 2004). Cones release glutamate constantly in the dark and the synaptic ribbons are believed to support this high rate of release.

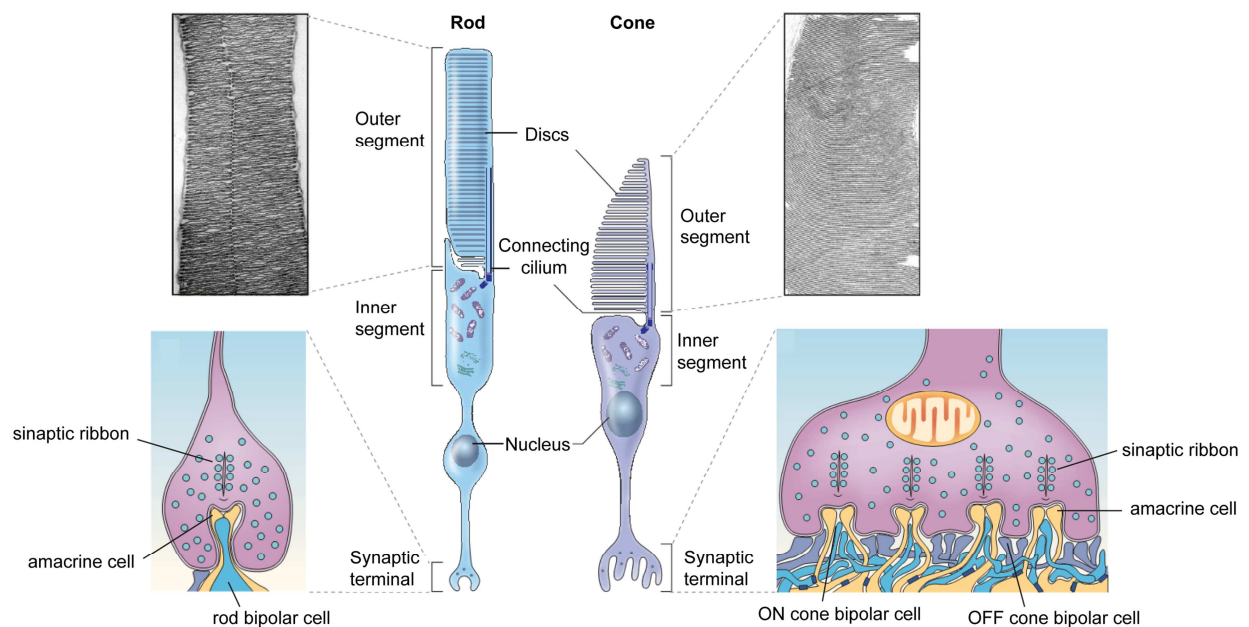


**Figure 1.4. An illustration of rod and cone photoreceptors and their subcellular compartments.**

Electron micrographs show close ups of rod (left) and cone (right) discs stacked inside the OSs. Detailed representations show synaptic terminals of rods (left) and cons (right). Adapted from Veleri et al., 2015, Wassle, 2004, and Mustafi et al., 2009 (Mustafi et al., 2009).

### 1.3.2 Bipolar cells

The photoreceptors synapse with bipolar cells, the secondary neurons of the retina.

The two main types of bipolar cells, ON and OFF bipolar cells, differ from each other in post-synaptic glutamate receptors. ON bipolar cells express metabotropic receptors, mainly metabotropic glutamate receptor 6 (mGluR6), and depolarize in response to light. OFF bipolar cells express ionotropic  $\alpha$ -amino-3-hydroxy-5-methyl-4-isoxazolepropionic acid (AMPA) and kainate receptors and hyperpolarize in the light.

Up until now, 15 distinct classes of bipolar cells have been recognized using three converging sets of high-throughput data – morphological (electron microscopic reconstruction) (Greene et al., 2016; Helmstaedter et al., 2013; Kim et al., 2014), physiological (calcium imaging) (Franke et al., 2017) and molecular (Drop-seq) (Shekhar et al., 2016) (see **Figure 1.5.**). Among the 15 types, there is only one that receives input directly from rods (rod bipolar cell). The other 14 types are cone bipolar cells, which are further subdivided into 8 ON and 6 OFF types (Zeng and Sanes, 2017), some of them transient and others sustained. The distinction is caused by the expression of either rapidly or slowly inactivating glutamate receptors (Masland, 2012).

ON and OFF bipolar cells synapse within specific planes of the IPL, which confines their possible synaptic partners to cells that occupy those same planes. The ON bipolar cells have their axon terminals in the inner half of the IPL, whereas OFF bipolar cells synapse in the outer half.

### 1.3.3 Horizontal cells

The signalling between photoreceptors and bipolar cells is modified by laterally interconnecting neurons, the horizontal cells. Through lateral inhibition, feedback, and feed-forward interactions to photoreceptors and bipolar cells, they are believed to enhance contrast between adjacent light and dark regions, improve colour discrimination and light adaptation. In most mammals, there are two morphologically distinct types of horizontal cells, mice and rats only have one type (Masland, 2001). In primates, a third type is sometimes mentioned (Kolb et al., 1994) (see **Figure 1.5.**).

### 1.3.4 Amacrine cells

Although all RGCs receive input from bipolar cells, direct synapses from bipolar cells are actually in minority. 50-70% of all RGC synapses, depending on the RGC type, are input from amacrine cells. The total number of amacrine cells in the retina is very high – they outnumber RGCs by 15 to 1. Their task is to modulate and integrate the visual message presented to the RGCs, either by direct contact with the RGCs, or by feedback inhibition onto axon terminals of bipolar cells. Amacrine cells also account for correlated firing of RGCs. RGCs that share input from the same amacrine cell fire together (Masland, 2001).

They are currently about 30 known types of amacrine cells classified (Masland, 2012). The many types differ among themselves in pre- and postsynaptic partners, neurotransmitters they use, width of the area of visual scene that they survey, branching style, exact location within the strata of the IPL, etc. (Masland, 2001) (see **Figure 1.5**).

### 1.3.5 Retinal ganglion cells (RGCs)

RGCs are the output neurons of the retina that convert the information gathered from the interneurons into changes in the action potential firing frequency. These nerve spikes are sent along their long axons (the optic nerve) to the brain.

In 2014, the number of mouse RGC types was estimated to be around 12 (Masland, 2004). By 2016, Baden et al. reported of a minimum of 32 RCG groups based on physiological studies, among them non-direction selective (9 OFF, 12 ON, 3 ON-OFF) and direction selective (2 OFF, 4 ON, 2 ON-OFF) (Baden et al., 2016). Their group, as well as preliminary electron microscopic reconstruction data (EyeWire, 2012) and transcriptomic studies, suggest that further sub-divisions are needed. They expect the total number of distinct RGC types to be over 50 (see **Figure 1.5**). One of the first RGCs identified were midget and parasol cells, followed by others such as the small bistratified RGCs and the intrinsically photosensitive retinal ganglion cells (ipRGCs) that are photosensitive and play an important role in the maintenance of circadian rhythms and the pupillary light response. The different RGC types selectively detect precise feature of a visual stimulus, such as colour, size, direction and speed of motion, etc. These different representations of the original image are

all simultaneously conveyed to the brain, where they are combined to form a realistic representation of the visual scene.

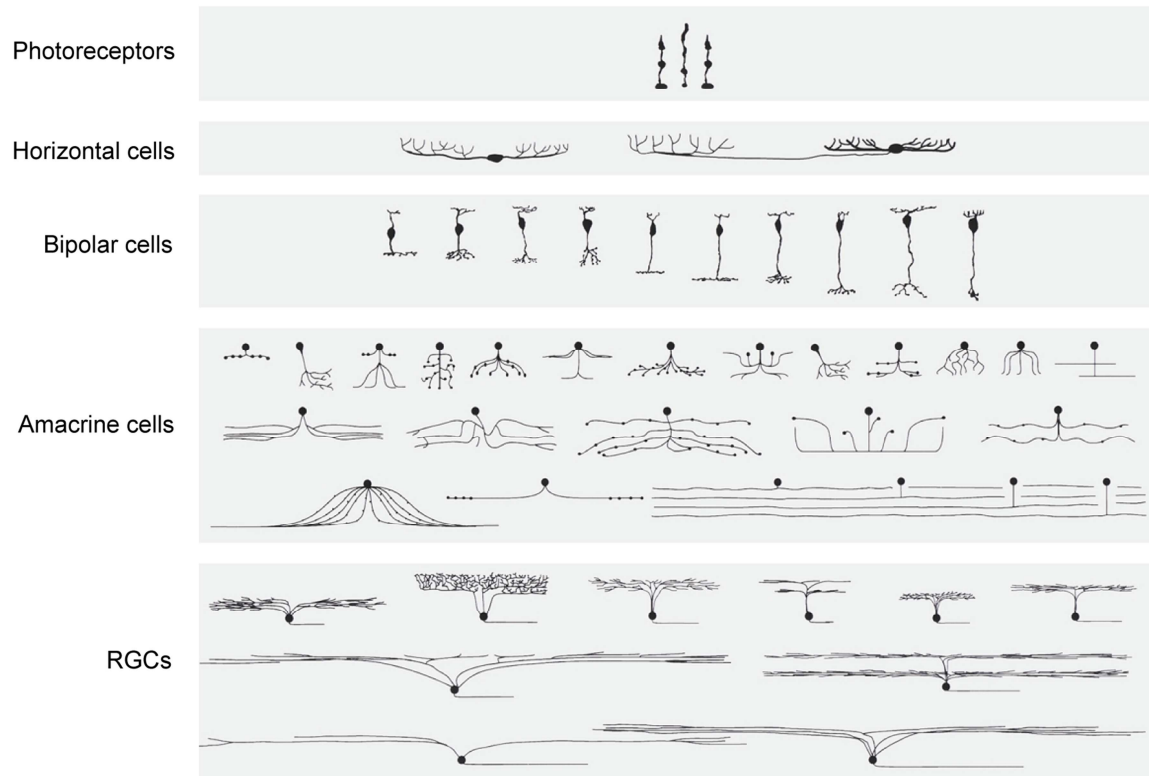


**Figure 1.5. The diversity within the major neural cell types of the retina.**

Note that the illustration is just showing a proportion of different cell types within each group, and not all the types discovered so far. Adapted from Masland, 2001.

## 1.4 How do we see?

### 1.4.1 Phototransduction cascade (in rods)

In the dark, rods are constitutively depolarized. Depolarization is a result of steady inflow of  $\text{Na}^+$  and  $\text{Ca}^{2+}$  ions into the cell along their concentration gradient, termed the dark current. The cations move into the cell through cyclic guanyl monophosphate (cGMP)-gated channels, located on OS plasma membrane, which remain open due to high concentrations of cGMP in the cell (**Figure 1.6.A**). The cation influx stimulates the rod to constantly release neurotransmitter glutamate at its synaptic terminal (**Figure 1.6.A'**).

Rhodopsin, the rod visual pigment, is densely packed within the disks of the rod OS. It consists of two components: a protein molecule, which is a light-sensitive transmembrane GPCR, and a covalently bound cofactor called retinal. In darkness, retinal is found in the form of 11-*cis*-retinal. Upon photon absorption, it isomerizes into all-*trans*-retinal (**Figure 1.6.E**), setting off a series of conformational changes in the opsin, eventually leading to its enzymatic activation (denoted as R\*). R\* catalyses the activation of the G protein transducin (T  $\alpha\beta\gamma$ ) by causing guanosine-5'-triphosphate (GTP) to bind to the  $\alpha$  subunit of the protein. As a result, activated  $\alpha$ -GTP (denoted G\*) dissociates from the complex and binds to the phosphodiesterase (PDE) activating it to PDE\*. PDE\* hydrolyses cGMP, reducing its cytoplasmic concentration. This causes closure of cGMP-gated channels in the plasma membrane, leads to reduced influx of cations into the OS and finally to membrane hyperpolarization (**Figure 1.6.B**). This decreases or terminates the dark glutamate release at the synaptic terminal (**Figure 1.6.B'**).

Following light activation, a recovery of the photoreceptor is essential so that it can respond to subsequently absorbed photons. This requires efficient inactivation of each of the activated components: R\* (**Figure 1.6.C**), G\* and PDE\* (**Figure 1.6.D**).

Because of low  $\text{Ca}^{2+}$  levels in the cell following phototransduction,  $\text{Ca}^{2+}$  are released from a calcium-binding protein called recoverin (RV). Recoverin normally forms a complex with rhodopsin kinase (RK), which is inhibiting its activity. Following  $\text{Ca}^{2+}$  release, RK dissociates from the complex and catalyses the inactivation of R\* to a phosphorylated form of rhodopsin, which then binds to a different cytoplasmic protein, arrestin (Arr). The amount of R\* for the activation of transducin is therefore reduced (**Figure 1.6.C**).

Low  $\text{Ca}^{2+}$  levels also trigger the  $\text{Ca}^{2+}$  release from guanylate cyclase-activating proteins (GCAP). This allows GCAP to bind to retinal guanylate cyclase, membrane-associated enzymes that catalyse the transition from GTP to cGMP (**Figure 1.6.D**).

GTPase-activating proteins bind to G\*, inducing hydrolysis of the bound GTP and causing  $\alpha$ -GDP to dissociate from PDE\*. This results in the inhibition of the PDE, halting the hydrolysis of cGMP. The increased levels of cGMP in the cytoplasm allows the cGMP-gated channels to reopen, causing influx of cations into the cell (**Figure 1.6.D**).

Finally, in order to maintain light sensitivity, all-*trans*-retinal needs to be re-converted to 11-*cis*-retinal, which occurs as part of the visual cycle (**Figure 1.6.E**). As photoreceptors are unable to perform this conversion themselves, retinal is transported from photoreceptors to the RPE, re-isomerized, and transported back to photoreceptors. This occurs through a series of steps involving specialized enzymes and retinoid binding proteins, such as lecithin:retinol acyltransferase (LRAT) and retinoid isomerohydrolase retinal pigment epithelium-specific 65kDa (RPE65).

In addition to the classical visual cycle, cones use a second mechanism independent of the RPE. In this pathway, the chromophore is recycled and then supplied back selectively to cones by Müller cells in the retina. This additional visual cycle is critical for extending the dynamic range of cones to bright light and for their rapid dark adaptation following exposure to light (Wang and Kefalov, 2011).

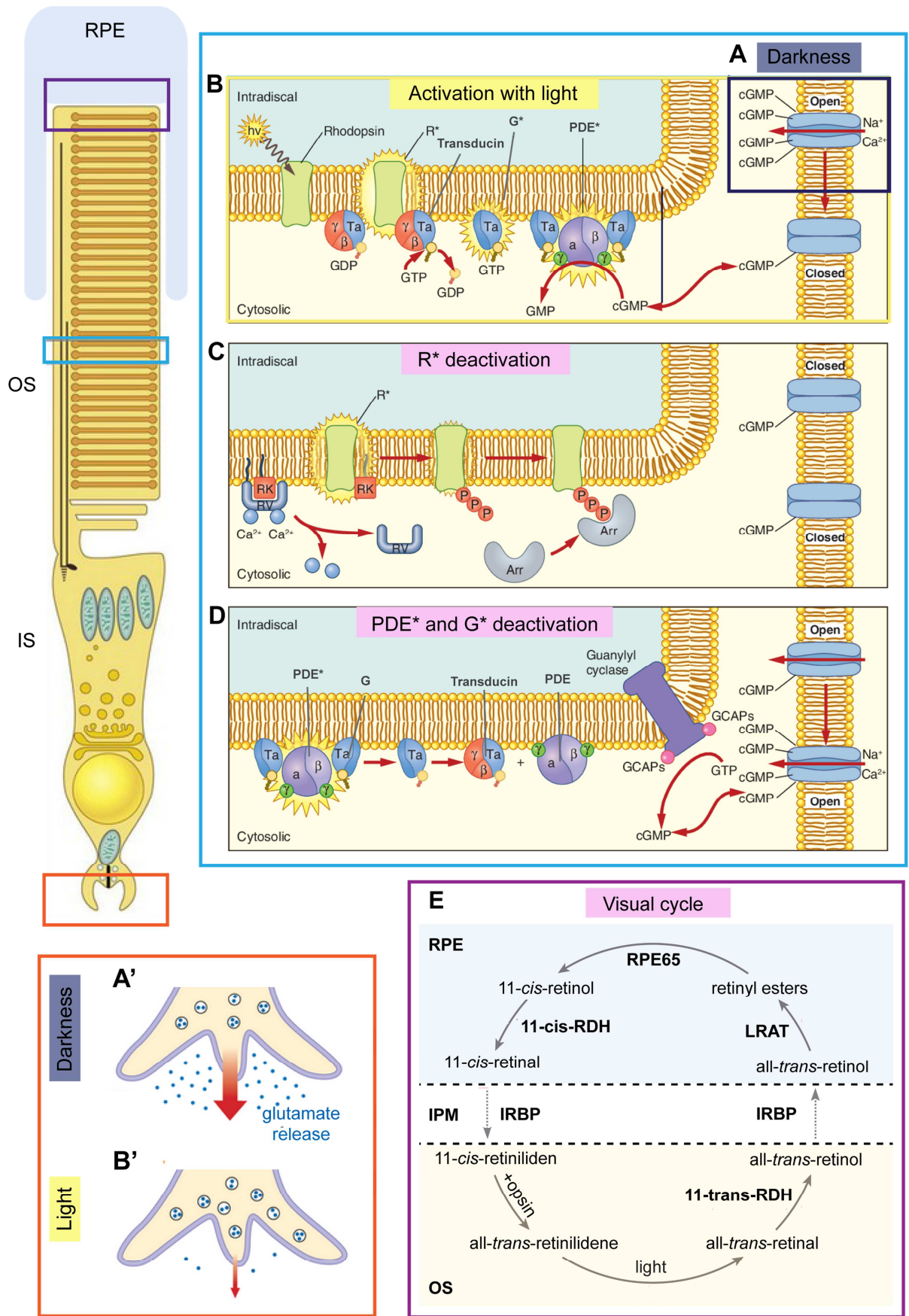


**Figure 1.6. Phototransduction cascade and the visual cycle.**

cGMP-gated channels on the photoreceptor OS membrane are opened in the dark, allowing inflow of  $\text{Na}^+$  and  $\text{Ca}^{2+}$  ions (**A**). Depolarization causes constant glutamate release at the photoreceptor synaptic terminal (**A'**). (**B**) A series of events triggered by light activation. These events cause the closure of cGMP-gated channels, hyperpolarizing the cell and inhibiting the release of glutamate at the synaptic terminal (**B'**). The recovery of photoreceptor requires efficient inactivation of all the components (**C, D**), as well as re-isomerization of the chromophore in the process of visual cycle (**E**). The photoreceptor illustration and the colour-coded frames help demonstrate the locations where these processes take place. For a more detailed description, refer to the text. Adapted from Chen and Sampath, 2013 and Openclass.com (Chen and Sampath, 2013; Openclass.com).

### 1.4.2 Retinal circuitry and cortical processing

In the retina, scotopic and photopic visual signals are propagated along separate pathways. This means that rods and cones synapse each to different types of second order bipolar cells, which then convey the signal further downstream. The dendrites of rod bipolar cells are highly branched and can receive input from as many as 120 rods. This allows for high sensitivity, but low acuity. On the contrary, especially in animals with foveae, cone bipolar cells receive synaptic input from only a few cones, which means that these RGCs have very small receptive fields and are capable of providing high acuity vision.

There are three known pathways leading from rods to RGCs (Goh, 2016; Seeliger et al., 2011; Wässle, 2004). In the classical primary rod pathway, rods synapse to rod ON bipolar cells, which express mGluR6. In the dark, glutamate is constantly bound to mGluR6, which inhibits the opening of cation channels and leaves the bipolar cell hyperpolarized. Light evokes a decrease in glutamate release, causes cation channels to open and results in cell depolarization – the ON response of ON bipolar cells. Interestingly, the majority of ON rod bipolar cells project onto All amacrine cells and not onto RGCs. This represents an important point of convergence with the cone pathway. Through All amacrine cells, rods can drive the signal to OFF cone bipolar cells via inhibitory synapses or ON cone bipolar cells via gap junctions. Through this mechanism, rods can generate both ON and OFF signals in scotopic conditions.

The gap junctions that exist between rods and cones allow rods to signal through cone pathways right from the level of photoreceptors. This is the so-called secondary rod pathway. Unlike rods, cones can synapse to both ON and OFF bipolar cells. This means that

by releasing glutamate, cones can signal either the presence or absence of light, depending on the type of bipolar cell they contact. While ON bipolar cells express mGluR6, OFF bipolar cells express either kainate or AMPA ionotropic receptors. In darkness, both of these channels are open, allowing  $\text{Ca}^{2+}$  influx, which depolarizes the OFF bipolar cell. In light, glutamate release drops, the  $\text{Ca}^{2+}$  channels close and the OFF cell hyperpolarizes.

The third rod pathway goes through a mixed rod-cone OFF bipolar cell. In this instance, glutamate release from rods is detected by AMPA receptors.

The three pathways are illustrated in **Figure 1.7**.

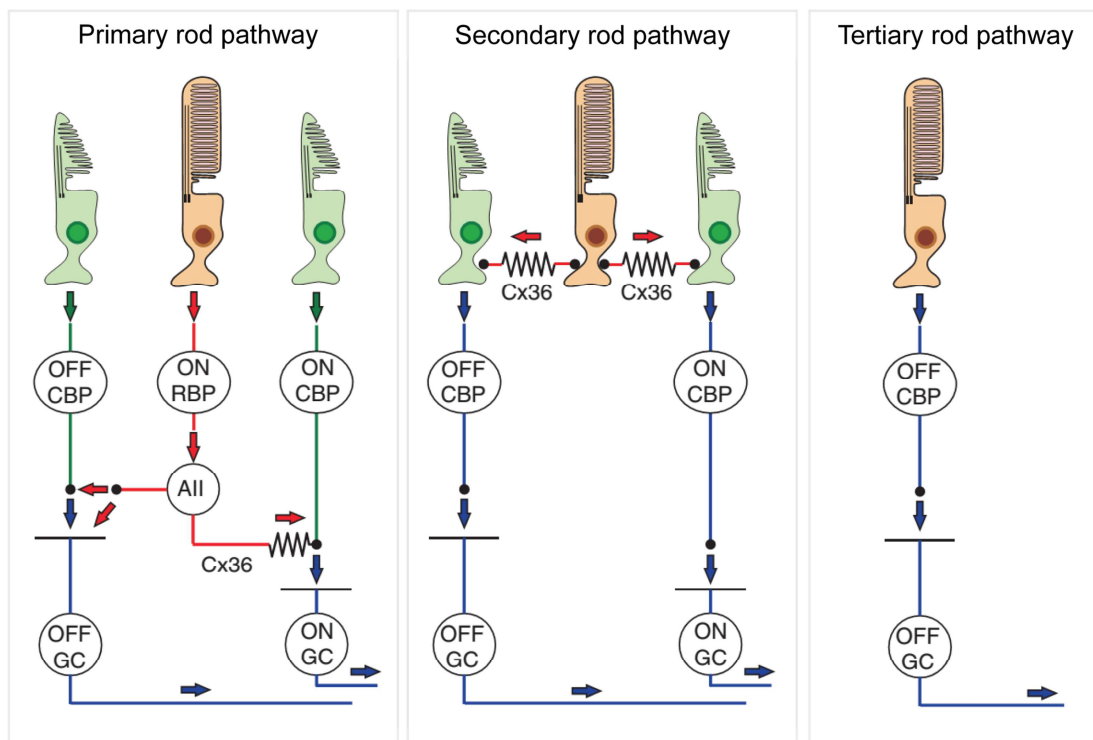


**Figure 1.7. The three rod pathways of the mammalian retina.**

CBP – cone bipolar cell, RBP – rod bipolar cell. Adapted from Seeliger et al., 2011.

Rods and cones do not only synapse to bipolar cells, but also to horizontal cells. Horizontal cells modulate multiple photoreceptor inputs to bipolar cells, controlling the resulting magnitude of bipolar cell activation. Amacrine cells carry out a similar task at the level of bipolar cell to RGC synapse.

RGCs, the output neurons of the retina, collect information about the visual world from retinal interneurons and encode this information as a change in the action potential firing frequency. Action potential refers to a rapid, transient change in membrane potential due to opening of voltage-gated  $\text{Na}^+$  and  $\text{K}^+$  channels. RGCs are the only cells in the retina that are capable of firing action potentials, all other cells in the retina respond to stimulation with graded membrane potential changes. Nerve spikes are transmitted along the long axons of the RGCs – the optic nerve - to the higher brain centres. The different types of RGCs convey independent channels of visual information that come together in the brain, forming a realistic representation of the visual scene. Most of RGC axons terminate in the lateral geniculate nucleus (LGN) in the dorsal thalamus, from where the information is relayed to the visual cortex (V1) for visual processing. Some axons project to the pretectal nucleus and are involved in reflexive eye movements, or to the suprachiasmatic nucleus, participating in sleep-wake cycle regulation. About 10% of the RGCs project to a part of the midbrain tectum called the superior colliculus and are involved in orienting the eyes in response to new stimuli in the visual periphery (Bear et al., 2007).

## 1.5 Retinal pigment epithelium (RPE) and its role in vision

RPE is the pigmented cell layer just outside the neurosensory retina that is firmly attached to the underlying choroid and overlying retinal visual cells. It is composed of a single layer of hexagonal cells that are densely packed with melanosomes. The RPE performs many functions that are of great importance for health and proper functioning of the neural retina (Strauss, 2005) (see **Figure 1.8.** for a summary).

RPE helps fight photo-oxidative stress and oxidative damage by absorbing scattered light, as well as by enzymatic and non-enzymatic antioxidants and cell's physiological ability to repair damaged DNA, lipids and proteins.

It transports ions and water from the subretinal space to the choroid, and eliminates metabolic end products such as lactic acid from the photoreceptors. In the other direction, RPE supplies nutrients such as glucose and fatty acids, as well as 11-*cis*-retinal from blood to the photoreceptors. 11-*cis*-retinal is a  $\beta$ -carotene derivative, derived entirely from the

animal's diet and delivered to the photoreceptors through choroidal capillaries through the RPE.

Furthermore, RPE is involved in re-isomerization of the chromophore after light isomerizes it into all-*trans* retinal. Photoreceptors are unable of this conversion themselves, therefore retinal is transported from photoreceptors to the RPE, re-isomerized to 11-*cis*-retinal, and transported back to photoreceptors. This process is known as the visual cycle and is crucial to maintain photoreceptor light sensitivity.

Spatial buffering of ions in the subretinal space maintains excitability of photoreceptors. The voltage-dependent ion conductance of the apical membrane enables the RPE to compensate for fast occurring changes in the ion composition in the subretinal space.

RPE cells take an important part in photoreceptor OS renewal by phagocytosing the material that has been shed from the OS. Because photoreceptors are exposed to intense light, their OSs need to go through constant renewal process in order to avoid the accumulation of photo-damaged proteins and lipids and maintain the excitability of photoreceptors. The photoreceptor OSs are digested by the RPE and essential substances such as retinal are recycled and brought back to photoreceptors to rebuild the OSs from the base of the photoreceptors. One RPE cell supports 30–50 photoreceptors (Bonilha, 2008), which shed daily around 10% of their OS volume.

In order to communicate with the neighbouring tissues, the RPE is able to secrete a large variety of growth factors such as fibroblast growth factors (FGF-1, FGF-2, FGF-5), transforming growth factor- $\beta$  (TGF- $\beta$ ), insulin-like growth factor-1 (IGF-1), ciliary neurotrophic factor (CNTF), vascular endothelial growth factor (VEGF), pigment epithelium-derived factor (PEDF), etc. These factors help maintain the structural integrity of choriocapillaris endothelium and photoreceptors.

By secreting immunosuppressive factors, RPE plays a role in establishing the immune privilege of the eye. It does so also by being an important component of the blood-retinal barrier that isolates the inner retinal from the systemic influences.

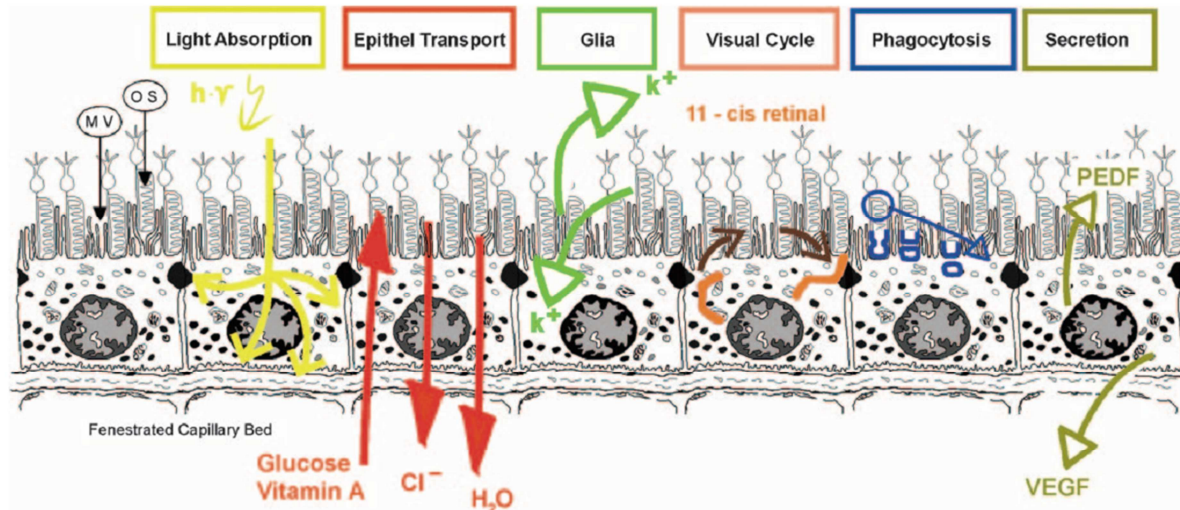


**Figure 1.8. The summary of RPE functions.**

From Strauss, 2005.

The importance of the functional interaction between photoreceptors and the RPE is supported by the studies demonstrating that mutations in genes which are expressed in the photoreceptors can lead to a primarily RPE dysfunction and the loss of photoreceptors occurring secondarily (for example mutations in ATP-binding cassette protein (ABC) (Sparrow et al., 2003)). The contrary is also true – gene mutations in the RPE can lead primarily to photoreceptor degeneration (for example mutations in tyrosine-protein kinase Mer (MERTK) (Goldman and O'Brien, 1978) and RPE65 (Cideciyan, 2010)) (Strauss, 2005).

## 2 OUTER RETINAL DYSTROPHIES

Outer retinal dystrophies are caused by progressive loss of light-sensitive photoreceptors and are accounted for about half of the blindness cases in the developed countries. While inherited photoreceptor degenerations are linked entirely to mutations in genes expressed in photoreceptors or the RPE, complex multifactorial diseases are caused by a combination of both genetic predispositions and environmental factors.

### 2.1 Inherited retinal diseases (IRDs)

IRDs are genetically and clinically very heterogeneous disorders (*Figure 2.1.*). Over 100 different forms have been described and combined, they have an incidence of about 1:2000, making IRDs the leading cause of blindness in people between 15 and 45 years of age (Cremers et al., 2018).

IRDs can be classified based on disease progression into stationary and progressive forms. Examples of stationary IRDs are congenital stationary night blindness and achromatopsia, whereas retinitis pigmentosa (RP) and cone-rod dystrophy are typically progressive IRDs.

IRDs can be further clinically differentiated in respect of the retinal cell type that is primarily affected. They can be rod dominated (rod-cone dystrophies), cone dominated (cone-rod dystrophies), or generalized (with both rods and cones affected simultaneously). In cone-rod dystrophies, cones are involved in disease pathogenesis first, followed by the degeneration of rods. The patients first experience central vision defects, which later progress towards the periphery. Rod-cone dystrophy-affected individuals first suffer from night blindness and tunnel vision due to rod degeneration. With the progression of the disease, cone-guided central vision also gets affected, eventually leading to legal blindness. The most common form of rod-cone dystrophy is RP. Leber congenital amaurosis (LCA) is the most severe form of IRD with both rods and cones affected in parallel, and in some cases also the RPE primarily involved.

Furthermore, IRDs can either be non-syndromic with only the ocular system affected, or syndromic, with ocular phenotype associated with pathologies of other tissues.

The mode of inheritance can be dominant, recessive, or X-linked. In most IRDs, mutations in different genes can cause very similar phenotypes. At the same time, mutations in the same gene can cause a range of clinical phenotypes. IRDs are considered as possibly the most genetically heterogeneous group of diseases in humans.

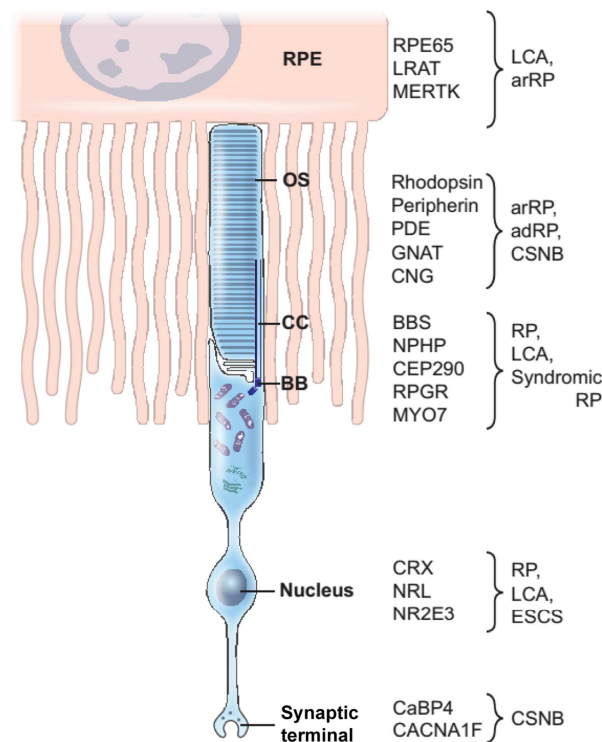


**Figure 2.1. Classification of the more important proteins associated with IRDs according to their localization in photoreceptors or RPE cells.**

arRP – autosomal recessive RP, adRP – autosomal dominant RP, CSNB – stationary night blindness, ESCS – enhanced S-cone syndrome. From Veleri et al., 2015.

### 2.1.1 Rod-dominated diseases

**Congenital stationary night blindness** is a typical stationary rod disorder, whereas the most common among rod-dominated diseases in general is the progressive **retinitis pigmentosa (RP)**, characterized by photoreceptor and RPE abnormalities, that lead to progressive vision loss. The worldwide prevalence of RP is approximately one in 4000 people, although reports vary from 1:9000 to 1:750, depending on the geographic location (Verbakel et al., 2018).

RP is characterized by primary degeneration of rods, causing loss of night vision and peripheral vision. This is followed by secondary cone degeneration leading to central vision deprivation. Other characteristics of the disease are atrophy in the RPE, RPE cell migration

into the outer retina, abnormal fundus with bone-spicule pigment deposits and attenuated retinal vessels, etc. (Pierrottet et al., 2014). The INL and the GCL are fairly well preserved until late in the disease course.

There are more than 30 different syndromic forms of RP. The two most prevalent are Usher syndrome which manifests as early-onset hearing impairment followed by RP, and Bardet-Biedl syndrome which includes RP, polydactyly, obesity, renal abnormalities, hypogonadism, and mental retardation. Non-syndromic RP can be inherited in an autosomal dominant, autosomal recessive, or X-linked manner, and there are some more rare forms such as mitochondrial and digenic (Chang et al., 2011; Pierrottet et al., 2014).

The big heterogeneity of RPE includes (1) genetic heterogeneity – many different genes may cause the same genotype; (2) allelic heterogeneity – many different mutations in the same gene may cause the disease; (3) phenotypic heterogeneity – different mutations in the same gene may cause different diseases; and (4) clinical heterogeneity – the same mutation in different individuals may result in different clinical consequences (Daiger et al., 2013). In 1990, Dryja and colleagues reported of the first gene involved in autosomal dominant RP – the rhodopsin (RHO) gene. Since then, more than 80 genes have been implicated in non-systemic RP, with additional 18 causing Usher syndrome and 18 associated with Bardet-Biedl syndrome (RetNet, 2019). New causative genes and mutations are being discovered continuously.

According to their function, RP-associated genes have been categorized into five distinct groups: phototransduction, retinal metabolism, tissue development and maintenance, cellular structure, and splicing (Berger et al., 2010). Most mutations are related to genes that are specifically expressed in photoreceptors, but there are some RPE specific gene mutations as well, for example *RPE65* which encodes an isomerohydrolase that is crucial for the derivation of *cis*-retinal, and *MERTK* involved in the phagocytosis of the photoreceptor OSs.

### **2.1.2 Cone-dominated diseases**

Cone-dominated diseases such as **cone dystrophy**, **cone-rod dystrophy**, and **monogenic macular dystrophy**, lead to severe visual impairment, with patients experiencing a decrease

in visual acuity, photophobia, nystagmus, colour vision abnormalities, etc. In progressive forms, night blindness also joins the symptoms later in the course of the disease. Macular dystrophy is restricted to the macula, whereas cone dystrophy and cone-rod dystrophy affect both macular and peripheral cones. Juvenile macular degeneration – **Stargardt disease** - is most commonly the result of a mutation in the *ABCA4* gene, which encodes an ATP-binding cassette transporter. **Achromatopsia** is a stationary form of cone dysfunction, it can be complete or incomplete, and is usually congenital. Patient with complete achromatopsia are unable to distinguish colours and along with that suffer from nystagmus, poor visual acuity and photophobia. Individuals with incomplete achromatopsia retain some colour vision.

### 2.1.3 Generalized photoreceptor diseases

The most well known disease from this group is **Leber congenital amaurosis (LCA)**. LCA represents a group of hereditary retinal dystrophies causing blindness or severe visual impairment within the first year of life. It is characterized by congenital visual loss, nystagmus, poor pupil responses, and absent electrical signals on electroretinogram (ERG). So far, 25 genes have been associated with LCA, accounting for 70-80% of cases (Kumaran et al., 2017). Associated genes encode proteins with a wide variety of retinal functions, such as photoreceptor morphogenesis (*CRB1*, *CRX*), phototransduction (*AIPL1*, *GUCY2D*), vitamin A cycling (*LRAT*, *RDH12*, *RPE65*), outer segment phagocytosis (*MERTK*), and intra-photoreceptor ciliary transport processes (*CEP290*, *LCA5*, *RPGRIP1*, *TULP1*) (den Hollander et al., 2008).

## 2.2 Multifactorial retinal diseases

The most typical multifactorial retinal disorder is **age-related macular degeneration (AMD)**. AMD is the leading cause of worldwide blindness in the elderly. This disease is not a classic monogenic disease, but the result of complex interactions between multiple genetic and environmental factors. In addition to age; hypertension, smoking, high lifetime exposure to

sunlight, diet, obesity, and chronic inflammation are considered as important environmental risk factors (Berger et al., 2010). Mutations in several genes are known to predispose people to AMD, including mutations in *APOE*, *LOC387715*, *CFH*, *CFB* and *C2* (de Jong, 2006).

AMD affects the central area of retina known as the macula, leading to progressive loss of high acuity central vision. AMD is associated with degeneration involving photoreceptors, RPE and Bruch's membrane, as well as alterations in choroidal capillaries.

The stages of AMD are categorised as early, in which a spectrum of changes is observed in the ageing eye, but the onset of apparent loss of vision has not yet occurred, and late, in which severe loss of vision is common. The first clinical features of AMD include the presence of extracellular deposits (drusen) between the RPE and Bruch's membrane, and pigmentation abnormalities in the RPE. Late AMD can manifest as atrophic (dry) or exudative (wet) AMD. Sometimes, both forms appear in the same patient simultaneously, or one form can develop into the other (de Jong, 2006). In the **dry** form of the disease, increased accumulation of drusen is thought to disrupt RPE's interface with choroid, causing RPE degeneration and secondarily the death of photoreceptors. The **wet** form is the more debilitating and rapidly progressing form of the disease. It is characterized by pathogenic proliferation of choroidal neovascularization, subsequently leading to detachment of the RPE or the retina, RPE tears, haemorrhages and lipid exudation (Kinnunen et al., 2012).

## 2.3 Animal models of retinal degeneration

**Mouse models** of human retinal disease are widely used in retina research. Mice are phylogenetically related and physiologically similar to humans, and at the same time easily maintained and bred in the laboratory. Numerous very well characterised mouse models exist and are often commercially available. Mouse models can be either naturally occurring or generated by genetic modulation (transgenic, knockout mice, knockin mice, etc.). The two models that we used in our study are described below.

### ***Cpfl1/Rho*<sup>-/-</sup> mouse**

Tg(*Cpfl1*; *Rho*<sup>-/-</sup>) mice are the result of crossing Cone photoreceptor function loss 1 (*Cpfl1*) mice (Chang et al., 2009; Chang et al., 2002) with rhodopsin knockout mice (*Rho*<sup>-/-</sup>) (Humphries et al., 1997).

The *Cpfl1* mouse is a spontaneously arising mutant that carries a 116-bp cDNA insertion and a 1-bp deletion in the catalytic subunit of the cone photoreceptor phosphodiesterase gene (*Pde6c*). ERGs of *Cpfl1* mice show no cone mediated response from the earliest age that can be tested, although they at first appear structurally normal under electron microscope. Cone photoreceptors start to rapidly degenerate in the first weeks after birth, with very few (non-functional) cones persisting for up to several months. Rod-mediated responses are not affected. The phenotypic characteristics of *Cpfl1* mice are comparable to those observed in patients with complete achromatopsia (Chang et al., 2009; Chang et al., 2002).

*Rho*<sup>-/-</sup> mice develop normal numbers of rod and cone nuclei, but the rods form no OSs and lack rhodopsin mRNA and protein (Humphries et al., 1997). There is no rod-mediated ERG response detected at any time. The ONL begins to thin by P30 and by P90 only a single row of cone nuclei remains (Toda et al., 1999).

Crossing the *Cpfl1* and the *Rho*<sup>-/-</sup> mouse model resulted in mice with no functional photoreceptors, rods or cones, starting from eye opening. The ONL in these mice degenerates to one row of cell bodies by 10 to 12 weeks after birth (Santos-Ferreira et al., 2016b) (**Figure 2.2.A**).

### **Rd1 mouse**

The rd1 (rd/rd) mouse is a well-known and well-characterized model of severe RP possessing a null mutation in the rod cGMP-specific *Pde6b* gene encoding the  $\beta$ 6-subunit of rod PDE (Bowes et al., 1990). This leads to accumulation of cGMP and triggers rod photoreceptor degeneration (Farber and Lolley, 1976). The same mutation occurs in humans suffering from autosomal recessive RP (McLaughlin et al., 1993), so the pathogenesis in mice mimics well the condition observed in humans.

Photoreceptor degeneration in the rd1 mouse starts at around P8, and by 3 weeks of age, there are no OSs and only a single row of cell bodies remaining in the ONL, consisting of cone photoreceptors (Carter-Dawson et al., 1978; Drager and Hubel, 1978; Farber et al., 1994; LaVail and Sidman, 1974) (**Figure 2.2.B**). These are subsequently lost through a secondary mechanism, but a small number of cone cell bodies can remain for over 250 days (Buskamp et al., 2010).

It has recently been discovered that the rd1 strain used in the majority of studies since 1948 possesses a naturally occurring mutation in the G protein-coupled receptor 179 (*Gpr179*) gene, which abolishes function in the ON bipolar cells (Nishiguchi et al., 2015). We used the C3H rd/rd mouse strain (Vicgian et al., 1992) to overcome this problem.

Despite the many advantages of rodent disease models, the results acquired from rodents cannot always be extrapolated to humans. Mouse and human eyes differ significantly in size and volume. In addition, mice are nocturnal animals and do not have the specific configuration of the high-acuity fovea as found in humans.

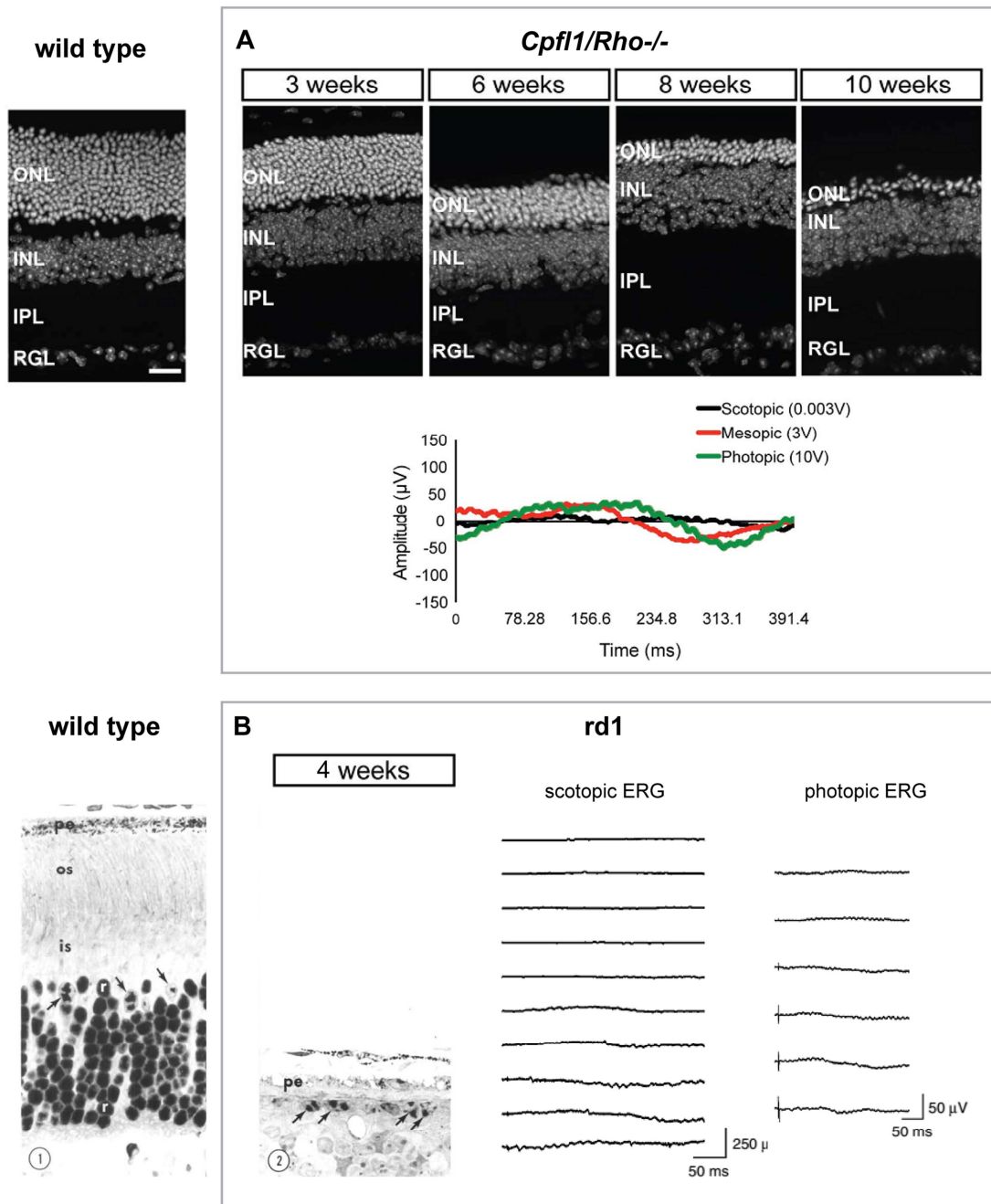


**Figure 2.2. Characterization of the two mouse models used in our study, *Cpfl1/Rho<sup>-/-</sup>* (A) and *rd1* (B) mouse.**

(A) Top, cross-sectional images of *Cpfl1/Rho<sup>-/-</sup>* retinas at ages 3 to 10 weeks, showing complete loss of the ONL at 10 weeks. Bottom, flattened ERG curves in scotopic, mesopic and photopic conditions in 12-week old *Cpfl1/Rho<sup>-/-</sup>*. Adapted from Santos-Ferreira et al., 2016b. (B) A light micrograph of a *rd1* retina at 4 weeks. All rod nuclei, OSs and ISs have degenerated, leaving only a small number of cone nuclei (arrows). ERG in scotopic and photopic conditions show no responses. Images from wild type mouse are shown on the left for better comparison. Adapted from Carter-Dawson et al, 19798 and Nishiguchi et al. 2015.

**Nonhuman primates** have a highly similar retinal organization to the one in humans, with a macula with cone-only foveal pit in its centre and a trichromatic vision. However, until very recently, only chemically or light/laser induced acute models of retinal degeneration have been available, which cannot fully recapitulate the pathogenesis of the disease (Shirai et al., 2016). Last year, the first inherited retinal dystrophies have been detected in nonhuman primates (Ikeda et al., 2018; Moshiri et al., 2019). In addition to this, generation of specific nonhuman primate disease models is becoming possible with the recent advances in gene editing tools such as CRISPR/Cas9 (Sato and Sasaki, 2018).

**Pig** eye size is very comparable to human and has a cone-enriched area (area centralis), which makes pigs an interesting large animal model. Targeted transgenic pig models of retinal degeneration have already been generated for dominant and recessive forms of RP and for Stargardt disease (Petters et al., 1997; Sommer et al., 2011).

A number of spontaneous mutations leading to inherited retinal degeneration have been identified in **dogs** (Petersen-Jones and Komaromy, 2015). One of the most well-known dog models is a naturally occurring model of LCA, a briar dog carrying a mutation in the REP65 gene (Veske et al., 1999). This model was used in the preclinical testing of gene augmentation therapy for LCA (Acland et al., 2001).

### 3 THERAPEUTIC APPROACHES FOR TREATING PHOTORECEPTOR DEGENERATION

Treatment options for most degenerative retinal diseases are still very limited and there is big interest and need for advancement. Multiple approaches for treating outer retina dystrophies are currently being explored, including pharmacotherapy, gene replacement, gene editing, neuroprotection, optogenetics, optopharmacology, cell replacement, induced retinal regeneration, and retinal prostheses. Some of them are effective only in the early stages of the disease, whereas others target later disease stages, where most or all of the photoreceptors are lost (**Figure 3.1.**).

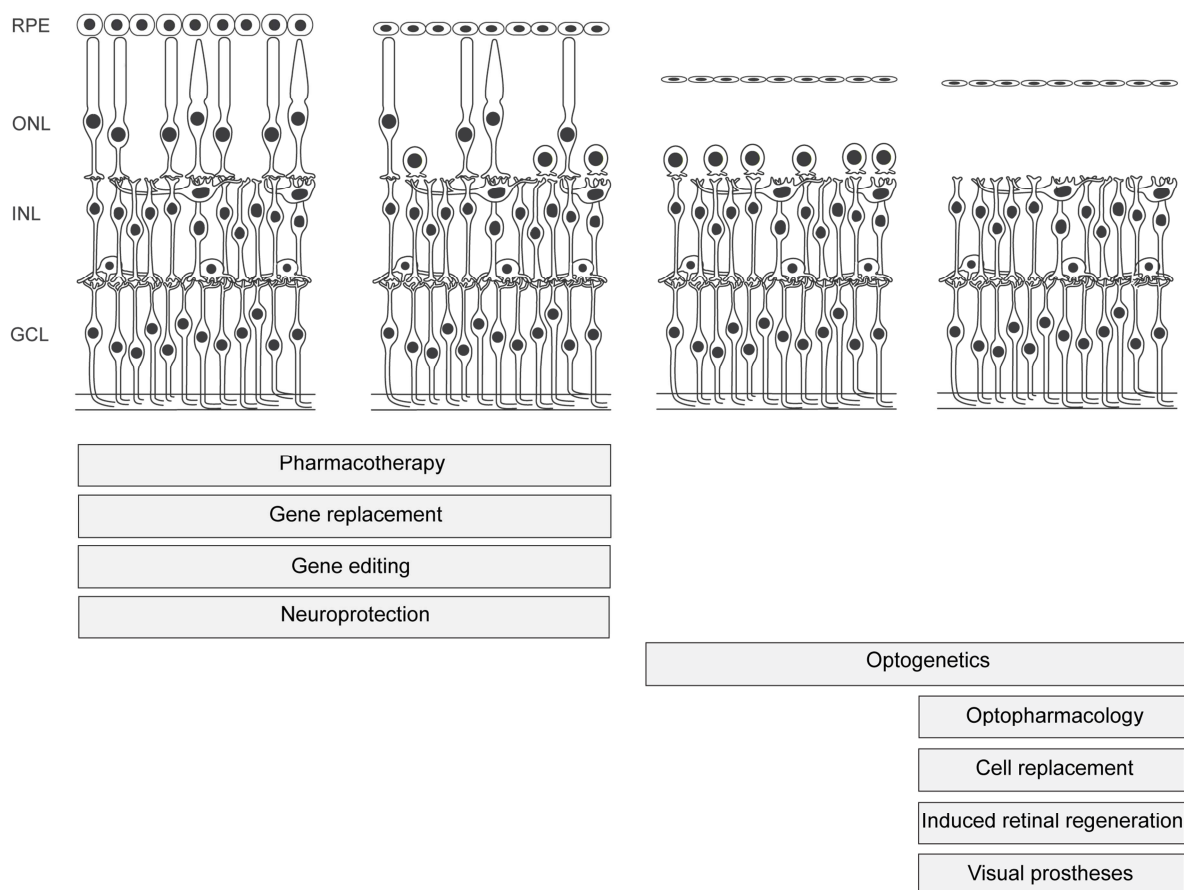


**Figure 3.1. An overview of therapeutic approaches and their application based on photoreceptor degeneration progression.**

Some treatment strategies such as neuroprotection and gene replacement require the presence of endogenous photoreceptors to be effective, whereas others such as cell replacement and visual prostheses aim to treat patients in the late stages of disease where no photoreceptors are left.

### 3.1 Pharmacotherapy

RPE65 and LRAT are two key enzymes of the visual cycle. Mutations in genes encoding these two proteins cause RP and LCA in humans. *Rpe65* and *LRAT* knockout mice display absence of 11-*cis*-retinal and rhodopsin, leading to severe impairment of rod photoreceptor function and retinal degeneration. Oral delivery of 9-*cis*-retinal resulted in formation of photopigment and dramatic improvement in rod physiology (Van Hooser et al., 2000). Two recent clinical studies showed safety and efficacy in treating RPE65 and LRAT-related LCA and RP with 9-*cis*-retinyl-acetate (Koenekoop et al., 2014; Scholl et al., 2015).

In diseases caused by mutations in the *ABCA4* gene, such as Stargardt disease, cone dystrophy, and cone-rod dystrophy, the defective visual cycle exacerbates the dimerization of vitamin A, leading to accumulation of lipofuscin. Possible approach could be to reduce vitamin A availability in photoreceptors using RPE65 inhibitors or retinoid-binding protein 4 (RBP4) antagonist (Scholl et al., 2016).

### 3.2 Gene replacement therapy

Gene therapy aims to treat, cure, or prevent a disease by providing to the cells a gene with therapeutic action. This gene can either introduce genetic material to compensate for abnormal genes, or to make a beneficial protein. Diseases caused by loss-of-function mutations can be treated with gene replacement therapy (gene supplementation), whereas diseases associated with gain-of-function mutations require elimination of the abnormal gene in addition to the supplementation.

Most gene therapy studies use viral vectors to deliver genes to the target cells, such as adeno-associated virus (AAV) and lentivirus. AAV is the preferred vector of choice for gene delivery in the retina. It has minimal immunogenicity and lacks pathogenicity, provides long-lasting transgene expression, can diffuse easily across biological barriers due to its small size, and can be easily modified using genetic engineering. A weakness of AAVs is that they can hold a maximum of 4.7 kb of genetic material, which can pose a problem for treating diseases caused by mutations in big genes (Dalkara et al., 2016). Non-viral gene delivery

approaches are also being explored, such as laser, ultrasound, and electrical discharges that create transient pores in cell membranes, allowing DNA or RNA fragments to enter the cells (Roska and Sahel, 2018). These could be used to transfect target cells with longer stretches of DNA, but for the moment they lack to provide long-lasting gene expression (Dalkara et al., 2016).

The first success in gene replacement for an IRD was documented following a clinical trial in patients with LCA caused by a mutation in the *RPE65* gene (LCA2). The patient received a single subretinal injection of AAV2 carrying the *RPE65* gene (Bainbridge et al., 2008; Hauswirth et al., 2008; Maguire et al., 2008). The initial results were very promising, but some long-term follow-up results showed that the retinal degeneration continued despite the treatment. The areas with improved visual sensitivity seemed to be sustained for 1 to 3 years, but after this time the effect declined or was lost (Bainbridge et al., 2015; Jacobson et al., 2015).

Since then, other clinical trials have been initiated or are in preparation, for example treatment for LCA1 (*GUCY2D* gene supplementation), LCA4 (*AIPL1* supplementation), Stargardt disease (*ABCA4* supplementation), choroideremia (*CHM* supplementation), X-linked retinoschisis (*RS1* supplementation), Leber hereditary optic neuropathy (*ND4* and *ND1* supplementation), Usher syndrome 1b, RP (*MERTK* supplementation), achromatopsia (*CNGB3* supplementation), etc. (Dalkara et al., 2016)

### **3.3 Gene editing**

While classical gene augmentation therapies hold promise for patients with loss-of-function mutations involving small sized genes, they cannot be applied to patients affected by dominant gain-of-function mutations, where the pathogenic mutation would need to be silenced or corrected in order to regain normal cell function.

Gene editing aims to modify the genome of a cell or an organism. Prokaryotic immune components known as clustered regularly interspaced short palindromic repeats (CRISPR) and CRISPR-associated nucleases such as Cas9 are to this day the most promising gene editing tools. CRISPR/Cas9 system only needs three components for proper functioning: the

presence of a short sequence called the PAM site adjacent to the target site, the endonuclease Cas9, and a custom made piece of RNA which directs the nuclease to the target site. In addition, The CRISPR/Cas9 system is small enough to enable AAV-mediated delivery (Peddle and MacLaren, 2017). The engineered nuclease creates a double strand break at a desired location. This is followed by an endogenous DNA repair process through either non-homologous end joining (NHEJ) or homologous recombination (HR). NHEJ occurs in all phases of the cell cycle. Insertion or deletion of random nucleotides can be targeted to the double strand break, causing a reading frame shift. This method is often used to achieve gene knockout. The error-free repair mechanism by HR only occurs in late S phase or G2 phase of the cell cycle. It involves the copying of DNA from a homologous template, which can be introduced to the cell along with the nuclease (Yu and Wu, 2018).

At present, direct silencing of dominant negative mutations is the more commonly adopted approach for developing treatments. After the disruption of the allele possessing the pathogenic mutation, the remaining wild type allele restores the functionality of the gene. Several studies have used CRISPR/Cas9 to knockout the mutant *RHO* genes ((Bakondi et al., 2016; Giannelli et al., 2018), and mutant *CEP290* gene – one of the most common causes of LCA (Ruan et al., 2017).

In principle, the HR pathway would allow precise insertion of a DNA portion that would restore the wild type functioning of the gene. However, HR only occurs in S and G2 stages of the cell cycle, and in post-mitotic cells such as retinal cells, HR rate is too low to have therapeutic value. In 2016, a new technique called homology-independent targeted integration (HITI) was described that allows precise gene knockin in absence of the HR pathway. It was used to partially restore MERTK expression, retinal morphology and function in the Royal College of Surgeons' (RCS) rats (Suzuki et al., 2016).

Despite the encouraging preliminary results, CRISPR/Cas9 still has several unsolved issues before being ready for clinical application. The efficiency of gene editing is rather low – about 30% *in vivo*, and very variable between studies. The success rate depends on many factors that are not yet well understood. Despite this, studies are reporting of improved disease phenotypes and patients' quality of life after the treatment. Non-specific gene editing is a huge concern, since it could silence essential genes or cause cancers. To reduce

the risks of off-target effects, several artificial high fidelity Cas9 molecules are being tested (Peddle and MacLaren, 2017).

Due to the heterogeneity of the inherited retinal diseases with hundreds of existing causative mutations, several alternative uses of CRISPR/Cas9 system have been suggested that could be applied to patients regardless of the disease-causing mutation. For example, the symptom of the disease could be targeted instead of its cause, as was demonstrated by Kim et al. (2017) who disrupted the *VEGFA* gene that is crucial for choroidal neovascularisation in wet AMD (Kim et al., 2017). Cellular reprogramming aims is to convert mutation-sensitive cells into a similar cell type that is less prone to be affected by this mutation, for example turning rods into cones by disrupting the neural retina-specific leucine zipper (*NRL*) gene in models of RP (Yu et al., 2017; Zhu et al., 2017b).

### **3.4 Neuroprotection**

Neuroprotective treatments aim to slow down the degeneration process and cell death. Several neuroprotective factors such as rod-derived cone viability factor (RdCVF), ciliary neurotrophic factor (CNTF), brain-derived neurotrophic factor (BDNF), basic fibroblast growth factor (FGF), pigment epithelium derived factor (PEDF), glial cell-derived growth factor (GDNF), and X-linked inhibitor of apoptosis (XIAP), have been examined in preclinical studies (Scholl et al., 2016).

These factors have traditionally been administered by intravitreal injections. However, with most of them losing biological activity rapidly after being delivered, repeated injections were necessary. Therefore, novel methods for achieving sustained delivery of therapeutic agents were explored. These include gene therapy to induce local expression of neurotrophic factors, vitreous implants to enable a slow steady release of these agents, and implanting genetically modified cells, preferably enclosed in a capsule, to continuously produce the neuroprotective protein (Lee, 2011).

CNTF is the most extensively studied neurotrophic factor so far. LaVail and collaborators first reported that intraocular injection of CNTF prevented photoreceptor death from light-induced damage in rats (LaVail et al., 1992). Injections of adenovirus or AAV coding for CNTF

in degenerated mouse retinas reduced photoreceptor loss, conserving ONL thickness and OS length (Cayouette et al., 1998; Cayouette and Gravel, 1997; Liang et al., 2001; Schlichtenbrede et al., 2003). An alternative delivery method tested was the intravitreal implantation of encapsulated RPE cells engineered to secrete this factor (Tao et al., 2002). However, controversially, despite the rescue from cell death, continuous exposure to CNTF changed photoreceptor cell profiles altering the expression of a large number of genes, caused disorganization of bipolar and Müller cells, and reduced visual function compared to controls, as confirmed by ERG recordings (Rhee et al., 2007; Schlichtenbrede et al., 2003). This evoked scepticism on the utility of CNTF as a trophic factor for the retina.

GDNF has been shown to delay photoreceptor OS collapse *in vitro* (Carwile et al., 1998) and to induce histological and functional protection of photoreceptors in RP models (Frasson et al., 1999), seemingly without significant side effects. John G. Flannery's group drove GDNF expression via AAV transduction into photoreceptors and RPE cells using a subretinal injection (McGee Sanftner et al., 2001), and later overexpressed this factor in retinal glial cells where it is normally produced, using the preferred intravitreal delivery route (Dalkara et al., 2011). This led to sustained functional rescue for over 5 months (Dalkara et al., 2011). Slow release formulations of GDNF, for example the use of biodegradable intravitreal implants were also tested as an alternative (Garcia-Caballero et al., 2018).

Although initial studies administering BDNF using intravitreal injections in models of IRD showed little survival-promoting activity for photoreceptors (LaVail et al., 1992), continuous expression was reported to significantly delay photoreceptor cell death and help maintain visual function assessed by ERG recordings (Okoye et al., 2003). Adenovirus-mediated gene delivery to Müller cells successfully protected photoreceptor from light-induced damage (Gauthier et al., 2005). Subretinal transplantation of iris pigment epithelial cells transduced with the AAV-mediated *BDNF* gene also showed a protective effect (Hojo et al., 2004).

In most forms of RP, rods are damaged first, followed by cone degeneration due to increased exposure to light and oxygen and the loss of endogenous trophic factors promoting their survival (Leveillard and Sahel, 2010). Mohand-Said and collaborators showed that transplantation of rods could limit and delay cone cell loss (Mohand-Said et al., 1998; Mohand-Said et al., 1997). A protein with cone rescue effect was identified several years later and named RdCVF (Leveillard et al., 2004). Subretinal injections of RdCVF protein

were found to protect cones against secondary degeneration in rodent models of RP (Yang et al., 2009). Later, RdCVF was also successfully delivered via AAV vectors (Byrne et al., 2015).

Regardless of the underlying mutation, the final common pathway prior to irreversible visual loss is photoreceptor death involving the apoptosis pathway. XIAP has been shown to block cellular apoptosis and to protect photoreceptors. Subretinal injections of AAV coding for XIAP resulted in overexpression of this neuroprotective factor in photoreceptors, which coincided with preserved ONL morphology in a rat outer retinal dystrophy model (Leonard et al., 2007).

### **3.5 Optogenetics**

Optogenetics is a mutation-independent approach that aims to introduce a gene for light-sensitive protein into the plasma membrane of cells that are not sensitive to light by nature, or have lost their sensitivity. The expressed protein acts as a light-gated ion channel or light-driven pump, thereby producing membrane current in the cell (microbial opsins), or as a light-sensitive GPCR (vertebrate opsins). This technique has been widely studied in vision restoration, targeting retinal cell types from RGCs to photoreceptors.

As this is one of the techniques applied directly in our study, it is discussed in more detail in Chapter 4.

### **3.6 Optopharmacology**

Photoswitches are light-sensitive molecules that confer light sensitivity onto certain endogenous ion channels without requiring genetic manipulation. These molecules have two components: a ligand that is a channel blocker or a receptor agonist or antagonist, and a photoisomerisable group allowing conformation change upon illumination. The light induced isomerisation alters the ability of the ligand interact with ion channels, or to activate or inactivate receptors.

An early example of a photoswitch used in vision restoration is AAQ. It is a photoswitchable  $K^+$  channel blocker. Upon photoisomerization, driven by 380 nm light,  $K^+$  channels are unblocked and outward currents silence the cell. Polosukhina et al. injected AAQ into rd1 mice and generated light-driven activity in RGCs (Polosukhina et al., 2012). The photosensitivity of this molecule is very poor and its half-life is only several hours, which means that unacceptably frequent intravitreal injections of the molecule would be required for therapeutic use. The development of a second generation of photoswitchable molecules DENAQ (Tochitsky et al., 2014), and later BENAQ (Tochitsky et al., 2017) followed. BENAQ is much more potent, non-toxic, and persists longer to restore visual responses in the retina for nearly 1 month after injection. Still, regular intravitreal injections would be needed, or a development of a controlled-release implant for human use. On the other hand, the temporal nature of chemical photoswitches might also present an advantage in the early phases of clinical trials. Because this strategy does not involve genetic modification of patient's cells (unlike optogenetics, for example), the treatment could be easily interrupted in case unwanted effects occurred.

### **3.7 Cell transplantation based treatments**

Stem cell treatments can aim either to replace lost neurons, restoring neural circuits, or to protect compromised endogenous retinal cells through expressing neurotrophic factors (NTFs). The paracrine-mediated effects are mostly mediated by non-retinal-derived adult stem cells, such as neural stem cells and mesenchymal stem cells derived from bone marrow, adipose tissues and dental pulp. They provide neuroprotection and axon regeneration directly through secretion of NTFs, or possibly indirectly by activating endogenous cells to provide additional paracrine support. The support from these stem cells can induce the growth of new connections (Mead et al., 2015).

Retinal stem cells, retinal progenitors, neural stem cells and pluripotent stem cells can act as cell sources for cell replacement therapy. Cell replacement using donor-derived and stem cell-derived RPE and photoreceptors will be extensively discussed in Chapter 5.

### 3.8 Induced retinal regeneration

A drug-based therapy aiming to mobilise endogenous retinal progenitor cells for retinal repair could present an approach with several advantages over cell replacement strategy. This type of treatment would be less invasive, with fewer concerns about immune rejection, tumour formation and ethics issues compared to cell replacement. Possible sources of RPCs are Müller cells, ciliary epithelia-derived cells, RPE and bone marrow derived cells.

The ciliary marginal zone in lower vertebrates, such as teleost and amphibians, is a life-long source of RPCs capable of producing new neurons. In rodents and humans, a population of multipotent RPCs has been isolated from ciliary epithelium that was able to generate several retinal cells types *in vitro*. This ability stays very limited *in vivo*, although some mitogens and transcription factor seemed to have a positive effect on the neurogenic potential (Yu et al., 2014).

In salamanders, RPE cells are able to transdifferentiate into neurons to regenerate the entire retina. The capacity to transdifferentiate is still present in rodents, but only in the earliest developmental stage. A very low level of the capacity to re-enter the cell cycle is preserved in adult rats *in vivo* in peripheral RPE, but mammalian RPE seems to lack the regulatory elements required for induction of transdifferentiation (Yu et al., 2014).

Bone marrow cells can migrate to the subretinal space in damaged retina in mice, but there has been no evidence of transdifferentiation into cells with the characteristics of retinal neurons.

To date, Müller cells present the most promising cell type with RPC properties. In teleost fish such as zebrafish and goldfish, as well as in some other non-mammalian vertebrates, Müller cells can return to stem-cell-like state upon retinal damage, differentiate into various cell types and integrate into the retina. After injury, Müller cells first exhibit reactive gliosis, and after undergo changes in gene expression that enable them to regain their stemness.

In mammals, Müller cells do undergo reactive gliosis following injury, which includes changes in morphology, up-regulation of various markers, etc., but neurogenesis has long been believed to be absent. However, in 2004, Ooto et al. demonstrated that Müller cells in adult rat retina are able to produce new bipolar and rod cells after N-methyl-D-aspartate

(NMDA)-induced neurotoxic damage that caused the loss of RGC and decreased the thickness of IPL. They were able to increase the number of newly formed bipolar cells by intravitreal injections of retinoic acid, as well as to promote the regeneration of other retinal cell types by misexpression of basic helix-loop-helix and homeobox genes in retinal explants of NMDA-treated rats (amacrine, horizontal, rod cells) (Ooto et al., 2004). Karl et al. observed dedifferentiation of Müller glial cells into amacrine cells *in vivo* in NMDA-treated mouse retinas that were depleted of RGCs and amacrine cells, upon stimulation with specific growth factors (Karl et al., 2008). A portion of Müller cells transdifferentiated into rhodopsin-expressing cells following N -methyl- N -nitrosourea (MNU) administration that damaged specifically photoreceptors (Wan et al., 2008). In culture, rodent and human Müller cells can generate glia and neurons. When transplanted into GCL or photoreceptor depleted retinas, Müller cell-derived neurons migrated and integrated into the appropriate layer, and led to improvements in rod or RGC function, respectively (Jayaram et al., 2014; Singhal et al., 2012).

Proneural transcription factor achaete-scute homolog 1 (*Ascl1*) is necessary for retinal regeneration in fish, but it is not expressed in mice. Transgenic expression of *Ascl1* in mouse Müller glia *in vivo* after retinal injury by neurotoxin or excessive light caused some cells to migrate from their normal layer and re-enter the mitotic cell cycle. In young mice, the effect of *Ascl1* expression was even more prominent, giving rise to amacrine, BC and photoreceptors (Ueki et al., 2015).

Various factors that could be used to regain the regenerative potential of Müller glia are being investigated, such as glutamate, FGF, EGF, and insulin, as well as stimulation of key signalling factors such as Wnt, Notch and Hedgehog. Reduced proliferative capability in mammalian Müller cells might also be the result of limited pro-mitogenic factors or inhibitory mechanisms, epigenetic regulation, or the more advanced immune system (Hamon et al., 2016).

In 2018, Yao and colleagues were able to reprogram Müller cells *in vivo* to generate new rod photoreceptors in mature mouse retina using a two-step protocol. They first stimulated Müller glia proliferation by intravitreal injection of AAV carrying a gene for  $\beta$ -catenin under control of the glial fibrillary acidic protein (GFAP) promoter. This was followed by a second injection to transfer three transcription factors – *Otx2*, *Crx* and *Nrl* – which reprogrammed

the cell-cycle activated Müller cells into rods. The Müller glia-derived rods expressed rod specific markers and correctly formed OSs, connecting cilium and the classic triad synapse. They successfully applied this method to restore vision in a mouse model of congenital stationary night blindness. Calcium currents were recorded from the newly formed rods, as well as responses at the GCL and visually evoked potentials from the primary visual cortices (Yao et al., 2018).

Nevertheless, currently, the number of Müller cells that can be activated to re-enter the cell cycle remains low, making this the primary limiting factor that needs to be overcome in order for this treatment to be relevant (Yu et al., 2014).

### **3.9 Visual prostheses**

A visual prosthesis is a device intended to restore functional vision in those suffering total blindness by electrically stimulating the retina or other parts of the visual pathway such as the optic nerve, LGN, and primary visual cortex.

The conversion of the visual image into electrical stimulation can be done using two different mechanisms. The “classical visual prosthesis” comprises of three main parts. A camera that is usually mounted on special goggles captures the visual scene, a video-processing unit, often worn on patient’s belt, translates this information into points of electrical stimulation, and the multi-electrode array implanted in or close to the eye activates the retina. The communication between the three units must be ensured by either a wireless system or a wired link. “Optical sensor prostheses” on the other hand use photodiodes implanted in the eye that do all of the three tasks themselves: catch visible light, convert it into electric current, and directly stimulate the retina (Brandli et al., 2016). The photodiode array-based system is more compact and takes into account natural eye movements, but may be hindered by opacities in the eye and has limited prospects for image processing. On the other hand, extraocular camera-based devices can generate larger electrical impulses, allow the use of light-processing algorithms to highlight features such as contrast and edges, object magnification, etc., but camera’s field of view does not follow the movement of the eye (Weiland et al., 2016).

The electrode or photodiode array can be placed at various sites along the visual pathway. Within the retina, the possible placements of the prosthesis are epiretinal, subretinal, and suprachoroidal. Epiretinal prostheses are placed on the GCL surface within the vitreous space, and stimulate directly the output neurons of the retina. Because of close proximity to the RGCs, this type of device theoretically allows higher resolution and acuity compared to devices positioned in other locations of the retina. Subretinal devices are located between bipolar cells and the RPE – where the photoreceptors usually reside. This allows for the neural processing that occurs within the outer and middle layers of the retina. Suprachoroidal prosthetic devices are located between the choroid and the sclera or contained within the sclera. Because the distance between the electrode array and the retinal tissue in this case is greater, this approach is expected to have limited potential for high-acuity restoration. However, the surgical procedure required is much simpler than in the former two cases (Shepherd et al., 2013). There are several retinal prostheses under development: Argus II, EPIRET3, IMI Retinal Implant, Alpha IMS, Boston Retinal Implant, PRIMA Vision Restoration System, BVA Implant, STS System, etc. (Weiland et al., 2016).

The main disadvantage of retinal locations is that the patients need an intact inner retina in order to be able to use this type of device. In glaucoma, diabetic retinopathy, or trauma, inner retina cells are often damaged. In this case, locations downstream the retina can be targeted, for example the optic nerve, LGN, and primary visual cortex.

Retinal prostheses have demonstrated improved visual acuity and improved performance in daily living activities in patients, such as navigating their surroundings, identifying objects and reading very large letters. Despite this success, the best restored visual acuity is still considered legally blind. Main areas to be improved in the future are density of electrodes, size of arrays, and adjustments of video capture properties. So far, the highest number of electrodes on an implant was 1500, which only brought a 20/546 visual acuity. They estimate that 1.44 million electrodes within a 7-mm square area of the retina would be required in order to achieve a 20/20 vision (Shepherd et al., 2013). Increased size of arrays would mean vision restoration across larger visual angle. In normal vision, this angle is about 160°, whereas it is only about 20° in currently available prosthetic devices. Feature detection algorithms are being developed and improved continuously to optimize pattern stimulation on the retina. Another big challenge is associating eye movements with the field

of view of the extraocular camera. This could be achieved by inserting an additional device in the periphery of the eye to track eye movements and synchronise them with the camera (Weiland et al., 2016). Certain plasticity in the central visual pathway is required in order to improve patient's performance, which means that the ongoing training post-operation will present an important factor in clinical success.

## 4 OPTOGENETICS

The expression of light-sensitive opsins in the plasma membrane of light-insensitive cells is a promising mutation-independent approach to restore vision in retinal degenerative diseases.

Opsins are a family of retinal-binding, seven-transmembrane, light-sensitive proteins, and are divided in two distinct families – microbial opsins (type I) and animal opsins (type II).

### 4.1 Microbial opsins

Microbial opsins are directly photoactivatable ion channels or pumps, which means that the conformational change caused by the light absorption is directly coupled to ion movement through the membrane. No complex cell machinery is required, as is the case for G-protein coupled vertebrate opsins. Another big advantage is that they are able to recycle their visual pigment autonomously, with both isomers remaining covalently attached to the protein. Animal opsins rely on RPE and Müller cells to recycle their visual pigment. Microbial opsins have very fast kinetics, often even faster than the intrinsic retinal responses – ~50-200 ms, and follow high frequency modulation of light (~20 Hz). The negative side to their simplicity is the absence of the phototransduction cascade that would provide amplification of the light signal. Their sensitivity is very low and they require light intensities of very bright outdoor light in order to be activated - from  $10^{14}$  to  $10^{16}$  photons  $\text{cm}^{-2} \text{s}^{-1}$  (Busskamp et al., 2010; Mace et al., 2015; Sengupta et al., 2016). Therefore, the optogenetic treatment with microbial opsins would need to be combined with a device that could offer intensity enhancement of the visual scene. The special goggles would capture the scene in real time with a camera, amplify the signal and translate it to a wavelength to which the photosensors respond. This image would then be projected to the eye (Cepko, 2010).

The most commonly used microbial optogenetic proteins are members of the channelrhodopsin (ChR) and halorhodopsin (HR) family. HR was first identified by Sugiyama and Mukohata in 1984 (Sugiyama and Mukohata, 1984). It is a light-driven inward chloride pump that causes hyperpolarization upon yellow light (~580 nm) stimulation. The HR that

was first used for optogenetic applications in neurons was the one isolated from an archaea species *Natronomonas pharaonis* (NpHR) (Zhang et al., 2007). ChRs are light-activatable cation channels from green algae, most sensitive to blue light (~470 nm), that cause depolarization of the cell when activated. ChR1 and ChR2 were both isolated from *Chlamydomonas reinhardtii* (Nagel et al., 2002; Nagel et al., 2003). The mechanisms of action of ChR and NpHR are illustrated in **Figure 4.1**.

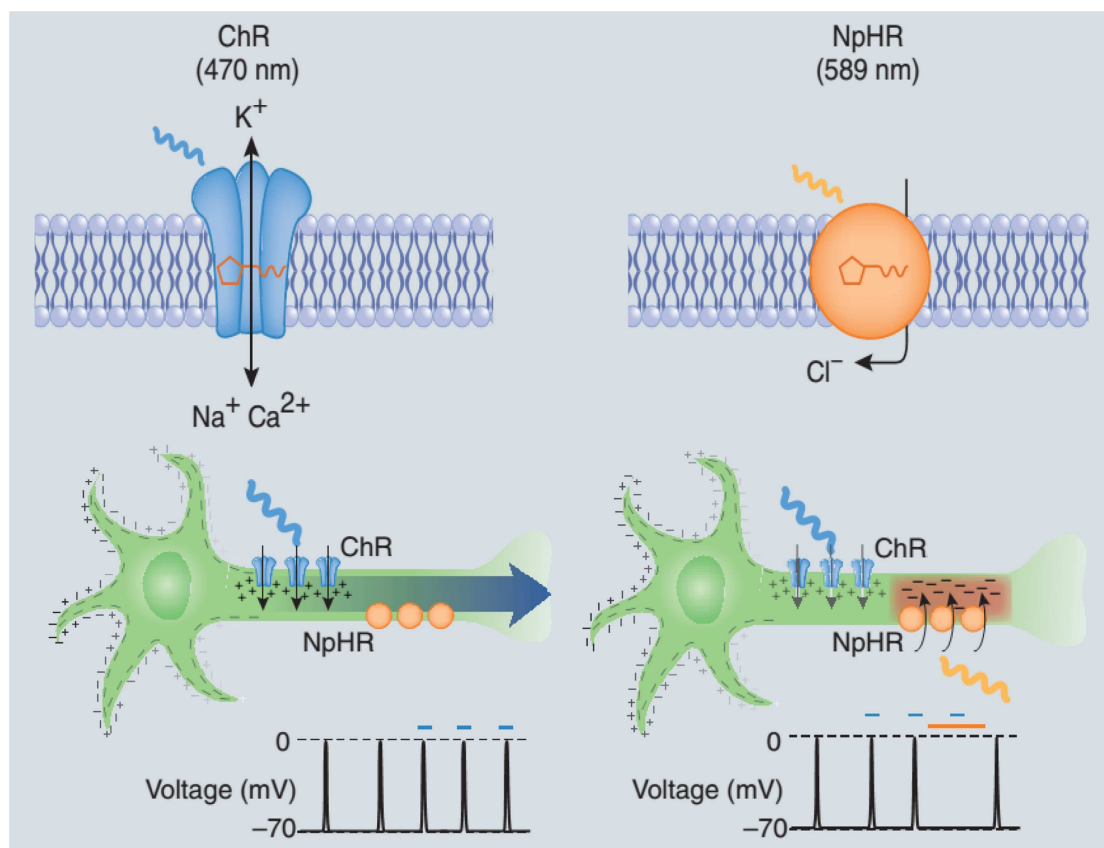


**Figure 4.1. Mechanisms of action of ChR, an activating microbial opsin, and NpHR, an inhibitory microbial opsin.**

ChR is a nonselective cation channel that depolarizes the cell upon blue light stimulation, leading to the spike formation and activation on this cell. NpHR, a chloride pump, hyperpolarizes a cell and inhibits spikes in response to yellow/orange light. Adapted from Pastrana, 2010 (Pastrana, 2010).

Since the discovery of these first optogenetic tools, the microbial opsin toolbox has been rapidly expanding through molecular engineering of the existing molecules and discovery of new variants in nature. The traits that are being sought for are faster kinetics (ChR2 (*E123A*), ChIEF, Chronos, ReaChR), increased light sensitivity (H234R, ChRGR, CatCh), altered spectral

sensitivity (VChR1, ReaChR, Chrimson; Arch, Jaws), improved trafficking to the cell membrane (ReaChR; eNpHR 1.0-3.0, Jaws), improved photocurrents (Jaws), etc. (Pan et al., 2015). In microbial opsins, increased light sensitivity generally correlates with decreased temporal kinetics, so a good balance between the two is desired in the newly discovered variants. The wavelength required for stimulation is of great importance safety wise. Red part of the spectrum is considered much safer than the blue, which is more likely to induce photochemical damage in the eye. As a result, when using light of longer wavelengths, one is allowed to apply a much higher light intensity without surpassing the safety threshold (European Parliament and Council of the European Union, 2006; International Commission on Non-ionizing Radiation Protection, 2013). For this reason, much effort is made towards developing safer, red-shifter variants of opsins (Duebel et al., 2015). View **Figure 4.2.** for detailed characteristics of some of these microbial proteins.

The two microbial opsins that we used in our study are eNpHR (eNpHR2.0) and Jaws. They are both hyperpolarizing chloride pumps, therefore appropriate for targeting photoreceptors, which under physiological conditions hyperpolarize in response to light. eNpHR was developed after the first generation of NpHR was found to form aggregates that led to cellular toxicity when expressed at high levels. Gradinaru et al. (2008) significantly improved the membrane targeting and endoplasmatic reticulum export of the protein by grafting signal peptides from mammalian membrane receptors onto NpHR (Gradinaru et al., 2008). Jaws is also a hyperpolarizing chloride pump, a red-shifted cruxhalorhodopsin, derived from *Haloarcula (Halobacterium) salinarum* and engineered to result in red light-induced photocurrents three times those of earlier silencers (Chuong et al., 2014). In addition to better response amplitudes, Jaws also shows better expression level and improved membrane trafficking in human tissue (Garita-Hernandez et al., 2018), which is why we transitioned to this microbial opsin for the work done on human induced pluripotent stem cell (hiPSC)-cones.

## 4.2 Vertebrate opsins

The two big advantages of animal (vertebrate) opsins are their increased light sensitivity that is enabled by the amplification of the light responses through G-protein coupled cascades, and their physiological compatibility that reduces the risk of immune reaction. However, they are usually associated with slow response kinetics, and need their photopigment renewed after each photoisomerization.

The first vertebrate opsin used in vision restoration was **melanopsin**, the light sensor of ipRGCs. Melanopsin is much more sensitive than microbial opsins (activatable by indoor light), but its kinetics are very slow, with hundreds of milliseconds to several seconds to activate and even longer to turn off (De Silva et al., 2017; Lin et al., 2008). While this might be enough for some basic light perception, it is not appropriate to mediate movie-rate vision (Lin et al., 2008).

Another attractive option is **rhodopsin**, the exceedingly light-sensitive GPCR found in rod photoreceptors. Its sensitivity when expressed in non-photoreceptor cells is similar to that of melanopsin, but it has a 10 times faster response rate (Cehajic-Kapetanovic et al., 2015; Gaub et al., 2015). However, these times are still considerably slow compared to rod photoreceptors, presumably due to the lack of other phototransduction cascade proteins in the targeted cells. Nevertheless, rhodopsin-treated mice were able to perform visually guided tasks (Gaub et al., 2015) and detect visual stimuli presented using LCD visual display in a dimly lit room, such as flicker of frequencies up to 10 Hz and elements of natural movie (Cehajic-Kapetanovic et al., 2015).

Berry and colleagues (2019) expressed vertebrate medium wavelength cone opsin in RGCs of blind mice and observed light sensitivity comparable to that of rhodopsin, but with 10-fold faster kinetics. In addition, the cone opsin-expressing RGCs adapted to light covering 2-3 orders of magnitude, from dim room light to outdoor light. Treated rd1 mice had restored patterned vision and visually guided exploration of novel objects under normal incidental room light (Berry et al., 2019).

Several groups have focused on engineered optically controlled channels or GPCRs (Broichhagen et al., 2015; Caporale et al., 2011; Gaub et al., 2014; van Wyk et al., 2015) that have been constructed or modified to become light-sensitive.

LiGluR is a genetically engineered ion channel ionotropic glutamate receptor 6 (iGluR6) with a mutation that allows for the covalent binding of a photoswitch. When expressed in the retina, it restored responses in the primary visual cortex, light-avoidance and visually guided behaviour (Caporale et al., 2011; Gaub et al., 2014). SNAG-mGluR2 is a modified mGluR2 receptor that uses a similar principle - allows covalent attachment of a synthetic photoswitch (Broichhagen et al., 2015). Although they both have very fast kinetics, the light intensities required for activation are comparable to those for ChR. Berry et al. (2017) used a combination of these two tools – an excitatory LiGluR ion channel and an inhibitory SNAG-mGluR2 GPCR to generate diverse light responses and further improve visual behaviour of treated mice (Berry et al., 2017).

Opto-mGluR6 is the optogenetic construct with the highest light sensitivity tested so far, eliciting a response at  $5 \times 10^{11}$  photons  $\text{cm}^{-2} \text{s}^{-1}$  at 473 nm. The generated light responses were observed to have similar kinetics to photoreceptor evoked light responses (van Wyk et al., 2015). Opto-mGluR6 is engineered by combining the transmembrane domains from melanopsin with the intracellular loops from mGluR6.

Refer to **Figure 4.2.** to view information on the excitation spectrum, sensitivity and kinetics of some of the proteins mentioned.

Taken together, the optogenetic protein toolbox is expanding rapidly, providing more and more candidates with favourable characteristics such as high light sensitivity, fast rise and decay times, and luminance adaptation. With these new tools, we can envisage visual function restoration in normal light conditions in not so far future.

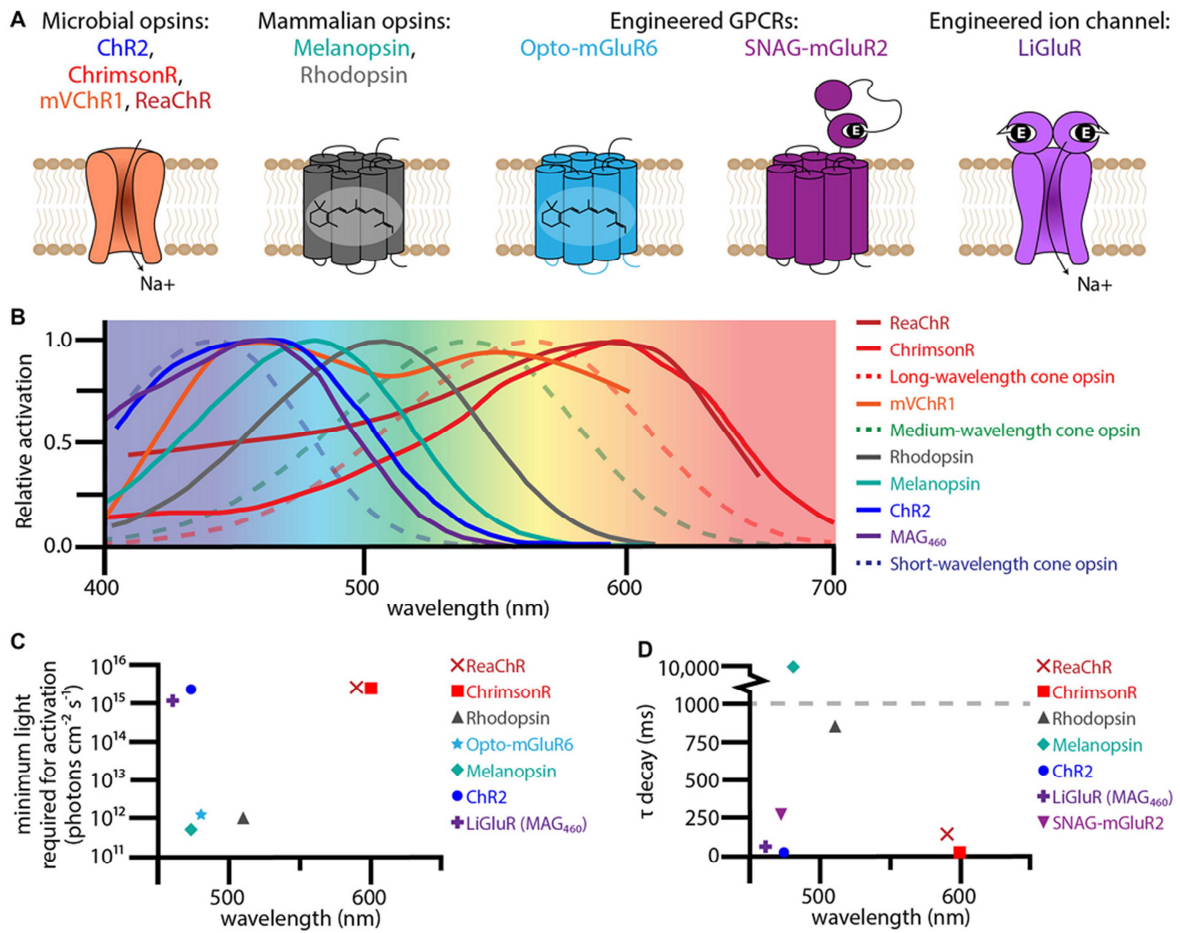


**Figure 4.2. A comparison of different optogenetic proteins used to restore visual responses in degenerated retinas.**

(A) Structural diagrams of optogenetic microbial opsins, mammalian opsins, and engineered GPCRs and ion channels. (B) Excitation spectra of various optogenetic sensors (solid lines) and human cone photoreceptors (dotted lines). (C) The minimum light intensity required for excitation, and (D) decay constant plotted against wavelength for different optogenetic effectors. From Baker and Flannery, 2018 (Baker and Flannery, 2018).

### 4.3 Choice of strategy – which retinal cells to target

The choice of optogenetic strategy to be applied depends on the degenerative state of the retina at the time of treatment. The first study reporting the reactivation of degenerated retina using a microbial opsin (ChR2) featured an intravitreal injection of AAV vectors with a ubiquitous promoter, that mostly drove ChR2 expression to the RGCs (Bi et al., 2006). This was followed by other studies using viral vectors with more favourable properties, improved optogenetic constructs, a combination of several optogenetic proteins, or using a different

animal model (Berry et al., 2017; Caporale et al., 2011; Ivanova et al., 2010; Sengupta et al., 2016; Zhang et al., 2009). A big disadvantage of this approach however, is that it bypasses all information processing normally conducted by the retinal circuitry, the OPL as well as IPL. As a result, only ON responses were successfully recovered using this strategy. Concerns have been raised that the retina might be missing the type of image pre-processing needed to achieve optimal vision with this approach. However, results gained from clinical studies for epiretinal implants give hope that the human brain might nevertheless possess the capability to adapt to an altered visual code (Shepherd et al., 2013). Today, optogenetic targeting of RGCs is entering the first phases of clinical trials. It would be a good option especially for patients with late stage degeneration and advanced remodelling of inner retinal circuits.

Bipolar cells may stay relatively well conserved in late degeneration. Conferring light sensitivity to bipolar cells would allow to keep image processing that occurs on the IPL level and elicit RGC responses that are closer to the natural activity patterns. Lagali et al. drove the expression Chr2 into ON bipolar cells of blind rd1 mice, regaining visually evoked potentials in the cortex and visually guided behaviour (Lagali et al., 2008). Several studies using a similar approach were able to generate ON and OFF responses in the RGCs despite only targeting the ON bipolar cells (Cronin et al., 2014; Mace et al., 2015; van Wyk et al., 2015), likely through indirect activation of the OFF pathway through rod bipolar cells and All amacrine cells.

Some patients were found to still have remaining cone bodies in advanced stages of retinal degeneration, even though these cones have long lost their OSs and with them light sensitivity. Busskamp et al. reactivated these dormant cones by expressing NpHR on their surface. The result was the restoration of all visual functions at the GCL, including all three types of classical responses (ON, OFF, ON-OFF), centre-surround opposition and direction selectivity, as well as mediated cortical processing and visually guided behaviour (Busskamp et al., 2010). These sophisticated retinal circuit functions were impossible to recover when conferring light to bipolar cells or RGCs.

## 4.4 Delivery of the optogene to the cells

Introduction of optogenes into target cells is usually achieved by using viral vectors, preferably AAV, due to their nonpathogenic and nonimmunogenic properties, the efficient transduction rate, broad cell and tissue tropism, and the fact that they have already been used in several clinical trials. Successful transgene delivery is vital for the favourable outcome of optogenetic procedures. Natural variants successfully target RGCs through intravitreal injection, and photoreceptor and RPE cells through subretinal injection. However, bipolar cells are more difficult to target, especially due to the physical barriers that hinder penetration of the viral particles. Through *in vivo* directed evolution, novel variants with improved diffusional properties are being engineered. These are able to target bipolar cells and even photoreceptors after administering the virus intravitreally (Dalkara et al., 2013; Mace et al., 2015). Intravitreal injection is the preferred injection route, because subretinal injections are associated with possible damage due to the retinal detachment that follows the procedure, and because they enable panretinal expression. Challenges still remain in restricting expression to specific subtypes of retinal cells, mainly because there are no specific promoters available for some of the cell types (for example, promoters to exclusively target only the ON or the OFF RGCs).

Preclinical studies on larger animals like dogs and nonhuman primates have shown substantially different transduction patterns compared to those observed in rodents. For example, only a ring of RGCs around the fovea can be targeted with AAV vectors in primate species. More efforts need to be put into testing promoter and viral capsids in models that more closely relate to humans (Planul and Dalkara, 2017). The challenge in optogenetics will be to express a functional amount of the opsin without eliciting immune responses to the AAV vector or the optogenetic sensor itself. First clinical trials investigating the safety of the procedure have been recently launched (RetroSense Therapeutics, GenSight Biologics).

## 5 CELL REPLACEMENT

Patients with retinal degeneration most typically lose RPE cells, photoreceptors, or both. Consequently, these two retinal cell types are most commonly considered in cell replacement therapies. RPE cells aim to replace dysfunctional or degenerated RPE and prevent further photoreceptor cell loss, whereas photoreceptors aim to repair the degenerating neural retina.

### 5.1 RPE transplantation

In AMD, photoreceptor cell death and the resulting vision loss are preceded by degenerative changes in the RPE and the underlying choroid. This creates a window of opportunity for RPE transplantation at the earlier stages of disease with the aim of delaying photoreceptor degeneration. The pioneering study of RPE cell therapy was performed by Peter Gouras in the early 1980s who transplanted human RPE cells in a monkey (Gouras et al., 1984). The reports demonstrating that the addition of RPE can delay photoreceptor degeneration in RCS rat followed soon after (Lopez et al., 1989). These and other studies resulted in several human trials in the 1990s that examined the effects of allogeneic transplantations of RPE cells, but failed to prove any lasting effects, which was partially attributed to rejection of the graft (Algvere et al., 1999; Weisz et al., 1999). This was followed by a development of two approaches for autologous RPE transplantation – macular translocation and RPE-choroid patch graft transplantation. In the former case, the retina is detached and repositioned so that the macula land over a different region with healthy RPE (Machemer and Steinhorst, 1993). In the alternative approach, patches of RPE with the underlying choroid are harvested from peripheral areas of the patient’s retina and placed under the macula (Stanga et al., 2002). Both these techniques showed to maintain visual acuity for at least up to 3-5 years, but were technically very challenging and could cause serious complications during surgery (Bobba et al., 2018).

More recently, significant research efforts have focused on efficiently deriving RPE cells from PSCs. The initial methods took advantage of PSCs’ capacity to spontaneously

differentiate to RPE, either using continuous adherent culture methods or embryoid body method, but the efficiency was quite low. Many protocols implemented the knowledge of developmental biology of the eye, using growth factors and small molecules to drive the differentiation towards the RPE fate. The newest approaches aim to generate RPE simultaneously with the neural retina from 3D retinal organoids (Reichman et al., 2014; Zhong et al., 2014).

Two main strategies have been used to deliver RPE cells to the recipient's eye; cell suspensions and polarized cell sheets. Injecting dissociated RPE cells proved less effective, because these cells failed to correctly polarize or survive at long term. The majority of later attempts focused on implanting a polarized monolayer of RPE on different types of scaffolds such as polyester, parylene, poly-lactic-co-glycolic acid (PLGA) (Liu et al., 2014) and human amniotic membrane (Ben M'Barek et al., 2017), or sheets of RPE cells without any matrix or scaffold (Kamao et al., 2014).

A number of animal studies using ESC and iPSC-derived RPE cells demonstrated that the grafted cells reduced degeneration of photoreceptors and improve vision (Li et al., 2012; Pan et al., 2013). Clinical trials using ESC-derived RPE showed that the transplants were safely tolerated, but reported of serious side effects of immunosuppressing treatment that was required (Schwartz et al., 2015). The use of autologous iPSC-generated RPE would prevent rejection of the graft and would surpass the need for immunosuppression. A woman from Japan was the first person to have her own skin cells reprogrammed and subsequently guided to produce an autologous hiPSC-derived RPE cell sheet, that was then transplanted into the patient (Cyranoski, 2013; Mandai et al., 2017b). One year after the surgery, visual acuity of the patient remained unchanged without any adverse events. The second patient was transplanted with allogenic hiPSC-derived RPE, but since, the trial was put on hold after two small genetic mutations were identified in the hiPSC and hiPSC-derived tissue from the second patient.

## 5.2 Photoreceptor cell suspension transplantation

### 5.2.1 Donor-derived dissociated photoreceptor precursors

Transplanting dissociated cells in the retina started to be explored in the late 1980s (Gouras et al., 1991). The advantages for this strategy are transplantation of an accurate number of cells, better contact between donor cells and the host retina, and minimal surgical invasion (Gasparini et al., 2018).

Several early studies examined the potential of neural stem or progenitor donor cells derived from brain or retina, but these cells failed to migrate and integrate correctly in the retina, develop into mature photoreceptors or form synapses (Sakaguchi et al., 2004; Young et al., 2000).

In the following years, most of the studies have moved towards using dissociated photoreceptor precursors – a population of young post-mitotic photoreceptors that are isolated from young animals. In 2006, MacLaren et al. demonstrated that transplantation of post-mitotic Nrl-expressing rod precursors isolated from donors at postnatal days 4-7 (P4-7) are the optimal source for rod photoreceptor replacement (MacLaren et al., 2006). Indeed, P1-7 is the peak of rod generation in mice. Many others studies later confirmed the importance of the developmental stage of donor cells at the time of transplantation (Bartsch et al., 2008; Lakowski et al., 2010; Lakowski et al., 2011). Gust and Reh reported that adult photoreceptors are still capable of integration, but show significantly reduced integration potential (Gust and Reh, 2011). Subretinal transplantation of optimally staged post-mitotic photoreceptor precursors labelled with green fluorescent protein (GFP) reporter into various murine models of retinal degeneration resulted in the presence of GFP<sup>+</sup> cells with rod-like morphology within the ONL of the host retina. These GFP<sup>+</sup> cells demonstrated robust expression of photoreceptor proteins that were genetically absent from the host photoreceptors, and displayed other morphological characteristics of mature photoreceptors such as synaptic terminals and OSs (Barber et al., 2013; Eberle et al., 2012; Pearson et al., 2012; Singh et al., 2013). These cells responded to light in a manner similar to wild type rods, as shown from single cell (Pearson et al., 2012) and whole retinal recordings (Lamba et al., 2009; MacLaren et al., 2006; Santos-Ferreira et al., 2015). For example,

Pearson and colleagues recorded a functional rescue following transplantation of *Nrl-GFP* donor-derived rod precursors into guanine nucleotide-binding protein G(t) subunit alpha-1 knockout (*Gnat1*<sup>-/-</sup>) mice – a model of congenital night blindness. After transplantation, labelled cells were light-sensitive, robust responses to scotopic stimuli in the visual cortex were observed, as well as head-tracking abilities and improved visually-guided task-solving behaviour in scotopic conditions (Pearson et al., 2012).

A significantly smaller amount of work has been implemented in transplanting cone precursors instead of rod precursors. This was largely because it has been very challenging to isolate big enough numbers of cones from donor mice where they represent only a very small portion of all photoreceptors. Santos-Ferreira and colleagues used neural zipper-deficient (*Nrl*<sup>-/-</sup>) mice crossed with GFP reporter line as a source of cone cells for transplantation. *Nrl* mutant mice develop rod-depleted retinas containing only cones and cone-like photoreceptors. The cone-like cells resemble S-cones on the morphological and functional level. After transplanting these cells into *Cpf1* mice, multi-electrode array (MEA) recordings showed responses to photopic stimuli (Santos-Ferreira et al., 2016b). The group led by Valerie Wallace generated another reporter line, where GFP is trapped in the coiled-coiled domain containing 136 (*Ccdc136*) locus. Even though this system labels a heterogeneous population of cells – S-cones and rod bipolar cells, it only expresses in cones until P14, which allows for their selection via fluorescent activated cell sorting (FACS) (Smiley et al., 2016).

#### **5.2.1.1 Delivery method for photoreceptor suspension**

Photoreceptor suspension can be delivered to the subretinal space either by trans-vitreous or trans-scleral injections (**Figure 5.1**). Trans-vitreous injection enters the eye diagonally through the vitreous cavity and pierces the retina to reach subretinal space. The exact location of the injection is more easily determinable with these injections, which can circumvent blood vessel damage by the procedure. However, the piercing of the retina can induce some local retinal gliosis. Trans-scleral injections on the other hand do not damage the retina itself, but can more easily lead to haemorrhages and subsequent infiltration of immune cells into the retina.

Pearson et al. (2012) performed dual subretinal injections (both in the superior and the inferior retina), as well as experimented with performing a scleral puncture to anterior chamber to introduce a deflation and minimise reflux, and pre-detachment of the retina two days prior to cell transplantation. These techniques significantly increased the number and spread of GFP-labelled cells in the host ONL following transplantation, but also led to higher failure rate (Pearson et al., 2012) (see **Figure 5.2.E**).

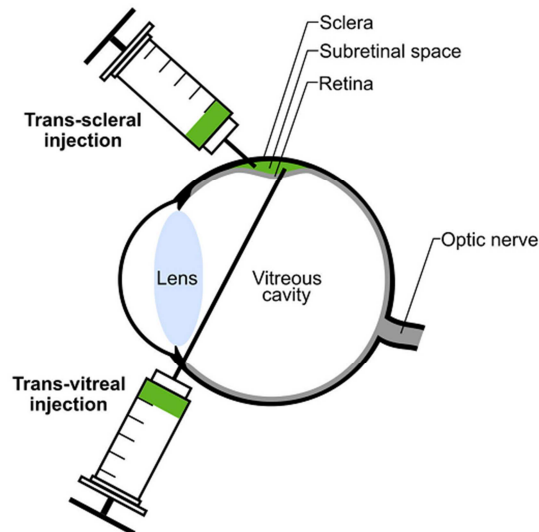


**Figure 5.1. Subretinal transplantation via trans-scleral or trans-vitreous injections.**

From Santos-Ferreira et al., 2017.

Disadvantages of using cell suspensions include high cell death and efflux of transplanted cells during the injection procedure, poor long-term survival and integration rates, and lack of graft structure and orientation (Gasparini et al., 2018).

### **5.2.1.2 Cell enrichment approaches**

A major limitation in photoreceptor transplantation is the low number of integrating cells. In order to achieve better integration, photoreceptor content from the cell suspension generated by dissociating whole donor retinas was enriched by either fluorescent activated cell sorting (FACS) or magnetic activated cell sorting (MACS). By using transgenic mice with rod-specific expression of GFP, donor photoreceptors could be enriched up to 95% by FACS, which significantly increased the numbers of integrated photoreceptors after transplantation (Barber et al., 2013; Lakowski et al., 2011; MacLaren et al., 2006; Pearson et

al., 2012). However, MACS represents a more suitable option for clinical application for several reasons (**Figure 5.2.C**). The establishment of flow cytometers in a good manufacturing practice (GMP) environment is very challenging. FACS also causes considerable stress to the cells due to high pressure and shearing forces, and is a rather slow procedure. MACS uses antibodies conjugated to magnetic beads, which means that millions of cells can be sorted simultaneously based on magnetism. Therefore, it has great scalability potential, and can be more easily adapted to GMP conditions and automated processing. Cluster of differentiation 73 (CD73) has been identified as a rod-specific cell surface marker in mice (Koso et al., 2009) and has been used for successful enrichment of rod precursors up to 90%, that resulted an increased integration rate following transplantation (Eberle et al., 2012; Eberle et al., 2011; Lakowski et al., 2011; Santos-Ferreira et al., 2015) (see **Figure 5.2.A and B**). A combination of four markers (CD73, CD24, CD133 and DC47) selecting exclusively post-mitotic precursors from mouse retinal organoids further improved integration outcomes compared to selection methods using a single marker (Lakowski et al., 2015).

### **5.2.1.3 Manipulation of the host environment**

In 2013, Barber et al. tested numerous mouse models of retinal degeneration and showed the importance of host environment and disease aetiology in the cell transplantation outcome. This was associated to several factors, namely the OLM, reactive gliosis, and the extracellular matrix (ECM) (Barber et al., 2013).

OLM, a series of adherens junctions between photoreceptors and Müller glia, represents a significant barrier for cell migration into the ONL. Mouse models with disrupted OLM showed higher integration rates. Several trials disrupted OLM by siRNAs against components of the OLM - Crumbs homologue 1 (Crb1) and zonula occludens-1 (ZO-1) (Pearson et al., 2010), or the glial toxin alpha-aminoadipic acid (AAAA) (West et al., 2008), increasing the number of integrated donor cells in the host retina (see **Figure 5.2.D**).

Glial cells in degeneration often undergo reactive gliosis and form a glial scar, which presents a physical barrier between host retina and transplanted cells. Mouse models of retinal degeneration with high reactive gliosis are less permissive for cell integration (Barber

et al., 2013) and transplantations into mouse models lacking GFAP and vimentin led to higher level of cell migration into the host retina (Kinouchi et al., 2003).

Components of the ECM such as chondroitin sulphate proteoglycans can pose a barrier for integration and synapse formation. Assays to digest the ECM with matrix metalloprotease 2 (MMP2) or bacterial enzymes such as chondroitinase ABC improved the outcome of transplantations (Barber et al., 2013; Ma et al., 2011; Suzuki et al., 2007; Yao et al., 2011) (see **Figure 5.2.D**).

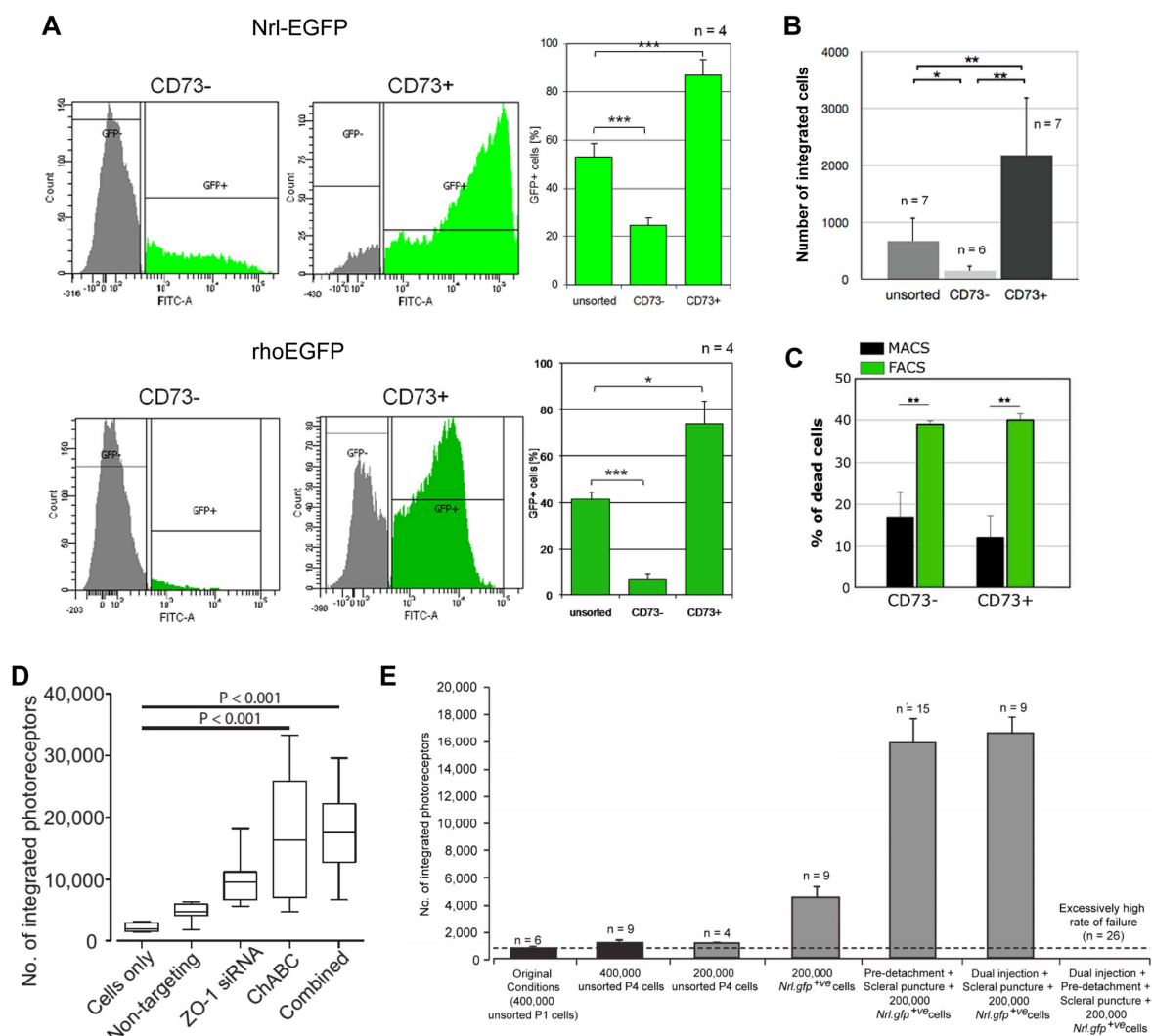


**Figure 5.2. Efforts to improve cell integration rates through CD73 marker enrichment (A-C), manipulation of host environment (D) and optimization of the injecting procedure for subretinal delivery.**

**(A)** Quantification of dissociated retinal tissue from *Nrl-EGFP* (top) and *rhoEGFP* mice (bottom) by flow cytometry directly after the retinal cells have been sorted via CD73-based MACS. Note the increased proportions of EGFP-labelled cells in the CD73<sup>+</sup> fraction. **(B)** Transplantation of CD73<sup>+</sup> led to improved integration rates. **(C)** Cell death during the sorting procedure is significantly lower with MACS (black)

compared to FACS (green). Adapted from Eberle et al., 2011 and Gasparini et al., 2018. **(D)** The impact of OLM disruption (using ZO-1 siRNA) and chondroitin sulphate proteoglycans (ECM component associated with glial scarring) degradation (using chondroitinase ABC), singularly or combined, on transplantation outcome in  $Rho^{-/-}$  mice. From Barber et al., 2013. **(E)** A histogram summarizing the impact of donor age (P1 versus P4), number of injected cells, cell population enrichment (unsorted versus *Nrl.gfp*<sup>+</sup> rod precursors), pre-detachment of the retina 2 days before transplantation, scleral puncture to anterior chamber, dual injections, and combinations of these techniques. The highest numbers of integrated cells were achieved when transplanting rod precursors using a combination of pre-detachment and scleral puncture, or a combination of dual injection and scleral puncture. From Pearson et al., 2012.

### 5.2.2 Dissociated pluripotent stem cell-derived photoreceptors

The ontogenetic equivalent of P4-7 mice in human foetuses is in their early second trimester of development. The use of foetus-derived precursors for the purpose of treatment would not be able to meet the supply needs, and would be ethically questionable. Recent advances in pluripotent stem cell technology are now allowing the use of this potentially unlimited source of transplantable cells.

The classical definition of a stem cell requires two properties: self-renewal – the ability to undergo numerous cycles of cell division while maintaining undifferentiated state, and potency – the capacity to differentiate into specialized cell types. Totipotent stem cells can differentiate into all embryonic and extraembryonic structures and construct a complete organism. These cells are produced after the fusion of an egg and sperm cells, and remain totipotent throughout the first few divisions of the fertilized egg. Pluripotent stem cells (PSCs) can develop into all body tissues, including germ line cells, except for trophoblast cells. Multipotent stem cells can produce various cells types within a closely related family of cells (for example, hematopoietic cells can give rise to new blood cells), whereas oligopotent stem cells can only form a few cell types (for example, lymphoid stem cells). Unipotent cells can only give rise to one cell type, but they keep the self-renewing property. Similarly, progenitor cells have a tendency to differentiate into a specific cell type, but have already been pushed to differentiate into their “target” cells. Progenitors are not stem cells, since they lost their ability to multiply indefinitely by this time. They can be considered as the transitional stage of differentiation between stem cells and fully differentiated cells. Precursor cells already exited the cell cycle – they are immature post-mitotic cells.

PSCs are the preferred cell type for innovative cell treatments, because of their capacity for extensive proliferation, relatively easy maintenance in culture and the potential to be directed into any cell type when given the right cues. Embryonic stem cells (ESCs) are PSCs that can be isolated from the inner cell mass of the mammalian blastocyst. Since their first establishment in 1981 (mouse) (Evans and Kaufman, 1981) and 1998 (human) (Thomson et al., 1998), ESCs were involved in numerous preclinical and clinical trials. However, their use remains the object of ethical, religious and political debates, which results in very strict regulations of research involving human ESCs in most countries.

In 2006, Takahashi and Yamanaka made a breakthrough discovery that led them to win the Nobel Prize in physiology or medicine in 2012. They were able to reprogram mouse somatic cells into a pluripotent state by over-expressing four transcription factors - *Oct4*, *Sox2*, *Klf4*, and *c-Myc* (Takahashi and Yamanaka, 2006) - and to successfully use the same technology to reprogram human fibroblasts (Takahashi et al., 2007). These pluripotent cells were termed induced pluripotent stem cells (iPSCs).

First attempts to differentiate photoreceptors from PSCs used mouse ESCs (mESCs) and a combination of embryoid body formation with subsequent 2D culture system (Ikeda et al., 2005). In 2006, the group of Tom Reh reported of the first production of retinal cells from human ESCs (Lamba et al., 2006). The early protocols only managed to obtain ESC-derived neural progenitors in culture. In order to further differentiate the cells towards photoreceptors, neural progenitors needed to be either transplanted in the subretinal space of adult rats (Banin et al., 2006), or co-cultured with mouse embryonic (Ikeda et al., 2005), postnatal (Zhao et al., 2002) or adult retinal cells (Lamba et al., 2006). Osakada and colleagues were the first to achieve complete generation of photoreceptor precursors from mouse, monkey and human ESCs *in vitro* under defined culture conditions, in the absence of retinal tissue (Osakada et al., 2008). Soon after, several groups confirmed that iPSCs, too, have the competence to differentiate towards photoreceptors (Hirami et al., 2009; Lamba et al., 2010). All these protocols aimed to imitate developmental signalling pathways using ECM or Wnt, Nodal and bone morphogenetic protein (BMP) antagonists, in combination with growth factors, retinoic acid and taurine. Unfortunately, the efficacy of these protocols was very poor, with only about 20% of cells expressing photoreceptor-specific markers.

The group of Yoshiki Sasai reported of the capacity of mouse and human ESCs to self-organize and generate optic cups in 3D culture system, which presented a breakthrough discovery for photoreceptor generation (Eiraku et al., 2011; Nakano et al., 2012). Since then, most of the laboratories that work on photoreceptor replacement adopted 3D retinal organoid technology, improving the initial protocol in many aspects and moving closer to clinical-grade quality of retinal transplants (Barnea-Cramer et al., 2016; Gonzalez-Cordero et al., 2017; Reichman et al., 2014; Wiley et al., 2016; Zhong et al., 2014). Additional research is underway to increase efficiency and reproducibility of differentiation protocols, accelerate and enhance full maturation of photoreceptors, adapt to GMP-compliant conditions, and develop conservation methods.

The first report of PSC-derived retinal cell transplantation was published in 2009 by the group of Thomas Reh (Lamba et al., 2009). They transplanted human ESCs (hESC) into wild type and cone-rod homeobox (*Crx*<sup>-/-</sup>) mice – a mouse model that fails to develop photoreceptor OSs, and observed integration and expression of rod and cone markers, as well as a partial restoration of light response by ERG analysis (Lamba et al., 2009). Mouse (miPSC) and hiPSC-derived photoreceptor transplantations followed soon after (Homma et al., 2013; Lamba et al., 2010; Tucker et al., 2011). Tucker et al. used a step-wise protocol for the generation of photoreceptors from mouse dsRed-iPSC reporter line, developed in their laboratory, and injected these cells into rhodopsin knockout mice (*Rho*<sup>-/-</sup>). After transplantation, labelled cells were present in the host ONL and displayed OS formation, mature photoreceptor markers and accounted for some functional recovery as indicated by improved b-wave in ERG measurements. Up to 6,4% of transplanted cells were reported to be integrated at 3-4 weeks post-transplantation (Tucker et al., 2011). Homma and colleagues generated a mouse iPSC cell line from fibroblasts of *Nrl-GFP* mice to allow them to select rods by FACS before transplanting them into wild type and dystrophic retina. They performed calcium imaging several weeks after the procedure and found the calcium oscillations of grafted cells alike to those of endogenous rods, suggesting similar functionality (Homma et al., 2013). After the introduction of retinal organoid technology for the generation of photoreceptors in 2011 (Eiraku et al., 2011; Nakano et al., 2012), most of the groups transitioned to this system, sequentially publishing studies proving that these cells, too, are capable of integration into the ONL of wild type and degenerated hosts

(Decembrini et al., 2014; Gonzalez-Cordero et al., 2013; Santos-Ferreira et al., 2016b). The team of Robin Ali fluorescently labelled rods using an AAV vector under the control of Rhodopsin promoter that allowed them rod enrichment of the cell suspension via FACS before transplantation. They engrafted the cells into three different mouse models: *Gnat1*<sup>-/-</sup>, *Rho*<sup>-/-</sup> and peripherin 2 mutant mouse (*Prph2*<sup>rd2/rd2</sup>) (Gonzalez-Cordero et al., 2013). Decembrini et al. used a transgenic ESC line expressing GFP under the control of Crx promoter. Engrafted cells showed mature photoreceptor morphology with expressed synaptic and phototransduction markers. However, in both these studies, the percentage of integrated cells was very low, 0,3% and 0,4%, respectively (Decembrini et al., 2014; Gonzalez-Cordero et al., 2013). The group of Marius Ader compared the integration rates following transplantation of AAV-labelled and CD73-enriched rods into wild type, prominin 1 knockout (*Prom1*<sup>-/-</sup>) and *Cpfl1/Rho*<sup>-/-</sup> mice. ESC-derived rods seemed to develop normal rod morphology in the two models with still existing ONL structure, but failed to do so in the model of complete photoreceptor degeneration (Santos-Ferreira et al., 2016b). Similar reports are found in three articles by the group of Robin Ali after using severely degenerated rd1 mice (Barnea-Cramer et al., 2016) or Aryl hydrocarbon receptor-interacting protein-like 1 knockout (*Aipl1*<sup>-/-</sup>) mice (Gonzalez-Cordero et al., 2017; Kruczek et al., 2017) as hosts for their ESC- and iPSC-derived photoreceptors. The transplanted cells survived in the subretinal space, often forming a distinct layer adjacent to the host ONL. They expressed photopigments, some OS and synaptic markers, but lacked morphological features of mature photoreceptor cells. Gagliardi et al. transplanted CD73<sup>+</sup> hiPSC-derived photoreceptors into dystrophic R23H rats and noticed some surviving cells in immunosuppressed rats up to 10 weeks post-transplantation, but they, too, as in previous examples, failed to develop major photoreceptor characteristics (Gagliardi et al., 2018).

### 5.3 Retinal sheet transplantation

Early studies in the 1990s attempted to isolate full-thickness retinal sheets, with or without RPE, from neonatal rats, or from foetal or post-mortem human eyes, and transplant them into wild type rats or models of retinal degeneration (del Cerro et al., 1985; Ehinger et al., 1991; Kaplan et al., 1997; Seiler and Aramant, 1998). Compared to injections of dissociated

cells, retinal sheets were more likely to retain the layered structure of the retina and correct photoreceptor morphology with OSs oriented toward the recipient RPE, and showed increase survival times (Aramant and Seiler, 2002; Seiler and Aramant, 1998). Grafts also formed apparent synapses with host tissue (Seiler et al., 2010). Light-evoked responses were recorded in the superior colliculus of treated S443ter<sup>-/-</sup> line-3 degenerated rats after rat foetal retinal transplant (Seiler et al., 2010; Seiler et al., 2017), with response region and quality of visual responses correlating with transplant organization and placement (Seiler et al., 2017). Human foetal retinal grafts (11-15.7 days of gestation) transplanted into nude S443ter<sup>-/-</sup> line-3 rats survived long-term in an environment of advanced retinal degeneration, matured and developed into different retinal cells (but not RGCs), formed a laminated structure, integrated into the host retina, and improved visual function (Lin et al., 2018). Promising results obtained in preclinical studies led to first clinical trials with 7 out of 10 patients showing visual improvement after being transplanted with human foetal sheets including the RPE (Radtke et al., 2008; Radtke et al., 2002).

More recently, the team of Masayo Takahashi transplanted mESC and miPSC-derived retinal tissue into rd1 mice (Assawachananont et al., 2014; Mandai et al., 2017a). They compared sheets cut out of *in vitro* developed optical vesicles at various days of differentiation (DD) – from DD11 to DD24. DD21 corresponded to the differentiation stage of mice at postnatal day 1. 2-4 weeks after transplantation into the subretinal space they observed three types of outcomes in terms of maturation and structural integrity of the graft: 1) sheets with almost complete ONL and INL, 2) sheets with structured ONL and partial INL, and 3) disorganized structures. Younger grafts (DD11-17) that were still at the neuroblastic stages at the time of transplantation, showed better potency to develop into almost complete retinal layers. 88% and 75% of grafts younger than DD17 formed structured ONL with or without the INL, respectively. The results after transplanting DD18 or older grafts were comparable to what one would expect after injecting dissociated retinal cells – the cells did not form a layered structure but appeared disorganized in 80% of the cases. They also observed different patterns of graft integration into the host retina (refer to **Figure 5.3.A-F**). In the case of laminar interception, graft INL was located between the graft ONL and host INL, interfering with direct contact of grafted photoreceptors to recipient interneurons. The second, preferred pattern was direct contact, where the structured ONL of the graft was

adjacent to recipient INL. Graft ONL formed rosette-like structures in most cases, with the graft INL surrounding the ONL. This means that the grafted photoreceptors were not in contact with the RPE of the host, which could present a problem in long-term survival of these cells. In rare cases, rosettes were disrupted allowing direct contact with the RPE. Direct contact was the most often observed with grafts that formed structured ONL, but not the INL (in 63% of these cases). The third pattern was cell integration of photoreceptors from disorganized grafts that migrated individually into the host retina (Assawachananont et al., 2014).

Several years later, this same group directly visualized synapses between the graft and host tissue by using PSC lines that expressed a reporter protein at photoreceptor synaptic terminals (Nrl-GFP/ ROSA::Nrl-CtBP2-tdTomato) to produce retinal sheets, and a rd1 mouse model with genetically GFP-labelled rod bipolar cells (L7-GFP/rd1) as recipients (**Figure 5.3.G**). Due to rosette formation, they estimated that approximately 50% of the total graft area may have access to host retina to form synapses. They observed host RGC light sensitivity by MEA tests, as well as light-guided behaviour by an adaptation of a shuttle-avoidance system. As mentioned previously, the direct contact of grafted photoreceptors to host RPE is often blocked by the graft INL after rosette formation, so mice were supplemented with 9-*cis* retinol acetate during functional tests (Mandai et al., 2017a).

In 2016, they developed retinal sheet graft technology using human ESC (hESC) and hiPSC lines (Shirai et al., 2016). They transplanted the sheets in nude rats with or without retinal degeneration, as well as in newly established monkey models with focal selective photoreceptor degeneration induced by cobalt chloride injection or 577 nm optically pumped semiconductor laser photocoagulation. Grafted hESC-derived sheets at DD50-150 were transplanted into rats and analysed at DD200-280. The grafts differentiated into a range of retinal cell types, including a structured ONL containing rods and cones with well-aligned photoreceptor OS membranous disks, connecting cilia and mitochondria in the ISs, as visualized under electron microscope. Host-graft synaptic connections were observed by immunochemical analysis. The hESC-derived sheets grafted into monkey models (at DD60) were found to increase in thickness until approximately DD120 and remained stable thereafter. Consistently with this, immunohistological analysis performed at DD90 demonstrated that proliferating cells (Ki67<sup>+</sup>) were still largely present within rosettes, and

cells at this stage did not express photoreceptor markers such as rhodopsin and cone opsin, indicating that the photoreceptors were still immature. In samples tested at DD150 or later, mature photoreceptor markers were abundant and IS/OS structures often observed. Proliferating cells were no longer present in samples at DD180 or older (Shirai et al., 2016). In the following study, Iraha et al. transplanted hESC and hiPSC-derived retinal sheets into a newly established immune-compromised rd1 mouse model and detected light responses at the RGC level by MEA 20-27 weeks later (Iraha et al., 2018).

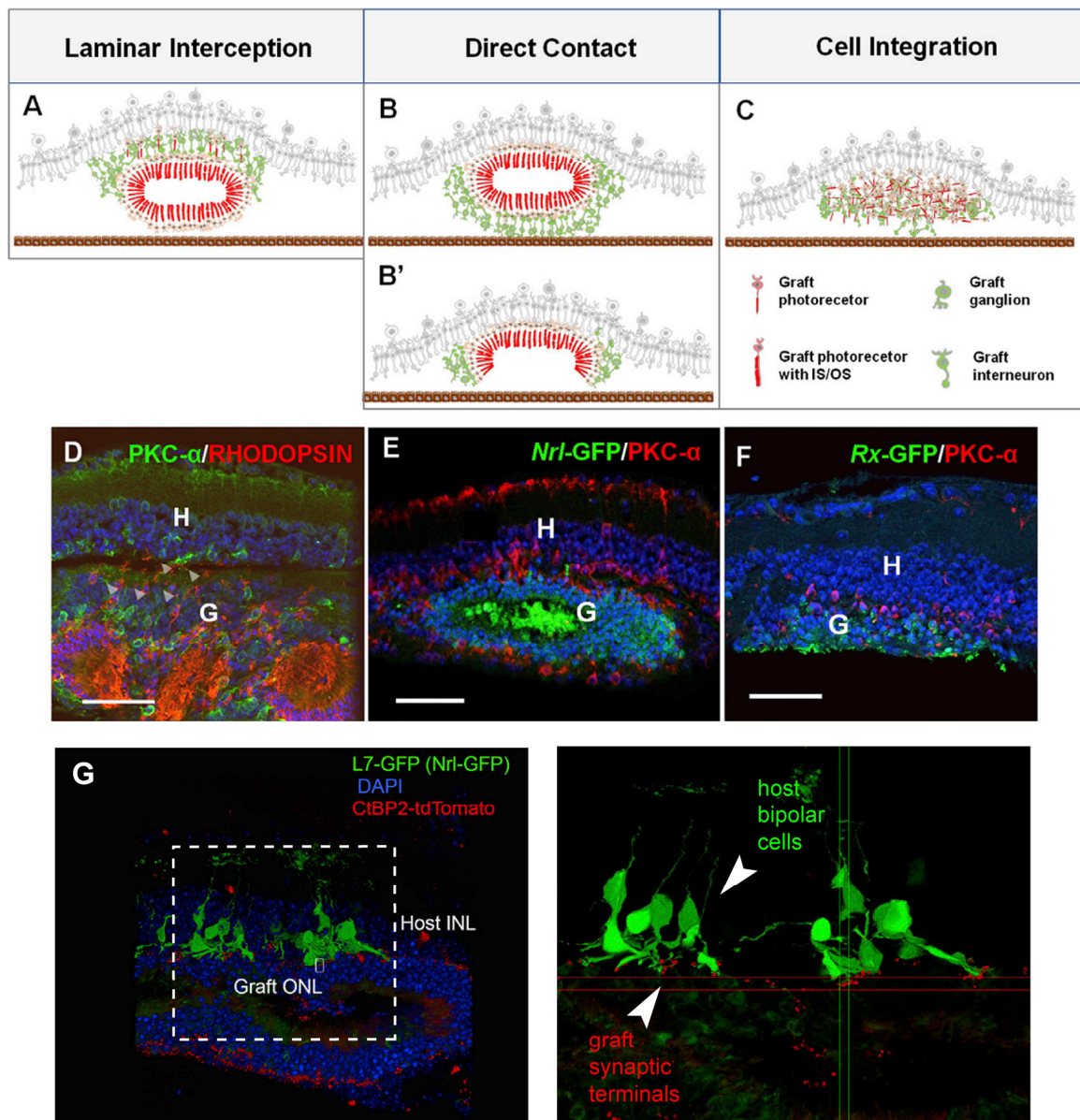


### **Figure 5.3. Transplantation of PSC-derived retinal sheets.**

Representations of the three typical patterns of integration after transplantation of retinal sheets (**A-C**) with associated immunohistochemical images illustrating these patterns in rd1 mice (**D-F**). G, graft; H, host. From Assawachananont et al., 2014. (**G**) 3D observation of contact between GFP<sup>+</sup> host bipolar cells and CtBP2-tdTomato in graft photoreceptor synaptic terminals. iPSC lines that express CtBP2-tdTomato at photoreceptor synaptic terminals after differentiation (Nrl-GFP/ ROSA::Nrl-CtBP2-tdTomato) were used to generate retinal sheets, and end-stage retinal-degeneration model mouse that expresses GFP in rod bipolar cells (L7-GFP/rd1) as hosts. Adapted from Mandai et al., 2017a.

The same year, Magdalene Seiler's laboratory, too, showed the potential for hESC-derived retinal sheets to restore visual function. Retinal sheets transplanted at DD30-65 into immunodeficient rd1 mice showed growth and survival up to 10 months post-surgery. Cells within the graft differentiated, integrated and produced functional photoreceptors and other retinal cells. The optokinetic tests and electrophysiological recordings from the superior colliculus showed visual improvement. The difference between the treated and untreated eye increased with time, in accordance with the maturation of the graft (McLelland et al., 2018).

## **5.4 Cell-seeded scaffold transplantation**

The main idea behind using scaffolds for photoreceptor transplantation is to deliver them in a more structured way – as a correctly organized layer, but without the remaining retinal cell as in the case of retinal sheet transplantation. Using scaffolds also permits adding cues for survival and differentiation towards photoreceptor fate.

An early study by Silverman and Hughes (1989) embedded retinal sheets harvested from neonatal mice into gelatin, subsequently retrieved exclusively the photoreceptor layer via vibratome sectioning and transplanted it into rats with eliminated ONL. Gelatin is flexible, non-neurotoxic and dissolves after transplantation, at body temperature, allowing donor photoreceptors to interact with the host retina (Silverman and Hughes, 1989). Future studies focused on seeding mouse or pig retinal precursors onto scaffolds before transplantation (Ballios et al., 2010; Redenti et al., 2009; Redenti et al., 2008; Tucker et al., 2010; Yao et al., 2015). The main polymers used were poly-(L-lactic acid) (PLLA), poly(lactic-

co-glycolic acid) (PLGA), poly(glycerol sebacate)(PGS), poly( $\epsilon$ -caprolactone)(PCL), hyaluronic acid (HA), polydimethylsiloxane (PDMS) and methylcellulose (MC).

An ideal photoreceptor scaffold should be biocompatible, biodegradable, flexible and easily injectable. A good example is the scrollable scaffold, which is injected folded thanks to its flexibility, and then unfolds upon transplantation, minimizing the surgical intervention (Redenti et al., 2009). Surface modifications such as coating with laminin can promote cell adhesion (Pritchard et al., 2010; Redenti et al., 2009; Redenti et al., 2008). Scaffolds also allow controlled delivery of molecules aiming to improve photoreceptor integration and survival. Tucker and colleagues loaded pre-activated MMP2 into a PLGA polymer scaffold before seeding it with retinal progenitor cells and transplanting it into  $Rho^{-/-}$  mice. MMP2 was previously shown to degrade deposits of several inhibitory ECM proteins at the outer limits of the dystrophic retina, where they act as a barrier against cellular migration and axonal extension. As a result, the number of donor cells that were able to cross the glial barrier and reach the degenerating host retina increased significantly (Tucker et al., 2010).

More recently, new technologies have allowed the making of 3D micropatterned films designed to support natural cell morphology. Jung et al. developed a biodegradable scaffold with wine glass-shaped micropattern that promotes photoreceptor capture, adherence and axon elongation. Since photoreceptors are highly polarized cells, it is crucial to ensure their polarity upon inserting them into the retina lacking the ONL. The produced scaffolds were seeded with hPSC-derived photoreceptors, which revealed mitochondria-rich photoreceptor ISs along the apical surface of the scaffold and axon terminals reaching out through the scaffold openings (**Figure 5.4.**). The present study did not report of photoreceptor OS formation, but did notice photoreceptor maturation continuing after seeding (Jung et al., 2018). The maturation process might be enhanced *in vivo*, therefore future work should focus on evaluating these constructs in animal models.

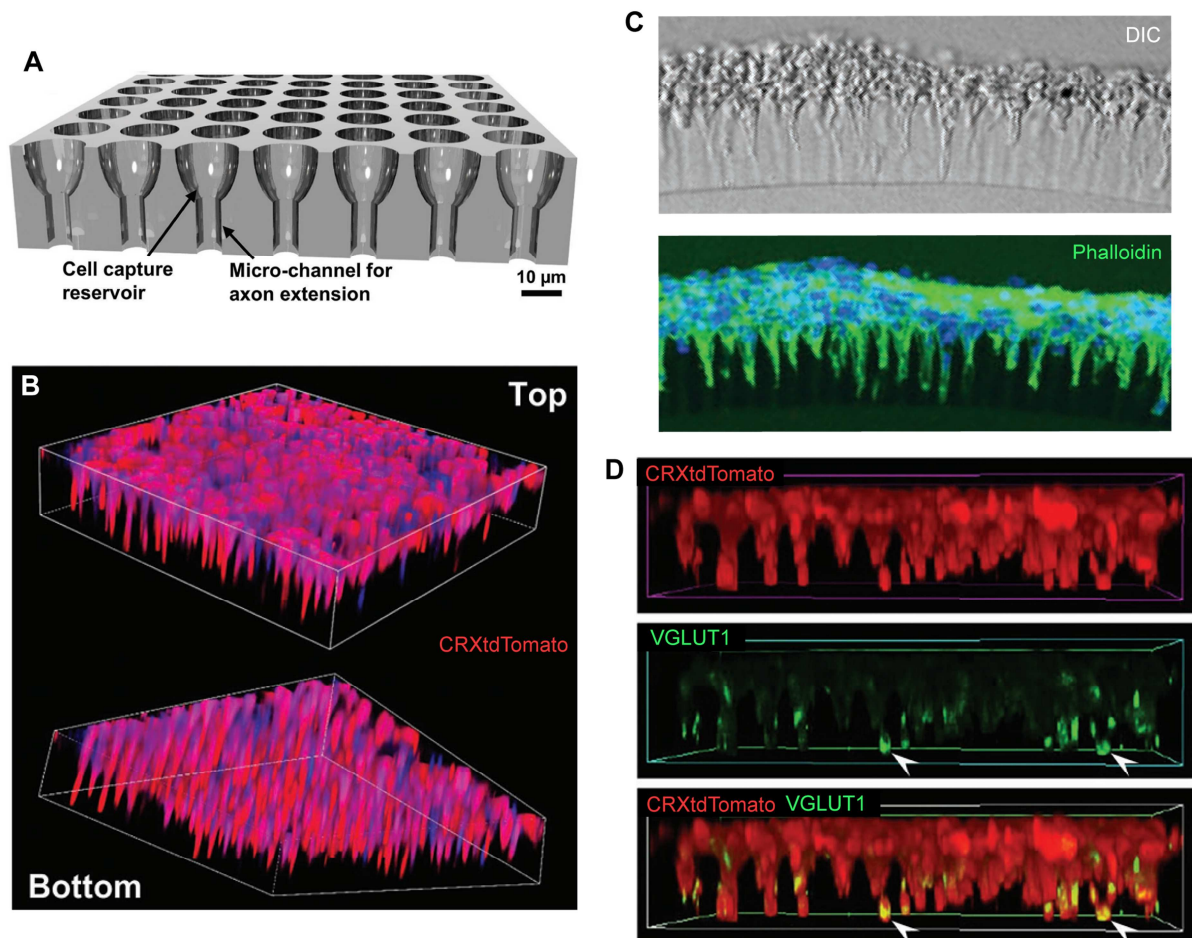


**Figure 5.4. A scaffold supporting photoreceptor cell polarisation, developed by Jung et al., 2018.**

(A) The design of the 3D microstructured scaffold, allowing the capture of photoreceptors in the upper reservoir, and extension of axonal processes through the narrowed section. (B) 3D top and bottom view of the scaffold seeded with tdTomato-labelled photoreceptors. (C) A differential interference contrast image of seeded cells and a staining for cytoskeleton F-actin thin filaments present in photoreceptor axons extending through the microchannels. (D) Extending photoreceptor axons express a presynaptic protein VGLUT1 in their terminals.

## 5.5 Issues with stem cell transplantation today

### 5.5.1 Cytoplasmic material exchange - paradigm shift in photoreceptor replacement therapy

Until recently, it has been believed that transplanted photoreceptors migrate and structurally integrate into the ONL of the recipient. This paradigm was challenged in 2016 by several groups (Pearson et al., 2016; Santos-Ferreira et al., 2016a; Singh et al., 2016)

providing strong evidence that, instead, material transfer occurs between transplanted cells, residing in subretinal space, and the remaining photoreceptors of the host (see **Figure 5.5** for a short summary).

After transplantation of FAC-sorted GFP<sup>+</sup> photoreceptor rods from the *Nrl-GFP* donors into *DsRed* hosts, 76-94% of the GFP<sup>+</sup> cells in the ONL showed double labelling for GFP and DsRed (Pearson et al., 2016; Santos-Ferreira et al., 2016a; Singh et al., 2016). Interestingly, the transfer of material also occurs for membrane-targeted proteins. After transplantation of donor cells derived from red fluorescent membrane-reporter mice into GFP hosts, cells in the hosts' ONL were found to express green labelling in the cytoplasm and red in the membrane simultaneously (Ortin-Martinez et al., 2017).

Fluorescence *in situ* hybridization (FISH) against Y chromosome after transplanting GFP-labelled female mice-derived photoreceptor precursors into male recipient mice showed similar results. Only about 1% of GFP<sup>+</sup> cells were positive for Y chromosome (Pearson et al., 2016; Santos-Ferreira et al., 2016a; Singh et al., 2016). This strongly supports the notion that the transfer is cytoplasmic rather than nuclear. Nuclear fusion was observed between Purkinje neurons or Müller glia following injection of bone marrow cells, for example, but is extremely rare between post-mitotic cells and has been previously ruled out in photoreceptor transplantation studies (Bartsch et al., 2008; MacLaren et al., 2006).

Furthermore, when transplanting previously 5-ethynyl-2'-deoxyuridine (EdU)-labelled *Nrl-GFP* photoreceptors into wild type mice, no GFP<sup>+</sup> cells residing within the ONL expressed the EdU nuclear marker simultaneously, suggesting that none of them were donor cells (Santos-Ferreira et al., 2016a).

Further evidence was collected using Cre/LoxP technology. Donor photoreceptors were isolated from a Cre-dependent mouse reporter line and transplanted into photoreceptor-specific Cre-expressing hosts (Santos-Ferreira et al., 2016a; Singh et al., 2016) or the inverse (Pearson et al., 2016). Reporter positive cells were detected in both the hosts' ONL and the subretinal cell mass, suggesting that the transfer between the donor and the host is bi-directional. At the same time, this indicates that, in addition to cytoplasmic and membrane-located material, even nuclear-targeted proteins such as Cre-recombinase can transfer between cells.

The capacity to exchange cytoplasmic material has been subsequently also proven for cones (Decembrini et al., 2017; Ortin-Martinez et al., 2017; Waldron et al., 2018). Nuclear hetero/euchromatin architecture of the rods and cones can serve as a good indicator when distinguishing between integration and material transfer. Cone nuclei contain several clumps of heterochromatin surrounded by a substantial amount of euchromatin, while rod nuclei have a single central clump of heterochromatin that almost fills up the whole nucleus with just a small amount of peripheral euchromatin (Carter-Dawson et al., 1978). Several groups reported of a big mismatch in nuclear morphology between starting cells and labelled cells found within ONL several weeks after transplantation (Ortin-Martinez et al., 2017; Waldron et al., 2018). Subretinally injecting rods into a cone-rich mouse model (*Nrl*<sup>-/-</sup>) or cones into a predominantly rod model (wild type) resulted in an 80->99% mismatch. On the contrary, the cells remaining in the subretinal space after transplantation kept the initial nuclear architecture. Fate switch was excluded with EdU staining of donor cells prior to transplanting, leading them to the idea of material exchange (Ortin-Martinez et al., 2017).

Cytoplasmic material transfer can result in the presence of various structural proteins that are otherwise absent from recipient mice, such as rod  $\alpha$ -transducin in *Gnat1*<sup>-/-</sup> mouse and Peripherin-2 in *Prph2*<sup>rd2/rd2</sup> mice (Pearson et al., 2016). It is likely that the observed visual improvements detected in the studies in the past (Barber et al., 2013; Pearson et al., 2012; Santos-Ferreira et al., 2015) emerged from donor cell-provided functional proteins that were enough to partially restore their function. However, it is yet to be further investigated to what extent this phenomenon takes place in different disease models. Morphology of labelled cells often resembles that of the photoreceptors of the donor mouse model itself, which is a good indicator that this is the case (Barber et al., 2013). However, cell integration might remain an important actor in regeneration in some disease models. Significant numbers of integration events were found by Waldron et al. (2018) after transplanting cone-like precursors and ESC-derived cones into degenerated *Prph2*<sup>rd2/rd2</sup> or cone-enriched *Nrl*<sup>-/-</sup> mice (14% and 23%, respectively), compared to only 1% after transplanting into wild type mice (Waldron et al., 2018). This confirms that the host environment and the aetiology of the disease remain a very important factor for the success of integration, as well as cytoplasmic transfer.

Cytoplasmic transfer has been confirmed in mouse PSC-derived cones (Waldron et al., 2018), but it is still unclear whether this phenomenon also occurs between human and mouse cells and whether human PSC-derived photoreceptors have a similar potential for material exchange. Gonzalez-Cordero and colleagues found most of the hPSC-derived cones after transplantation into *Nrl*<sup>-/-</sup> mice to be incorporated cells. They confirmed human origin of these cells by staining for human-specific nuclear and mitochondrial markers, as well as by comparing the sizes of human versus mice nuclei. However, they occasionally found GFP<sup>+</sup> cells that did not express human markers, suggesting that material transfer might also be possible between human and mouse cells (Gonzalez-Cordero et al., 2017). Similarly, Zhu and colleagues interpreted the GFP<sup>+</sup> cells within the host ONL as integrated cells. They merely used the localization of human-specific nuclear proteins such as human nuclear antigen (HNA) for distinguishing between the two processes (Zhu et al., 2017a). Since the Cre/LoxP experiments pointed to the facts that material exchange is not restricted to only cytoplasmic and membrane-bound proteins, but may also translocate nuclear-targeted proteins, further proof to support the integration theory would be preferred.

The described material exchange seems to be restricted to photoreceptor-photoreceptor interactions. This explains why very limited numbers of labelled cells were observed after transplantations of non-photoreceptor fraction (CD73<sup>-</sup> fraction, for example) (Eberle et al., 2011) or non-retinal cells such as fibroblasts (Pearson et al., 2016). Studies engrafting labelled photoreceptors into models of severe degeneration never reported of any fluorescent cells in the host INL, which makes seem heterotypic transfer unlikely. Ortin-Martinez et al., however, did report of a low-level GFP signal in bipolar and Müller cells after transplanting *Nrl-GFP* rods into *Nrl*<sup>-/-</sup> mice (Ortin-Martinez et al., 2017). Further clarification is needed to determine whether other retinal cells than photoreceptors can engage in material exchange.

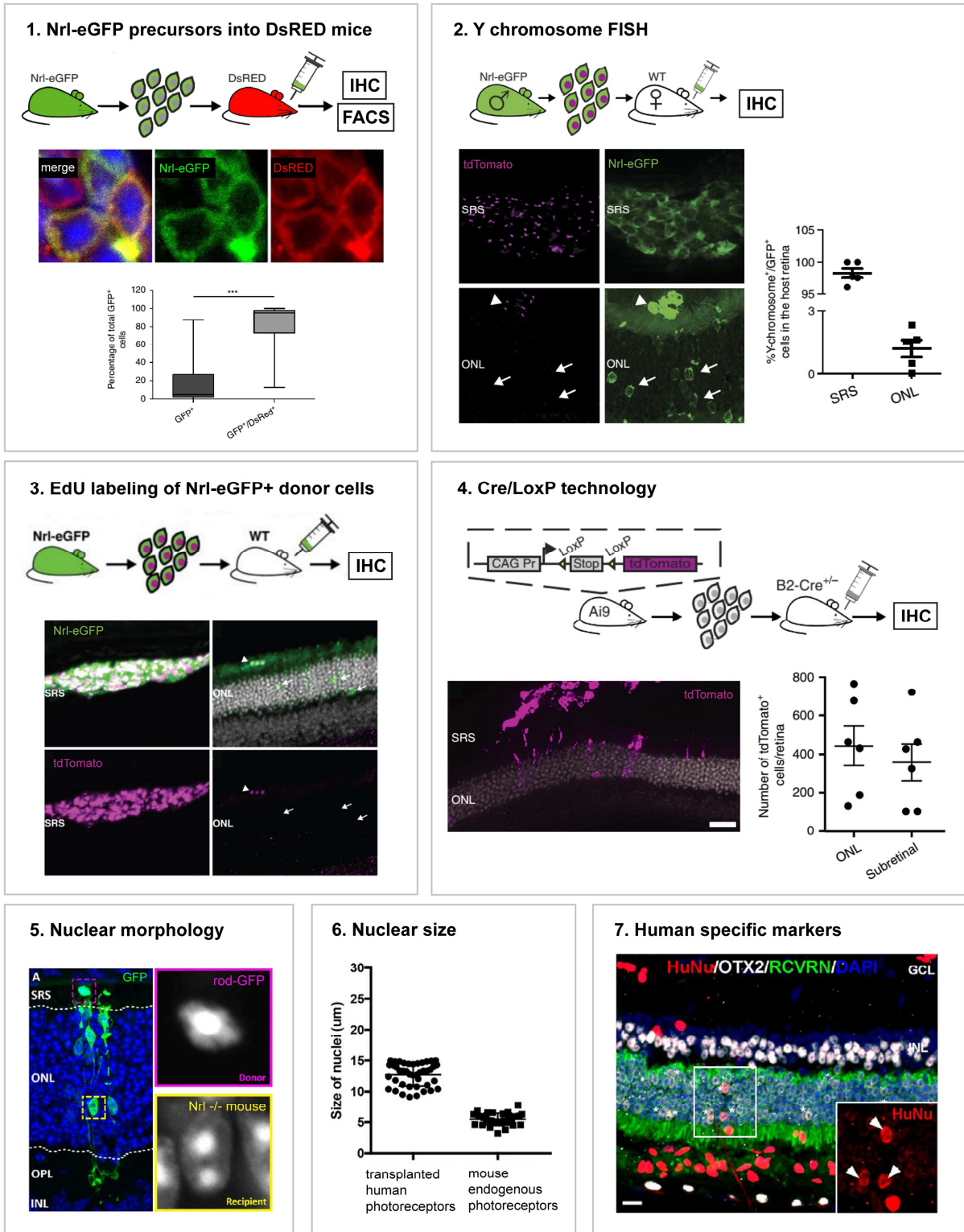


**Figure 5.5. A summary of methods for distinguishing material transfer event from structural integration.**

**1.** Analysis of DsRED host retinas grafted with *Nrl-eGFP* photoreceptors by immunohistochemistry or flow cytometry. Transplanted photoreceptors coexpressing eGFP and DsRed (top). From Singh et al., 2016. More than 80% of photoreceptor were eGFP<sup>+</sup>/DsRed<sup>+</sup> several weeks after injection, indicating that the vast majority of eGFP<sup>+</sup> cells were endogenous photoreceptor that underwent material exchange with donor cells. Data obtained from flow cytometry analysis (bottom). From

Pearson et al., 2016. The values range from 76-94%, depending on the study (Pearson et al., 2016; Santos-Ferreira et al., 2016a; Singh et al., 2016). **2. Y chromosome FISH analysis.** 3 weeks after transplanting male *Nrl-eGFP* rod precursors into female host, the majority of eGFP<sup>+</sup> cells in the subretinal space expressed eGFP and stained for Y chromosome (donor cells), whereas only over 1% of eGFP<sup>+</sup> cells in the ONL contained Y chromosome (host cells that underwent material transfer). From Santos-Ferreira et al., 2016a. **3. Transplantation of EdU-labelled *Nrl-eGFP* photoreceptors.** The majority of cells in the subretinal space, but very few in the ONL, were eGFP<sup>+</sup>/Edu<sup>+</sup>, therefore donor photoreceptors. From Santos-Ferreira et al., 2016a. **4. Cre/LoxP technology.** Donor photoreceptors isolated from floxed reporter mice (Ai9) and transplanted into rod photoreceptor-specific Cre mice (*B2-Cre<sup>+/+</sup>*) show expression of the tdTomato reporter in cells located in the subretinal space as well as ONL, bidirectional transport of intracellular content between donor and host photoreceptors. From Santos-Ferreira et al., 2016a. **5. Nuclear morphology.** After transplantation of GFP<sup>+</sup> rods into *Nrl<sup>-/-</sup>* mouse (with all photoreceptors cone-like), GFP<sup>+</sup> cells in the subretinal space showed rod nuclear morphology as would be expected, whereas GFP<sup>+</sup> cells in the ONL showed cone nuclear architecture, suggesting material exchange. From Ortin-Martinez et al., 2017. **6. Nuclear size.** The size of photoreceptors nuclei of human origin are larger compared to those of mouse origin (13  $\mu\text{m}$  versus 6  $\mu\text{m}$ ). From Gonzalez-Cordero et al., 2017. **7. Human specific markers** can be used to selectively label human-derived photoreceptors in human-to-mouse transplantation settings. From Zhu et al., 2018.

The mechanisms leading to the material transfer are yet to be illuminated. Cytoplasmic and membrane-targeted reporter proteins can be transferred, as well as nuclear-targeted proteins and various endogenous vision-related proteins such as Peripherin-2,  $\alpha$ -transducin, rhodopsin, S opsin and cone-arrestin. It is unclear if this information is transferred as protein or/and as mRNA. The exchange could occur by merging of plasma membranes of two cells, membrane nanotubes, endocytosis, gap junctions, or other. It is not the result from the uptake of free protein that would be released into the extracellular environment by donor cells (before or after transplantation) or resident macrophages (Pearson et al., 2016). The fact that only photoreceptors seem to be capable of this type of transfer can lead one to hypothesize that photoreceptor-specific structures, for example OSs, might be involved in this process (Gasparini et al., 2018).

Whatever the underlying mechanism is, this paradigm switch calls for a reevaluation of all the photoreceptor transplantation studies conducted at an earlier date, including the reports of functional synapses, examining the proportion of integration versus material transfer in different models of retinal degeneration, ways of improving integration by manipulating OLM integrity and glial scar formation, etc.

### **5.5.2 Reaching proper PSC-derived photoreceptor differentiation and morphology *in vitro***

Since the ontogenetic equivalent of P4-7 mice in human are fetuses in their early second trimester of development, and their use would be ethically problematic and would not be able to meet the supply needs, cell transplantation studies are now mainly focussing on deriving appropriate cells for transplantation from PSCs. There have been immense advances in this field in the last years, as discussed previously. However, the effort to develop protocols that are capable to further bias the differentiation of RPCs within retinal organoids towards specific cell fates is still ongoing. In parallel, various cell surface antigens are being tested as potential means of selecting the desired cells from the retinal organoid (Gagliardi et al., 2018; Lakowski et al., 2018). It will be important to maximize the level of cellular maturity and function of these cells. So far, complete differentiation with the establishment of connecting cilia and robust elaboration of OSs, has not yet been achieved *in vitro*. The existing protocols are also extremely time-consuming, and it would be desirable to develop accelerated methods of differentiation (Aghaizu et al., 2017).

To be able to translate cell therapies to humans, all the steps of preparing the therapeutic cells need to be in total compliance with GMP. This means that the cell products must be consistently manufactured to reach a certain criteria in terms of viability, function, purity and sterility during the generation and differentiation process. Chemically undefined media and materials of animal origin need to be avoided.

The development of appropriate cryopreservation methods of either organoids or photoreceptors after its isolation will be important in order to have cells at the right stage of development readily available at all times.

### **5.5.3 Orientation, cell morphology and synaptogenesis *in vivo* post-transplantation**

One of the big drawbacks of using photoreceptor cell suspensions is that the transplanted cells mostly fail to orientate themselves appropriately and do not exhibit clear apical-basal polarisation. This presents a problem for various reasons. First, it lessens the chances of synapse formation with the remaining INL cells. Second, it disturbs the contact between

photoreceptors and the cells of the RPE. The RPE plays a crucial role in photoreceptor OS maintenance and in the visual cycle, and is therefore indispensable to retain the structure and function of photoreceptors.

So far, the formation of correctly developed OSs has been impossible to achieve in models of severe degeneration (Barber et al., 2013; Eberle et al., 2012; Gonzalez-Cordero et al., 2017; Singh et al., 2013). Diffused transplanted photoreceptors often express synaptic markers (Gonzalez-Cordero et al., 2017; Santos-Ferreira et al., 2016b; Singh et al., 2013), but direct evidence of synapse formation in models of severe degeneration with no or little remaining ONL has not been provided.

These issues have been partially resolved in PSC-derived retinal sheets, although in that case, their contact with the RPE and their potential of forming synapses is often disturbed because of the formation of rosettes (Mandai et al., 2017a).

#### **5.5.4 Immune response related concerns (and recent efforts to overcome them)**

The eye is believed to be one of the immune privileged sites of the vertebrate body. The ocular environment is largely isolated from the blood stream by the blood-retinal barrier, and certain cells in the eye (such as the RPE) express molecules that suppress T cell function. Due to these intrinsic protective mechanisms, it was initially believed that transplantations in the eye would not require immunosuppressive treatment. However, numerous cases of graft rejection and inflammatory responses have been reported after subretinal injections (Kennelly et al., 2017; Santos-Ferreira et al., 2015; West et al., 2010; Zhu et al., 2017a). Infiltration of immune cells such as macrophages and T cells into the subretinal space, and microglia migration into the graft, was associated with reduced numbers of integrated donor cells (West et al., 2010). The extent of immune response is effected by different modes of cell delivery (trans-vitreous versus trans-scleral injection), potential mismatch of haplotypes, and the use of unsorted cells that might contain a bigger proportion of immunoreactive cells such as microglia and Müller cells (Gasparini et al., 2018). Cell survival also varies dramatically among different mouse models of photoreceptor degeneration (Barber et al., 2013). It must be kept in mind that diseases such as AMD and RP cause the

loss of RPE cells, leading to breaches in the blood-retinal barrier as well as to disturbed secretion of the immunosuppressive factors. In this respect, it is to be expected that the eye would be less protected from the immune response in patients with such conditions compared to healthy individuals.

From the immunological standpoint, it would be ideal to use **autologous hiPSC cell lines**. However, creating a separate cell line for every single patient will not be feasible in a clinical setting when trying to treat a high number of patients. The process of production, validation and subsequent differentiation into appropriate cell type takes months and is excessively expensive. In addition, the disease causing mutation would need to be corrected by gene editing prior to producing the hiPSC cell line from patient's cells. On the other hand, most studies suggest that using allografts would require at least some extent of immunosuppression. Immunosuppressive drugs that are commonly used in organ transplantation such as cyclosporine and glucocorticoids are associated with grave side effects, and since blindness is not a life-threatening condition, it is debatable whether it would be justifiable to succumb the patient to the immunosuppression-related risks. Recently, **local delivery of immunosuppressive agents** has shown satisfactory results in monkeys (Sugita et al., 2017).

Deepak Lamba's group identified mesencephalic astrocyte-derived neurotrophic factor (**MANF**) as an evolutionary conserved immune modulator that plays a critical role in the regulatory network mediating tissue repair in the retina. MANF enhanced the integration success of transplanted cells and improved restoration of visual function. Modulating the immune environment could be used as a strategy to improve regenerative therapies in the future (Neves et al., 2016).

In the past, several studies pointed to the importance in major histocompatibility complex (MHC) matching in the survival of subretinally delivered transplants in monkeys (Sugita et al., 2017). Establishing human leukocyte antigen (**HLA – the MHC in human**)-**haplotype-based stem cell banks** is considered as an attractive option. In ethnically homogenous populations such as Japan, it is estimated that 50 of such cell lines would be enough to provide cells for about 90% of the population (Nakatsuji et al., 2008). 150 cell lines could provide a haplotype match for 93% of the UK population (Taylor et al., 2012). The number of cell lines necessary to cover a satisfactory proportion of the population depends strongly on

the heterogeneity of that population. An iPSC bank of the 100 most common HLA types population wide would offer a match to 78% of individuals of European origin, 63% of Asians, 52% of Hispanics, and 45% of African Americans (Garreta et al., 2018). An alternative approach to this offers to **knockout HLA expression in donor cells**. This type of cells could potentially represent a universally tolerated cell source (Gornalusse et al., 2017; Torikai et al., 2016).

# RESULTS

Inherited retinal diseases are genetically and clinically very heterogeneous disorders with an estimated incidence of 1:2000. One of the possible strategies to treat late stage retinal degeneration is photoreceptor replacement therapy, but there are still many challenges that lie ahead. In order to achieve visual improvement, the transplanted photoreceptors need to 1) develop light-sensitive OSs, 2) form functional synapses with the cells of the INL, and 3) keep in close contact with the RPE. In animals with severely degenerated ONL, transplanted photoreceptors fail to develop normal OS structures, so light sensitivity is under question. What is more, the RPE is often damaged along with the photoreceptors, especially in later stages of the disease (RP, AMD, LCA, etc.). RPE plays a crucial role in photoreceptor maintenance (disk shedding, providing nutrients, etc.) and in the visual cycle (chromophore re-isomeration), therefore is absolutely necessary for vision.

In the present study, we tried to overcome some of these challenges by combining photoreceptor transplantation with optogenetics. More precisely, we introduced a hyperpolarizing microbial opsin into photoreceptor precursors from newborn mice, or photoreceptors developed *in vitro* from hiPSCs (the part of the project using hiPSC was led by Marcela Garita-Hernandez), and transplanted them into blind mice lacking the photoreceptor layer. The key advantage of these optogenetically transformed photoreceptors is that they stay functional based on the activity of the microbial opsin, even in the absence of properly formed OSs and without the support from the RPE. Microbial opsins operate in a much simpler way than animal opsins. The conformational change caused by the light absorption is directly coupled to ion movement through the membrane. Furthermore, the photoisomerization of the chromophore is reversible and both isomers remain covalently attached to the protein.

After transplantation, optogenetically transformed photoreceptors were located in the subretinal space and were light-sensitive, as shown by two-photon targeted patch clamp recordings. Furthermore, by using MEA recordings we detected light responses in RGCs. This demonstrates that the transplanted photoreceptors form synaptic connections with the inner retinal neurons and that microbial opsin-induced signals are transmitted to the retinal output neurons. Treated mice also displayed robust light avoidance behaviour. We detected no responses on the photoreceptor, RGC or behavioral level in mice transplanted with photoreceptors that were not optogenetically engineered.

Taken all this together, these results demonstrate that structural and functional retinal repair is possible by combining stem cell therapy and optogenetics.

# Restoration of visual function by transplantation of optogenetically engineered photoreceptors

**Authors:** Marcela Garita-Hernandez<sup>1#</sup>, Maruša Lampič<sup>1#</sup>, Antoine Chaffiol<sup>1</sup>, Laure Guibbal<sup>1</sup>, Fiona Routet<sup>1</sup>, Tiago Santos-Ferreira<sup>2</sup>, Sylvia Gasparini<sup>2</sup>, Oliver Borsch<sup>2</sup>, Giuliana Gagliardi<sup>1</sup>, Sacha Reichman<sup>1</sup>, Serge Picaud<sup>1</sup>, José-Alain Sahel<sup>1,3,4</sup>, Olivier Goureau<sup>1</sup>, Marius Ader<sup>2</sup>, Deniz Dalkara<sup>1\*#</sup>, Jens Duebel<sup>1\*#</sup>

## Affiliations:

<sup>1</sup> Sorbonne Université, Institut de la Vision, INSERM, CNRS, 75012 Paris, France

<sup>2</sup> CRTD/Center for Regenerative Therapies Dresden, CMCB, TU Dresden, Germany.

<sup>3</sup> CHNO des Quinze-Vingts, DHU Sight Restore, INSERM-DGOS CIC 1423, Paris, France.

<sup>4</sup>Department of Ophthalmology, The University of Pittsburgh School of Medicine, USA.

\* correspondence, # equal contribution

## Abstract

A major challenge in the treatment of retinal degenerative diseases, with the transplantation of replacement photoreceptors, is the difficulty in inducing the grafted cells to grow and maintain light-sensitive outer segments (OS) in the host retina, which depends on proper interaction with the underlying retinal pigment epithelium (RPE). For an RPE-independent treatment approach, we introduced a hyperpolarizing microbial opsin into photoreceptor precursors from new-born mice, and transplanted them into blind mice lacking the photoreceptor layer. These optogenetically transformed photoreceptors were light responsive and their transplantation led to the recovery of visual function, as shown by ganglion cell recordings and behavioral tests. Subsequently, we generated cone photoreceptors from human induced pluripotent stem cells (hiPSCs), expressing the chloride pump Jaws. After transplantation into blind mice, we observed light-driven responses at the

photoreceptor and ganglion cell level. These results demonstrate that *structural* and *functional* retinal repair is possible by combining *stem cell therapy* and *optogenetics*.

## Introduction

Cell replacement therapy offers hope for the treatment of late stage retinal degeneration, when the outer retinal photoreceptor layer is lost (Jayakody et al., 2015; Santos-Ferreira et al., 2017; West et al., 2009). However, a remaining obstacle of photoreceptor replacement is that transplanted cells have to develop into functional photoreceptors with light-sensitive outer segments (OS). Indeed, in mouse models of severe degeneration, the formation of light-sensitive OS by transplanted photoreceptors has been difficult to achieve (Barber et al., 2013; Eberle et al., 2012; Singh et al., 2013). Recent studies, using retinal sheet transplantation led to major improvements in terms of OS formation and light sensitivity (Iraha et al., 2018; Mandai et al., 2017a). Despite these promising results, a major problem has not yet been solved: photoreceptors need tight interaction with the retinal pigment epithelium (RPE) in order to maintain their structure and function via continuous disc shedding and renewal (Strauss, 2005). Since in retinal degenerative diseases the RPE is often also compromised (Strauss, 2005; Wright et al., 2010), the probability that transplanted photoreceptors stay sensitive to light is very low (Chiba, 2014; Milam et al., 1998). To tackle this problem, we introduced optogenetic light sensors into photoreceptors, derived from the developing mouse retina as well as from human induced pluripotent stem cells (hiPSCs), and transplanted them into mouse models of severe retinal degeneration. The key point of our approach is that these optogenetically transformed photoreceptors stay functional based on the activity of the microbial opsin, even in the absence of properly formed OS and without the support from the RPE.

## Results

### ***Transplantation of optogenetically transformed photoreceptor precursors from neo-natal mice to blind mouse retinas***

For optogenetic transformation of mouse photoreceptors, eyes of new-born wild-type mice at postnatal day (P) 2 were injected with an adeno-associated viral (AAV) vector encoding enhanced *Natronomonas pharaonis* halorhodopsin eNpHR2.0 (NpHR) (Gradinaru et al., 2008) under the control of the rhodopsin promoter (AAV-Rho-NpHR-YFP) (Fig. 1A and Fig. S1). At P4, photoreceptor precursors were sorted by magnetic activated cell sorting (MACS) using the photoreceptor specific cell surface marker CD73 (Eberle et al., 2011; Koso et al., 2009). The harvested cells were transplanted via sub-retinal injections into two blind mouse models of late stage retinal degeneration (*Cpfl1/Rho*<sup>-/-</sup> mice (Santos-Ferreira et al., 2016b) aged 9 to 18 weeks and *C3H rd/rd* (rd1) mice (Vicgian et al., 1992) aged 4 to 11 weeks; see Table S4 for a complete overview of mouse ages). At these ages, the vast majority of outer nuclear layer (ONL) cells were lost in host mice (Fig. 1, B and E). *Cpfl1/Rho*<sup>-/-</sup> mice are left with 2-3 rows of photoreceptors at the age of 9 weeks, and a single row of photoreceptors by 10-12 weeks of age. These mice are born with non-functional rods and cones (Santos-Ferreira et al., 2016b). Rd1 mice lose photoreceptor OS and only a single row of cone cell bodies in the ONL remains by 3 weeks after birth (Carter-Dawson et al., 1978). Four weeks after transplantation, we investigated the morphology of the transplanted donor cells and their ability to integrate into the host retina. In both mouse models, we found NpHR-positive donor cells in close contact to cell bodies of rod bipolar cells, but none of the transplanted cells displayed correctly formed OS (Fig. 1, C,D,F,G). Transplanted cells expressed the synaptic marker Synaptophysin (Fig. S2) suggesting synapse formation between donor photoreceptors and the downstream neurons. We quantified the number of YFP<sup>+</sup> cells in the subretinal space transplanted with donor-derived NpHR-expressing rod precursors and found substantial numbers of cells to survive at four weeks post transplantation (Fig. S3). Next, we assessed potential material transfer between transplanted cells and remaining photoreceptors by fluorescence in situ hybridization with Y chromosome-specific probe (Y chromosome FISH). NpHR-expressing rod precursors derived from male P4 mice were injected into female *Cpfl1/Rho*<sup>-/-</sup> mice at 9 weeks of age, and

imaged after 4 weeks using structured illumination microscopy (Fig. 1H). Y chromosome<sup>+</sup>/YFP<sup>+</sup> cells (transplanted donor cells) and Y chromosome<sup>-</sup>/YFP<sup>+</sup> cells (endogenous photoreceptor that underwent material transfer) were quantified. 90% of YFP<sup>+</sup> cells co-stained with Y chromosome probe, leaving only very few cells exclusively YFP<sup>+</sup>. This could either be due to an artefact or very rare events of cytoplasmic exchange among donor and host photoreceptors (Fig. 1H,I). We then tested if we can elicit light responses from these NpHR-positive donor cells in the absence of functional OS. Two-photon targeted patch-clamp recordings revealed robust responses to orange light pulses (580 nm, 10<sup>16</sup> photons cm<sup>-2</sup>s<sup>-1</sup>) (Fig. 2B and Fig. S4). There were no measurable light-evoked currents in transplanted photoreceptors expressing GFP only, which is consistent with the finding that the transplanted cells lacked their light-sensitive OS. Stimulation at different wavelengths showed a spectral sensitivity matching the action spectrum of NpHR (Fig. 2B). To measure the temporal properties of NpHR-positive photoreceptors, we recorded photocurrents using light pulses at increasing frequencies, and we observed that they could follow up to 25 Hz (Fig. 2C and Fig. S4). Although, frequencies above 10 Hz are filtered out by the bipolar cells, the ability of optogenetically engineered photoreceptors to respond to light in a faster than natural pace implies that retinal ganglion cells (RGCs) receiving signal from these cells should follow high-frequency stimulation in a similar manner to normal retina (Crevier and Meister, 1998). The rise constants were significantly faster compared to photocurrents of wild-type mice (Fig. 2D). Both, from the spectral (peak current at 580 nm) and the temporal (Tau<sub>ON</sub> < 10ms) response properties we concluded that the photocurrents were driven by the introduced NpHR (Fig. 2, A-D, and Fig. S4).

### ***Connectivity and signal transmission from optogenetically transformed mouse photoreceptor precursors to downstream host neurons***

Next, we investigated if the signals from transplanted photoreceptors are transmitted to RGCs, the output neurons of the retina. By using extracellular spike recordings, we measured ON- and OFF-light responses in RGCs. These results demonstrate that NpHR-induced signals are transmitted to the retinal output neurons via ON- and OFF-pathways suggesting that the transplanted photoreceptors can form functional synaptic connections with the inner retinal neurons (Fig. 3A and Fig. S5), which was supported by histologica

analysis (Fig. S2). Recordings performed under pharmacological block of photoreceptor input to ON-bipolar cells (50  $\mu$ M L-AP4) showed complete abolition of ON light responses, which recovered after 20 minutes of L-AP4-washout. These control experiments confirmed that light induced signals were indeed transmitted via photoreceptor-to-bipolar cell synapses (Fig. 3, B and C). By stimulating treated retinas at different wavelengths we determined the spectral sensitivity of the light responses, which peaked at 580-600nm, reflecting the action spectrum of NpHR (Fig. 3, D and E). To assess the light intensities required to trigger spike responses, we used light pulses (580 nm) at different intensities. Importantly, the intensities required to evoke light responses were well below the safety limit for optical radiation in the human eye (European Parliament and Council of the European Union, 2006; International Commission on Non-ionizing Radiation Protection, 2013) (Fig. 3, F and G, and Fig. S5). We did not observe measurable light responses in retinas from age-matched control-mice, where photoreceptor precursors expressing only GFP were transplanted (Fig. 3, H and I, and Fig. S5). Lastly, to test whether the behaviour of treated mice could be modulated by light, we used the light/dark box test (Bourin and Hascoet, 2003) employing high intensity orange light (Fig. 3J). Treated *Cpfl1/Rho*<sup>-/-</sup> mice displayed robust light avoidance behavior (40.8 $\pm$ 3.5% of time in the illuminated compartment), compared to non-injected (59.8 $\pm$ 2.2%) mice and mice transplanted with photoreceptor precursors expressing GFP (56.6 $\pm$ 4.5%) (Fig. 3K).

### ***Generation of optogenetically transformed photoreceptors derived from hiPSC***

To evaluate the translatability of our approach to human subjects, we asked if it is possible to replace the mouse donor cells with optogenetically-transformed hiPSCs (Fig. 4A). To do so, we first optimized a previous protocol of differentiation based on the self-generation of 3D neural-retina-like structures (Reichman et al., 2017). Using this system, we generated cone-enriched retinal organoids, expressing the pan-photoreceptor markers Cone Rod Homeobox (CRX) and recoverin (RCVRN) alongside the cone-specific marker cone arrestin (CAR) (Fig. 4, B-F and Fig. S6). Contrary to nocturnal rodents, cone photoreceptors are responsible for high acuity daylight vision in humans, and are therefore the preferred choice for transplantation. To render these immature cones light-sensitive, we used the hyperpolarizing chloride pump Jaws, a red-shifted cruxhalorhodopsin, Jaws, derived from

*Haloarcula (Halobacterium) salinarum* and engineered to result in red light-induced photocurrents three times those of earlier silencers (Chuong et al., 2014). Jaws was chosen for iPSC experiments based on its enhanced expression level and improved membrane trafficking in human tissue, compared to NpHR (Chuong et al., 2014; Garita-Hernandez et al., 2018; Khabou et al., 2018). By using an AAV vector, encoding Jaws-GFP under the control of CAR promoter, we delivered the microbial opsin to the hiPSC-derived cone photoreceptors (Fig. 4, G and H). Single cell recordings from optogenetically transformed cones in retinal organoids revealed solid light responses, matching the response properties of Jaws, while recordings from hiPSC-derived cones, expressing GFP only, showed no light responses (Fig. 4, I-L). Additionally, monolayer cultures of these human cones expressing Jaws, maintained their ability to strongly respond to light after dissociation of the retinal organoids (Fig. S7). These results collectively demonstrate the possibility to induce robust optogenetic light responses in photoreceptors derived from hiPSCs in the absence of light-sensitive OS.

#### ***Transplantation and integration of optogenetically transformed photoreceptors derived from hiPSC to blind mouse retina***

In order to transplant Jaws-positive photoreceptors, we dissociated the retinal organoids and injected the cell suspension subretinally into the blind hosts (*Cpfl1/Rho*<sup>-/-</sup>, age 10 to 15 weeks; rd1, age 4 to 5 weeks). In both *Cpfl1/Rho*<sup>-/-</sup> and rd1 mice we observed Jaws-expressing donor cells in close proximity to the host INL several weeks after transplantation (Fig. 5, A-C). Due to recent concerns about material transfer in photoreceptor transplantation (Pearson et al., 2016; Santos-Ferreira et al., 2016a; Singh et al., 2016), we stained cryosections from the transplanted retinas with the human nuclear antigen (HNA) and we examined the size of the transplanted cells (HNA<sup>+</sup>) in relation to the chromatin structure and diameter of host cells. HNA stained cell counts confirmed that only a very small portion (5%) of the GFP-labelled cells could potentially be endogenous mouse cells that underwent material transfer (HNA<sup>-</sup>/GFP<sup>+</sup>) (Fig. 5D and Fig. S8). Both the HNA staining and nuclei comparison confirmed the human identity of transplanted cells in close proximity of the host INL. The transplanted GFP<sup>+</sup> cells were RCVRN positive (Fig. S8) and located next to PKC $\alpha$ -positive bipolar cells (Fig. 5A). They expressed the synaptic marker Synaptophysin

in close apposition to the bipolar cell dendrites (Fig. 5B), suggesting that the human cells form synaptic connections with the host bipolar cells. The transplanted cells displayed robust Jaws-induced photocurrents by patch clamp, demonstrating the functionality of the microbial opsin in the host environment (Fig. 5E). The measured photocurrents peaked at 575 nm and showed fast kinetics ( $\tau_{ON} < 10\text{ms}$ ) (Fig. 5, F-H), reflecting the response properties of Jaws. At the ganglion cell level, we observed ON- and OFF responses from different ganglion cell types, which shows that Jaws-driven signals from transplanted photoreceptors were transmitted via second order neurons (Fig. S9) to ON and OFF ganglion cells (Fig. 5I and Fig. S10). The light intensity requirements were again below the safety threshold for the human retina (European Parliament and Council of the European Union, 2006; International Commission on Non-ionizing Radiation Protection, 2013) (Fig. 5J and Fig. S10). After transplantation of control human donor cells, expressing GFP only, no light responses were detected (Fig. 4K and Fig. S10), as expected in absence of OS-like structures.

## Discussion

Transplantation of healthy photoreceptors holds great promise to restore vision in patients with outer retinal degeneration. This approach has received significant attention over the past years as it can restore vision independently from the cause of photoreceptor cell loss (Dalkara et al., 2016). Significant progress has been made in the generation (Garita-Hernandez et al., 2018; Gonzalez-Cordero et al., 2017; Reichman et al., 2017; Reichman et al., 2014; Wiley et al., 2016; Wright et al., 2014; Zhong et al., 2014), purification (Gagliardi et al., 2018; Lakowski et al., 2018) and transplantation of photoreceptors (Barnea-Cramer et al., 2016; Gagliardi et al., 2018; Gonzalez-Cordero et al., 2017; Mandai et al., 2017a; Santos-Ferreira et al., 2017; Shirai et al., 2016; Zhu et al., 2017a) from hiPSCs. However, photoreceptor replacement faces a three-fold challenge: transplanted cells need to develop (1) synaptic contact to bipolar cells for signal transmission, (2) functional photoreceptor OS, and (3) tight contact to RPE cells to maintain OS light-sensitivity (Fig. 6). This makes photoreceptor transplantation complex and challenging. Recent studies have shown that the recipient environment is of great importance for successful integration and survival of transplanted photoreceptor cells. In animals with severely degenerated ONL, transplanted

photoreceptor precursors derived from postnatal mouse retina (Barber et al., 2013; Eberle et al., 2012; Singh et al., 2013) or from hiPSCs (Gonzalez-Cordero et al., 2017) failed to develop normal OS structure and establish correct OS polarity with respect to host RPE. The RPE cells are indispensable for OS renewal as they phagocytose the shed OS discs. Moreover, they re-isomerize the chromophore all-*trans*-retinal into 11-*cis*-retinal. Thus, in the absence of intimate contact with the RPE photoreceptors cannot maintain their light sensitivity (Sparrow et al., 2010).

For an OS and RPE-independent treatment approach, we introduced a hyperpolarizing microbial opsin into photoreceptors derived from either neo-natal mouse retinas or from human retinal organoids derived from iPSCs. We transplanted these optogenetically transformed photoreceptors into blind mice lacking the photoreceptor layer. We have shown that these cells can mediate visual function, as demonstrated by a battery of tests from retinal ganglion cell recordings to behavioral tests. The paradigm that transplanted photoreceptors migrate and structurally integrate into the ONL of the recipient has been challenged recently by several groups (Pearson et al., 2016; Santos-Ferreira et al., 2016a; Singh et al., 2016) providing strong evidence that cytoplasmic material transfer occurs between transplanted cells, residing in the sub-retinal space, and remaining photoreceptor cells of the host. In these experiments, however, late stage degeneration animals were used to model patients with advanced disease, thus there are only few remaining photoreceptors, minimising the potential contribution of material transfer (Nickerson et al., 2018). To distinguish between potential 'fusion' events and structural integration of donor photoreceptors, we performed Y chromosome FISH and HNA staining in the *Cpfl1/Rho*<sup>-/-</sup> model where some remaining cells were visible in earlier transplantation time-points. Our Y chromosome FISH experiments revealed a very limited number of events of potential material transfer (<10%). In our blind rd1 mice, only sparse population of cones and no rods remain after 36 days of age (Carter-Dawson et al., 1978). We confirmed this observation in our control animals, obviating the possibility of material transfer from the transplanted NpHR-expressing mouse progenitors to remnant ONL cells of the host. Moreover, NpHR-positive cells that were attached to the host INL visibly show rod nuclear morphology, indicating that these are indeed donor cells and not remaining cones. As for the transplantation of Jaws expressing hiPSCs, histological analysis using a human-specific

nuclear marker (HNA) in transplanted mice, confirmed that the vast majority (95%) of GFP-expressing cells were HNA positive. This result along with the measured nuclei size confirmed the human origin of the transplanted cells, ruling out material exchange between human donor photoreceptors and mouse host cells. Although these do not fully rule out that material transfer may contribute to the improved functional responses, we have observed that the level of functional improvement is independent of the host age at time of transplantation, further supporting the optogenetically transformed photoreceptors are the major source of functional light responses. Moreover, material transfer is rare between human donor and mouse host photoreceptors (Gagliardi et al., 2018; Gonzalez-Cordero et al., 2017) (Fig. 5 and Fig. S8), arguing against a significant contribution of material transfer to the observed functional improvements.

Lastly, any possible rescue effect mediated by remaining host photoreceptors is expected to be very minor as our control groups transplanted at the same ages with wild type donor-derived photoreceptor precursors or hiPSC-derived photoreceptors expressing GFP only, never showed any detectable functional responses. This confirms that any possible rescue effect on remaining host photoreceptors cannot be a result of the transplantation itself and suggests that the functional outcomes are a direct consequence of the presence of an optogenetic protein expressed in the transplanted photoreceptors.

In conclusion, by using immature photoreceptors equipped with a microbial opsin, we went beyond the current limitations of optogenetic gene therapy approaches. Optogenetic approaches commonly target bipolar cells or RGCs that are viable targets in late stages of retinal degenerative diseases such as retinitis pigmentosa or age-related macular degeneration . Unfortunately, conferring light sensitivity to cells downstream from photoreceptors, bypasses the important information processing normally conducted by the inner retinal circuitry. Photoreceptor-directed optogenetic therapy that aims to rescue the function of remaining 'dormant' cones harnesses the information processing of the inner retina allowing the recovery of complex visual responses such as lateral inhibition and directional selectivity in previously blind mice (Busskamp et al., 2010), but this strategy can only be useful in patients with remaining cones which represent a minor portion of late stage retinitis pigmentosa patients (Azoulay-Sebban, 2015). Here, we use the synergy of cell replacement and optogenetic therapy that allows the restoration of retinal *structure* with

stem cell derivatives and visual *function* with microbial opsins. In a future perspective, optogenetically engineered hiPSC-derived cones could serve as donor cells for photoreceptor transplantation in late stage retinal degeneration. In patients, degenerative diseases of the retina such as retinitis pigmentosa, age-related macular degeneration, and Leber congenital amaurosis, often manifest RPE degeneration along with photoreceptor degeneration, especially in their late stages (Athanasίου et al., 2013; Cideciyan, 2010; Li et al., 1995; Wright et al., 2010). Our approach bodes well for applications in such patients who can only obtain limited benefit from transplantation of photoreceptors in the absence of chromophore replenishment from their dystrophic RPE.

# Figures and figure legends

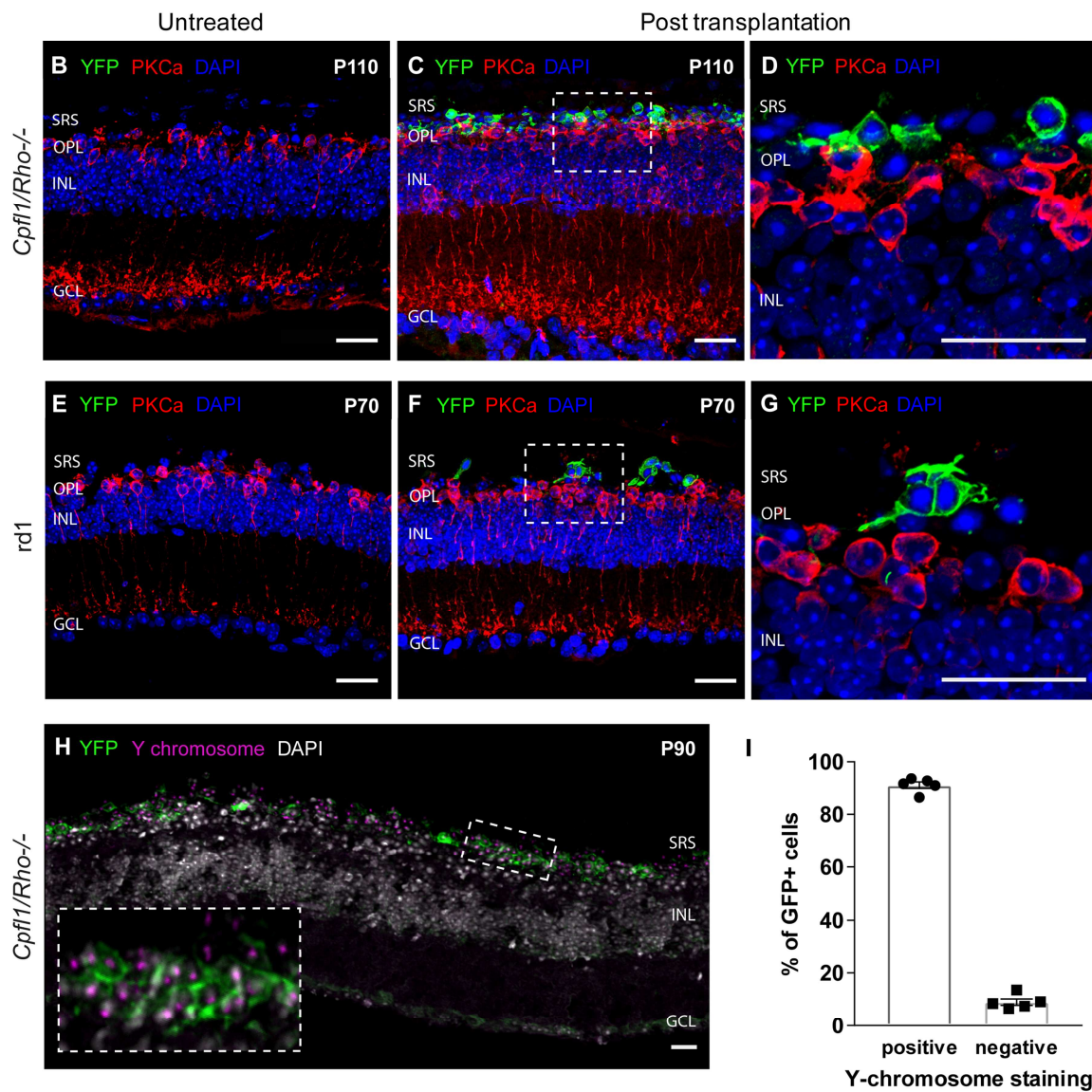
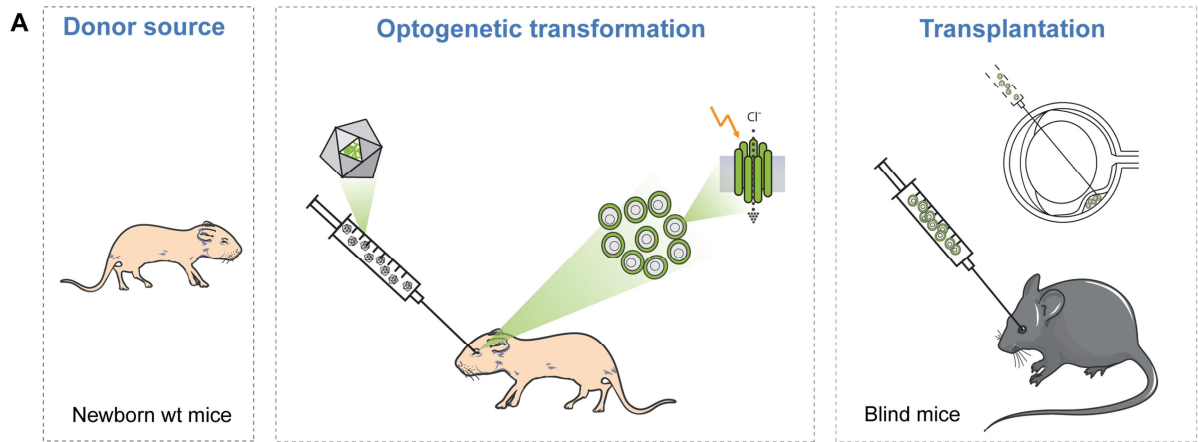


**Figure 1. Transplanted photoreceptor precursors, expressing NpHR, integrate into the retina of blind mice.**

**(A)** Eyes of wild type mice at P2 were injected with AAV-Rho-NpHR-YFP. Two days later, retinas were dissected and photoreceptor precursors sorted out. These cells were transplanted via sub-retinal injections into blind mice. **(B-G)** Immunofluorescence analysis on vertical sections of *Cpfl1/Rho*<sup>-/-</sup> (B-D) and rd1 (E-G) retinas. **(B)** Age-matched non-transplanted *Cpfl1/Rho*<sup>-/-</sup> retina. **(C,D)** *Cpfl1/Rho*<sup>-/-</sup> retina transplanted with NpHR-photoreceptors showing YFP<sup>+</sup> cells (green) located on top of host PKC $\alpha$  bipolar cells (red). **(E)** Age-matched non-transplanted rd1 retina. **(F,G)** Rd1 retina transplanted with NpHR-photoreceptors. **(H,I)** Y chromosome FISH. **(H)** A retinal section showing Y chromosome labelling (magenta) and immunohistochemistry staining of YFP (green) with DAPI counterstaining (white) 4 weeks after transplantation of NpHR-expressing rods from male donors into a female *Cpfl1/Rho*<sup>-/-</sup> mouse (P60 at the time of transplantation). **(I)** Quantification of YFP<sup>+</sup> cells containing Y chromosome from 5 individual experimental retinas (N=5). The vast majority of YFP<sup>+</sup> cells also contained a Y chromosome (90.9  $\pm$  1.2%; mean  $\pm$  SEM), proving that they originate from donor mice. Scale bars: 25  $\mu$ m. SRS – subretinal space, OPL – outer plexiform layer, INL – inner nuclear layer, GCL – ganglion cell layer, P – postnatal day.

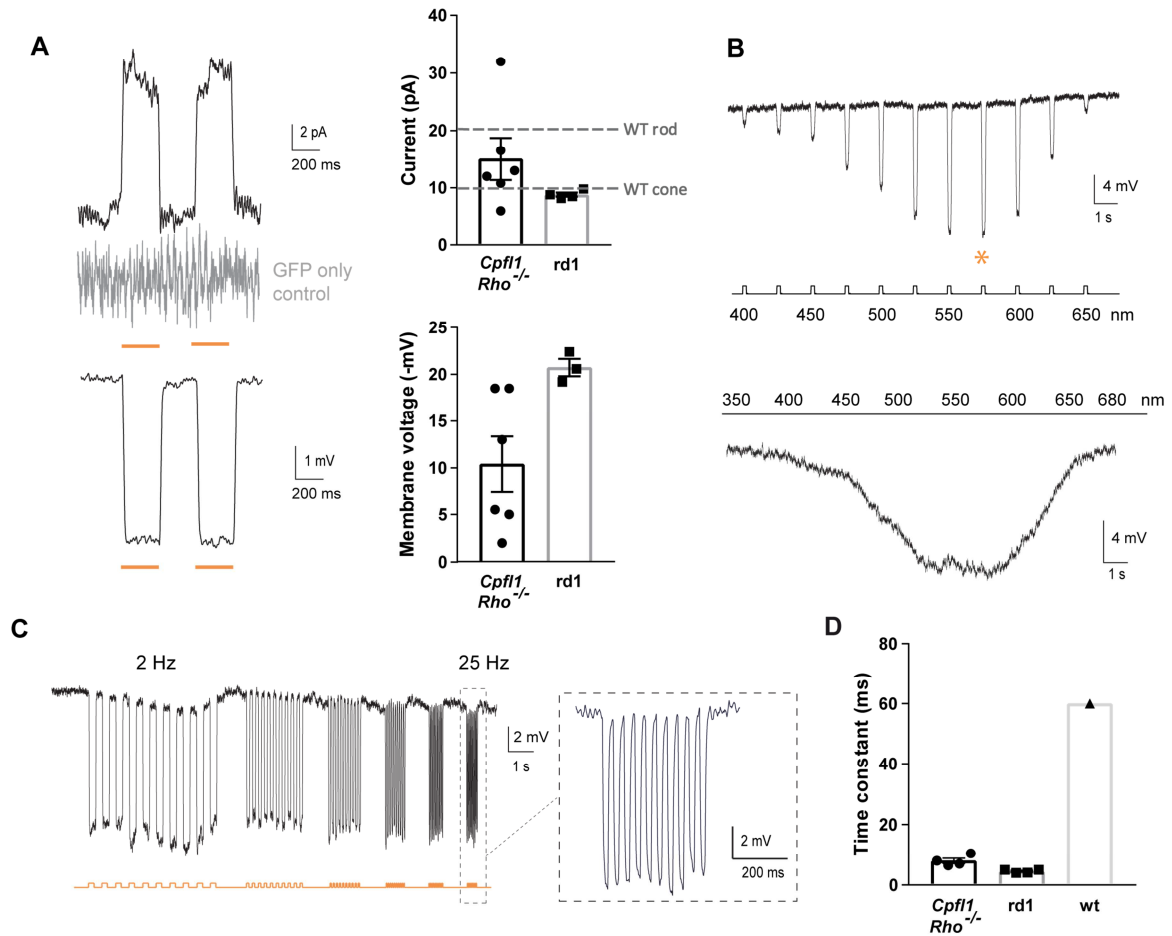


**Figure 2. Transplanted NpHR-expressing photoreceptor precursors respond to light.**

(A-D) Light response characteristics from cells recorded by whole-cell patch-clamp technique in treated *Cpf1/Rho<sup>-/-</sup>* mice. The resting membrane potential (RMP) of transplanted photoreceptors in the dark (at 0 current) for the recordings presented in the figure was  $-36 \pm 1,5$  mV. **(A)** Left, light-evoked responses of NpHR- photoreceptors stimulated with 2 consecutive flashes (top, current response; bottom, voltage response), absence of the response in GFP only-expressing photoreceptor shown in grey. Right, comparison of response amplitudes. Mean photocurrent peak (top) and mean peak voltage response (bottom). Mean values observed in wild type rods and cones are indicated with a dashed line(Nikonov et al., 2006). **(B)** Representative action spectrum from a NpHR photoreceptor stimulated at different wavelengths. Top, stimuli ranging from 400 nm to 650 nm, separated by 25 nm steps. Maximal voltage responses were obtained at 575 nm. Bottom, continuous ‘rainbow’ stimulation between 350 and 680 nm. **(C)** Temporal properties: Modulation of NpHR-induced voltage responses at increasing stimulation

frequencies from 2 to 25 Hz. **(D)** Comparison of rise time constants in the two models and in wild type cones. In all panels: Light stimulations were performed at  $8.7 \cdot 10^{16}$  photons  $\text{cm}^{-2} \text{s}^{-1}$  and 590 nm, if not stated otherwise. n = number of cells. Values are mean  $\pm$  SEM.

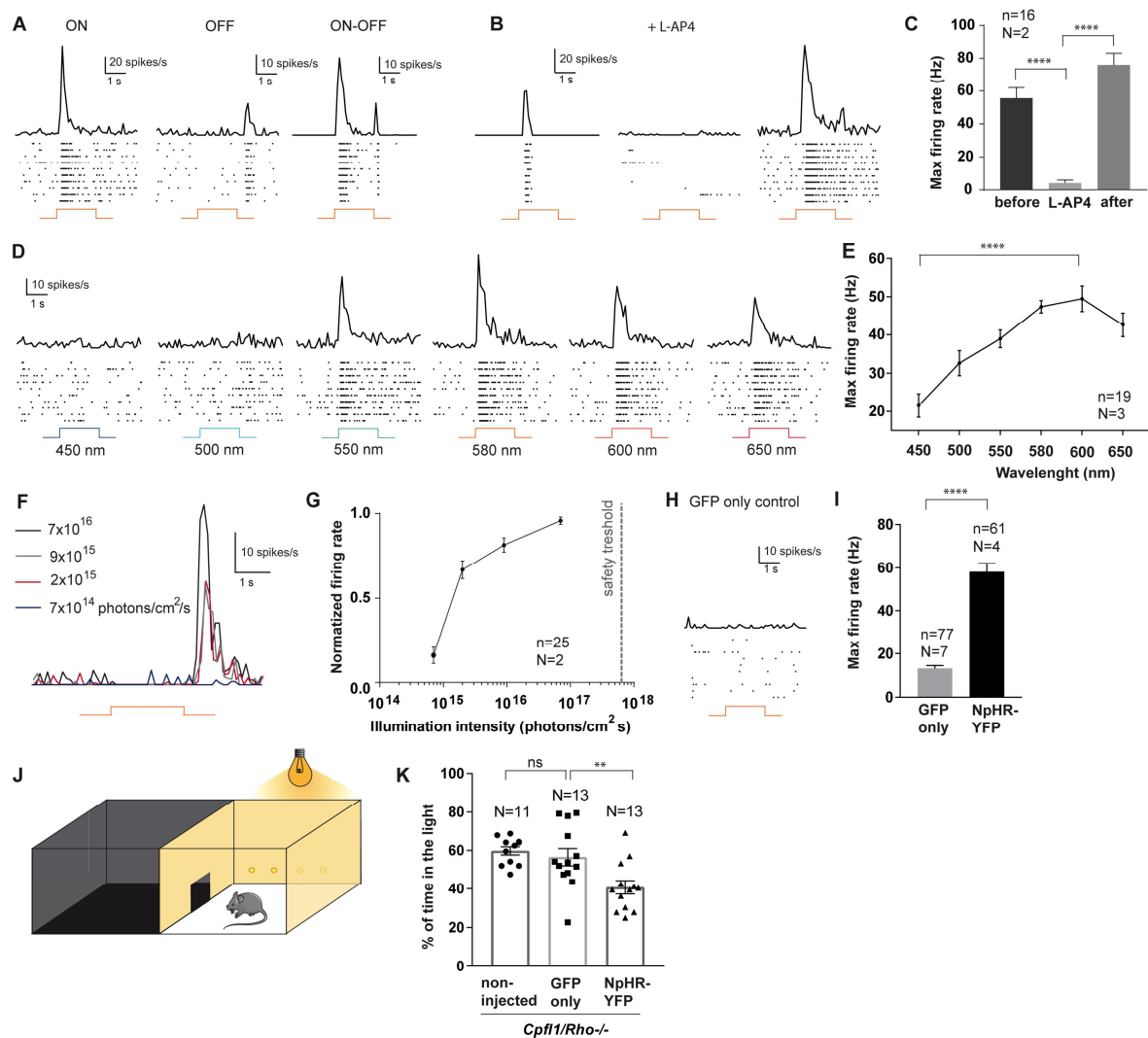


**Figure 3. NpHR-triggered responses from transplanted photoreceptors are transmitted to retinal ganglion cells (RGCs) and induce light avoidance behaviour in blind mice.**

(A-I) Averaged spike responses obtained from multi-electrode array (MEA) recordings shown as PSTH (peristimulus time histograms) and raster plots recorded in transplanted *Cpfl1/Rho*<sup>-/-</sup> mice (stimulation: 580 nm,  $7 \times 10^{16}$  photons  $\text{cm}^{-2} \text{s}^{-1}$ ). **(A)** Representative traces from three RGCs responding either with an ON-, OFF-, or ON/OFF-response pattern. **(B)** Representative traces from a cell before, during ON bipolar cell blockade, and after wash-out, and **(C)** quantification of maximum firing rates for these conditions. **(D)** Representative responses to wavelengths ranging from 450 nm to 650 nm. **(E)** Quantification of RGC action spectrum (shown for OFF responses). The cells reach their peak firing rate at 580 nm (ON responses, data not shown) and 600 nm (OFF responses). **(F)** PSTHs of a single RGC responding to

stimuli of increasing intensities (from  $7 \times 10^{14}$  to  $7 \times 10^{16}$  photons  $\text{cm}^{-2} \text{s}^{-1}$ ). **(G)** Intensity curve. The dashed line indicates the maximum light intensity allowed in the human eye at 590nm (European Parliament and Council of the European Union, 2006; International Commission on Non-ionizing Radiation Protection, 2013). **(H)** Unresponsive cell from a control retina transplanted with GFP only-expressing photoreceptors. **(I)** Maximum firing rate in mice treated with GFP only photoreceptors versus mice treated with NpHR-photoreceptors (shown for ON responses). **(J)** Schematic representation of the dark/light box test. **(K)** Percentage of time spent in the light compartment for: non-treated *Cpfl1/Rho*<sup>-/-</sup> mice, *Cpfl1/Rho*<sup>-/-</sup> mice treated with GFP only photoreceptors, and *Cpfl1/Rho*<sup>-/-</sup> mice treated with NpHR-photoreceptors (illumination: 590 nm,  $2.11 \times 10^{15}$  photons  $\text{cm}^{-2} \text{s}^{-1}$ ). In all panels: N = number of retinas, n = number of cells. Values are mean  $\pm$  SEM. Statistical significance assessed using Mann-Whitney Student's test (\*\* p<0,01; \*\*\*\* p<0,0001; ns – not significant).

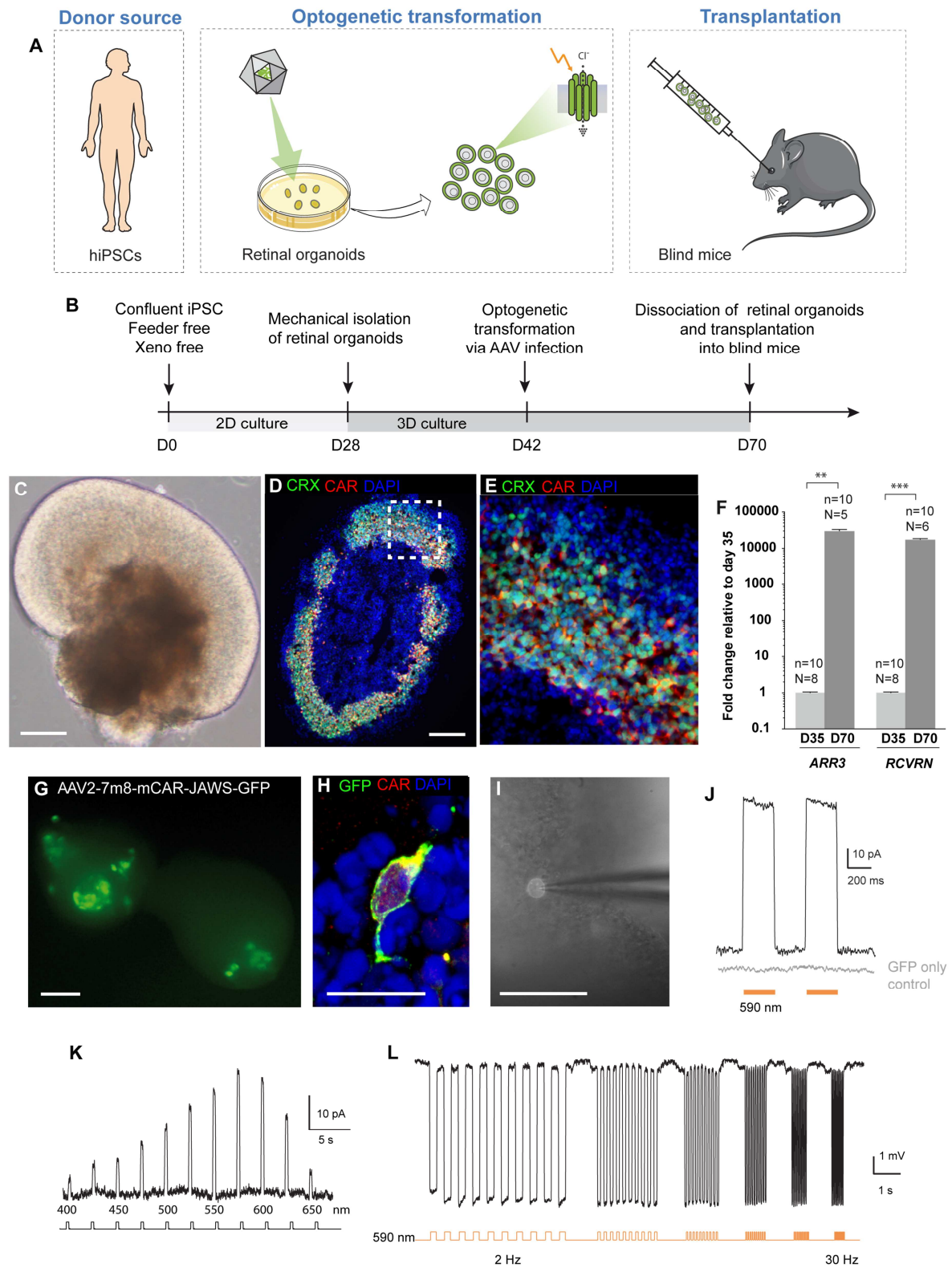


**Figure 4. Jaws-expressing photoreceptors, derived from hiPSCs, are sensitive to light.**

**(A)** Human iPSCs were differentiated towards retinal organoids and were infected with AAV-mCar-Jaws-GFP. After further maturation, cells were dissociated and iPSC-derived photoreceptors were transplanted into blind mice. **(B)** Schematic diagram of the differentiation and viral transformation of retinal organoids. **(C)** Bright-field image of a retinal organoid at D30 of differentiation. **(D, E)** Characterization of a representative retinal organoid at D70, depicting a thick layer of photoreceptors immunoreactive for CRX (green) and CAR (red). **(F)** Real time qRT-PCR analysis of photoreceptor specific markers *CAR (ARR3)* and *RCVRN*. N = number of biological replicates, n = number of organoids. Values are mean  $\pm$  SEM. Statistical significance assessed using Mann-Whitney Student's test (\*\*  $p < 0,01$ ; \*\*\*  $p < 0,001$ ). **(G)** Live GFP fluorescence observed at D54 (12 days post infection). **(H)** A single cone photoreceptor stained with GFP (green) and CAR (red) at D70. **(I)** Bright field/epifluorescence image of a GFP<sup>+</sup> cell patched inside a retinal organoid at D70 of differentiation. Scale bars: C,D,G,I: 100  $\mu$ m; E,H: 25  $\mu$ m. **(J-L)** Patch-clamp data from Jaws-cones within organoids. The resting membrane potential (RMP) of Jaws-expressing photoreceptors in the dark (at 0 current) for the recordings presented in the figure was  $-41,7 \pm 3,9$  mV. Stimulation at 590 nm if not stated otherwise. **(J)** Photocurrent responses after stimulation with 2 consecutive flashes at  $3.5 \cdot 10^{17}$  photons  $\text{cm}^{-2} \text{s}^{-1}$ , absence of response in GFP only-expressing cones is shown in grey. **(K)** Photocurrent action spectrum corresponding to a Jaws-cone stimulated at wavelengths ranging from 400 nm to 650 nm. Maximal responses were obtained at 575 nm (at  $8.7 \cdot 10^{16}$  photons  $\text{cm}^{-2} \text{s}^{-1}$ ). **(L)** Modulation of Jaws-induced voltage responses at increasing stimulation frequencies from 2 to 30 Hz.

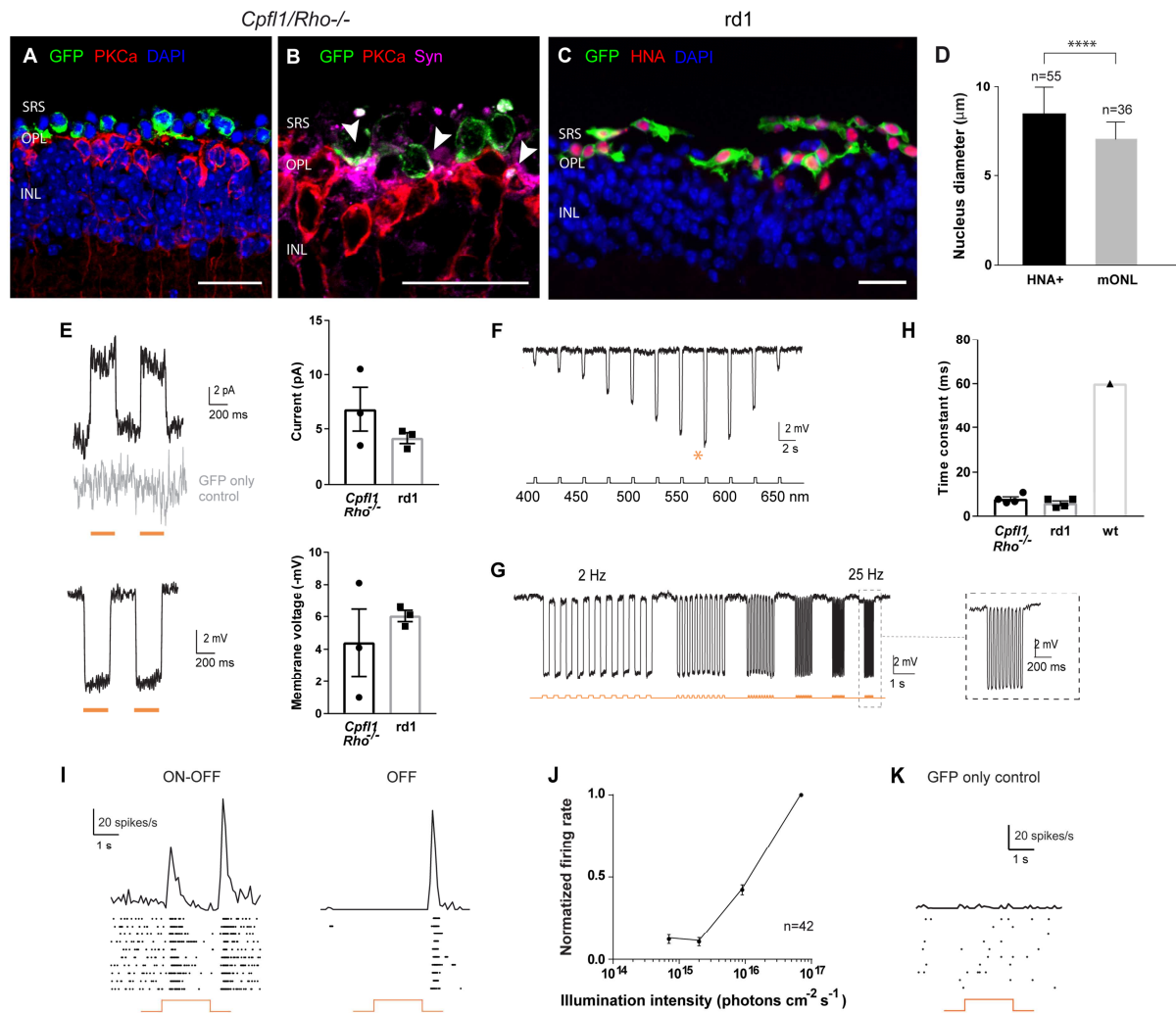


**Figure 5. Transplanted photoreceptors, derived from hiPSCs, integrate into the retina of blind mice and display Jaws induced light responses that are transmitted to retinal ganglion cells (RGCs).**

Immunofluorescence analysis on vertical sections 4 weeks after transplantation of Jaws-cone-treated *Cpfl1/Rho*<sup>-/-</sup> (A,B) and rd1 (C) retinas. **(A)** Transplanted cells (green) overlies host PKC $\alpha$  bipolar cells (red), DAPI counterstaining (blue). **(B)** Immunofluorescence against GFP (green), PKC $\alpha$  (bipolar cells, red) and synaptophysin (synapses, magenta). Arrows point to synaptic connections. **(C)** GFP<sup>+</sup> Jaws-cones co-express Human Nuclear Antigen (HNA). Scale bars: 20  $\mu\text{m}$ . SRS – subretinal space, OPL – outer plexiform layer, INL – inner nuclear layer. **(D)** Measurement of nuclear size of HNA<sup>+</sup> cells, transplanted in end-stage rd1 mice, and cells in the ONL of a wild type mouse. (E-H) Patch-clamp data from Jaws-cones after transplantation into blind mice. The RMP of Jaws-photoreceptors at 0 current was  $-40,8 \pm 5,2$  mV. Stimulation at 590 nm if not stated otherwise. **(E)** Left, representative

photocurrents (top) and voltage hyperpolarization (bottom) after stimulation with 2 consecutive flashes, absence of the response in GFP only cones shown in grey. Right, comparison of response amplitudes of Jaws-cones in different models (top, mean photocurrent peak; bottom, mean voltage peak). **(F)** Voltage action spectrum corresponding to a Jaws-expressing cell stimulated at wavelengths from 400 nm to 650 nm. Maximal responses were obtained at 575 nm. **(G)** Temporal properties: Jaws-induced hyperpolarization at increasing stimulation frequencies from 2 to 25 Hz. **(H)** Comparison of response rise time constant between Jaws-cones transplanted in *Cpfl1/Rho<sup>-/-</sup>* and rd1 models, and wild type cones. (I-K) Averaged spike responses obtained from MEA recordings shown as PSTH and raster plots from a transplanted *Cpfl1/Rho<sup>-/-</sup>* mouse. **(I)** Representative examples of two RGCs responding either with an ON/OFF or OFF-response (stimulation: 580 nm,  $7 \times 10^{16}$  photons  $\text{cm}^{-2} \text{s}^{-1}$ ). **(J)** Intensity curve. **(K)** Unresponsive cell from a control retina transplanted with GFP only cones. In all panels: n = number of cells. Values are mean  $\pm$  SEM. Statistical significance assessed using Mann-Whitney Student's test (\*\*\*\* p<0,0001).

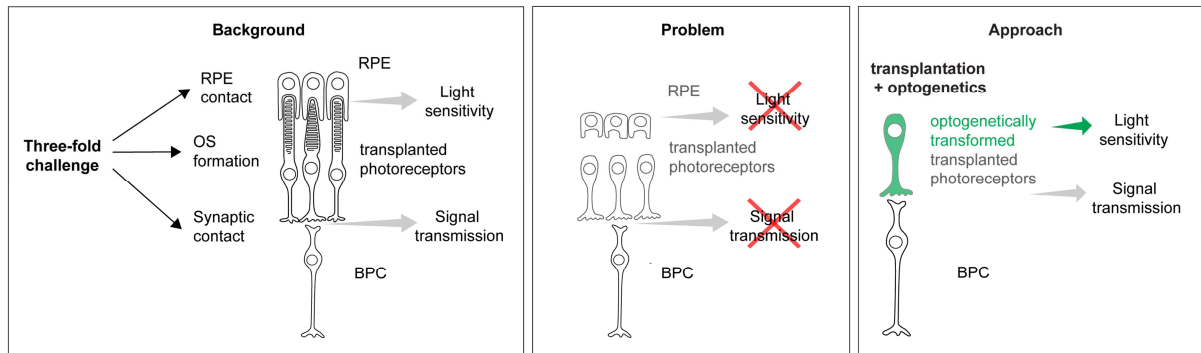


**Figure 6. Schematic illustrating the three-fold challenge in photoreceptor cell replacement.**

In order to provide visual improvement, transplanted photoreceptors need to form functional OS, retain in close contact to the RPE to maintain light sensitivity, and develop synaptic connection to host bipolar cells for signal transmission. After transplantation into animals with severely degenerated ONL, photoreceptors fail to develop normal OS structure and establish correct polarity with respect to host RPE. In addition, in retinal degeneration, the RPE is often compromised alongside photoreceptors. All this undermines the success of photoreceptor replacement. We therefore introduced a hyperpolarizing microbial opsin into the photoreceptors before transplantation, developing an OS- and RPE-independent approach for vision restoration in late stage retinal degeneration. RPE – retinal pigment epithelium, PR – photoreceptors, BPC – bipolar cells.

## Materials and methods

### ***Animals***

Wild type C57BL/6 mice (Janvier Laboratories) were used as a source of photoreceptor precursor donor cells. The following two models are both models of late stage degeneration and were used as cell recipients. Cone photoreceptor function loss 1/rhodopsin-deficient double-mutant *Cpfl1/Rho*<sup>-/-</sup> mice (Santos-Ferreira et al., 2016b) were provided by Marius Ader and rederived by Charles River Laboratory. The line was the result of crossing Cone photoreceptor function loss 1 (*Cpfl1*) mice (Chang et al., 2002) with rhodopsin knock-out mice (*Rho*<sup>-/-</sup>) (Humphries et al., 1997). The outcome were mice with no functional photoreceptors starting from eye opening and with the ONL degenerating to one row of cell bodies by 10 to 12 weeks (Santos-Ferreira et al., 2016b). Retinal degeneration 1 (rd1) mice (*C3Hrd/rd*) (Vicgian et al., 1992) were provided by Thierry Leveillard. The retina in these mice degenerates to a single row of cones by 3 weeks of age (Carter-Dawson et al., 1978; LaVail and Sidman, 1974).

All mice were housed under a 12-hour light-dark cycle with free access to food and water. All animal experiments and procedures were approved by the local animal experimentation ethics committee (Le Comité d'Ethique pour l'Expérimentation Animale Charles Darwin) and were carried out according to institutional guidelines in adherence with the National Institutes of Health guide for the care and use of laboratory animals as well as the Directive 2010/63/EU of the European Parliament.

### ***AAV production***

Recombinant AAVs were produced as previously described using the co-transfection method on HEK293 cells (ATCC CRL-1573), harvested 24-72 hours post transfection and purified by iodixanol gradient ultracentrifugation (Choi et al., 2007). The 40% iodixanol fraction was collected after a 90 minute spin at 59 000 rpm. Concentration and buffer exchange was performed against PBS containing 0.001% Pluronic. AAV vector stocks titers were then determined based on real-time quantitative PCR titration method (Aurnhammer et al., 2012) using SYBR Green (Thermo Fischer Scientific).

### ***AAV-infection of photoreceptor precursors***

Wild type mice (C57BL/6J) at P2 were anesthetized on ice. Eyelids were cut and 1  $\mu$ l of AAV9 2YF carrying eNpHR gene under the control of human rhodopsin promoter and fused to the fluorescent reporter eYFP (AAV9 2YF hRho-eNpHR-eYFP), or of AAV9 2YF hRho-GFP in the case of GFP only-expressing controls, was injected bilaterally using an ultrafine 34-gauge Hamilton syringe.

### ***Isolation and purification of rod precursors with magnetic activated cell sorting (MACS)***

2 days following the AAV injections in P2 mice, at P4, retinas were isolated from the injected wild type mice and cells were enriched using CD73 cell surface marker before transplantation, as described previously (Eberle et al., 2011; Koso et al., 2009). Shortly, retinas were dissociated, pelleted by centrifugation (5 minutes at 300g), resuspended in 500  $\mu$ L MACS buffer (phosphate-buffered saline [PBS; pH 7.2], 0.5% BSA, 2 mM EDTA) and incubated with 10  $\mu$ g/mL rat anti-mouse CD73 antibody (BD Biosciences) for 5 minutes at 4°C. After washing in MACS buffer, cells were centrifuged for 5 minutes at 300g. The cell pellet was resuspended in 480  $\mu$ L MACS buffer and 120  $\mu$ L goat anti-rat IgG magnetic beads (Miltenyi Biotec). The suspension was incubated for 15 minutes at 4°C followed by a washing step with MACS buffer and centrifugation. Before magnetic separation, the cells were resuspended in MACS buffer and filtered through a 30- $\mu$ m pre-separation filter.

The cell suspensions were applied onto a LS column fixed to a MACS separator. The column was rinsed with 3 x 3 mL MACS buffer and the flow through was collected (CD73 negative cells). The column was removed from the magnet and placed in a new collection tube. The CD73-positive fraction was eluted by loading 5 mL MACS buffer and immediately applying the plunger supplied with the column. The cells were then counted and concentrated to about 200.000 cells/ $\mu$ l.

### ***Maintenance of hiPSC culture***

All experiments were carried out using hiPSC-2 cell line, previously established from human dermal fibroblasts from an 8-year-old boy (gift from P. Rustin, INSERM U676, Paris) by co-

transfecting OriP/EBNA1-based epi-somal vectors pEP4EO2SEN2K (3µg), pEP4EO2SET2K (3µg) and pCEP4-M2L (2µg) (Addgene) via nucleofection (Nucleofector 4D, V4XP, withDT-130 program; Lonza) 31, and recently adapted to feeder-free conditions 23. Cells were kept at 37°C, under 5% CO<sub>2</sub> /95% air atmosphere, and 20% Oxygen tension and 80-85% of humidity. Colonies were cultured with Essential 8™ medium (Thermo Fisher Scientific) in culture dishes coated with truncated recombinant human Vitronectin and passaged once a week, as previously described (Reichman et al., 2017).

### ***Generation of retinal organoids from human iPS cells***

Human iPSC were differentiated towards retinal organoids following an optimised protocol based on the one published by Reichman et al. (Reichman et al., 2017). Briefly, hiPSC-2 cell line was expanded to 80% confluence in Essential 8™ medium were switched in Essential 6™ medium (Thermo Fisher Scientific). After 3 days, cells were moved to the Proneural medium (Table S1). The medium was changed every 2-3 days. After 4 weeks of differentiation, neural retina-like structures grew out of the cultures and were mechanically isolated. Pigmented parts, giving rise to RPE were carefully removed. The extended 3D culture in Maturation medium (Table S1) allowed the formation of retinal organoids. Addition of 10 ng/ml Fibroblast growth factor 2 (FGF2, Preprotech) at this point favoured the growth of retinal organoids and the commitment towards retinal neurons instead of RPE lineage (Fuhrmann, 2010). In order to promote the commitment of retinal progenitors towards photoreceptors, we specifically blocked Notch signalling for a week starting at day 42 of differentiation using the gamma secretase inhibitor DAPT (10 µM, Selleckchem) (Jadhav et al., 2006). Floating organoids were cultured in 6 well-plates (10 organoids per well) and medium was changed every 2 days. Table S1 summarizes the formulations for the different media used.

### ***Infection of retinal organoids with AAV expressing Jaws***

Introduction of Jaws optogene was done by one single infection at day 42 at a  $5 \times 10^{10}$  vg per organoid. Retinal organoids were infected with an AAV with an engineered capsid, AAV2-7m8 (Dalkara et al., 2013) carrying Jaws gene under the control of mouse cone arrestin promoter and fused to the fluorescent reporter GFP (AAV2-7m8-mCAR-Jaws-GFP). For GFP

only-expressing controls, an infection with AAV2-7m8-mCAR-GFP was carried out in the same manner as mentioned above.

### ***Monolayer cultures of dissociated cells***

After removal of any pigmented tissue, 70-day old retinal organoids were collected and washed 3 times in Ringer solution (Table S1) before dissociation with two units of pre-activated papain at 28.7 u/mg (Worthington) in Ringer solution for 25 min at 37°C. Once a homogeneous cell suspension was obtained after pipetting up and down, papain was deactivated with Proneural medium (Table S1). Cells were centrifuged and resuspended in pre-warmed Proneural medium. Dissociated retinal cells were plated onto coverslips coated with human recombinant 30 µg/cm<sup>2</sup> Laminin (Sigma-Aldrich) and 150 µg/cm<sup>2</sup> Poly-L-Ornithine in 24 well-plates (Garita-Hernandez et al., 2013). Monolayers were incubated at 37°C in a standard 5% CO<sub>2</sub> / 95% air incubator and medium was changed every 2 days for the next 15-20 days, before immunostaining.

### ***Preparation of cells for transplantation***

At day 70 of differentiation retinal organoids were dissociated using papain as described above to obtain a single cell suspension in Proneural medium (Table S1). Cell suspension was filtered through a 30 µm mesh (Miltenyi Biotec) to remove residual aggregates. After counting, cells were centrifuged and resuspended in Proneural medium at a concentration of 300.000 cells/µl.

### ***RNA isolation and Real time RT-qPCR***

Total RNA isolation was performed using a NucleoSpin RNA XS kit (Macherey-Nagel), according to the manufacturer's instructions. RNA concentration and purity were determined using a NanoDrop ND-1000 Spectrophotometer (Thermo Fisher Scientific).

Reverse transcription was carried out with 250 ng of total RNA using the QuantiTect retrotranscription kit (Qiagen). Quantitative PCR (qPCR) reactions were performed using Taqman Array Fast plates and Taqman Gene expression master mix (Thermo Fisher Scientific) in an Applied Biosystems real-time PCR machine (7500 Fast System). All samples

were normalized against a housekeeping gene (18S) and the gene expression was determined based on the  $\Delta\Delta\text{CT}$  method. Average values were obtained from at least 4 biological replicates. The primer sets and MGB probes (Thermo Fisher Scientific) labelled with FAM for amplification are listed in Table S2.

### ***Transplantation procedure***

Mice were sedated by intraperitoneal injection of ketamine (50mg/kg) and xyazine (10mg/kg) and the pupils were dilated with tropicamide drops. The mice were placed onto a heating pad to maintain the temperature at 37 °C. A drop of Lubrithal eye gel (Dechra) was used to keep the eyes hydrated during the surgery. A small glass slip was put on the eye to enable visualization through the Leica Alcon ophthalmic microscope while a syringe with a blunt, 34-gauge needle was inserted tangentially through the conjunctiva and sclera. 1  $\mu\text{l}$  of cell suspension including 200.000-300.000 cells was injected between the retina and RPE, into the subretinal space, creating a bullous retinal detachment. Injections were performed bilaterally. Mice were placed into a warm chamber after the surgery until their awakening.

### ***Tissue preparation and immunostaining***

70-day old organoids were washed in PBS and fixed in 4% paraformaldehyde for 10 min at 4°C before they were incubated overnight in 30% sucrose (Sigma-Aldrich) in PBS. Organoids were embedded in gelatin blocks (7.5% gelatin (Sigma-Aldrich), 10% sucrose in PBS) and frozen using isopentane at -50°C.

At least 4 weeks after transplantation, mice were sacrificed by CO<sub>2</sub> inhalation followed by a cervical dislocation. The eyeballs were removed, fixed in 4% paraformaldehyde for 30 minutes at room temperature (RT) and incubated overnight at 4°C in PBS containing 30% (w/v) sucrose (Sigma-Aldrich). The eyes were then dissected to obtain only the back of the eye with the retina and the RPE. The samples were embedded in gelatin blocks (7.5% gelatin (Sigma-Aldrich), 10% sucrose in PBS), frozen with liquid nitrogen and stored at -80°C.

10 $\mu\text{m}$  thick sections were obtained using a Cryostat Microm and mounted on Super Frost Ultra Plus® slides (Menzel Gläser). Cryosections were washed in PBS (5 min, RT) and then

permeabilised in PBS containing 0.5 % Triton X-100 during 1 hour at RT. Blocking was done with PBS containing 0.2% gelatin, 0.25% Triton X-100 for 30 min at RT and incubation with primary antibodies was performed overnight at 4°C. Primary antibodies used are listed in Table S3. After incubation with primary antibodies, sections were washed with PBS containing 0.25% Tween20 and incubated with fluorochrome-conjugated secondary antibodies (1/500 dilution) for 1 hour at RT. After successive washing in PBS-Tween20, nuclei were counterstained with DAPI (4'-6'-diamino-2-phenylindole, dilactate; Invitrogen-Molecular Probe, Eugene, OR) at a 1/1000 dilution. Samples were further washed in PBS and dehydrated with 100% ethanol before mounting using fluoromount Vectashield (Vector Laboratories).

### ***FISH for Y chromosome detection***

For combined chromosomal fluorescence in situ hybridization (Y chromosome FISH) and immunohistochemistry, retinas from female *Cpfl1/Rho<sup>-/-</sup>* mice transplanted with male donor-derived rod precursors (N=5) were collected 4 weeks post-surgery, fixed for 1 h at 4 °C with freshly prepared 4% paraformaldehyde (Merck Millipore), incubated in 30% sucrose overnight, followed by cryopreservation. After embedding and freezing in OCT medium, cryosections of 12 µm were rehydrated with 10mM sodium citrate buffer pH 6, antigen retrieval performed (80 °C , 25 min). Sections were washed in PBS for 5min and incubated with a primary antibody against GFP (1:500; AbCam) overnight at RT, followed by incubation with secondary antibody conjugated to AlexaFluor 488 (1:1,000; Jackson ImmunoResearch) overnight at RT. Next, slides were post-fixed in 2% PFA for 10 minutes, pre-treated with 50% formamide for 1 hour at RT, then hybridization of the XMP Y orange probe (Metasystems) to the Y chromosome was performed. To allow the probe to penetrate the tissue, samples were incubated for 3 h at 45 °C in a HybEZ II oven. Then, samples were transferred to a hot block at 80 °C for 5min, to denature DNA. Afterwards, probes were hybridized with DNA for 2 days at 37 °C. Posthybridization consisted of 3x15 min washes with 2x SCC at 37 °C and 2x5min stringency washes with 0.1 x SCC at 60 °C. Finally, sections were counterstained with DAPI (1:15,000; Sigma). The samples were imaged and quantified using structured illumination microscopy (SIM; ApoTome, Zeiss).

For information on antibodies used, see Table S3.

### ***Quantification of YFP<sup>+</sup> cells after transplantation***

Transplanted host eyes (N=6) were processed and cryosectioned as described for the Y chromosome FISH experiment, and subsequently stained for GFP (1:800; Abcam) and photoreceptor specific marker RCVRN (1:5000; Millipore), followed by secondary antibody staining (1:1,000; Jackson Immunoresearch). Every fourth serial section from whole experimental retinas was used to quantify the total amount of YFP<sup>+</sup> photoreceptors. Cells were counted from images obtained with the NanoZoomer microscope (Hamamatsu Photonics). Following these cell counts, the resulting value was multiplied by four to estimate the total amount of labelled cells per retina.

For information on antibodies used, see Table S3.

### ***Nuclear size measurements***

Measurements of the nuclear size were performed with FIJI software (NIH) on immunostained sections of rd1 transplanted retinas and compared with the values in wild type mice.

### ***Image acquisition***

Immunofluorescence was observed using a Leica DM6000 microscope (Leica microsystems) equipped with a CCD CoolSNAP-HQ camera (Roper Scientific) or using an inverted or upright laser scanning confocal microscope (FV1000, Olympus) with 405, 488, 515 and 635 nm pulsing lasers. The images were acquired sequentially with the step size optimized based on the Nyquist–Shannon theorem. The analysis was conducted in FIJI (NIH). Images were put into a stack, Z-sections were projected on a 2D plane using the MAX intensity setting in the software's Z-project feature, and the individual channels were merged.

Images of Y chromosome labelled retinas were acquired using SIM (ApoTome, Zeiss). Samples stained to perform quantification of surviving YFP<sup>+</sup> photoreceptors were imaged with the NanoZoomer microscope (Hamamatsu Photonics).

### ***Light stimulation of NpHR-positive, Jaws-positive, and control cells***

Light-triggered responses were measured in donor cells before transplantation – *in vivo* in AAV-injected wild-type donor mice at P12 for NpHR<sup>+</sup>, and in retinal organoids and monolayer cultures from dissociated organoids for Jaws<sup>+</sup> cells. In order to measure light responses we used a monochromatic light source (Polychrome V, TILL photonics). After patching the cells we first stimulated them with a pair of 590 nm full-field light pulses. Then the activity spectrum was measured by using light flashes ranging from 400 nm to 650 nm (separated by 25 nm steps). Finally we generated light pulses at different frequencies ranging between 2 and 30 Hz in order to determine the temporal response properties of NpHR and Jaws in AAV-transduced cells. Stimulation and analysis were performed using custom-written software in Matlab (Mathworks) and Labview (National Instruments). We used light intensities ranging between  $1 \times 10^{16}$  and  $3.2 \times 10^{17}$  photons  $\text{cm}^{-2} \text{s}^{-1}$ .

### ***Live two-photon imaging and patch-clamp recordings of donor cells before and after transplantation into blind mouse***

Donor mouse retina (P12), retinal organoids or monolayer cultures from dissociated organoids were placed in the recording chamber of the microscope at 36°C in oxygenated (95% O<sub>2</sub>/5% CO<sub>2</sub>) Ames medium (Sigma-Aldrich) during the whole experiment. Transplanted mice were sacrificed by CO<sub>2</sub> inhalation followed by quick cervical dislocation, and eyeballs were removed. Retinas from *Cpfl1/Rho<sup>-/-</sup>* or rd1 mice were isolated in oxygenated (95% O<sub>2</sub>/5% CO<sub>2</sub>) Ames medium and whole mount retinas with ganglion cell side down were placed in the recording chamber of the microscope at 36°C for the duration of the experiment for both live two-photon imaging and electrophysiology.

A custom-made two-photon microscope equipped with a 25x water immersion objective (XLPlanN-25x-W-MP/NA1.05, Olympus) equipped with a pulsed femto-second laser (InSight™ DeepSee™ - Newport Corporation) were used for imaging and targeting AAV-transduced fluorescent photoreceptor cells (eYFP<sup>+</sup> or GFP<sup>+</sup> cells). Two-photon images were acquired using the excitation laser at a wavelength of 930 nm. Images were processed offline using ImageJ (NIH). A CCD camera (Hamamatsu Corp.) was also used to visualize the donor cells or the retina under infrared light.

For patch-clamp recordings, AAV-transduced fluorescent cells were targeted with a patch electrode under visual guidance using the reporter tag's fluorescence. Whole-cell recordings were obtained using the Axon Multiclamp 700B amplifier (Molecular Device Cellular Neurosciences). Patch electrodes were made from borosilicate glass (BF100-50-10, Sutter Instrument) pulled to 7-10 M $\Omega$  and filled with 115mM K Gluconate, 10mM KCl, 1mM MgCl<sub>2</sub>, 0.5mM CaCl<sub>2</sub>, 1.5mM EGTA, 10mM HEPES, and 4mM ATP-Na<sub>2</sub> (pH 7.2). Photocurrents were recorded while voltage-clamping cells at a potential of -40 mV. Some cells were also recorded in current-clamp (zero) configuration, hence allowing us to monitor the membrane potential during light stimulations.

A monochromatic light source (Polychrome V, TILL photonics) was used to stimulate cells during electrophysiological experiments and hence record photocurrents or changes in cells membrane potential. First, in order to measure the activity spectrum of NpHR and Jaws, we used 300 ms light flashes ranging from 650 to 400 nm (25 nm steps; interstimulus interval 1.5 s) at a constant light intensity of  $1.2 \times 10^{16}$  photons cm<sup>-2</sup> s<sup>-1</sup>. Then this light source was used at a constant wavelength of 590 nm to generate light pulses at different frequencies (ranging from 2 to 30 Hz) in order determine the temporal response properties of optogenetic proteins used. Stimuli were generated using custom-written software in LabVIEW (National Instruments) and output light intensities were calibrated using a spectrophotometer (USB2000+, Ocean Optics).

### ***Multi-electrode array recordings and data analysis***

The mice were euthanized, the retinas isolated, cut each in two pieces and placed in Ames medium bubbled with 95% O<sub>2</sub> and 5 % CO<sub>2</sub>. Each piece was mounted separately on a cellulose membrane soaked overnight in poly-L-lysine and gently pressed against a 60- $\mu$ m electrode spacing 252 channel multi-electrode array chip (256MEA60/10iR, Multi Channel Systems) with retinal ganglion cells facing the electrodes. The piece remained perfused with oxygenated Ames medium at 34°C throughout the experiment. Full field light stimuli were applied with a Polychrome V monochromator (TILL Photonics) driven by a STG2008 stimulus generator (Multichannel Systems) using custom written stimuli in MC\_Stimulus II (MC\_Stimulus II Version 3.4.4, Multichannel Systems).

The basic stimulus pattern applied was 10 repetitions of 2-second stimuli of 580 nm light (close to excitation maximum for NpHR and Jaws) and intensity of  $7 \times 10^{16}$  photons  $\text{cm}^{-2} \text{s}^{-1}$ , with 10 seconds intervals. To assess temporal dynamics of responding cells, stimuli ranging from 1 ms to 2 s were played to the retina. Action spectrum of optogenetic protein-expressing cells was examined by playing sets of stimuli of different wavelengths (450 nm, 500 nm, 550 nm, 580 nm, 600 nm, 650 nm; 10 stimuli of 2 seconds with 10 second intervals for each wavelength). To determine sensitivity of responding cells, stimuli of lower intensities were also used ( $1 \times 10^{14}$ ,  $7 \times 10^{14}$ ,  $2 \times 10^{15}$  and  $9 \times 10^{15}$  photons  $\text{cm}^{-2} \text{s}^{-1}$ ). During the experiments aiming to show that the light responses are really coming from the ONL, we perfused the tissue with L-AP4 (50  $\mu\text{M}$ ) for at least 20 minutes before the recordings in order to block input from photoreceptors to ON bipolar cells. This was followed by at least 15 minute rinse with Ames medium and another set of light stimulation to observe whether the response returned.

Data were acquired using the MC\_Rack software (MC\_Rack v4.5, Multi Channel Systems). RGC responses were amplified and sampled at 20 kHz. Data was then filtered with a 200 Hz high pass filter and individual channels were spike sorted using template matching and cluster grouping based on principal component analysis of the waveforms in Spike2 software v.7 (Cambridge Electronic Design Ltd). The raster plots and peristimulus time histogram data (bin size of 10 ms) were constructed in MATLAB using custom scripts from spike-sorted channels and further processed in Adobe Illustrator CS4 (Adobe Systems) for presentation.

Maximum firing rate for each responding cell was measured in the 2 seconds after the onset (for ON-responding cells) or 2 seconds after the offset (for OFF-responding cells) of the stimulus. The number of cells and mice that were used for quantitative analysis are stated in Figure legends. Error bars were calculated over cells.

### ***Light/dark box***

For light-avoidance behaviour, we used a custom-made dark-light box (Bourin and Hascoet, 2003; Sengupta et al., 2016) of dimensions 36 cm x 20 cm x 18 cm, divided longitudinally into two equal sized compartments with a non-transparent wall with a 7 cm x 5 cm hole in

the middle. The light compartment was equipped with eight 590 nm LEDs (Cree XP-E, amber, Lumitronix) 3 cm from the bottom of the box. A light intensity of  $2.05 \times 10^{16}$  photons  $\text{cm}^{-2} \text{s}^{-1}$  was used for all the experiments. The mice were habituated in the dark for at least 2 hours prior the testing. Each mouse was introduced into the light compartment and was left in the box for at least 5 minutes before the start of illumination. The lights were turned on when the mouse was in the light compartment and were left on for at least 5 minutes. The behaviour of the mice was recorded with a camera and subsequently analysed manually by recording the times spent in each compartment after the start of illumination, and using the Smart Vision Tracking Software (Harvard Apparatus). The mouse's head was used to define the compartment it occupied.

### ***Statistical analyses***

Data was analysed with GraphPad Prism and it was expressed as mean  $\pm$  standard error of mean (SEM). Comparisons between values were analysed using unpaired two-tailed non-parametric Mann-Whitney Student's test. A level of  $p < 0.05$  was considered significant. The labels used were: \* for  $p < 0.05$ , \*\* for  $p < 0.01$ , \*\*\* for  $p < 0.001$  and \*\*\*\* for  $p < 0.0001$ .

**Acknowledgments:** We thank Thierry Léveillard for providing the rd1 mice and Cheryl Craft for providing the hCAR antibody. We are thankful to Romain Caplette, Olivier Marre and Stéphane Deny for their help with the MEA recordings and analysis. We thank Abhishek Sengupta for the construction of the light/dark box. We are grateful to Mélissa Desrosiers and Camille Robert for AAV productions and the fundraising department of the Vision Institute for LCL fundraising.

**Funding:** This study was supported by an ERC Starting Grants (OPTOGENRET, 309776/JD, REGNETHER 639888/DD), the Centre National de la Recherche Scientifique (CNRS), the Institut National de la Santé et de la Recherche Médicale (INSERM), Labex-Lifesenses (DD, JD), Sorbonne Université, Marie Curie CIG (334130, Retinal Gene Therapy, DD), INSERM, ANR grant RHU Light4Deaf (DD,OG), LCL Foundation (DD), Deutsche Forschungsgemeinschaft (DFG) FZT 111, Center for Regenerative Therapies Dresden, FZT 111 Cluster of Excellence (MA), DFG Grant AD375/6-1 (MA), BMBF Research Grant 01EK1613A (MA).

**Author contributions:** MG optimized differentiation and AAV mediated transduction of hiPSC-derived retinal organoids, performed culture, histology, imaging, qPCR, designed experiments and wrote the manuscript. ML performed cell transplantation, imaging, histology, cell quantification, MEA recordings, behavioral experiments, designed experiments and wrote the manuscript. AC performed patch-clamp recordings and 2-photon imaging. LG generated hiPSC-derived retinal organoids, performed cell transplantation, imaging, histology and behavioral experiments. FR performed behavioral experiments. TF contributed to cell transplantation. SG and OB performed Y chromosome FISH experiments and quantification, cell transplantation, histology and imaging. GG and SR helped to optimize hiPSC cultures and differentiation protocols. SP and JAS provided scientific input, financial and administrative support. OG provided hiPSCs and gave feedback on the manuscript. MA provided *Cpfl1/Rho*<sup>-/-</sup> mice, contributed to cell transplantation and gave feedback on the manuscript. DD and JD designed experiments and wrote the manuscript.

**Competing interests:** The authors have submitted a patent application (application number PCT/EP2017/074125) based on the results reported in this paper.

**Reporting summary:** Further information on experimental design is available in the Nature Research Reporting Summary linked to this article.

**Data availability:** The data that support the findings of this study are available from the corresponding author upon reasonable request.

**Code availability:** The MATLAB codes that were used to represent MEA raster and PSTH data are available from the corresponding author upon reasonable request.

## Supplementary data

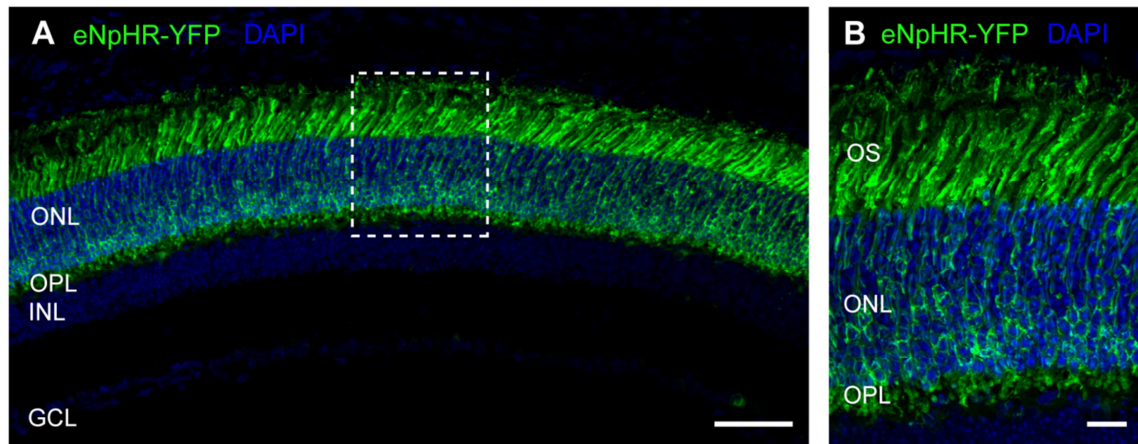


**Figure S1. NpHR expression in rod photoreceptors of donor mice.** (A, B) A vertical section of a wild type mouse retina at P10, after AAV9-2YF-hRho-NpHR-YFP has been intravitreally injected at P2. As the mouse retina is vastly dominated by rod photoreceptors, we selected a promoter that drives gene expression in rods, in order to generate a high number of donor cells for transplantation studies (see also Buskamp et al., 2010 (Buskamp et al., 2010)). NpHR-expressing cells are shown in green, the sample was counterstained with DAPI. Scale bars, A 50  $\mu$ m, B 10  $\mu$ m. OS – outer segments, ONL – outer nuclear layer, OPL – outer plexiform layer, INL – inner nuclear layer, GCL – ganglion cell layer.

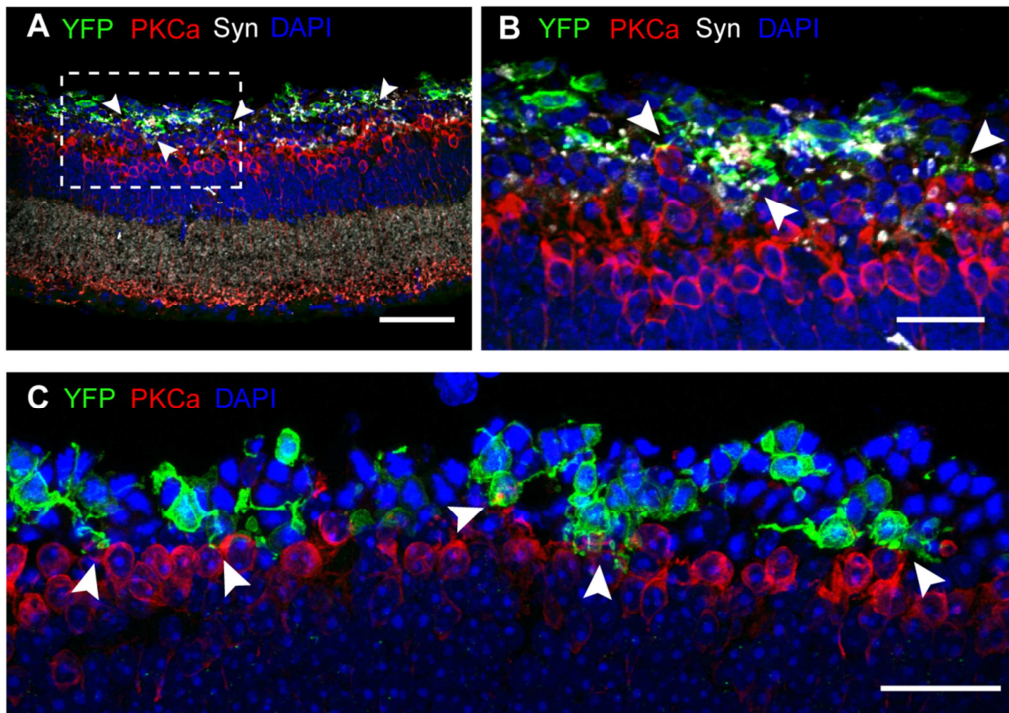


**Figure S2. Transplanted NpHR-rod precursors are located in close apposition to the host INL and express the synaptic marker synaptophysin.**

**(A-C)** *Cpfl1/Rho*<sup>-/-</sup> retinas transplanted with NpHR-photoreceptors showing YFP<sup>+</sup> cells (green) located on top of host PKC $\alpha$  bipolar cells (red), with (A,B) or without synaptophysin staining (C), 4 weeks after transplantation. Arrows point to potential synaptic connections with host rod bipolar cells. Scale bars: A: 50  $\mu$ m; B,C: 25  $\mu$ m. SRS – subretinal space, OPL – outer plexiform layer, INL – inner nuclear layer, GCL – ganglion cell layer.

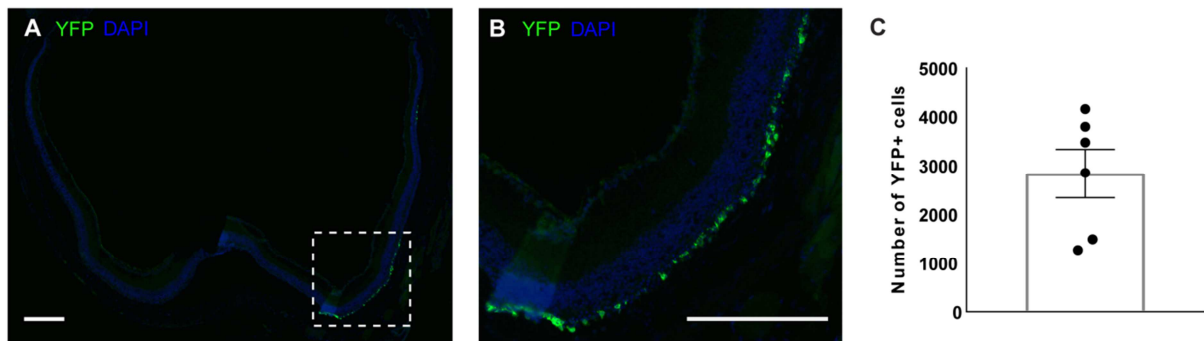


**Figure S3: Quantification of YFP<sup>+</sup> cells after transplantation of NpHR-rod precursors.**

**(A,B)** A section of a representative section of a *Cpfl1/Rho*<sup>-/-</sup> retina showing immunohistochemistry staining of YFP (green) with DAPI counterstaining (blue) 4 weeks after transplantation into a P60 animal. Scale bars: 200  $\mu$ m. **(C)** Quantification of YFP<sup>+</sup> cells from 6 individual experimental retinas (N=6). On average,  $2830 \pm 493$  cells (mean  $\pm$  SEM) per retina remained in the subretinal space 4 weeks post-transplantation, corresponding to  $1.42 \pm 0.25\%$  of all cells transplanted.

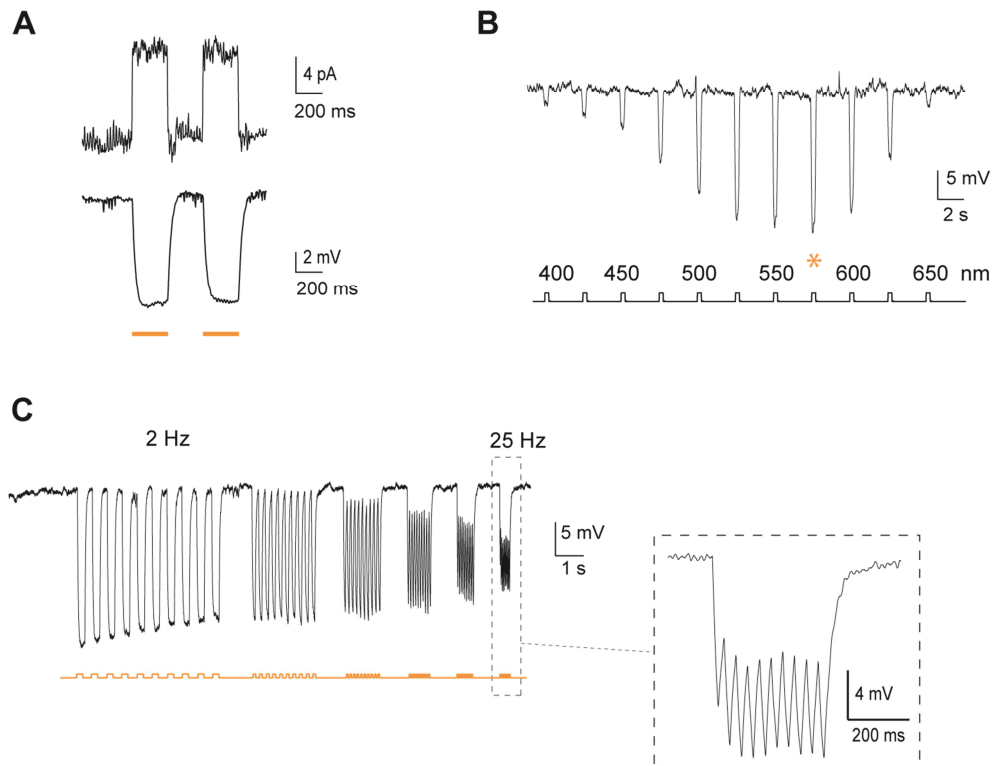


**Figure S4. NpHR-expressing photoreceptor precursors transplanted into rd1 mouse respond to light.**

**(A)** Light-evoked responses of NpHR-photoreceptor stimulated with two consecutive flashes at 590 nm (top, current response; bottom, voltage response). **(B)** Voltage response action spectrum corresponding to a NpHR-photoreceptor stimulated at wavelengths ranging from 400 nm to 650 nm, in rd1 retina. Maximal responses were obtained at 575 nm. **(C)** Temporal properties: Modulation of NpHR-induced voltage response at increasing stimulation frequencies from 2 to 25 Hz.

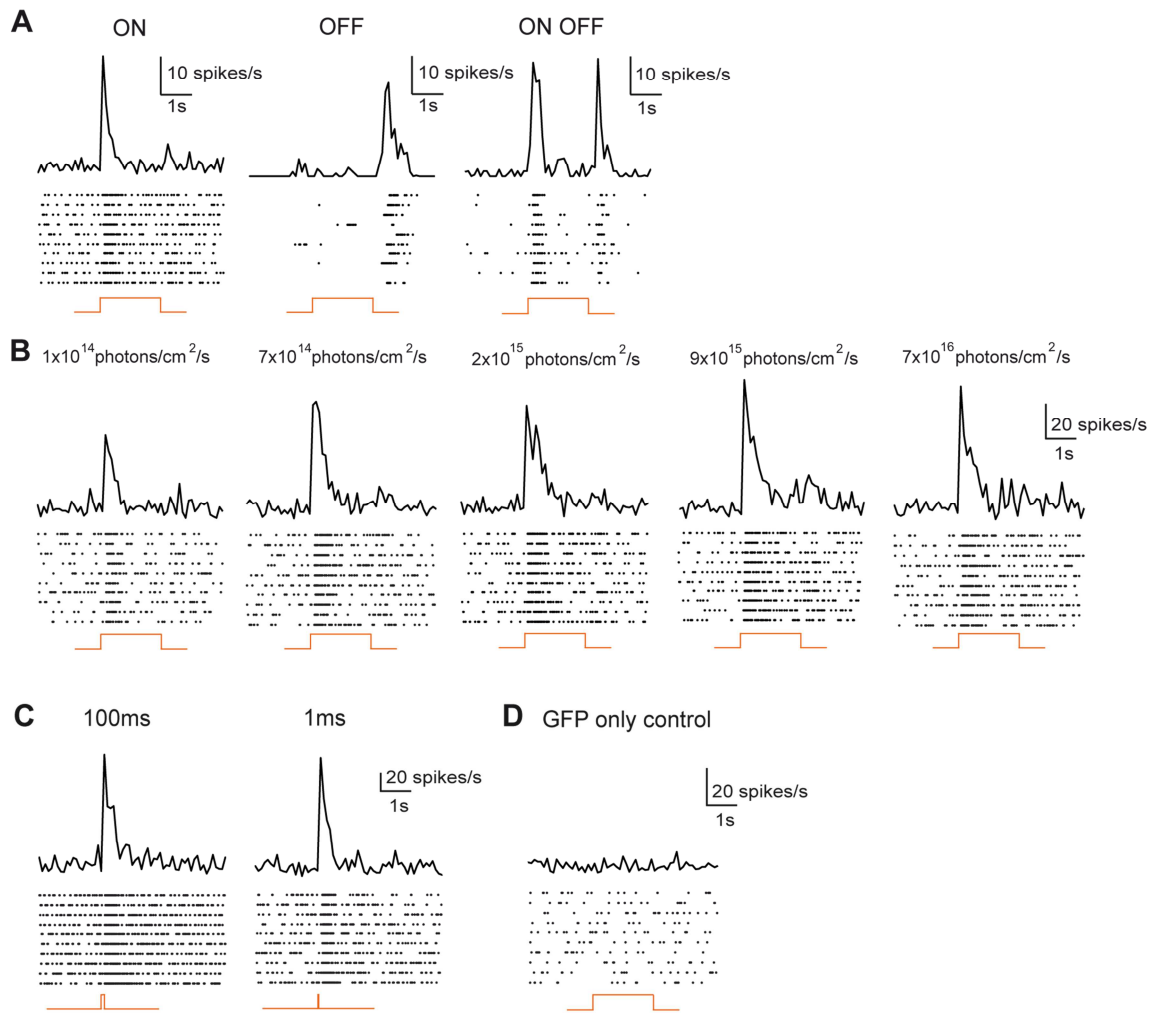


**Figure S5. Halorhodopsin-triggered RGC responses in rd1 mice.**

**(A)** RGCs firing responses shown as PSTH and raster plots recorded from transplanted rd1 mice, showing examples of cells responding with an ON-, OFF- or an ON/OFF-response (stimulation: 580 nm,  $7 \times 10^{16}$  photons cm<sup>-2</sup> s<sup>-1</sup>). **(B)** Responses from a representative cell at lower light intensities and **(C)** shorter light pulses. **(D)** Unresponsive cell from a control retina transplanted with GFP only photoreceptors.

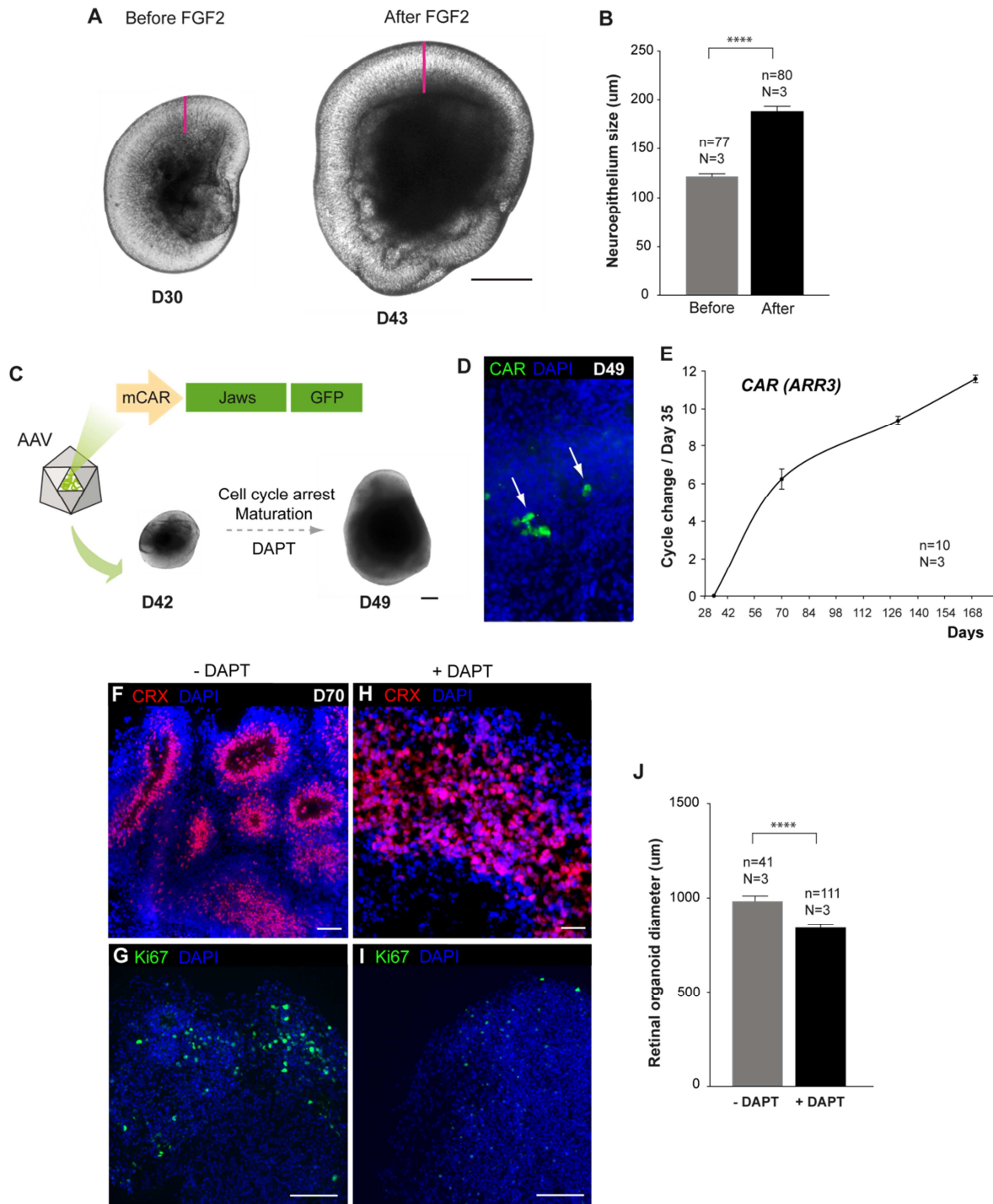


**Figure S6. Growth of the neuroepithelium in retinal organoids treated with FGF2 and the effect of Notch inhibition on retinal organoidogenesis and photoreceptor commitment.**

**(A)** Representative micrographs of a retinal organoid before (D30) and after (D43) treatment with FGF2. Pink bars show the neuroepithelium thickness quantified in **(B)**. **(B)** Neuroepithelium thickness before ( $111.5 \pm 5.30 \mu\text{m}$ ) and after ( $154.45 \pm 5.30 \mu\text{m}$ ) addition of FGF2. **(C)** Schematics of the introduction of Jaws using an AAV vector and representative

images of a retinal organoid before (D42) and after (D49) infection and treatment with DAPT. **(D)** Immunofluorescence analysis of retinal organoids showing the first CAR positive cells (green arrows) at D49 of differentiation. **(E)** Time course analysis of *CAR* by qPCR in differentiating retinal organoids. Data is expressed as cycle change in PCR expression level relative to D35 of differentiation. (F-I) Organoid cryosections after 70 days of differentiation without (F and G) or with DAPT (H and I). **(J)** Measurement of the diameter of retinal organoids on D56 of differentiation with and without DAPT treatment. Scale bars A,C,F,H 200  $\mu\text{m}$ ; E,G,I 50  $\mu\text{m}$ . In all panels: N = number of biological replicates, n = number of organoids. Values are mean  $\pm$  SEM. Statistical significance assessed using Mann-Whitney Student's test (\*\*\*\*  $p < 0,0001$ ).

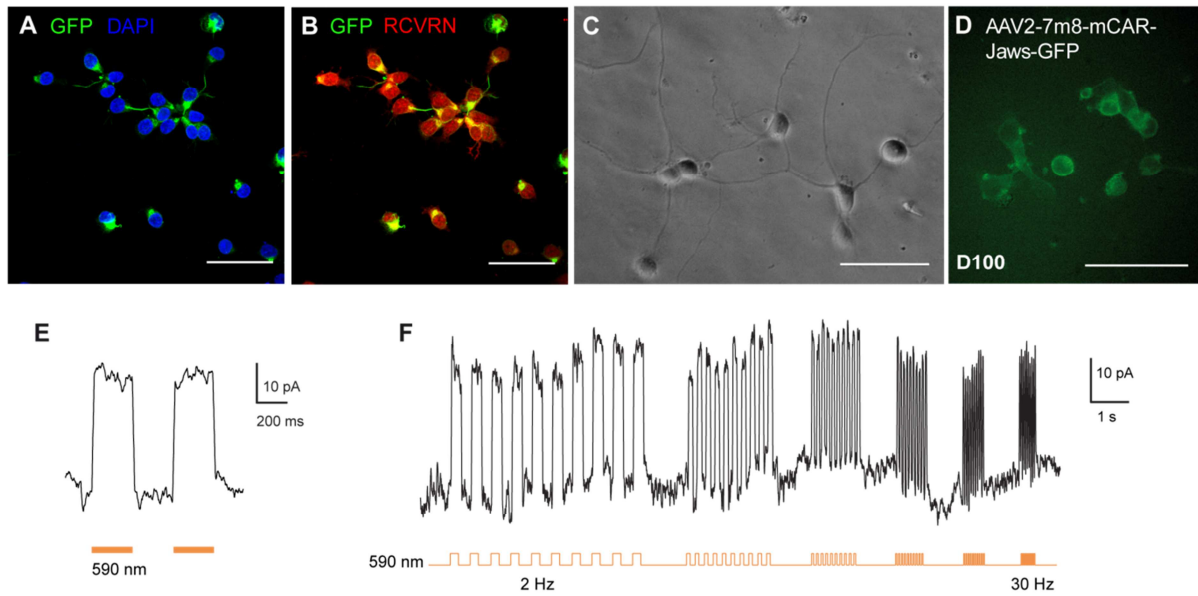


**Figure S7. Physiological analysis of monolayer cultures derived from dissociated retinal organoids.**

(A,B) Monolayer cultures stained with antibodies against GFP and DAPI **(A)**, and photoreceptor marker RCVRN and GFP **(B)**. **(C)** Jaws-cones used for patch-clamp recordings in D100 monolayer cultures. **(D)** A two-photon laser microscope image of Jaws-cones. Scale bars 50  $\mu\text{m}$ . **(E)** Light-evoked photocurrent responses of Jaws-cones in the monolayer stimulated with two consecutive flashes of light at 590 nm. **(F)** Modulation of Jaws-induced responses at increasing stimulation frequency (2 to 30 Hz).

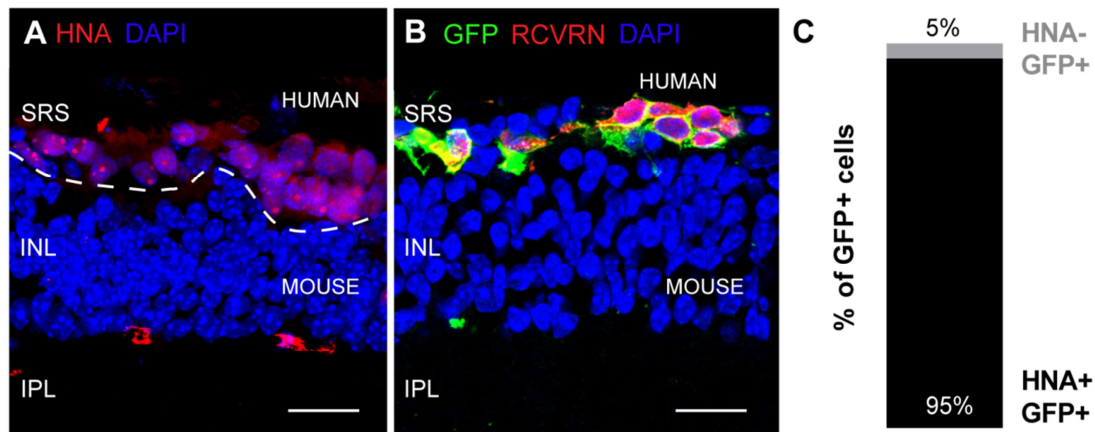


**Figure S8. Expression of human and photoreceptor markers in transplanted GFP<sup>+</sup> cells.**

**(A)** Immunostaining of transplanted cells against human nuclear antibody (HNA, red) showed human cells lie over the rd1 host INL. The white dashed line depicts the border between transplanted cells (top) and mouse host tissue (bottom). **(B)** Jaws-GFP transplanted cells co-expressed photoreceptor specific marker RCVRN (red) confirming the photoreceptor identity of GFP positive cells. Nuclei were counterstained with DAPI (blue). Scale bars 20  $\mu$ m. SRS – subretinal space, INL – inner nuclear layer, IPL – inner plexiform layer. **(C)** Quantification of HNA<sup>+</sup>/GFP<sup>+</sup> cells, representing transplanted hiPSC-derived photoreceptors, and HNA<sup>-</sup>/GFP<sup>+</sup> cells, representing cells where GFP<sup>+</sup> staining could be the result of material transfer, from 3 individual experimental rd1 retinas (5 weeks old at the time of transplantation; N=3). The vast majority of GFP<sup>+</sup> cells co-expressed HNA ( $95.07 \pm 1.6$  %; mean  $\pm$  SEM).

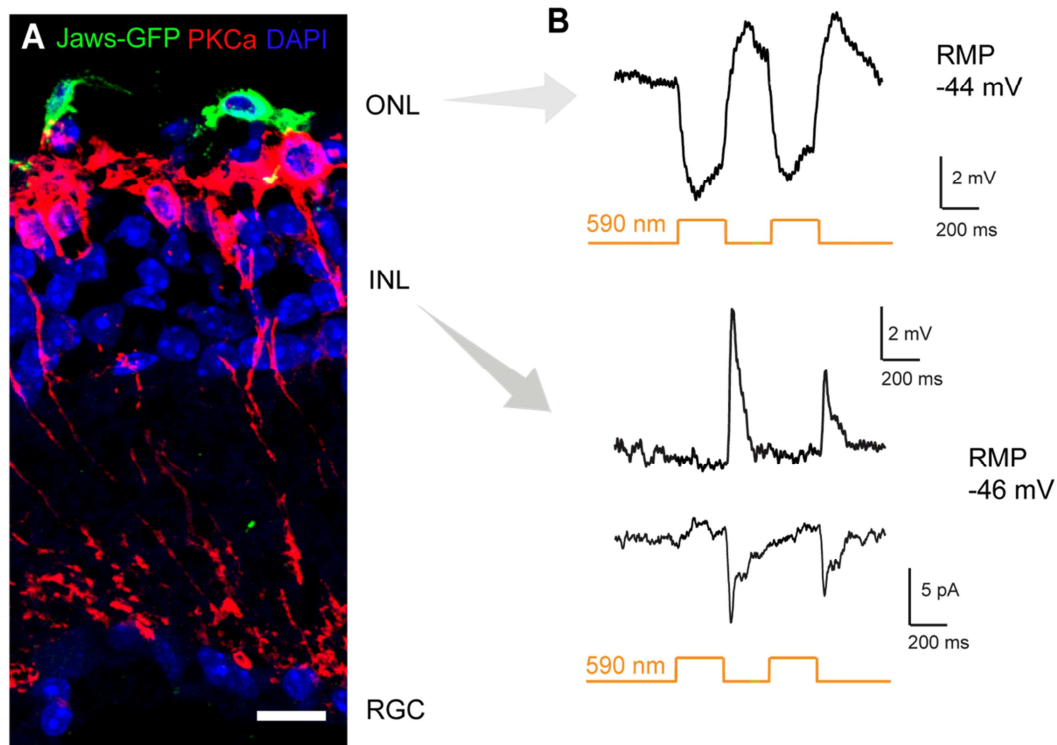


**Figure S9: Signal transduction from photoreceptors to the second order neurons in rd1 mouse transplanted with Jaws-photoreceptors.**

**(A)** An rd1 retina after transplantation, showing Jaws-cones located on top of the PKCa-stained recipient INL. ONL – outer nuclear layer, INL – inner nuclear layer, GCL – ganglion cell layer. **(B)** Photocurrents elicited by a Jaws-expressing donor cell transplanted in an rd1 retina (top) and the response (voltage and current) recorded from a second order OFF-neuron (bottom).

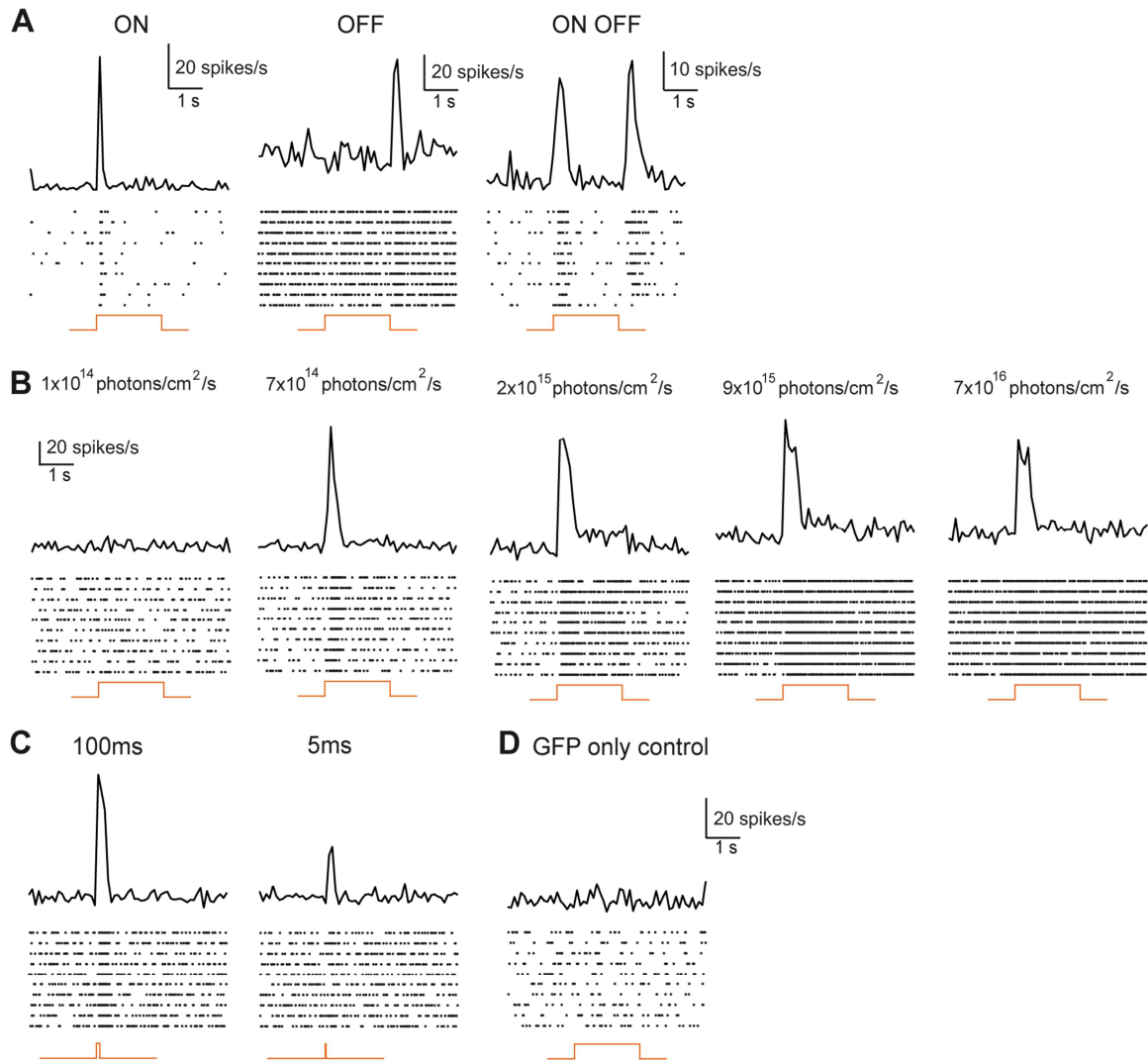


**Figure S10. Jaws-triggered RGC responses in rd1 mice.**

**(A)** RGCs firing responses shown as PSTH and raster plots recorded from transplanted rd1 mice, showing examples of cells responding with an ON-, OFF- or ON/OFF-response (stimulation: 580 nm,  $7 \times 10^{16}$  photons cm<sup>-2</sup> s<sup>-1</sup>). **(B)** Responses at lower light intensities and **(C)** shorter light pulses. **(D)** An unresponsive cell from a control retina transplanted with GFP only-expressing cones.

**Table S1. Media formulation.**

<i>Medium</i>	<i>Formulation</i>
<b>Proneural medium</b>	Essential 6™ Medium (Gibco, A1516401) N-2 supplement (100X) 1% (Gibco, 17502048) Penicillin-Streptomycin 1% (Gibco, 15140122)
<b>Maturation medium</b>	DMEM/F-12 (Gibco, 11320074) B-27™ Supplement (50X), serum free 2% (Gibco, 17504044) MEM Non-Essential Amino Acids Solution (100X) 1% (Gibco 11140035) Penicillin-Streptomycin 1% (Gibco, 15140122)
<b>Ringer solution</b>	NaCl 155 mM, KCl 5 mM, CaCl <sub>2</sub> 2 mM, NaCl <sub>2</sub> 1 mM, NaH <sub>2</sub> PO <sub>4</sub> 2 mM, HEPES 10 mM, glucose 10 mM

**Table S2. List of TaqMan® Gene Expression ID Assays used for qRT-PCR.**

<i>Gene symbols</i>	<i>Assays IDs</i>
<b>18S</b>	18S-Hs99999901_s1
<b>CONE ARRESTIN</b>	ARR3-Hs00182888_m1
<b>RECOVERIN</b>	RCVRN-Hs00610056_m1

**Table S3. List of primary antibodies used for immunostaining.**

<i>Antibody</i>	<i>Reference</i>	<i>Catalogue number</i>	<i>Species</i>	<i>Dilution</i>
<b>hCAR</b>	Gift from Cheryl Craft	-	Rabbit	1:20,000
<b>CRX</b>	Abnova	<a href="#">H00001406-M02</a>	Mouse	1:5,000
<b>GFP</b>	Abcam	<a href="#">ab13970</a>	Chicken	1:500
<b>HNA</b>	Millipore	<a href="#">MAB4383</a>	Mouse	1:200
<b>Ki67</b>	BD <a href="#">pharmagenPharmagen</a>	<a href="#">550609</a>	Mouse	1:200
<b>PKCα</b>	Santa Cruz	<a href="#">sc-208</a>	Rabbit	1:100
<b>RCVRN</b>	Millipore	<a href="#">AB5585</a>	Rabbit	1:5,000-1:2,000
<b>Synaptophysin</b>	Sigma	<a href="#">SAB4502906</a>	Mouse	1:200

**Table S4. A list of all mice used to generate figures, with specified strain, experimental group, experiment type, and ages at the time of transplantation and at the time of experiment.**

<i>Fig.</i>	<i>Strain</i>	<i>Experimental group</i>	<i>Experiment type</i>	<i>Age at trans-plantation (weeks)</i>	<i>Age at the time of experiment (weeks)</i>	<i>Number of mice (N)</i>	
<b>Fig. 1</b>	<b>B</b>	<i>Cpfl1</i> <i>Rho</i> <sup>-/-</sup>	Non-injected control	IHC	-	16	1
	<b>C, D</b>	<i>Cpfl1</i> <i>Rho</i> <sup>-/-</sup>	Mouse NpHR-precursors	IHC	13	16	1
	<b>E</b>	rd1	Non-injected control	IHC	-	10	1
	<b>F, G</b>	rd1	Mouse NpHR-precursors	IHC	4	10	1
	<b>I</b>	<i>Cpfl1</i> <i>Rho</i> <sup>-/-</sup>	Mouse NpHR-precursors	FISH	9	13	3

<b>Fig. 2</b>	<b>A</b>	<i>Cpfl1</i> <i>Rho</i> <sup>-/-</sup>	Mouse NpHR-precursors	Patch-clamp	9	11	1	
		<i>Cpfl1</i> <i>Rho</i> <sup>-/-</sup>	Mouse NpHR-precursors	Patch-clamp	10	14	1	
		<i>Cpfl1</i> <i>Rho</i> <sup>-/-</sup>	Mouse GFP only-precursors	Patch-clamp	6.5	11	1	
		rd1	Mouse NpHR-precursors	Patch-clamp	11	13	1	
	<b>B, C</b>	<i>Cpfl1</i> <i>Rho</i> <sup>-/-</sup>	Mouse NpHR-precursors	Patch-clamp	10	14	1	
		<b>D</b>	<i>Cpfl1</i> <i>Rho</i> <sup>-/-</sup>	Mouse NpHR-precursors	Patch-clamp	9	11	1
	<b>Fig. 3</b>	<b>A-G, I</b>	<i>Cpfl1</i> <i>Rho</i> <sup>-/-</sup>	Mouse NpHR-precursors	MEA	10	14	2
			<i>Cpfl1</i> <i>Rho</i> <sup>-/-</sup>	Mouse NpHR-precursors	MEA	10	13.5	1
			<i>Cpfl1</i> <i>Rho</i> <sup>-/-</sup>	Mouse NpHR-precursors	MEA	10	13	1
		<b>H, I</b>	<i>Cpfl1</i> <i>Rho</i> <sup>-/-</sup>	Mouse GFP only-precursors	MEA	5	9	2
<i>Cpfl1</i> <i>Rho</i> <sup>-/-</sup>			Mouse GFP only-precursors	MEA	5.5	10	1	
<i>Cpfl1</i> <i>Rho</i> <sup>-/-</sup>			Mouse GFP only-precursors	MEA	6.5	11	2	
<i>Cpfl1</i> <i>Rho</i> <sup>-/-</sup>			Mouse GFP only-precursors	MEA	12	16	1	
<b>K</b>		<i>Cpfl1</i> <i>Rho</i> <sup>-/-</sup>	Non-injected control	Light/dark box	-	7.5	4	
		<i>Cpfl1</i> <i>Rho</i> <sup>-/-</sup>	Non-injected control	Light/dark box	-	8	2	
		<i>Cpfl1</i> <i>Rho</i> <sup>-/-</sup>	Non-injected control	Light/dark box	-	9	2	
	<i>Cpfl1</i> <i>Rho</i> <sup>-/-</sup>	Non-injected control	Light/dark box	-	13	3		
	<i>Cpfl1</i> <i>Rho</i> <sup>-/-</sup>	Mouse GFP only-precursors	Light/dark box	5	8	4		
	<i>Cpfl1</i> <i>Rho</i> <sup>-/-</sup>	Mouse GFP only-precursors	Light/dark box	10.5	13.5	2		
	<i>Cpfl1</i> <i>Rho</i> <sup>-/-</sup>	Mouse GFP only-precursors	Light/dark box	12	15	2		
	<i>Cpfl1</i> <i>Rho</i> <sup>-/-</sup>	Mouse GFP only-precursors	Light/dark box	13	16	3		
	<i>Cpfl1</i> <i>Rho</i> <sup>-/-</sup>	Mouse GFP only-precursors	Light/dark box	16	21	1		
	<i>Cpfl1</i> <i>Rho</i> <sup>-/-</sup>	Mouse NpHR-precursors	Light/dark box	9	12	6		
	<i>Cpfl1</i> <i>Rho</i> <sup>-/-</sup>	Mouse NpHR-precursors	Light/dark box	10	13.5	4		
	<i>Cpfl1</i> <i>Rho</i> <sup>-/-</sup>	Mouse NpHR-precursors	Light/dark box	18	23	3		

<b>Fig. 5</b>	<b>A, B</b>	<i>Cpfl1</i> <i>Rho</i> <sup>-/-</sup>	Human Jaws- cones	IHC	10.5	14	1
	<b>C</b>	rd1	Human Jaws- cones	IHC	5	9	1
	<b>D</b>	rd1	Human Jaws- cones	IHC	5	9	3
	<b>E</b>	<i>Cpfl1</i> <i>Rho</i> <sup>-/-</sup>	Human Jaws- cones	Patch-clamp	10.5	14	2
		<i>Cpfl1</i> <i>Rho</i> <sup>-/-</sup>	Human GFP only-cones	Patch-clamp	7	10	1
		rd1	Human Jaws- cones	Patch-clamp	4	8	1
		rd1	Human Jaws- cones	Patch-clamp	5	9	1
	<b>F, G</b>	<i>Cpfl1</i> <i>Rho</i> <sup>-/-</sup>	Human Jaws- cones	Patch-clamp	10.5	14.5	1
	<b>H</b>	<i>Cpfl1</i> <i>Rho</i> <sup>-/-</sup>	Human Jaws- cones	Patch-clamp	10.5	14	2
		rd1	Human Jaws- cones	Patch-clamp	4	8	1
		rd1	Human Jaws- cones	Patch-clamp	5	9	1
	<b>I, J</b>	<i>Cpfl1</i> <i>Rho</i> <sup>-/-</sup>	Human Jaws- cones	MEA	10.5	14.5	1
	<b>K</b>	<i>Cpfl1</i> <i>Rho</i> <sup>-/-</sup>	Human GFP only-cones	MEA	7	10	1

# DISCUSSION

## Overcoming some of the present challenges of photoreceptor replacement therapy and optogenetics by combining the two

Despite many efforts in the field, vision restoration by photoreceptor replacement remains challenging. One of the key burning issues is the establishment and maintenance of OSs in transplanted photoreceptors under conditions of severe retinal degeneration. Recent studies have shown that the recipient environment is of great importance for successful integration and survival of transplanted cells (Barber et al., 2013). In animals with severely degenerated ONL at the time of transplantation, cells fail to develop **normal OS structures** (Barber et al., 2013; Barnea-Cramer et al., 2016; Eberle et al., 2012; Singh et al., 2013). The function of photoreceptor OSs is to absorb light and transduce this signal into a change of membrane potential, so it is difficult to fathom light sensitivity without these structures properly formed. However, there have been some reports of remaining photosensitivity in photoreceptors with short or no OSs (Reuter and Sanyal, 1984; Thompson et al., 2014). Thompson and colleagues used P90 rds mice that, as they stated, had a similar OS structural deficit than transplanted PSC-derived photoreceptors. These cells were able to support useful vision, suggesting that PCS-derived photoreceptor cell might have the potential to restore vision despite not having correctly formed OSs (Thompson et al., 2014). However, rds at P90 still have 60% of photoreceptors retained in the ONL, which accounts to many more cells than can currently be achieved by cell transplantation. As also supported by our own work, it is unlikely that low numbers of photoreceptors with profoundly abnormal OS morphology and significantly reduced light sensitivity could account for visual improvement. Cell grafts, transplanted as single cell suspensions, fail to establish **correct orientation and OS polarity with respect to host RPE** post-transplantation. RPE plays a critical role in photoreceptor structure and function maintenance. Due to constant light exposure and oxidative stress, photoreceptor OSs are constantly shed from the photoreceptors and phagocytosed by the RPE. This helps avoid photo-oxidative damage and maintains excitability of the photoreceptors. Furthermore, crucial steps of the visual cycle, the process in which all-*trans*-retinal is re-isomerized back into 11-*cis*-retinal, take place in the RPE cells. Photoreceptors are unable to make the conversion themselves. Thus, RPE plays a vital role in regenerating visual pigments in order to maintain their light sensitivity. The importance of

RPE-neural retina contact has been underlined by studies using experimental retinal detachment that have shown fast OS degeneration and photoreceptor cell death within a few days after RPE-retina separation (Sparrow et al., 2010).

Correct orientation of transplanted photoreceptors with their OSs facing and staying in close contact with the host RPE cells is therefore of great importance in photoreceptor replacement. The problem of orientation has been partially circumvented by transplanting retinal sheets, although due to frequent rosette formation, photoreceptors within these sheets also often end up not lying in apposition to RPE cells (Assawachananont et al., 2014; Mandai et al., 2017a). An additional complication in regard to RPE support to photoreceptors is that patients with degenerative diseases of the retina very often manifest **RPE degeneration along with photoreceptor degeneration**, especially in the late stages of disease (Wright et al., 2010). One of the main characteristic fundusoscopic features of RP is the bone spicule pigment, corresponding to melanin-containing RPE cells clustered around blood vessels in the inner retina, where they migrated after photoreceptor death (Li et al., 1995). AMD often displays progressive RPE degeneration, which results in degeneration of photoreceptors (Athanasίου et al., 2013). LCA patients can suffer severe and progressive loss of vision starting in the first years of life due to RPE65 retinol isomerase deficiency and photoreceptor degeneration (Cideciyan, 2010). This creates a worry that, even if correct orientation of grafted photoreceptors and OS formation could be achieved, defective RPE cells of the patients most probably would not be able to support the function of these newly provided photoreceptors. Cones require an additional intraretinal visual cycle that allows them rapid dark adaptation and continuous function under bright and rapidly changing light conditions. In **cone-specific visual cycle**, Müller cells within the neural retina convert all-*trans*-retinal back to 11-*cis*-retinol. Only cones, but not rods, can oxidize *cis*-retinol to *cis*-retinal, needed for pigment regeneration (Wang and Kefalov, 2011; Xue et al., 2017). It is yet to be examined if transplanted cones are capable of this complex interaction with Müller cells and chromophore oxidation.

Aiming to overcome these difficulties, we combined photoreceptor replacement with optogenetics. We expressed a hyperpolarizing microbial opsin in mouse donor-derived photoreceptor precursors or hiPSC-derived photoreceptors by AAV vector transduction before transplantation, and subsequently grafted these cells into the subretinal space of

blind mice lacking the ONL. What makes this approach so attractive is that the functionality of these optogenetically engineered photoreceptors is provided by the microbial opsin activity. In microbial opsins, conformational change caused by light absorption is directly coupled to ion movement across the membrane through these channels/pumps, creating a membrane current. Optogenetic proteins from the HR group such as the ones we used cause hyperpolarization in response to light, mimicking the normal physiological response of photoreceptors in light conditions. Optogenetic protein-expressing photoreceptors are functional regardless the lack of proper photoreceptor morphological traits, complex light-capturing apparatus within the OSs, or the phototransduction cascade. Furthermore, the photoisomerization of the chromophore in microbial opsins is reversible and both isomers remain covalently attached to the protein. This means, that no support from RPE or Müller cells is needed in order to recover the visual pigment.

We used two different hyperpolarizing microbial opsins in the course of this study, NpHR (NpHR2.0, **eNpHR**) and **Jaws**. This was because our work on donor-derived photoreceptor precursors started before Jaws was described (Chuong et al., 2014) and because NpHR performed well in mouse photoreceptors and photoreceptor precursors. However, NpHR is difficult to express at the cell membrane in primate tissues (Garita-Hernandez et al., 2018), likely because the trafficking signals used to engineer these bacterial proteins originated from rodent sequences (Gradinaru et al., 2008; Gradinaru et al., 2010). For these reasons, we transitioned to Jaws for the second part of the study using cells of human origin. Reports show that Jaws mediates higher photocurrents and is capable of restoring greater light sensitivity compared to previously described hyperpolarizing opsins. Its activation maximum is further shifted towards the red part of the spectrum (a 14-nm red shift compared to NpHR) (Chuong et al., 2014), which is important safely wise.

Because bipolar cells and RGCs can stay fairly intact for prolonged periods of time in patients with photoreceptor degeneration, **expressing optogenetic proteins in cells lying downstream from photoreceptors** has been widely explored (Berry et al., 2017; Bi et al., 2006; Chaffiol et al., 2017; Cronin et al., 2014; Lagali et al., 2008; Mace et al., 2015; Sengupta et al., 2016; Zhang et al., 2009). However, this approach bypasses the information processing normally conducted by the retinal circuitry. For example, studies that confer light sensitivity to RGCs lost both the processing occurring on the OPL as well as the IPL, resulting

in recovery of only ON RGC responses. In this approach, the retina might be missing the type of image pre-processing needed to achieve optimal vision.

Targeting bipolar cells allows keeping the IPL processing, and both ON and OFF responding RGCs were documented in some of these studies (Cronin et al., 2014; Mace et al., 2015; van Wyk et al., 2015). However, this approach was unable to recover complex visual functions such as lateral inhibition and directional selectivity. Furthermore, the number and density of bipolar cells is fairly small and targeting them with AAV vectors has proven difficult in primates. The very limited numbers of targeted bipolar cells would further limit the resolution of re-established vision.

Lastly, optogenetics has been implemented in the so-called **dormant cones** (Buskamp et al., 2010; Chuong et al., 2014). By this approach, re-sensitized photoreceptors activated all retinal cone pathways, drove sophisticated retinal circuit functions including directional selectivity and lateral inhibition, activated cortical circuits, and mediated visually guided behaviours. It was demonstrated that persisting cone cell bodies (~25%) were enough to induce RGC activity, even during later stages of degeneration in mouse models. Later studies showed that around 17% of RP patients with average age of 56 maintain dormant cones (Azoulay-Sebban, 2015).

For patients who have already gone beyond the loss of photoreceptors, transplantation of functional cones therefore offers all of the advantages of photoreceptor targeted optogenetics but can be applied in the majority of late stage RP patients that have already lost their cells. Our approach potentially allows recovery of sophisticated visual functions that cannot be recovered when conferring light sensitivity to bipolar cells or RGCs. At present, we have not yet conducted any tests to determine whether there was any recovery of directional selectivity or lateral inhibition in our treated retinas. It would be interesting to foresee such experiments in the future.

## Evaluation of synaptogenesis and considering alternative mechanisms

Once we have conferred light sensitivity to grafted photoreceptors by microbial opsin expression, the one thing that is still indispensable for visual improvement is transmission of the action potentials that were triggered by the photoreceptors, to the underlying retinal circuitry of the host. The majority of synaptogenesis occurs early in development and is not a general feature of adult retina. However, in the early stages of retinal degeneration, the loss of input from photoreceptors appears to trigger rewiring events in the inner retina (Marc and Jones, 2003; Marc et al., 2003). Bipolar cells have been observed to initially retract their dendrites, but then elongate them into the ONL in search of new synaptic partners (Haverkamp et al., 2006). Although this can eventually lead to inappropriate synaptic contacts, it may also represent an ideal time window for transplanted cells to initiate synaptic connections. It would be interesting to explore the reorganization mechanism and its time course more closely in mice and humans, and to determine whether intervening at the specific stage of retinal degeneration may allow us to use inner retinal remodeling to our advantage.

The numerous studies performed in the past that performed transplantations in mouse models with remaining endogenous photoreceptors and reported of proper synapse formation need to be re-evaluated in the light of the discovery of material transfer between host and graft photoreceptors. It is believed that the vast majority of labelled and at the time thought to be integrated cells, were indeed host photoreceptors that received reporter protein/RNA from overlaying grafted cells. It is not known whether any of the labelled cells displaying correctly formed synapses were indeed integrated transplanted cells.

Few studies attempted transplantation into severely degenerated models lacking the ONL (Barber et al., 2013; Barnea-Cramer et al., 2016; Eberle et al., 2012; Gonzalez-Cordero et al., 2017; Kruczek et al., 2017; Santos-Ferreira et al., 2016b; Singh et al., 2013). In addition, interestingly, the commonly used rd1 strain, the most popular mouse model of severe outer retinal degeneration, was recently discovered to possess a mutation in the *Gpr179* gene. This mutation affects a GPCR localized in the dendrites of ON bipolar cells, eliminating ON bipolar cell function (Nishiguchi et al., 2015). This explains the many failed earlier attempts

to repair retinal function in this model, our own included – we were unable to detect responses from the RGCs when transplanting microbial opsin-expressing photoreceptors into this classical rd1 model. However, after replacing this rd1 strain with one where the *Gpr179* mutation has been eliminated via backcrossing to a C57BL/6j background (Vicgian et al., 1992), we were able to detect functional restoration at the level of RGCs. However, several photoreceptor transplantation studies did report of functional improvements in the conventional rd1 model, such as blood flow changes in the visual cortices, functional improvements in light avoidance behaviour and/or the presence of optomotor response in cell-transplanted rd1 mice (Barnea-Cramer et al., 2016; Singh et al., 2013). Due to the mutation it is highly unlikely that the observed connections between transplanted rods and host rod bipolar cells could account for the reported improvements in visual function, therefore alternative signalling pathways should be considered for this functional rescue.

In our study, synaptogenesis with second order neurons has been implied through providing evidence of physical localization, expression of synaptic marker and functional rescue. Donor and hiPSC-derived optogenetically transformed photoreceptors were located in close apposition to cell bodies of rod bipolar cells several weeks post-transplantation and expressed synaptic marker Synaptophysin. Synaptophysin is an abundant synaptic vesicle membrane glycoprotein, present in neuronal presynaptic vesicles. Furthermore, we recorded a response from a second order OFF neuron lying directly underneath Jaws-expressing hiPSC-derived cones, further suggesting that Jaws-driven signals from transplanted photoreceptors were transmitted via second order neurons. Lastly, MEA recordings performed under pharmacological block of photoreceptor input to ON bipolar cells by L-2-amino-4-phosphonobutyric acid (**L-AP4**) showed complete abolition of ON light responses, which recovered after washout. Synaptic transmission from photoreceptors to ON bipolar cells is mediated by mGluR6, which is believed to be expressed uniquely in the nervous system by ON bipolar cells. L-AP4 is a group-selective agonist for the group III metabotropic glutamate receptors (mGluR4/6/7/8). Activation of mGluR6 couples negatively to a nonselective cation channel and leaves the cell hyperpolarized, mimicking the conditions in the absence of light. Therefore, by adding L-AP4 to the perfusion medium during MEA recordings, we block the transmission from rods to ON bipolar cells. These experiments confirm that light induced signals were indeed transmitted via photoreceptor-

to-bipolar cell synapses and were not, for example, triggered by ipRGCs, or by transplanted NpHR/Jaws-expressing photoreceptors that would somehow end up displaced in the GCL of the host after surgery. We can also dismiss these two alternative scenarios based on the following observations. Melanopsin, the opsin found in **ipRGCs**, shows its peak sensitivity at around 480 nm, whereas our responding cells' sensitivity was red shifted. Spikes coming from conventional RGCs that have received the information about light from the upstream retinal circuitry are transient at a broad range of intensities, such as RGCs in our recordings, whereas ipRGCs show a sustained response with a long onset latency and prolonged post-stimulus discharge (Wong et al., 2007). In melanopsin-expressing cells, light provokes membrane depolarization; therefore ipRGCs act as ON responding RGCs. In our recordings, we detected both ON and OFF responses. On the contrary – had the light sensitivity stemmed from **displaced hyperpolarizing opsin expressing transplanted cells**, we would have only detected OFF responses.

Despite the described data that strongly suggest that synapses did form between our transplanted photoreceptors and host bipolar cells, it will be important to show more direct proof of synaptogenesis in our transplanted mice in the future, for example via synaptic tracing in conjunction with functional assessment. However, when it comes to transplantation of human-derived photoreceptors, mouse models might not be a compatible enough model to answer our questions about synapse formation potential of these cells. Laver and Matsubara (2017) performed a computational study comparing several essential mouse and human triad ribbon synapse specific proteins with a predictive measure of structural divergence and by tertiary structural modeling, observing a high degree of divergence between the proteins of both species. This raised concerns about whether xenosynaptogenesis is possible (Laver and Matsubara, 2017). Despite this, several studies have reported of synapse formation between photoreceptors within hESC-derived retinal sheets and rat (McLelland et al., 2018) or mouse bipolar cells (Iraha et al., 2018), as suggested by immunostaining for synaptic markers, MEA-detected responses in the GCL and improved visual acuity in severely degenerated rodent models post-transplantation (Iraha et al., 2018; McLelland et al., 2018). This is in line with our own observations. Nevertheless, it would make sense to consider alternative preclinical animal models (such as nonhuman primates) for a more pertinent graft efficacy evaluation.

We identified and considered possible alternative mechanisms that could provide vision restoration observed in our study, including novel rewiring involving cone OFF bipolar cells, functional rescue of residual cones, virus carry-over, material transfer and **local hyperpolarization** or **glutamate spill-over** from the graft. Transplantation studies in severe degeneration models often report of a formation of distinct layer comprising of transplanted photoreceptors in the subretinal space of treated mice, resembling in a way the configuration of the subretinal electronic retina. Electrical current changes in the grafted cells could influence second order retinal cells even in the absence of conventional synapses, just by being closely apposed (Barnea-Cramer et al., 2016).

**Neuroprotection and functional rescue of remaining host cones** could be a mechanism for visual improvement in transplanted mice. Recent studies suggest that overexpression of RdCVF *in vivo* in the subretinal space is neuroprotective and can delay transition to cone dormancy in rodent RP models (Byrne et al., 2015; Sahel et al., 2013). Furthermore, in 2016, Wang and Lee showed that transplantation of wild type donor- or iPSC-derived rod precursors into a pig model of autosomal-dominant RP was able to not only delay transition to dormancy of cones, but also to reactivate cones that were already dormant. The pigs were injected at 18 months, when dormant cones lacking both ISs and OSs were the only cells remaining in the ONL of the visual streak. Transplanted rods restored ISs and OSs in endogenous cones in a region extending out to 1200  $\mu\text{m}$  from the transplant site, and resulted in an increase in cone electrophysiology in the corresponding regions, as demonstrated with photopic multifocal ERG (mfERG) (Wang et al., 2016). However, our age-matched control groups transplanted with donor-derived photoreceptor precursors or hiPSC-derived photoreceptors expressing YFP/GFP only, never showed any functional responses. In addition, the functional tests were performed in conditions that specifically activate the optogenetic protein. All this indicates that the rescue effect is unlikely the result of cell transplantation itself, but is directly correlated to the presence of an optogenetic protein expressed in the transplanted photoreceptors. However, when closely studying the results obtained from the light/dark box experiment, we did notice a trend (although the differences were not significant) of mice that were injected at a younger age, performing slightly better compared to older animals, in the mouse group treated with YFP only-expressing precursors as well as NpHR-expressing precursors. While this could well be a

result of a behavioural change that comes naturally with age (for example, generally moving less), it might also indicate that a small proportion of light avoidance behaviour could be accounted to residual cone rescue. However, the group treated with NpHR-precursors showed robust light avoidance behaviour compared to GFP only injected controls, and this significant difference is to be accounted to the optogenetic protein.

Lentiviruses and AAVs are often used to label cells with a reporter protein prior to transplanting them, in order to be able to subsequently visualize them. The possibility of reporter protein expression due to potential **carry-over of the virus** remaining in the cell solution has been addressed previously. Very small numbers of reporter-labelled cells in the ONL have been accounted to virus transduction on several occasions (Gonzalez-Cordero et al., 2013; West et al., 2012). However, control subretinal injections of lentivirus-transduced fibroblasts (Lamba et al., 2009), AAV-transduced ESC-derived FAC-sorted neuronal population (Gonzalez-Cordero et al., 2013) or supernatant from the final cell wash (Gonzalez-Cordero et al., 2017; Pearson et al., 2016; West et al., 2012) showed no labelled cells in the ONL. With our recent knowledge of material transfer existence, we could speculate that the rare reporter-labelling events that they reported of in the past were in reality due to the cytoplasmic exchange. The occurrence of virus carry-over becomes even more unlikely after extensive washing, FACS and prolonged incubation periods (Blomer et al., 2005). In order to retrieve the NpHR-expressing photoreceptor precursors in our study, we injected AAV *in vivo* into P2 mice, isolated and dissociated the retinas two days later, which was followed by numerous washing steps and the MACS. Only then were the cells transplanted into recipient mice. To gain Jaws-expressing iPSC-derived cones, embryoid bodies were AAV-transduced at D42 in culture and then further stayed in culture until D70, going through many changes of medium and several washes before being injected into host mice. The possibility of viral particles remaining in the injected cell solution in any of these cases is extremely low. Furthermore, control injections of final cell wash supernatant resulted in no reporter-labelled cells.

As mentioned earlier, the common belief that transplanted photoreceptors migrate and structurally integrate into the ONL of the host has been disputed recently by several groups (Pearson et al., 2016; Santos-Ferreira et al., 2016a; Singh et al., 2016). They provided strong evidence that instead, material transfer occurs between grafted cells remaining in the

subretinal space after transplantation, and the remnant photoreceptors of the host. We only used models of late stage retinal degeneration with very little cells remaining in the ONL at the time of treatment. *Cpfl1/Rho*<sup>-/-</sup> mice were injected at ages ranging from 9 and 18 weeks, and rd1 mice at ages from 4 to 11 weeks. *Cpfl1/Rho*<sup>-/-</sup> are left with 2-3 rows of photoreceptors at the age of 9 weeks (the youngest mice injected), and a single row of photoreceptors by 10-12 weeks of age. Rd1 mice degenerate even faster, to a single row of cell bodies in the ONL by 3 weeks after birth (Carter-Dawson et al., 1978). It is believed that labelled cells observed after transplantation in mouse models that are degenerated to a such extent are very unlikely to be the result of material transfer (Gagliardi et al., 2018; Gonzalez-Cordero et al., 2017; Kruczek et al., 2017). However, to distinguish between potential cytoplasmic exchange events and structural integration of transplanted photoreceptors with more certainty, we performed Y chromosome FISH combined with GFP immunostaining on retinal slices of female mice that were transplanted with NpHR-expressing rod precursors coming from male donors. In this setting, cells that are YFP<sup>+</sup> and carry Y chromosome represent donor-derived transplanted cells, and cells that are YFP<sup>+</sup> in the absence of Y chromosome are possibly cells that got reporter-labelled by exchanging material with the neighbouring donor cells, but are in fact remaining photoreceptors of the host. Our data shows co-expression of YFP and Y chromosome in more than 90% of labelled cells, confirming that the vast majority of NpHR<sup>+</sup> cells are of donor origin. The remaining 10% could be the result of an artefact or/and rare events of cytoplasmic exchange among donor and host photoreceptors. Although this result does not allow us to entirely rule out the possibility that material exchange contributed to the functional improvements that we observed, we do think that the contribution of material transfer towards visual improvement is minor, if present at all. We concluded so based on the following observations. We compared the ages of mice at the time of injection between two groups; 1) mice that showed functional recovery at the GCL, and 2) mice where no restoration of function was detected at the RGC level. A bigger number of remaining photoreceptors in the ONL leads to more common events of cytoplasmic exchange. Therefore, if the functional improvement were the result of predominantly cytoplasmic material transfer, we would expect younger mice to perform better. This was not the case – younger mice did not demonstrate a higher level of improvement compared to older mice. Furthermore, there

was no significant difference in light-avoidance test performance between mice treated at a younger versus older age.

In addition, to further evaluate the possibility of material transfer between transplanted mouse-derived rod photoreceptors and remaining cones in the recipient, we investigated the nuclear morphology of NpHR<sup>+</sup> donor cells. Nuclear hetero/euchromatin architecture of mouse rods and cones can serve as an indicator when distinguishing between integration and material transfer (Ortin-Martinez et al., 2017). While cone nuclei contain several clumps of heterochromatin and a substantial amount of euchromatin, mouse rod nuclei display an inverted architecture with a single big central clump of heterochromatin and very little surrounding euchromatin (Carter-Dawson et al., 1978; Solovei et al., 2009). In rd1 mice, only sparse population of cones and no rods are remaining after P36 (Carter-Dawson et al., 1978), as also seen in our control mice. NpHR<sup>+</sup> cells that were attached to the host INL visibly show rod nuclear morphology (single clump of heterochromatin), indicating that these are indeed the transplanted rods.

To tackle the possibility of cytoplasmic exchange between hiPSC-derived photoreceptors and mouse endogenous cells, we performed an immunohistochemical analysis using a human-specific nuclear marker (Human Nuclear Antigen, HNA) along with staining for GFP. The quantification analysis of GFP<sup>+</sup>/HNA<sup>+</sup> cells (hiPSC-derived photoreceptors) and GFP<sup>+</sup>/HNA<sup>-</sup> cells (mouse host photoreceptors that underwent material transfer) showed that 95% of GFP<sup>+</sup> cells co-stain with HNA. It needs to be taken into account, however, that material exchange of nuclear-targeted proteins is also possible amongst photoreceptors, as demonstrated with the Cre/LoxP experiments (Pearson et al., 2016; Santos-Ferreira et al., 2016a; Singh et al., 2016). Nonetheless, in addition to human specific markers, human photoreceptors can also be easily distinguishable from mouse cells according to the size of their nuclei (Gagliardi et al., 2018; Gonzalez-Cordero et al., 2017), which we confirmed with our own measurements, so this, too, can serve as a mean for telling the two apart. Taking this together, cytoplasmic exchange between human and rodent photoreceptors seems to be a very rare even, which is in accordance with what was reported previously (Gagliardi et al., 2018; Gonzalez-Cordero et al., 2017).

Finally, as the mechanisms of material transfer are still poorly understood, we cannot entirely rule out the possibility of heterotypic transfer from transplanted photoreceptors to bipolar cells, horizontal cells, or Müller cells. Ortin-Martinez et al. (2017) noticed low-level GFP signal in bipolar and Müller cells after transplanting *Nrl-GFP* rods into *Nrl*<sup>-/-</sup> mice, proposing second order transfer (Ortin-Martinez et al., 2017), although we found no other group previously reporting of a similar observation, nor have we noticed any reporter labelling in cells of the INL. Against this possibility speaks also the previously discussed experiment in which pharmacological block of photoreceptor input to ON bipolar cells silenced all ON responses in the GCL, providing proof that light-induced responses commenced in the photoreceptor layer.

## **The rationale behind the methods used to assess visual function improvement**

Functional assessment is considered the gold standard for evaluating the success of photoreceptor transplantation. These include electrophysiological, reflex-based and behavioural testing. In vision function testing, full-field ERG is a commonly used non-invasive *in vivo* method to measure light-driven electrical responses. However, this method has not proven very useful for measuring subtle differences, because it takes into consideration electrical activity generated by the whole retina. Pearson and colleagues (2012) estimated that about 150.000 functional photoreceptors are needed to reach the baseline of detection for ERG (Pearson et al., 2012). In our and other photoreceptor transplantation studies, the numbers of surviving cells after treatment are much lower. Furthermore, stimulating our optogenetically engineered photoreceptors would require a specially designed ERG machine that would be able to generate light of appropriate wavelengths and of 'optogenetic' intensities to stimulate microbial opsins. For these reasons, we turned to *ex vivo* electrophysiological tests, as transplantation studies in the past often have. We used single cell recordings - patch-clamp - to assess light responsiveness of reporter protein labelled photoreceptors. A patch-clamp recording was also performed on a second order neuron that was lying directly underneath transplanted photoreceptors, implying synaptic connectivity and signal transduction. To assess whether

the signal is transmitted all the way to the output neurons of the retina, we used MEA, a highly sensitive method that allows the recording of hundreds of single RGCs in parallel. The retina is very amenable to MEA recordings as RGCs are very accessible and can be easily brought to close proximity of the recording electrodes. These electrodes detect the final retinal output, generated as extracellular action potentials in RGC axons. Spikes recorded by each electrode can be further spike sorted and analysed to isolate single neuron responses, thereby overcoming a limitation fundamental to most extracellular recording techniques.

As a behavioural test, we chose the light/dark box that was adapted to enable strong orange light illumination. We used orange light because the microbial opsins that were used are most sensitive to wavelengths of around 580-590 nm. At the same time, this helped us avoid stimulation of ipRGCs (melanopsin activation maximum is in the blue spectrum (Berson et al., 2002)). Because mice are nocturnal animals, they display a natural avoidance of brightly lit areas. The rationale behind this test is that animals that are able to detect light, prefer to retreat to the dark part of the chamber, whereas mice that do not detect light cannot tell the lit up and the dark part of the box apart, so will spend about 50% of time in each of the compartments.

## The remaining challenges

Disadvantages of using cell suspensions include high cell death in the preparation procedure, uncontrolled placement and reflux of donor cells during the injection procedure, ectopic migration of transplanted cells away from the injection area, poor long-term survival and integration rates, and lack of graft structure and orientation (Gasparini et al., 2018; Jung et al., 2018).

The high enough **number of surviving and integrating cells** is important in order to regain visual function, and to recover complex retinal circuit functions, such as directional selectivity and lateral inhibition. In the study that targeted dormant cones with NpHR, Busskamp et al. (2010) estimated that about 25% of remaining cone bodies was sufficient to trigger responses in the RGCs. Taking into account that a healthy mouse retina has an estimate of 150.000 cones, 25% would account to about 35.000-40.000 cells. This is the

lowest number they tested at the time. Several previous photoreceptor replacement studies, however, reported of functional improvement despite much lower numbers of labelled cells in the ONL (Lamba et al., 2009; MacLaren et al., 2006; Pearson et al., 2012; Santos-Ferreira et al., 2015). Lamba et al. (2006), for example, was able to record light-evoked extracellular field potential in the GCL of transplanted retinas with as little as 100-400 cells per retina (Lamba et al., 2006). However, all these studies performed transplantations in disease models with remaining ONL. It is now believed that the vast majority of labelled cells in this case regained function via cytoplasmic exchange, and so that a large part (if not all) of them already had previously established synapses formed with the underlying second order neurons. Few studies transplanted photoreceptor precursors in severely degenerated models without any remaining OS. Singh et al. (2013) reported of an 8% survival rate of labelled donor-derived cells after transplantation into rd1, which was enough to trigger changes in cerebral visual cortical blood flow and improvements in light avoidance behaviour (Singh et al., 2013). In this case, most of the labelled and quantified cells were indeed donor cells, since material exchange is unlikely to occur in retinas with so little remaining endogenous photoreceptors. Many of them surely did not form functional synapses reaching out to host bipolar cells, and an even smaller number of them formed functional synapses and at the same time an OS well enough developed to be capable of light detection.

In our hands, on average, about 2800 (minimum 1272, maximum 4152) cells out of 200.000 injected per retina were still detectable in the subretinal space 4 weeks after transplantation, which is only about 1.5% of all cells injected. It needs to be mentioned at this point, however, that the quantification of transplanted cells that we have performed is an underestimate in terms of cell survival, because we established YFP labelling in our cells using an AVV vector. With this method, we were unable to label all the cells expressing the rod precursor marker CD73 that were later used to select cells for transplantation, although the coverage appeared very good (see Figure S1). This means that a part of transplanted cells did not express the reporter protein, therefore was not included in our cell count. However, transplanted cells that do not express NpHR-YFP, do not appear to contribute to visual function gain. It would be interesting to quantify the proportion of transplanted cells

that form synapses with the host INL layer to appraise how many synaptic connections are enough for functional improvement.

The huge loss of cells can be accounted to previously mentioned causes such as poor cell condition at the time of injection due to preparation procedures (papain treatment, MACS, etc.), and efflux during suspension delivery into the subretinal space. Pearson et al. (2012) achieved a significantly higher numbers of labelled cells present in the ONL after performing two injections in the same eye (Pearson et al., 2012). The host environment – for example the state of outer limiting membrane, reactive gliosis and extracellular matrix – seems to be important for cell survival and integration. Methods for disrupting the OLM (Pearson et al., 2010; West et al., 2008) or digestion of the ECM (Barber et al., 2013) have been explored, but the results need to be re-evaluated in the light of new knowledge about material transfer. It is unclear whether these methods increase the ease for cytoplasmic exchange or cell integration. However, in severe degeneration, the ECM and OLM already become compromised in the course of the disease, so these types of procedures might not be necessary. Sorting exclusively photoreceptor precursor from the suspension of diverse retinal cells before transplantation also greatly effects integration/material transfer rates. To purify a suspension of cells intended for transplantation from retinas of newborn mice, we used a well-established cell surface marker CD73, enabling a successful enrichment of rod precursors to up to 90%, (Eberle et al., 2012; Eberle et al., 2011; Lakowski et al., 2011; Santos-Ferreira et al., 2015). This same purification method has been proven successful in enriching populations of mouse PSC-derived retinal cells (Decembrini et al., 2014; Gonzalez-Cordero et al., 2013; Kruczek et al., 2017; Lakowski et al., 2015; Santos-Ferreira et al., 2016b). Regarding human cells, it was recently confirmed that CD73 is a specific marker of both immature and mature rod and cone photoreceptors in retinal organoids (Reichman et al., 2017). CD73 based MACS allowed purification of hiPSC-derived dissociated retinal organoid cells at DD>100 to a rate consistent with the results obtained with mouse cells. However, the weak CD73 expression in retinal organoids before day 100 did not allow an efficient isolation of photoreceptor precursors by MACS, in agreement with recent data on CD73-based human foetal retina (Lakowski et al., 2018). For this reason, we instead aimed for the development of a protocol to obtain cone-enriched retinal organoids from hiPSC in the absence of proliferative cells. The procedure, based on a previously published protocol

by Reichman et al. (Reichman et al., 2017), involved blocking the Notch signalling pathway by DAPT in order to promote commitment of retinal progenitors towards photoreceptors.

Immune response plays a big role in survival of transplanted cells. Especially innate immunity seems to be important in the early stages after transplantation (Kennelly et al., 2017), and damaging a capillary during the course or subretinal surgery can cause an increase in infiltration of macrophages and neutrophils. To overcome the adverse effects of immune system on graft survival and to improve the **long-term survival** of transplanted cells, new immunosuppressive agents are being tested and alternative means of delivery (e.g. local delivery), as well as the effect that MHC matching has on the outcome of transplantation (discussed in Chapter 5.5.4.). All retinal degenerative diseases, regardless their aetiology, involve a certain extent of oxidative stress, inflammation and apoptosis, compromising the survival of transplanted cells. The administration of neuroprotective compounds, such as neurotrophic factors, anti-apoptotic or anti-inflammatory molecules (preferably in a sustained manner that could avoid repeated intraocular injections) as an adjunctive treatment along with transplantation might improve the health and long-term survival of grafted cells. At the same time, they may also positively influence the state of host retina itself, making it more receptive for donor photoreceptors.

One of the biggest downsides of applying photoreceptors in the form of cell suspensions is the **lack of their structure and orientation** post-transplantation. We have partially avoided the need to establish proper photoreceptor apical-basal polarisation, because our approach is believed to be RPE-independent and because transplanted cells do not need OSs to be functional. However, our grafted cells still need to establish synapses with the existing retinal circuitry, in order for the signal to be sent forward from the light-sensing photoreceptor cell bodies. I would expect a large increase of the proportion of cells forming functional synapses, if we were capable to provide proper orientation of the grafted photoreceptors.

In addition to the two **RPE functions** that are most directly associated with the OS light sensitivity and function (visual pigment re-isomerization and phagocytosis of the damaged photoreceptor OSs), RPE also has other important functions for the maintenance of photoreceptors that cannot be overcome with optogenetics. These include transport of nutrients and O<sub>2</sub> from the blood to the photoreceptors, controlling the chemical

composition and the volume of the subretinal space, secretion of various growth factors, etc. It is conceivable that RPE would still be needed for the long-term survival of the transplanted photoreceptors, even if these photoreceptors were genetically transformed to stay light-sensitive.

**Optogenetics-related drawbacks** are mostly linked to the high light intensities needed to stimulate microbial opsin-expressing photoreceptors. In fact, this is especially problematic with microbial opsins that need blue light for their activation, because blue light more easily induces photochemical damage. NpHR and Jaws are both red-shifted opsins, and because orange light needed for their activation has a vastly lower damage potential, we were able to induce functional improvement using intensities below the safety threshold for the human retina (European Parliament and Council of the European Union, 2006; International Commission on Non-ionizing Radiation Protection, 2013). Nevertheless, the treatment that we are suggesting would need to, in addition to the transplantation, take use of a device that would capture the visual scene, amplify the signal, translate it into an appropriate wavelength, and project this signal back to the eye to be detected by grafted NpRH/Jaws-expressing photoreceptors in the retina.

Another consideration to take into account is the possibility of an immune reaction against the microbial opsin. Although we have not tested this, it is probable that the optogenetically transformed cells are more immunogenic than cells that do not express this “foreign” protein derived from bacteria. This is something that should be explored in the future.

## **Considerations for the future**

Grafts are significantly more structured when inserted as retinal sheets, and they also show improved long-term survival. Retinal graft sheet in a clinical trial was observed to survive 3 years after the transplantation (del Cerro et al., 1985). However, this approach grafts a mix of retinal cells and does not aim to select photoreceptors exclusively beforehand. As a result, in some cases, the INL of the graft gets caught between the graft ONL and the host INL, blocking the direct contact of transplanted photoreceptors and host interneurons. This approach is also currently limited by morphological changes – frequent rosette formation

within the grafted sheet. It would be much preferred to reconstruct a structured ONL itself without the presence of other retinal cell types.

Recently, a 3D microstructured scaffold designed to support natural cell morphology enabled polarization of seeded photoreceptors and allowed elongation of processes (Jung et al., 2018). The study did not report of photoreceptor OS formation though, and the developed scaffold is still to be tested *in vivo*.

The synergistic approach combining photoreceptor replacement and optogenetics, proposed in this work, efficiently bypasses the need of photoreceptor OSs and RPE for light sensitivity and functionality of transplanted photoreceptors. As mentioned previously, big improvements in developing optogenetic constructs have been achieved in the last years. It would be worth testing alternative opsins with this same approach - improved microbial opsins, constructs using synthetic optoswitches, or vertebrate opsins. Animal opsins have several advantages over opsins derived from bacteria, especially the much increased light sensitivity (1000-10.000-fold (Berry et al., 2017)) that could enable vision restoration in normal light conditions. This could circumvent the use of specialized intensifying goggles with this treatment and avoid the potential toxicity to remaining retinal cells due to high light intensities. High sensitivity of animal opsins is enabled through GPCR cascades. It is unknown to what extent the proteins that allow for this amplification of the signal are expressed in, say, iPSC-derived photoreceptors. Studies conferring light sensitivity to bipolar cells or RGCs by expressing rhodopsin or cone opsin on their surface showed diminished light sensitivity (although still much higher than microbial opsins) and slower kinetics of these opsins compared to when naturally present in photoreceptors (Berry et al., 2019; Cehajic-Kapetanovic et al., 2015; Gaub et al., 2015). This was possibly due to the lack of other phototransduction cascade proteins in these cells, especially the proteins involved in terminating the light response (for example, rhodopsin kinase and arrestin in rods). Because vertebrate opsins need their chromophore recovered after each photoisomerization, it is unclear whether this method could be RPE-independent.

The other possible future direction, avoiding the use of optogenetics, would be to further work towards establishing functional OSs in PSC-derived photoreceptors. During the embryonic development, the functional differentiation of the photoreceptor layer and the RPE depend on each other. Photoreceptors complete their differentiation through their

interaction with the apical surfaces of RPE cells and orient their axons pointing away from the pigment epithelium. Enabling the correctly oriented developing photoreceptors (for example, seeded on a scaffold) to stay in close proximity to the RPE upon transplantation might help initiate and/or complete OS formation. Alternatively, a combined scaffold containing both polarized photoreceptors and overlying RPE cells could be developed *in vitro*, and then grafted into the subretinal space. This approach would be beneficial for the many patients who display both photoreceptor and RPE malformation concurrently.

In the long run, it is worth keeping in mind that one of the most common outer retinal degenerative diseases in today's aging population, wet AMD, is a combination of chronic deficiencies in not only photoreceptors and the RPE, but also in the underlying Bruch's membrane and the capillary system (choroid). Therefore, the logical next step would be to transplant Bruch's membrane replacement and the choriocapillaris along with the photoreceptors and the RPE.

# BIBLIOGRAPHY

- Acland, G.M., G.D. Aguirre, J. Ray, Q. Zhang, T.S. Aleman, A.V. Cideciyan, S.E. Pearce-Kelling, V. Anand, Y. Zeng, A.M. Maguire, S.G. Jacobson, W.W. Hauswirth, and J. Bennett. 2001. Gene therapy restores vision in a canine model of childhood blindness. *Nature genetics*. 28:92-95.
- Aghaizu, N., K. Kruczek, A. Gonzalez-Cordero, R.R. Ali, and R.A. Pearson. 2017. Pluripotent stem cells and their utility in treating photoreceptor degenerations. *In Progress in brain research*. Vol. 231. Elsevier B.V.
- Ahnelt, P.K. 1998. The photoreceptor mosaic. *Eye*. 12 ( Pt 3b):531-540.
- Alvarez, P.V., P. Gouras, and E. Døving. 1999. Long-term outcome of RPE allografts in non-immunosuppressed patients with AMD. *European journal of ophthalmology*. 9:217-230.
- Aramant, R.B., and M.J. Seiler. 2002. Transplanted sheets of human retina and retinal pigment epithelium develop normally in nude rats. *Experimental eye research*. 75:115-125.
- Assawachananont, J., M. Mandai, S. Okamoto, C. Yamada, M. Eiraku, S. Yonemura, Y. Sasai, and M. Takahashi. 2014. Transplantation of embryonic and induced pluripotent stem cell-derived 3D retinal sheets into retinal degenerative mice. *Stem cell reports*. 2:662-674.
- Athanasiou, D., M. Aguila, D. Bevilacqua, S.S. Novoselov, D.A. Parfitt, and M.E. Cheetham. 2013. The cell stress machinery and retinal degeneration. *FEBS letters*. 587:2008-2017.
- Aurnhammer, C., M. Haase, N. Muether, M. Hausl, C. Rauschhuber, I. Huber, H. Nitschko, U. Busch, A. Sing, A. Ehrhardt, and A. Baiker. 2012. Universal real-time PCR for the detection and quantification of adeno-associated virus serotype 2-derived inverted terminal repeat sequences. *Human gene therapy methods*. 23:18-28.
- Azoulay-Sebban, L. 2015. Etude des corrélations anatomiques et fonctionnelles au cours de la rétinopathie pigmentaire : identification et validation de nouveaux marqueurs prédictifs. *In École doctorale Cerveau, cognition, comportement*. Vol. Sciences Recherche Clinique. Paris 6, Paris. 250.
- Baden, T., P. Berens, K. Franke, M. Roman Roson, M. Bethge, and T. Euler. 2016. The functional diversity of retinal ganglion cells in the mouse. *Nature*. 529:345-350.
- Bainbridge, J.W., M.S. Mehat, V. Sundaram, S.J. Robbie, S.E. Barker, C. Ripamonti, A. Georgiadis, F.M. Mowat, S.G. Beattie, P.J. Gardner, K.L. Feathers, V.A. Luong, S. Yzer, K. Balaggan, A. Viswanathan, T.J. de Ravel, I. Casteels, G.E. Holder, N. Tyler, F.W. Fitzke, R.G. Weleber, M. Nardini, A.T. Moore, D.A. Thompson, S.M. Petersen-Jones, M. Michaelides, L.I. van den Born, A. Stockman, A.J. Smith, G. Rubin, and R.R. Ali. 2015. Long-term effect of gene therapy on Leber's congenital amaurosis. *The New England journal of medicine*. 372:1887-1897.
- Bainbridge, J.W., A.J. Smith, S.S. Barker, S. Robbie, R. Henderson, K. Balaggan, A. Viswanathan, G.E. Holder, A. Stockman, N. Tyler, S. Petersen-Jones, S.S. Bhattacharya, A.J. Thrasher, F.W. Fitzke, B.J. Carter, G.S. Rubin, A.T. Moore, and R.R. Ali. 2008. Effect of gene therapy on visual function in Leber's congenital amaurosis. *The New England journal of medicine*. 358:2231-2239.
- Baker, C.K., and J.G. Flannery. 2018. Innovative Optogenetic Strategies for Vision Restoration. *Frontiers in cellular neuroscience*. 12:316.
- Bakondi, B., W. Lv, B. Lu, M.K. Jones, Y. Tsai, K.J. Kim, R. Levy, A.A. Akhtar, J.J. Breunig, C.N. Svendsen, and S. Wang. 2016. In Vivo CRISPR/Cas9 Gene Editing Corrects Retinal Dystrophy in the S334ter-3 Rat Model of Autosomal Dominant Retinitis Pigmentosa. *Molecular therapy : the journal of the American Society of Gene Therapy*. 24:556-563.
- Ballios, B.G., M.J. Cooke, D. van der Kooy, and M.S. Shoichet. 2010. A hydrogel-based stem cell delivery system to treat retinal degenerative diseases. *Biomaterials*. 31:2555-2564.
- Banin, E., A. Obolensky, M. Idelson, I. Hemo, E. Reinhardt, E. Pikarsky, T. Ben-Hur, and B. Reubinoff. 2006. Retinal incorporation and differentiation of neural precursors derived from human embryonic stem cells. *Stem cells*. 24:246-257.
- Barber, A.C., C. Hippert, Y. Duran, E.L. West, J.W. Bainbridge, K. Warre-Cornish, U.F. Luhmann, J. Lakowski, J.C. Sowden, R.R. Ali, and R.A. Pearson. 2013. Repair of the degenerate retina by

- photoreceptor transplantation. *Proceedings of the National Academy of Sciences of the United States of America*. 110:354-359.
- Barnea-Cramer, A.O., W. Wang, S.J. Lu, M.S. Singh, C. Luo, H. Huo, M.E. McClements, A.R. Barnard, R.E. Maclaren, and R. Lanza. 2016. Function of human pluripotent stem cell-derived photoreceptor progenitors in blind mice. *Scientific reports*. 6:29784.
- Bartsch, U., W. Oriyakhel, P.F. Kenna, S. Linke, G. Richard, B. Petrowitz, P. Humphries, G.J. Farrar, and M. Ader. 2008. Retinal cells integrate into the outer nuclear layer and differentiate into mature photoreceptors after subretinal transplantation into adult mice. *Experimental eye research*. 86:691-700.
- Bear, M.F., B.W. Connors, and M.A. Paradiso. 2007. The central visual system. In *Neuroscience - Exploring the brain*. Lippincott Williams and Wilkins.
- Ben M'Barek, K., W. Habeler, A. Plancheron, M. Jarraya, F. Regent, A. Terray, Y. Yang, L. Chatrousse, S. Domingues, Y. Masson, J.A. Sahel, M. Peschanski, O. Goureau, and C. Monville. 2017. Human ESC-derived retinal epithelial cell sheets potentiate rescue of photoreceptor cell loss in rats with retinal degeneration. *Science translational medicine*. 9.
- Berger, W., B. Kloeckener-Gruissem, and J. Neidhardt. 2010. The molecular basis of human retinal and vitreoretinal diseases. *Prog Retin Eye Res*. 29:335-375.
- Berry, M.H., A. Holt, J. Levitz, J. Broichhagen, B.M. Gaub, M. Visel, C. Stanley, K. Aghi, Y.J. Kim, K. Cao, R.H. Kramer, D. Trauner, J. Flannery, and E.Y. Isacoff. 2017. Restoration of patterned vision with an engineered photoactivatable G protein-coupled receptor. *Nature communications*. 8:1862.
- Berry, M.H., A. Holt, A. Salari, J. Veit, M. Visel, J. Levitz, K. Aghi, B.M. Gaub, B. Sivyer, J.G. Flannery, and E.Y. Isacoff. 2019. Restoration of high-sensitivity and adapting vision with a cone opsin. *Nature communications*. 10:1221.
- Berson, D.M., F.A. Dunn, and M. Takao. 2002. Phototransduction by retinal ganglion cells that set the circadian clock. *Science*. 295:1070-1073.
- Bi, A., J. Cui, Y.P. Ma, E. Olshevskaya, M. Pu, A.M. Dizhoor, and Z.H. Pan. 2006. Ectopic expression of a microbial-type rhodopsin restores visual responses in mice with photoreceptor degeneration. *Neuron*. 50:23-33.
- Blomer, U., I. Gruh, H. Witschel, A. Haverich, and U. Martin. 2005. Shuttle of lentiviral vectors via transplanted cells in vivo. *Gene Ther*. 12:67-74.
- Bobba, S., N. Di Girolamo, M. Munsie, F. Chen, A. Pebay, D. Harkin, A.W. Hewitt, M. O'Connor, S. McLenachan, A.M.A. Shadforth, and S.L. Watson. 2018. The current state of stem cell therapy for ocular disease. *Experimental eye research*. 177:65-75.
- Bonilha, V.L. 2008. Age and disease-related structural changes in the retinal pigment epithelium. *Clinical ophthalmology*. 2:413-424.
- Bourin, M., and M. Hascoet. 2003. The mouse light/dark box test. *European journal of pharmacology*. 463:55-65.
- Bowes, C., T. Li, M. Danciger, L.C. Baxter, M.L. Applebury, and D.B. Farber. 1990. Retinal degeneration in the rd mouse is caused by a defect in the beta subunit of rod cGMP-phosphodiesterase. *Nature*. 347:677-680.
- Brandli, A., C.D. Luu, R.H. Guymer, and L.N. Ayton. 2016. Progress in the clinical development and utilization of vision prostheses: an update. *Eye and brain*. 8:15-25.
- Broichhagen, J., A. Damijonaitis, J. Levitz, K.R. Sokol, P. Leippe, D. Konrad, E.Y. Isacoff, and D. Trauner. 2015. Orthogonal Optical Control of a G Protein-Coupled Receptor with a SNAP-Tethered Photochromic Ligand. *ACS central science*. 1:383-393.
- Busskamp, V., J. Duebel, D. Balya, M. Fradot, T.J. Viney, S. Siegert, A.C. Groner, E. Cabuy, V. Forster, M. Seeliger, M. Biel, P. Humphries, M. Paques, S. Mohand-Said, D. Trono, K. Deisseroth, J.A. Sahel, S. Picaud, and B. Roska. 2010. Genetic reactivation of cone photoreceptors restores visual responses in retinitis pigmentosa. *Science*. 329:413-417.

- Byrne, L.C., D. Dalkara, G. Luna, S.K. Fisher, E. Clerin, J.A. Sahel, T. Leveillard, and J.G. Flannery. 2015. Viral-mediated RdCVF and RdCVFL expression protects cone and rod photoreceptors in retinal degeneration. *The Journal of clinical investigation*. 125:105-116.
- Caporale, N., K.D. Kolstad, T. Lee, I. Tochitsky, D. Dalkara, D. Trauner, R. Kramer, Y. Dan, E.Y. Isacoff, and J.G. Flannery. 2011. LiGluR restores visual responses in rodent models of inherited blindness. *Molecular therapy : the journal of the American Society of Gene Therapy*. 19:1212-1219.
- Carlson Stock Art. Eye Anatomy 1 Illustration. Vol. 2019.
- Carter-Dawson, L.D., M.M. LaVail, and R.L. Sidman. 1978. Differential effect of the rd mutation on rods and cones in the mouse retina. *Investigative ophthalmology & visual science*. 17:489-498.
- Carwile, M.E., R.B. Culbert, R.L. Sturdivant, and T.W. Kraft. 1998. Rod outer segment maintenance is enhanced in the presence of bFGF, CNTF and GDNF. *Experimental eye research*. 66:791-805.
- Cayouette, M., D. Behn, M. Sendtner, P. Lachapelle, and C. Gravel. 1998. Intraocular gene transfer of ciliary neurotrophic factor prevents death and increases responsiveness of rod photoreceptors in the retinal degeneration slow mouse. *The Journal of neuroscience : the official journal of the Society for Neuroscience*. 18:9282-9293.
- Cayouette, M., and C. Gravel. 1997. Adenovirus-mediated gene transfer of ciliary neurotrophic factor can prevent photoreceptor degeneration in the retinal degeneration (rd) mouse. *Hum Gene Ther*. 8:423-430.
- Cehajic-Kapetanovic, J., C. Eleftheriou, A.E. Allen, N. Milosavljevic, A. Pienaar, R. Bedford, K.E. Davis, P.N. Bishop, and R.J. Lucas. 2015. Restoration of Vision with Ectopic Expression of Human Rod Opsin. *Current biology : CB*. 25:2111-2122.
- Cepko, C. 2010. Neuroscience. Seeing the light of day. *Science*. 329:403-404.
- Chang, B., T. Grau, S. Dangel, R. Hurd, B. Jurklies, E.C. Sener, S. Andreasson, H. Dollfus, B. Baumann, S. Bolz, N. Artemyev, S. Kohl, J. Heckenlively, and B. Wissinger. 2009. A homologous genetic basis of the murine cpfl1 mutant and human achromatopsia linked to mutations in the PDE6C gene. *Proceedings of the National Academy of Sciences of the United States of America*. 106:19581-19586.
- Chang, B., N.L. Hawes, R.E. Hurd, M.T. Davisson, S. Nusinowitz, and J.R. Heckenlively. 2002. Retinal degeneration mutants in the mouse. *Vision research*. 42:517-525.
- Chang, S., L. Vaccarella, S. Olatunji, C. Cebulla, and J. Christoforidis. 2011. Diagnostic challenges in retinitis pigmentosa: genotypic multiplicity and phenotypic variability. *Current genomics*. 12:267-275.
- Chen, J., and A.P. Sampath. 2013. Structure and function of rod and cone photoreceptors. In *Retina*. S.J. Ryan, A.P. Schachat, and C.P. Wilkinson, editors. 342-359.
- Chiba, C. 2014. The retinal pigment epithelium: an important player of retinal disorders and regeneration. *Experimental eye research*. 123:107-114.
- Choi, V.W., A. Asokan, R.A. Haberman, and R.J. Samulski. 2007. Production of recombinant adeno-associated viral vectors. *Current protocols in human genetics*. Chapter 12:Unit 12 19.
- Chuong, A.S., M.L. Miri, V. Busskamp, G.A. Matthews, L.C. Acker, A.T. Sorensen, A. Young, N.C. Klapoetke, M.A. Henninger, S.B. Kodandaramaiah, M. Ogawa, S.B. Ramanlal, R.C. Bandler, B.D. Allen, C.R. Forest, B.Y. Chow, X. Han, Y. Lin, K.M. Tye, B. Roska, J.A. Cardin, and E.S. Boyden. 2014. Noninvasive optical inhibition with a red-shifted microbial rhodopsin. *Nature neuroscience*. 17:1123-1129.
- Cideciyan, A.V. 2010. Leber congenital amaurosis due to RPE65 mutations and its treatment with gene therapy. *Prog Retin Eye Res*. 29:398-427.
- Cremers, F.P.M., C.J.F. Boon, K. Bujakowska, and C. Zeitz. 2018. Special Issue Introduction: Inherited Retinal Disease: Novel Candidate Genes, Genotype-Phenotype Correlations, and Inheritance Models. *Genes*. 9.

- Crevier, D.W., and M. Meister. 1998. Synchronous period-doubling in flicker vision of salamander and man. *Journal of neurophysiology*. 79:1869-1878.
- Cronin, T., L.H. Vandenbergh, P. Hantz, J. Juttner, A. Reimann, A.E. Kacso, R.M. Huckfeldt, V. Busskamp, H. Kohler, P.S. Lagali, B. Roska, and J. Bennett. 2014. Efficient transduction and optogenetic stimulation of retinal bipolar cells by a synthetic adeno-associated virus capsid and promoter. *EMBO molecular medicine*. 6:1175-1190.
- Curcio, C.A., K.R. Sloan, R.E. Kalina, and A.E. Hendrickson. 1990. Human photoreceptor topography. *The Journal of comparative neurology*. 292:497-523.
- Cyranoski, D. 2013. Stem cells cruise to clinic. *Nature*. 494:413.
- Daiger, S.P., L.S. Sullivan, and S.J. Bowne. 2013. Genes and mutations causing retinitis pigmentosa. *Clinical genetics*. 84:132-141.
- Dalkara, D., L.C. Byrne, R.R. Klimczak, M. Visel, L. Yin, W.H. Merigan, J.G. Flannery, and D.V. Schaffer. 2013. In vivo-directed evolution of a new adeno-associated virus for therapeutic outer retinal gene delivery from the vitreous. *Science translational medicine*. 5:189ra176.
- Dalkara, D., O. Goureau, K. Marazova, and J.A. Sahel. 2016. Let There Be Light: Gene and Cell Therapy for Blindness. *Hum Gene Ther*. 27:134-147.
- Dalkara, D., K.D. Kolstad, K.I. Guerin, N.V. Hoffmann, M. Visel, R.R. Klimczak, D.V. Schaffer, and J.G. Flannery. 2011. AAV mediated GDNF secretion from retinal glia slows down retinal degeneration in a rat model of retinitis pigmentosa. *Molecular therapy : the journal of the American Society of Gene Therapy*. 19:1602-1608.
- Dartnall, H.J., J.K. Bowmaker, and J.D. Mollon. 1983. Human visual pigments: microspectrophotometric results from the eyes of seven persons. *Proceedings of the Royal Society of London. Series B, Biological sciences*. 220:115-130.
- de Jong, P.T. 2006. Age-related macular degeneration. *The New England journal of medicine*. 355:1474-1485.
- De Silva, S.R., A.R. Barnard, S. Hughes, S.K.E. Tam, C. Martin, M.S. Singh, A.O. Barnea-Cramer, M.E. McClements, M.J. During, S.N. Peirson, M.W. Hankins, and R.E. MacLaren. 2017. Long-term restoration of visual function in end-stage retinal degeneration using subretinal human melanopsin gene therapy. *Proceedings of the National Academy of Sciences of the United States of America*. 114:11211-11216.
- Decembrini, S., U. Koch, F. Radtke, A. Moulin, and Y. Arsenijevic. 2014. Derivation of traceable and transplantable photoreceptors from mouse embryonic stem cells. *Stem cell reports*. 2:853-865.
- Decembrini, S., C. Martin, F. Sennlaub, S. Chemtob, M. Biel, M. Samardzija, A. Moulin, F. Behar-Cohen, and Y. Arsenijevic. 2017. Cone Genesis Tracing by the Chrnb4-EGFP Mouse Line: Evidences of Cellular Material Fusion after Cone Precursor Transplantation. *Molecular therapy : the journal of the American Society of Gene Therapy*. 25:634-653.
- del Cerro, M., D.M. Gash, G.N. Rao, M.F. Notter, S.J. Wiegand, and M. Gupta. 1985. Intraocular retinal transplants. *Investigative ophthalmology & visual science*. 26:1182-1185.
- den Hollander, A.I., R. Roepman, R.K. Koenekoop, and F.P. Cremers. 2008. Leber congenital amaurosis: genes, proteins and disease mechanisms. *Prog Retin Eye Res*. 27:391-419.
- Drager, U.C., and D.H. Hubel. 1978. Studies of visual function and its decay in mice with hereditary retinal degeneration. *The Journal of comparative neurology*. 180:85-114.
- Duebel, J., K. Marazova, and J.A. Sahel. 2015. Optogenetics. *Current opinion in ophthalmology*. 26:226-232.
- Eberle, D., T. Kurth, T. Santos-Ferreira, J. Wilson, D. Corbeil, and M. Ader. 2012. Outer segment formation of transplanted photoreceptor precursor cells. *PLoS one*. 7:e46305.
- Eberle, D., S. Schubert, K. Postel, D. Corbeil, and M. Ader. 2011. Increased integration of transplanted CD73-positive photoreceptor precursors into adult mouse retina. *Investigative ophthalmology & visual science*. 52:6462-6471.

- Ehinger, B., A. Bergstrom, M. Seiler, R.B. Aramant, C.L. Zucker, B. Gustavii, and A.R. Adolph. 1991. Ultrastructure of human retinal cell transplants with long survival times in rats. *Experimental eye research*. 53:447-460.
- Eiraku, M., N. Takata, H. Ishibashi, M. Kawada, E. Sakakura, S. Okuda, K. Sekiguchi, T. Adachi, and Y. Sasai. 2011. Self-organizing optic-cup morphogenesis in three-dimensional culture. *Nature*. 472:51-56.
- European Parliament and Council of the European Union. 2006. Directive 2006/25/EC on artificial optical radiation. *Official Journal of the European Union*. L 114:38-59.
- Evans, M.J., and M.H. Kaufman. 1981. Establishment in culture of pluripotential cells from mouse embryos. *Nature*. 292:154-156.
- EyeWire. 2012. Eyewire game to map the brain.
- Farber, D.B., J.G. Flannery, and C. Bowesrickman. 1994. The Rd Mouse Story - 70 Years of Research on an Animal-Model of Inherited Retinal Degeneration. *Prog Retin Eye Res*. 13:31-64.
- Farber, D.B., and R.N. Lolley. 1976. Enzymic basis for cyclic GMP accumulation in degenerative photoreceptor cells of mouse retina. *Journal of cyclic nucleotide research*. 2:139-148.
- Franke, K., P. Berens, T. Schubert, M. Bethge, T. Euler, and T. Baden. 2017. Inhibition decorrelates visual feature representations in the inner retina. *Nature*. 542:439-444.
- Frasson, M., S. Picaud, T. Leveillard, M. Simonutti, S. Mohand-Said, H. Dreyfus, D. Hicks, and J. Sabel. 1999. Glial cell line-derived neurotrophic factor induces histologic and functional protection of rod photoreceptors in the rd/rd mouse. *Investigative ophthalmology & visual science*. 40:2724-2734.
- Fuhrmann, S. 2010. Eye morphogenesis and patterning of the optic vesicle. *Current topics in developmental biology*. 93:61-84.
- Gagliardi, G., K. Ben M'Barek, A. Chaffiol, A. Slembrouck-Brec, J.B. Conart, C. Nanteau, O. Rabesandratana, J.A. Sahel, J. Duebel, G. Orieux, S. Reichman, and O. Goureau. 2018. Characterization and Transplantation of CD73-Positive Photoreceptors Isolated from Human iPSC-Derived Retinal Organoids. *Stem cell reports*. 11:665-680.
- Garcia-Caballero, C., B. Lieppman, A. Arranz-Romera, I.T. Molina-Martinez, I. Bravo-Osuna, M. Young, P. Baranov, and R. Herrero-Vanrell. 2018. Photoreceptor preservation induced by intravitreal controlled delivery of GDNF and GDNF/melatonin in rhodopsin knockout mice. *Molecular vision*. 24:733-745.
- Garita-Hernandez, M., F. Diaz-Corrales, D. Lukovic, I. Gonzalez-Guede, A. Diez-Lloret, M.L. Valdes-Sanchez, S. Massalini, S. Erceg, and S.S. Bhattacharya. 2013. Hypoxia increases the yield of photoreceptors differentiating from mouse embryonic stem cells and improves the modeling of retinogenesis in vitro. *Stem cells*. 31:966-978.
- Garita-Hernandez, M., L. Guibbal, L. Toualbi, F. Routet, A. Chaffiol, C. Winckler, M. Harinquet, C. Robert, S. Fouquet, S. Bellow, J.A. Sahel, O. Goureau, J. Duebel, and D. Dalkara. 2018. Optogenetic Light Sensors in Human Retinal Organoids. *Front Neurosci*. 12:789.
- Garreta, E., S. Sanchez, J. Lajara, N. Montserrat, and J.C.I. Belmonte. 2018. Roadblocks in the Path of iPSC to the Clinic. *Current transplantation reports*. 5:14-18.
- Gasparini, S.J., S. Llonch, O. Borsch, and M. Ader. 2018. Transplantation of photoreceptors into the degenerative retina: Current state and future perspectives. *Prog Retin Eye Res*.
- Gaub, B.M., M.H. Berry, A.E. Holt, E.Y. Isacoff, and J.G. Flannery. 2015. Optogenetic Vision Restoration Using Rhodopsin for Enhanced Sensitivity. *Molecular therapy : the journal of the American Society of Gene Therapy*. 23:1562-1571.
- Gaub, B.M., M.H. Berry, A.E. Holt, A. Reiner, M.A. Kienzler, N. Dolgova, S. Nikonov, G.D. Aguirre, W.A. Beltran, J.G. Flannery, and E.Y. Isacoff. 2014. Restoration of visual function by expression of a light-gated mammalian ion channel in retinal ganglion cells or ON-bipolar cells. *Proceedings of the National Academy of Sciences of the United States of America*. 111:E5574-5583.

- Gauthier, R., S. Joly, V. Pernet, P. Lachapelle, and A. Di Polo. 2005. Brain-derived neurotrophic factor gene delivery to muller glia preserves structure and function of light-damaged photoreceptors. *Investigative ophthalmology & visual science*. 46:3383-3392.
- Giannelli, S.G., M. Luoni, V. Castoldi, L. Massimino, T. Cabassi, D. Angeloni, G.C. Demontis, L. Leocani, M. Andreazzoli, and V. Broccoli. 2018. Cas9/sgRNA selective targeting of the P23H Rhodopsin mutant allele for treating retinitis pigmentosa by intravitreal AAV9.PHP.B-based delivery. *Human molecular genetics*. 27:761-779.
- Goh, D. 2016. Assessing visual function following the transplantation of mouse ESC-derived rod precursors. In Institute of Ophthalmology. Vol. Doctor of Philosophy (PhD). University College London, London, UK. 241.
- Goldman, A.I., and P.J. O'Brien. 1978. Phagocytosis in the retinal pigment epithelium of the RCS rat. *Science*. 201:1023-1025.
- Gonzalez-Cordero, A., K. Kruczek, A. Naeem, M. Fernando, M. Kloc, J. Ribeiro, D. Goh, Y. Duran, S.J.I. Blackford, L. Abelleira-Hervas, R.D. Sampson, I.O. Shum, M.J. Branch, P.J. Gardner, J.C. Sowden, J.W.B. Bainbridge, A.J. Smith, E.L. West, R.A. Pearson, and R.R. Ali. 2017. Recapitulation of Human Retinal Development from Human Pluripotent Stem Cells Generates Transplantable Populations of Cone Photoreceptors. *Stem cell reports*. 9:820-837.
- Gonzalez-Cordero, A., E.L. West, R.A. Pearson, Y. Duran, L.S. Carvalho, C.J. Chu, A. Naeem, S.J. Blackford, A. Georgiadis, J. Lakowski, M. Hubank, A.J. Smith, J.W. Bainbridge, J.C. Sowden, and R.R. Ali. 2013. Photoreceptor precursors derived from three-dimensional embryonic stem cell cultures integrate and mature within adult degenerate retina. *Nature biotechnology*. 31:741-747.
- Gornalusse, G.G., R.K. Hirata, S.E. Funk, L. Riobos, V.S. Lopes, G. Manske, D. Prunkard, A.G. Colunga, L.A. Hanafi, D.O. Clegg, C. Turtle, and D.W. Russell. 2017. HLA-E-expressing pluripotent stem cells escape allogeneic responses and lysis by NK cells. *Nature biotechnology*. 35:765-772.
- Gouras, P., J. Du, M. Gelanze, R. Lopez, R. Kwun, H. Kjeldbye, and W. Krebs. 1991. Survival and synapse formation of transplanted rat rods. *Journal of neural transplantation & plasticity*. 2:91-100.
- Gouras, P., M.T. Flood, and H. Kjeldbye. 1984. Transplantation of cultured human retinal cells to monkey retina. *Anais da Academia Brasileira de Ciencias*. 56:431-443.
- Gradinaru, V., K.R. Thompson, and K. Deisseroth. 2008. eNpHR: a Natronomonas halorhodopsin enhanced for optogenetic applications. *Brain cell biology*. 36:129-139.
- Gradinaru, V., F. Zhang, C. Ramakrishnan, J. Mattis, R. Prakash, I. Diester, I. Goshen, K.R. Thompson, and K. Deisseroth. 2010. Molecular and cellular approaches for diversifying and extending optogenetics. *Cell*. 141:154-165.
- Greene, M.J., J.S. Kim, H.S. Seung, and EyeWirers. 2016. Analogous Convergence of Sustained and Transient Inputs in Parallel On and Off Pathways for Retinal Motion Computation. *Cell reports*. 14:1892-1900.
- Gust, J., and T.A. Reh. 2011. Adult donor rod photoreceptors integrate into the mature mouse retina. *Investigative ophthalmology & visual science*. 52:5266-5272.
- Hagerman, G.S., and L.V. Johnson. 1991. The photoreceptor-retinal pigmented epithelial interface. In Principles and practice of clinical electrophysiology of vision. J.R.A. Heckenlively, G.B., editor. Mosby Year Book, St. Louis.
- Hamon, A., J.E. Roger, X.J. Yang, and M. Perron. 2016. Muller glial cell-dependent regeneration of the neural retina: An overview across vertebrate model systems. *Developmental dynamics : an official publication of the American Association of Anatomists*. 245:727-738.
- Hauswirth, W.W., T.S. Aleman, S. Kaushal, A.V. Cideciyan, S.B. Schwartz, L. Wang, T.J. Conlon, S.L. Boye, T.R. Flotte, B.J. Byrne, and S.G. Jacobson. 2008. Treatment of leber congenital amaurosis due to RPE65 mutations by ocular subretinal injection of adeno-associated virus gene vector: short-term results of a phase I trial. *Hum Gene Ther*. 19:979-990.

- Haverkamp, S., S. Michalakis, E. Claes, M.W. Seeliger, P. Humphries, M. Biel, and A. Feigenspan. 2006. Synaptic plasticity in CNGA3(-/-) mice: cone bipolar cells react on the missing cone input and form ectopic synapses with rods. *The Journal of neuroscience : the official journal of the Society for Neuroscience*. 26:5248-5255.
- Haverkamp, S., H. Wassle, J. Duebel, T. Kuner, G.J. Augustine, G. Feng, and T. Euler. 2005. The primordial, blue-cone color system of the mouse retina. *The Journal of neuroscience : the official journal of the Society for Neuroscience*. 25:5438-5445.
- Helmstaedter, M., K.L. Briggman, S.C. Turaga, V. Jain, H.S. Seung, and W. Denk. 2013. Connectomic reconstruction of the inner plexiform layer in the mouse retina. *Nature*. 500:168-174.
- Hirami, Y., F. Osakada, K. Takahashi, K. Okita, S. Yamanaka, H. Ikeda, N. Yoshimura, and M. Takahashi. 2009. Generation of retinal cells from mouse and human induced pluripotent stem cells. *Neuroscience letters*. 458:126-131.
- Hojo, M., T. Abe, E. Sugano, Y. Yoshioka, Y. Saigo, H. Tomita, R. Wakusawa, and M. Tamai. 2004. Photoreceptor protection by iris pigment epithelial transplantation transduced with AAV-mediated brain-derived neurotrophic factor gene. *Investigative ophthalmology & visual science*. 45:3721-3726.
- Homma, K., S. Okamoto, M. Mandai, N. Gotoh, H.K. Rajasimha, Y.S. Chang, S. Chen, W. Li, T. Cogliati, A. Swaroop, and M. Takahashi. 2013. Developing rods transplanted into the degenerating retina of Crx-knockout mice exhibit neural activity similar to native photoreceptors. *Stem cells*. 31:1149-1159.
- Humphries, M.M., D. Rancourt, G.J. Farrar, P. Kenna, M. Hazel, R.A. Bush, P.A. Sieving, D.M. Sheils, N. McNally, P. Creighton, A. Erven, A. Boros, K. Gulya, M.R. Capocchi, and P. Humphries. 1997. Retinopathy induced in mice by targeted disruption of the rhodopsin gene. *Nature genetics*. 15:216-219.
- Ikeda, H., F. Osakada, K. Watanabe, K. Mizuseki, T. Haraguchi, H. Miyoshi, D. Kamiya, Y. Honda, N. Sasai, N. Yoshimura, M. Takahashi, and Y. Sasai. 2005. Generation of Rx+/Pax6+ neural retinal precursors from embryonic stem cells. *Proceedings of the National Academy of Sciences of the United States of America*. 102:11331-11336.
- Ikeda, Y., K.M. Nishiguchi, F. Miya, N. Shimozawa, J. Funatsu, S. Nakatake, K. Fujiwara, T. Tachibana, Y. Murakami, T. Hisatomi, S. Yoshida, Y. Yasutomi, T. Tsunoda, T. Nakazawa, T. Ishibashi, and K.H. Sonoda. 2018. Discovery of a Cynomolgus Monkey Family With Retinitis Pigmentosa. *Investigative ophthalmology & visual science*. 59:826-830.
- International Commission on Non-ionizing Radiation Protection. 2013. ICNIRP guidelines on limits of exposure to incoherent visible and infrared radiation. *Health Physics*. 105:74-96.
- Iraha, S., H.Y. Tu, S. Yamasaki, T. Kagawa, M. Goto, R. Takahashi, T. Watanabe, S. Sugita, S. Yonemura, G.A. Sunagawa, T. Matsuyama, M. Fujii, A. Kuwahara, A. Kishino, N. Koide, M. Eiraku, H. Tanihara, M. Takahashi, and M. Mandai. 2018. Establishment of Immunodeficient Retinal Degeneration Model Mice and Functional Maturation of Human ESC-Derived Retinal Sheets after Transplantation. *Stem cell reports*. 10:1059-1074.
- Ivanova, E., G.S. Hwang, Z.H. Pan, and D. Troilo. 2010. Evaluation of AAV-mediated expression of Chop2-GFP in the marmoset retina. *Investigative ophthalmology & visual science*. 51:5288-5296.
- Jacobs, G.H., G.A. Williams, and J.A. Fenwick. 2004. Influence of cone pigment coexpression on spectral sensitivity and color vision in the mouse. *Vision research*. 44:1615-1622.
- Jacobson, S.G., A.V. Cideciyan, A.J. Roman, A. Sumaroka, S.B. Schwartz, E. Heon, and W.W. Hauswirth. 2015. Improvement and decline in vision with gene therapy in childhood blindness. *The New England journal of medicine*. 372:1920-1926.
- Jadhav, A.P., H.A. Mason, and C.L. Cepko. 2006. Notch 1 inhibits photoreceptor production in the developing mammalian retina. *Development*. 133:913-923.
- Jayakody, S.A., A. Gonzalez-Cordero, R.R. Ali, and R.A. Pearson. 2015. Cellular strategies for retinal repair by photoreceptor replacement. *Prog Retin Eye Res*. 46:31-66.

- Jayaram, H., M.F. Jones, K. Eastlake, P.B. Cottrill, S. Becker, J. Wiseman, P.T. Khaw, and G.A. Limb. 2014. Transplantation of photoreceptors derived from human Muller glia restore rod function in the P23H rat. *Stem cells translational medicine*. 3:323-333.
- Jung, Y.H., M.J. Phillips, J. Lee, R. Xie, A.L. Ludwig, G. Chen, Q. Zheng, T.J. Kim, H. Zhang, P. Barney, J. Min, K. Barlow, S. Gong, D.M. Gamm, and Z. Ma. 2018. 3D Microstructured Scaffolds to Support Photoreceptor Polarization and Maturation. *Advanced materials*. 30:e1803550.
- Kamao, H., M. Mandai, S. Okamoto, N. Sakai, A. Suga, S. Sugita, J. Kiryu, and M. Takahashi. 2014. Characterization of human induced pluripotent stem cell-derived retinal pigment epithelium cell sheets aiming for clinical application. *Stem cell reports*. 2:205-218.
- Kaplan, H.J., T.H. Tezel, A.S. Berger, M.L. Wolf, and L.V. Del Priore. 1997. Human photoreceptor transplantation in retinitis pigmentosa. A safety study. *Archives of ophthalmology*. 115:1168-1172.
- Karl, M.O., S. Hayes, B.R. Nelson, K. Tan, B. Buckingham, and T.A. Reh. 2008. Stimulation of neural regeneration in the mouse retina. *Proceedings of the National Academy of Sciences of the United States of America*. 105:19508-19513.
- Kennelly, K.P., T.M. Holmes, D.M. Wallace, C. O'Farrelly, and D.J. Keegan. 2017. Early Subretinal Allograft Rejection Is Characterized by Innate Immune Activity. *Cell transplantation*. 26:983-1000.
- Khabou, H., M. Garita-Hernandez, A. Chaffiol, S. Reichman, C. Jaillard, E. Brazhnikova, S. Bertin, V. Forster, M. Desrosiers, C. Winckler, O. Goureau, S. Picaud, J. Duebel, J.A. Sahel, and D. Dalkara. 2018. Noninvasive gene delivery to foveal cones for vision restoration. *JCI insight*. 3.
- Kim, J.S., M.J. Greene, A. Zlateski, K. Lee, M. Richardson, S.C. Turaga, M. Purcaro, M. Balkam, A. Robinson, B.F. Behabadi, M. Campos, W. Denk, H.S. Seung, and EyeWriters. 2014. Space-time wiring specificity supports direction selectivity in the retina. *Nature*. 509:331-336.
- Kim, K., S.W. Park, J.H. Kim, S.H. Lee, D. Kim, T. Koo, K.E. Kim, J.H. Kim, and J.S. Kim. 2017. Genome surgery using Cas9 ribonucleoproteins for the treatment of age-related macular degeneration. *Genome research*. 27:419-426.
- Kinnunen, K., G. Petrovski, M.C. Moe, A. Berta, and K. Kaarniranta. 2012. Molecular mechanisms of retinal pigment epithelium damage and development of age-related macular degeneration. *Acta ophthalmologica*. 90:299-309.
- Kinouchi, R., M. Takeda, L. Yang, U. Wilhelmsson, A. Lundkvist, M. Pekny, and D.F. Chen. 2003. Robust neural integration from retinal transplants in mice deficient in GFAP and vimentin. *Nature neuroscience*. 6:863-868.
- Koenekoop, R.K., R. Sui, J. Sallum, L.I. van den Born, R. Ajlan, A. Khan, A.I. den Hollander, F.P. Cremers, J.D. Mendola, A.K. Bittner, G. Dagnelie, R.A. Schuchard, and D.A. Saperstein. 2014. Oral 9-cis retinoid for childhood blindness due to Leber congenital amaurosis caused by RPE65 or LRAT mutations: an open-label phase 1b trial. *Lancet*. 384:1513-1520.
- Kolb, H., E. Fernandez, J. Schouten, P. Ahnelt, K.A. Linberg, and S.K. Fisher. 1994. Are there three types of horizontal cell in the human retina? *The Journal of comparative neurology*. 343:370-386.
- Koso, H., C. Minami, Y. Tabata, M. Inoue, E. Sasaki, S. Satoh, and S. Watanabe. 2009. CD73, a novel cell surface antigen that characterizes retinal photoreceptor precursor cells. *Investigative ophthalmology & visual science*. 50:5411-5418.
- Kruczek, K., A. Gonzalez-Cordero, D. Goh, A. Naeem, M. Jonikas, S.J.I. Blackford, M. Kloc, Y. Duran, A. Georgiadis, R.D. Sampson, R.N. Maswood, A.J. Smith, S. Decembrini, Y. Arsenijevic, J.C. Sowden, R.A. Pearson, E.L. West, and R.R. Ali. 2017. Differentiation and Transplantation of Embryonic Stem Cell-Derived Cone Photoreceptors into a Mouse Model of End-Stage Retinal Degeneration. *Stem cell reports*. 8:1659-1674.
- Kumaran, N., A.T. Moore, R.G. Weleber, and M. Michaelides. 2017. Leber congenital amaurosis/early-onset severe retinal dystrophy: clinical features, molecular genetics and therapeutic interventions. *The British journal of ophthalmology*. 101:1147-1154.

- Lagali, P.S., D. Balya, G.B. Awatramani, T.A. Munch, D.S. Kim, V. Busskamp, C.L. Cepko, and B. Roska. 2008. Light-activated channels targeted to ON bipolar cells restore visual function in retinal degeneration. *Nature neuroscience*. 11:667-675.
- Lakowski, J., M. Baron, J. Bainbridge, A.C. Barber, R.A. Pearson, R.R. Ali, and J.C. Sowden. 2010. Cone and rod photoreceptor transplantation in models of the childhood retinopathy Leber congenital amaurosis using flow-sorted Crx-positive donor cells. *Human molecular genetics*. 19:4545-4559.
- Lakowski, J., A. Gonzalez-Cordero, E.L. West, Y.T. Han, E. Welby, A. Naeem, S.J. Blackford, J.W. Bainbridge, R.A. Pearson, R.R. Ali, and J.C. Sowden. 2015. Transplantation of Photoreceptor Precursors Isolated via a Cell Surface Biomarker Panel From Embryonic Stem Cell-Derived Self-Forming Retina. *Stem cells*. 33:2469-2482.
- Lakowski, J., Y.T. Han, R.A. Pearson, A. Gonzalez-Cordero, E.L. West, S. Gualdoni, A.C. Barber, M. Hubank, R.R. Ali, and J.C. Sowden. 2011. Effective transplantation of photoreceptor precursor cells selected via cell surface antigen expression. *Stem cells*. 29:1391-1404.
- Lakowski, J., E. Welby, D. Budinger, F. Di Marco, V. Di Foggia, J.W.B. Bainbridge, K. Wallace, D.M. Gamm, R.R. Ali, and J.C. Sowden. 2018. Isolation of Human Photoreceptor Precursors via a Cell Surface Marker Panel from Stem Cell-Derived Retinal Organoids and Fetal Retinae. *Stem cells*. 36:709-722.
- Lamba, D.A., J. Gust, and T.A. Reh. 2009. Transplantation of human embryonic stem cell-derived photoreceptors restores some visual function in Crx-deficient mice. *Cell stem cell*. 4:73-79.
- Lamba, D.A., M.O. Karl, C.B. Ware, and T.A. Reh. 2006. Efficient generation of retinal progenitor cells from human embryonic stem cells. *Proceedings of the National Academy of Sciences of the United States of America*. 103:12769-12774.
- Lamba, D.A., A. McUsic, R.K. Hirata, P.R. Wang, D. Russell, and T.A. Reh. 2010. Generation, purification and transplantation of photoreceptors derived from human induced pluripotent stem cells. *PloS one*. 5:e8763.
- LaVail, M.M., and R.L. Sidman. 1974. C57BL-6J mice with inherited retinal degeneration. *Archives of ophthalmology*. 91:394-400.
- LaVail, M.M., K. Unoki, D. Yasumura, M.T. Matthes, G.D. Yancopoulos, and R.H. Steinberg. 1992. Multiple growth factors, cytokines, and neurotrophins rescue photoreceptors from the damaging effects of constant light. *Proceedings of the National Academy of Sciences of the United States of America*. 89:11249-11253.
- Laver, C.R.J., and J.A. Matsubara. 2017. Structural divergence of essential triad ribbon synapse proteins among placental mammals - Implications for preclinical trials in photoreceptor transplantation therapy. *Experimental eye research*. 159:156-167.
- Lee, E. 2011. Cone photoreceptor neuroprotection in inherited retinal degenerations. In Department of Genetics, University College London Institute of Ophthalmology. Vol. Doctor of Philosophy. University College London, London, UK. 379.
- Leonard, K.C., D. Petrin, S.G. Coupland, A.N. Baker, B.C. Leonard, E.C. LaCasse, W.W. Hauswirth, R.G. Korneluk, and C. Tsilfidis. 2007. XIAP protection of photoreceptors in animal models of retinitis pigmentosa. *PloS one*. 2:e314.
- Leveillard, T., S. Mohand-Said, O. Lorentz, D. Hicks, A.C. Fintz, E. Clerin, M. Simonutti, V. Forster, N. Cavusoglu, F. Chalmel, P. Dolle, O. Poch, G. Lambrou, and J.A. Sahel. 2004. Identification and characterization of rod-derived cone viability factor. *Nature genetics*. 36:755-759.
- Leveillard, T., and J.A. Sahel. 2010. Rod-derived cone viability factor for treating blinding diseases: from clinic to redox signaling. *Science translational medicine*. 2:26ps16.
- Li, Y., Y.T. Tsai, C.W. Hsu, D. Erol, J. Yang, W.H. Wu, R.J. Davis, D. Egli, and S.H. Tsang. 2012. Long-term safety and efficacy of human-induced pluripotent stem cell (iPS) grafts in a preclinical model of retinitis pigmentosa. *Molecular medicine*. 18:1312-1319.
- Li, Z.Y., D.E. Possin, and A.H. Milam. 1995. Histopathology of bone spicule pigmentation in retinitis pigmentosa. *Ophthalmology*. 102:805-816.

- Liang, F.Q., N.S. Dejneka, D.R. Cohen, N.V. Krasnoperova, J. Lem, A.M. Maguire, L. Dudus, K.J. Fisher, and J. Bennett. 2001. AAV-mediated delivery of ciliary neurotrophic factor prolongs photoreceptor survival in the rhodopsin knockout mouse. *Molecular therapy : the journal of the American Society of Gene Therapy*. 3:241-248.
- Lin, B., A. Koizumi, N. Tanaka, S. Panda, and R.H. Masland. 2008. Restoration of visual function in retinal degeneration mice by ectopic expression of melanopsin. *Proceedings of the National Academy of Sciences of the United States of America*. 105:16009-16014.
- Lin, B., B.T. McLelland, A. Mathur, R.B. Aramant, and M.J. Seiler. 2018. Sheets of human retinal progenitor transplants improve vision in rats with severe retinal degeneration. *Experimental eye research*. 174:13-28.
- Liu, Z., N. Yu, F.G. Holz, F. Yang, and B.V. Stanzel. 2014. Enhancement of retinal pigment epithelial culture characteristics and subretinal space tolerance of scaffolds with 200 nm fiber topography. *Biomaterials*. 35:2837-2850.
- Lopez, R., P. Gouras, H. Kjeldbye, B. Sullivan, V. Reppucci, M. Brittis, F. Wapner, and E. Goluboff. 1989. Transplanted retinal pigment epithelium modifies the retinal degeneration in the RCS rat. *Investigative ophthalmology & visual science*. 30:586-588.
- Ma, J., M. Kabiell, B.A. Tucker, J. Ge, and M.J. Young. 2011. Combining chondroitinase ABC and growth factors promotes the integration of murine retinal progenitor cells transplanted into Rho(-/-) mice. *Molecular vision*. 17:1759-1770.
- Mace, E., R. Caplette, O. Marre, A. Sengupta, A. Chaffiol, P. Barbe, M. Desrosiers, E. Bamberg, J.A. Sahel, S. Picaud, J. Duebel, and D. Dalkara. 2015. Targeting channelrhodopsin-2 to ON-bipolar cells with vitreally administered AAV Restores ON and OFF visual responses in blind mice. *Molecular therapy : the journal of the American Society of Gene Therapy*. 23:7-16.
- Machemer, R., and U.H. Steinhorst. 1993. Retinal separation, retinotomy, and macular relocation: II. A surgical approach for age-related macular degeneration? *Graefes archive for clinical and experimental ophthalmology = Albrecht von Graefes Archiv fur klinische und experimentelle Ophthalmologie*. 231:635-641.
- MacLaren, R.E., R.A. Pearson, A. MacNeil, R.H. Douglas, T.E. Salt, M. Akimoto, A. Swaroop, J.C. Sowden, and R.R. Ali. 2006. Retinal repair by transplantation of photoreceptor precursors. *Nature*. 444:203-207.
- Maguire, A.M., F. Simonelli, E.A. Pierce, E.N. Pugh, Jr., F. Mingozzi, J. Bennicelli, S. Banfi, K.A. Marshall, F. Testa, E.M. Surace, S. Rossi, A. Lyubarsky, V.R. Arruda, B. Konkle, E. Stone, J. Sun, J. Jacobs, L. Dell'Osso, R. Hertle, J.X. Ma, T.M. Redmond, X. Zhu, B. Hauck, O. Zelenaia, K.S. Shindler, M.G. Maguire, J.F. Wright, N.J. Volpe, J.W. McDonnell, A. Auricchio, K.A. High, and J. Bennett. 2008. Safety and efficacy of gene transfer for Leber's congenital amaurosis. *The New England journal of medicine*. 358:2240-2248.
- Mandai, M., M. Fujii, T. Hashiguchi, G.A. Sunagawa, S.I. Ito, J. Sun, J. Kaneko, J. Sho, C. Yamada, and M. Takahashi. 2017a. iPSC-Derived Retina Transplants Improve Vision in rd1 End-Stage Retinal-Degeneration Mice. *Stem cell reports*. 8:1112-1113.
- Mandai, M., Y. Kurimoto, and M. Takahashi. 2017b. Autologous Induced Stem-Cell-Derived Retinal Cells for Macular Degeneration. *The New England journal of medicine*. 377:792-793.
- Marc, R.E., and B.W. Jones. 2003. Retinal remodeling in inherited photoreceptor degenerations. *Molecular neurobiology*. 28:139-147.
- Marc, R.E., B.W. Jones, C.B. Watt, and E. Strettoi. 2003. Neural remodeling in retinal degeneration. *Prog Retin Eye Res*. 22:607-655.
- Masland, R.H. 2001. The fundamental plan of the retina. *Nature neuroscience*. 4:877-886.
- Masland, R.H. 2004. Neuronal cell types. *Current biology : CB*. 14:R497-500.
- Masland, R.H. 2012. The neuronal organization of the retina. *Neuron*. 76:266-280.
- McGee Sanftner, L.H., H. Abel, W.W. Hauswirth, and J.G. Flannery. 2001. Glial cell line derived neurotrophic factor delays photoreceptor degeneration in a transgenic rat model of retinitis

- pigmentosa. *Molecular therapy : the journal of the American Society of Gene Therapy*. 4:622-629.
- McLaughlin, M.E., M.A. Sandberg, E.L. Berson, and T.P. Dryja. 1993. Recessive mutations in the gene encoding the beta-subunit of rod phosphodiesterase in patients with retinitis pigmentosa. *Nature genetics*. 4:130-134.
- McLelland, B.T., B. Lin, A. Mathur, R.B. Aramant, B.B. Thomas, G. Nistor, H.S. Keirstead, and M.J. Seiler. 2018. Transplanted hESC-Derived Retina Organoid Sheets Differentiate, Integrate, and Improve Visual Function in Retinal Degenerate Rats. *Investigative ophthalmology & visual science*. 59:2586-2603.
- Mead, B., M. Berry, A. Logan, R.A. Scott, W. Leadbeater, and B.A. Scheven. 2015. Stem cell treatment of degenerative eye disease. *Stem cell research*. 14:243-257.
- Milam, A.H., Z.Y. Li, and R.N. Fariss. 1998. Histopathology of the human retina in retinitis pigmentosa. *Prog Retin Eye Res*. 17:175-205.
- Mohand-Said, S., A. Deudon-Combe, D. Hicks, M. Simonutti, V. Forster, A.C. Fintz, T. Leveillard, H. Dreyfus, and J.A. Sahel. 1998. Normal retina releases a diffusible factor stimulating cone survival in the retinal degeneration mouse. *Proceedings of the National Academy of Sciences of the United States of America*. 95:8357-8362.
- Mohand-Said, S., D. Hicks, M. Simonutti, D. Tran-Minh, A. Deudon-Combe, H. Dreyfus, M.S. Silverman, J.M. Ogilvie, T. Tenkova, and J. Sahel. 1997. Photoreceptor transplants increase host cone survival in the retinal degeneration (rd) mouse. *Ophthalmic research*. 29:290-297.
- Moshiri, A., R. Chen, S. Kim, R.A. Harris, Y. Li, M. Raveendran, S. Davis, Q. Liang, O. Pomerantz, J. Wang, L. Garzel, A. Cameron, G. Yiu, J.T. Stout, Y. Huang, C.J. Murphy, J. Roberts, K.N. Gopalakrishna, K. Boyd, N.O. Artemyev, J. Rogers, and S.M. Thomasy. 2019. A nonhuman primate model of inherited retinal disease. *The Journal of clinical investigation*. 129:863-874.
- Mustafi, D., A.H. Engel, and K. Palczewski. 2009. Structure of cone photoreceptors. *Prog Retin Eye Res*. 28:289-302.
- Nagel, G., D. Ollig, M. Fuhrmann, S. Kateriya, A.M. Musti, E. Bamberg, and P. Hegemann. 2002. Channelrhodopsin-1: a light-gated proton channel in green algae. *Science*. 296:2395-2398.
- Nagel, G., T. Szellas, W. Huhn, S. Kateriya, N. Adeishvili, P. Berthold, D. Ollig, P. Hegemann, and E. Bamberg. 2003. Channelrhodopsin-2, a directly light-gated cation-selective membrane channel. *Proceedings of the National Academy of Sciences of the United States of America*. 100:13940-13945.
- Nakano, T., S. Ando, N. Takata, M. Kawada, K. Muguruma, K. Sekiguchi, K. Saito, S. Yonemura, M. Eiraku, and Y. Sasai. 2012. Self-formation of optic cups and storable stratified neural retina from human ESCs. *Cell stem cell*. 10:771-785.
- Nakatsuji, N., F. Nakajima, and K. Tokunaga. 2008. HLA-haplotype banking and iPS cells. *Nature biotechnology*. 26:739-740.
- Neves, J., J. Zhu, P. Sousa-Victor, M. Konjikusic, R. Riley, S. Chew, Y. Qi, H. Jasper, and D.A. Lamba. 2016. Immune modulation by MANF promotes tissue repair and regenerative success in the retina. *Science*. 353:aaf3646.
- Nickerson, P.E.B., A. Ortin-Martinez, and V.A. Wallace. 2018. Material Exchange in Photoreceptor Transplantation: Updating Our Understanding of Donor/Host Communication and the Future of Cell Engraftment Science. *Frontiers in neural circuits*. 12:17.
- Nikonov, S.S., R. Kholodenko, J. Lem, and E.N. Pugh, Jr. 2006. Physiological features of the S- and M-cone photoreceptors of wild-type mice from single-cell recordings. *The Journal of general physiology*. 127:359-374.
- Nishiguchi, K.M., L.S. Carvalho, M. Rizzi, K. Powell, S.M. Holthaus, S.A. Azam, Y. Duran, J. Ribeiro, U.F. Luhmann, J.W. Bainbridge, A.J. Smith, and R.R. Ali. 2015. Gene therapy restores vision in rd1 mice after removal of a confounding mutation in Gpr179. *Nature communications*. 6:6006.
- Okoye, G., J. Zimmer, J. Sung, P. Gehlbach, T. Deering, H. Nambu, S. Hackett, M. Melia, N. Esumi, D.J. Zack, and P.A. Campochiaro. 2003. Increased expression of brain-derived neurotrophic

- factor preserves retinal function and slows cell death from rhodopsin mutation or oxidative damage. *The Journal of neuroscience : the official journal of the Society for Neuroscience*. 23:4164-4172.
- Ooto, S., T. Akagi, R. Kageyama, J. Akita, M. Mandai, Y. Honda, and M. Takahashi. 2004. Potential for neural regeneration after neurotoxic injury in the adult mammalian retina. *Proceedings of the National Academy of Sciences of the United States of America*. 101:13654-13659.
- Openclass.com. The eye and vision. Vol. 2019.
- Ortin-Martinez, A., E.L. Tsai, P.E. Nickerson, M. Bergeret, Y. Lu, S. Smiley, L. Comanita, and V.A. Wallace. 2017. A Reinterpretation of Cell Transplantation: GFP Transfer From Donor to Host Photoreceptors. *Stem cells*. 35:932-939.
- Osakada, F., H. Ikeda, M. Mandai, T. Wataya, K. Watanabe, N. Yoshimura, A. Akaike, Y. Sasai, and M. Takahashi. 2008. Toward the generation of rod and cone photoreceptors from mouse, monkey and human embryonic stem cells. *Nature biotechnology*. 26:215-224.
- Pan, C.K., G. Heilweil, R. Lanza, and S.D. Schwartz. 2013. Embryonic stem cells as a treatment for macular degeneration. *Expert opinion on biological therapy*. 13:1125-1133.
- Pan, Z.H., Q. Lu, A. Bi, A.M. Dizhoor, and G.W. Abrams. 2015. Optogenetic Approaches to Restoring Vision. *Annual review of vision science*. 1:185-210.
- Pastrana, E. 2010. Optogenetics: controlling cell function with light. *Nature Methods*. Special Feature: Method of the Year.
- Pearson, R.A., A.C. Barber, M. Rizzi, C. Hippert, T. Xue, E.L. West, Y. Duran, A.J. Smith, J.Z. Chuang, S.A. Azam, U.F. Luhmann, A. Benucci, C.H. Sung, J.W. Bainbridge, M. Carandini, K.W. Yau, J.C. Sowden, and R.R. Ali. 2012. Restoration of vision after transplantation of photoreceptors. *Nature*. 485:99-103.
- Pearson, R.A., A.C. Barber, E.L. West, R.E. Maclaren, Y. Duran, J.W. Bainbridge, J.C. Sowden, and R.R. Ali. 2010. Targeted disruption of outer limiting membrane junctional proteins (Crb1 and ZO-1) increases integration of transplanted photoreceptor precursors into the adult wild-type and degenerating retina. *Cell transplantation*. 19:487-503.
- Pearson, R.A., A. Gonzalez-Cordero, E.L. West, J.R. Ribeiro, N. Aghaizu, D. Goh, R.D. Sampson, A. Georgiadis, P.V. Waldron, Y. Duran, A. Naeem, M. Kloc, E. Cristante, K. Kruczek, K. Warre-Cornish, J.C. Sowden, A.J. Smith, and R.R. Ali. 2016. Donor and host photoreceptors engage in material transfer following transplantation of post-mitotic photoreceptor precursors. *Nature communications*. 7:13029.
- Peddle, C.F., and R.E. Maclaren. 2017. The Application of CRISPR/Cas9 for the Treatment of Retinal Diseases. *The Yale journal of biology and medicine*. 90:533-541.
- Petersen-Jones, S.M., and A.M. Komaromy. 2015. Dog models for blinding inherited retinal dystrophies. *Human gene therapy. Clinical development*. 26:15-26.
- Petters, R.M., C.A. Alexander, K.D. Wells, E.B. Collins, J.R. Sommer, M.R. Blanton, G. Rojas, Y. Hao, W.L. Flowers, E. Banin, A.V. Cideciyan, S.G. Jacobson, and F. Wong. 1997. Genetically engineered large animal model for studying cone photoreceptor survival and degeneration in retinitis pigmentosa. *Nature biotechnology*. 15:965-970.
- Pierrottet, C.O., M. Zuntini, M. Digiuni, I. Bazzanella, P. Ferri, R. Paderni, L.M. Rossetti, S. Cecchin, N. Orzalesi, and M. Bertelli. 2014. Syndromic and non-syndromic forms of retinitis pigmentosa: a comprehensive Italian clinical and molecular study reveals new mutations. *Genetics and molecular research : GMR*. 13:8815-8833.
- Planul, A., and D. Dalkara. 2017. Vectors and Gene Delivery to the Retina. *Annual review of vision science*. 3:121-140.
- Polosukhina, A., J. Litt, I. Tochitsky, J. Nemargut, Y. Sychev, I. De Kouchkovsky, T. Huang, K. Borges, D. Trauner, R.N. Van Gelder, and R.H. Kramer. 2012. Photochemical restoration of visual responses in blind mice. *Neuron*. 75:271-282.
- Pritchard, C.D., K.M. Arner, R.S. Langer, and F.K. Ghosh. 2010. Retinal transplantation using surface modified poly(glycerol-co-sebacic acid) membranes. *Biomaterials*. 31:7978-7984.

- Redenti, S., W.L. Neeley, S. Rompani, S. Saigal, J. Yang, H. Klassen, R. Langer, and M.J. Young. 2009. Engineering retinal progenitor cell and scrollable poly(glycerol-sebacate) composites for expansion and subretinal transplantation. *Biomaterials*. 30:3405-3414.
- Redenti, S., S. Tao, J. Yang, P. Gu, H. Klassen, S. Saigal, T. Desai, and M.J. Young. 2008. Retinal tissue engineering using mouse retinal progenitor cells and a novel biodegradable, thin-film poly( $\epsilon$ -caprolactone) nanowire scaffold. *Journal of ocular biology, diseases, and informatics*. 1:19-29.
- Reichman, S., A. Slembrouck, G. Gagliardi, A. Chaffiol, A. Terray, C. Nanteau, A. Potey, M. Belle, O. Rabesandratana, J. Duebel, G. Orioux, E.F. Nandrot, J.A. Sahel, and O. Goureau. 2017. Generation of Storable Retinal Organoids and Retinal Pigmented Epithelium from Adherent Human iPS Cells in Xeno-Free and Feeder-Free Conditions. *Stem cells*.
- Reichman, S., A. Terray, A. Slembrouck, C. Nanteau, G. Orioux, W. Habeler, E.F. Nandrot, J.A. Sahel, C. Monville, and O. Goureau. 2014. From confluent human iPS cells to self-forming neural retina and retinal pigmented epithelium. *Proceedings of the National Academy of Sciences of the United States of America*. 111:8518-8523.
- RetNet. 2019. Summaries of genes and loci causing retinal diseases. Vol. 2019.
- Reuter, J.H., and S. Sanyal. 1984. Development and degeneration of retina in rds mutant mice: the electroretinogram. *Neuroscience letters*. 48:231-237.
- Rhee, K.D., A. Ruiz, J.L. Duncan, W.W. Hauswirth, M.M. Lavail, D. Bok, and X.J. Yang. 2007. Molecular and cellular alterations induced by sustained expression of ciliary neurotrophic factor in a mouse model of retinitis pigmentosa. *Investigative ophthalmology & visual science*. 48:1389-1400.
- Roorda, A., and D.R. Williams. 1999. The arrangement of the three cone classes in the living human eye. *Nature*. 397:520-522.
- Roska, B., and J.A. Sahel. 2018. Restoring vision. *Nature*. 557:359-367.
- Ruan, G.X., E. Barry, D. Yu, M. Lukason, S.H. Cheng, and A. Scaria. 2017. CRISPR/Cas9-Mediated Genome Editing as a Therapeutic Approach for Leber Congenital Amaurosis 10. *Molecular therapy : the journal of the American Society of Gene Therapy*. 25:331-341.
- Sahel, J.A., T. Leveillard, S. Picaud, D. Dalkara, K. Marazova, A. Safran, M. Paques, J. Duebel, B. Roska, and S. Mohand-Said. 2013. Functional rescue of cone photoreceptors in retinitis pigmentosa. *Graefe's archive for clinical and experimental ophthalmology = Albrecht von Graefes Archiv fur klinische und experimentelle Ophthalmologie*. 251:1669-1677.
- Sakaguchi, D.S., S.J. Van Hoffelen, E. Theusch, E. Parker, J. Orasky, M.M. Harper, A. Benediktsson, and M.J. Young. 2004. Transplantation of neural progenitor cells into the developing retina of the Brazilian opossum: an in vivo system for studying stem/progenitor cell plasticity. *Developmental neuroscience*. 26:336-345.
- Santos-Ferreira, T., S. Llonch, O. Borsch, K. Postel, J. Haas, and M. Ader. 2016a. Retinal transplantation of photoreceptors results in donor-host cytoplasmic exchange. *Nature communications*. 7:13028.
- Santos-Ferreira, T., K. Postel, H. Stutzki, T. Kurth, G. Zeck, and M. Ader. 2015. Daylight vision repair by cell transplantation. *Stem cells*. 33:79-90.
- Santos-Ferreira, T., M. Volkner, O. Borsch, J. Haas, P. Cimalla, P. Vasudevan, P. Carmeliet, D. Corbeil, S. Michalakis, E. Koch, M.O. Karl, and M. Ader. 2016b. Stem Cell-Derived Photoreceptor Transplants Differentially Integrate Into Mouse Models of Cone-Rod Dystrophy. *Investigative ophthalmology & visual science*. 57:3509-3520.
- Santos-Ferreira, T.F., O. Borsch, and M. Ader. 2017. Rebuilding the Missing Part-A Review on Photoreceptor Transplantation. *Frontiers in systems neuroscience*. 10:105.
- Sato, K., and E. Sasaki. 2018. Genetic engineering in nonhuman primates for human disease modeling. *Journal of human genetics*. 63:125-131.
- Schlichtenbrede, F.C., A. MacNeil, J.W. Bainbridge, M. Tschernutter, A.J. Thrasher, A.J. Smith, and R.R. Ali. 2003. Intraocular gene delivery of ciliary neurotrophic factor results in significant

- loss of retinal function in normal mice and in the Prph2Rd2/Rd2 model of retinal degeneration. *Gene Ther.* 10:523-527.
- Scholl, H.P., A.T. Moore, R.K. Koeneke, Y. Wen, G.A. Fishman, L.I. van den Born, A. Bittner, K. Bowles, E.C. Fletcher, F.T. Collison, G. Dagnelie, S. Degli Eposti, M. Michaelides, D.A. Saperstein, R.A. Schuchard, C. Barnes, W. Zein, D. Zobor, D.G. Birch, J.D. Mendola, E. Zrenner, and R.I.S. Group. 2015. Safety and Proof-of-Concept Study of Oral QLT091001 in Retinitis Pigmentosa Due to Inherited Deficiencies of Retinal Pigment Epithelial 65 Protein (RPE65) or Lecithin:Retinol Acyltransferase (LRAT). *PLoS one.* 10:e0143846.
- Scholl, H.P., R.W. Strauss, M.S. Singh, D. Dalkara, B. Roska, S. Picaud, and J.A. Sahel. 2016. Emerging therapies for inherited retinal degeneration. *Science translational medicine.* 8:368rv366.
- Schwartz, S.D., C.D. Regillo, B.L. Lam, D. Elliott, P.J. Rosenfeld, N.Z. Gregori, J.P. Hubschman, J.L. Davis, G. Heilwell, M. Spirn, J. Maguire, R. Gay, J. Bateman, R.M. Ostrick, D. Morris, M. Vincent, E. Anglade, L.V. Del Priore, and R. Lanza. 2015. Human embryonic stem cell-derived retinal pigment epithelium in patients with age-related macular degeneration and Stargardt's macular dystrophy: follow-up of two open-label phase 1/2 studies. *Lancet.* 385:509-516.
- Seeliger, M.W., A. Brombas, R. Weiler, P. Humphries, G. Knop, N. Tanimoto, and F. Muller. 2011. Modulation of rod photoreceptor output by HCN1 channels is essential for regular mesopic cone vision. *Nature communications.* 2:532.
- Seiler, M.J., and R.B. Aramant. 1998. Intact sheets of fetal retina transplanted to restore damaged rat retinas. *Investigative ophthalmology & visual science.* 39:2121-2131.
- Seiler, M.J., R.B. Aramant, B.B. Thomas, Q. Peng, S.R. Sadda, and H.S. Keirstead. 2010. Visual restoration and transplant connectivity in degenerate rats implanted with retinal progenitor sheets. *The European journal of neuroscience.* 31:508-520.
- Seiler, M.J., R.E. Lin, B.T. McLelland, A. Mathur, B. Lin, J. Sigman, A.T. De Guzman, L.M. Kitzes, R.B. Aramant, and B.B. Thomas. 2017. Vision Recovery and Connectivity by Fetal Retinal Sheet Transplantation in an Immunodeficient Retinal Degenerate Rat Model. *Investigative ophthalmology & visual science.* 58:614-630.
- Sengupta, A., A. Chaffiol, E. Mace, R. Caplette, M. Desrosiers, M. Lampic, V. Forster, O. Marre, J.Y. Lin, J.A. Sahel, S. Picaud, D. Dalkara, and J. Duebel. 2016. Red-shifted channelrhodopsin stimulation restores light responses in blind mice, macaque retina, and human retina. *EMBO molecular medicine.* 8:1248-1264.
- Shekhar, K., S.W. Lapan, I.E. Whitney, N.M. Tran, E.Z. Macosko, M. Kowalczyk, X. Adiconis, J.Z. Levin, J. Nemes, M. Goldman, S.A. McCarroll, C.L. Cepko, A. Regev, and J.R. Sanes. 2016. Comprehensive Classification of Retinal Bipolar Neurons by Single-Cell Transcriptomics. *Cell.* 166:1308-1323 e1330.
- Shepherd, R.K., M.N. Shivdasani, D.A. Nayagam, C.E. Williams, and P.J. Blamey. 2013. Visual prostheses for the blind. *Trends in biotechnology.* 31:562-571.
- Shirai, H., M. Mandai, K. Matsushita, A. Kuwahara, S. Yonemura, T. Nakano, J. Assawachananont, T. Kimura, K. Saito, H. Terasaki, M. Eiraku, Y. Sasai, and M. Takahashi. 2016. Transplantation of human embryonic stem cell-derived retinal tissue in two primate models of retinal degeneration. *Proceedings of the National Academy of Sciences of the United States of America.* 113:E81-90.
- Silverman, M.S., and S.E. Hughes. 1989. Transplantation of photoreceptors to light-damaged retina. *Investigative ophthalmology & visual science.* 30:1684-1690.
- Singh, M.S., J. Balmer, A.R. Barnard, S.A. Aslam, D. Moralli, C.M. Green, A. Barnea-Cramer, I. Duncan, and R.E. MacLaren. 2016. Transplanted photoreceptor precursors transfer proteins to host photoreceptors by a mechanism of cytoplasmic fusion. *Nature communications.* 7:13537.
- Singh, M.S., P. Charbel Issa, R. Butler, C. Martin, D.M. Lipinski, S. Sekaran, A.R. Barnard, and R.E. MacLaren. 2013. Reversal of end-stage retinal degeneration and restoration of visual

- function by photoreceptor transplantation. *Proceedings of the National Academy of Sciences of the United States of America*. 110:1101-1106.
- Singhal, S., B. Bhatia, H. Jayaram, S. Becker, M.F. Jones, P.B. Cottrill, P.T. Khaw, T.E. Salt, and G.A. Limb. 2012. Human Muller glia with stem cell characteristics differentiate into retinal ganglion cell (RGC) precursors in vitro and partially restore RGC function in vivo following transplantation. *Stem cells translational medicine*. 1:188-199.
- Smiley, S., P.E. Nickerson, L. Comanita, N. Daftarian, A. El-Sehemy, E.L. Tsai, S. Matan-Lithwick, K. Yan, S. Thurig, Y. Touahri, R. Dixit, T. Aavani, Y. De Repentingy, A. Baker, C. Tsilfidis, J. Biernaskie, Y. Sauve, C. Schuurmans, R. Kothary, A.J. Mears, and V.A. Wallace. 2016. Establishment of a cone photoreceptor transplantation platform based on a novel cone-GFP reporter mouse line. *Scientific reports*. 6:22867.
- Solovei, I., M. Kreysing, C. Lanctot, S. Kosem, L. Peichl, T. Cremer, J. Guck, and B. Joffe. 2009. Nuclear architecture of rod photoreceptor cells adapts to vision in mammalian evolution. *Cell*. 137:356-368.
- Sommer, J.R., J.L. Estrada, E.B. Collins, M. Bedell, C.A. Alexander, Z. Yang, G. Hughes, B. Mir, B.C. Gilger, S. Grob, X. Wei, J.A. Piedrahita, P.X. Shaw, R.M. Petters, and K. Zhang. 2011. Production of ELOVL4 transgenic pigs: a large animal model for Stargardt-like macular degeneration. *The British journal of ophthalmology*. 95:1749-1754.
- Sparrow, J.R., D. Hicks, and C.P. Hamel. 2010. The retinal pigment epithelium in health and disease. *Current molecular medicine*. 10:802-823.
- Sparrow, J.R., H.R. Vollmer-Snarr, J. Zhou, Y.P. Jang, S. Jockusch, Y. Itagaki, and K. Nakanishi. 2003. A2E-epoxides damage DNA in retinal pigment epithelial cells. Vitamin E and other antioxidants inhibit A2E-epoxide formation. *The Journal of biological chemistry*. 278:18207-18213.
- Stanga, P.E., A. Kychenthal, F.W. Fitzke, A.S. Halfyard, R. Chan, A.C. Bird, and G.W. Aylward. 2002. Retinal pigment epithelium translocation after choroidal neovascular membrane removal in age-related macular degeneration. *Ophthalmology*. 109:1492-1498.
- Strauss, O. 2005. The retinal pigment epithelium in visual function. *Physiological reviews*. 85:845-881.
- Sugita, S., K. Makabe, S. Fujii, Y. Iwasaki, H. Kamao, T. Shiina, K. Ogasawara, and M. Takahashi. 2017. Detection of Retinal Pigment Epithelium-Specific Antibody in iPSC-Derived Retinal Pigment Epithelium Transplantation Models. *Stem cell reports*. 9:1501-1515.
- Sugiyama, Y., and Y. Mukohata. 1984. Isolation and characterization of halorhodopsin from *Halobacterium halobium*. *Journal of biochemistry*. 96:413-420.
- Suzuki, K., Y. Tsunekawa, R. Hernandez-Benitez, J. Wu, J. Zhu, E.J. Kim, F. Hatanaka, M. Yamamoto, T. Araoka, Z. Li, M. Kurita, T. Hishida, M. Li, E. Aizawa, S. Guo, S. Chen, A. Goebel, R.D. Soligalla, J. Qu, T. Jiang, X. Fu, M. Jafari, C.R. Esteban, W.T. Berggren, J. Lajara, E. Nunez-Delicado, P. Guillen, J.M. Campistol, F. Matsuzaki, G.H. Liu, P. Magistretti, K. Zhang, E.M. Callaway, K. Zhang, and J.C. Belmonte. 2016. In vivo genome editing via CRISPR/Cas9 mediated homology-independent targeted integration. *Nature*. 540:144-149.
- Suzuki, T., M. Akimoto, H. Imai, Y. Ueda, M. Mandai, N. Yoshimura, A. Swaroop, and M. Takahashi. 2007. Chondroitinase ABC treatment enhances synaptogenesis between transplant and host neurons in model of retinal degeneration. *Cell transplantation*. 16:493-503.
- Takahashi, K., K. Tanabe, M. Ohnuki, M. Narita, T. Ichisaka, K. Tomoda, and S. Yamanaka. 2007. Induction of pluripotent stem cells from adult human fibroblasts by defined factors. *Cell*. 131:861-872.
- Takahashi, K., and S. Yamanaka. 2006. Induction of pluripotent stem cells from mouse embryonic and adult fibroblast cultures by defined factors. *Cell*. 126:663-676.
- Tao, W., R. Wen, M.B. Goddard, S.D. Sherman, P.J. O'Rourke, P.F. Stabila, W.J. Bell, B.J. Dean, K.A. Kauper, V.A. Budz, W.G. Tsiaras, G.M. Acland, S. Pearce-Kelling, A.M. Laties, and G.D. Aguirre. 2002. Encapsulated cell-based delivery of CNTF reduces photoreceptor

- degeneration in animal models of retinitis pigmentosa. *Investigative ophthalmology & visual science*. 43:3292-3298.
- Taylor, C.J., S. Peacock, A.N. Chaudhry, J.A. Bradley, and E.M. Bolton. 2012. Generating an iPSC bank for HLA-matched tissue transplantation based on known donor and recipient HLA types. *Cell stem cell*. 11:147-152.
- Thompson, S., F.R. Blodi, S. Lee, C.R. Welder, R.F. Mullins, B.A. Tucker, S.F. Stasheff, and E.M. Stone. 2014. Photoreceptor cells with profound structural deficits can support useful vision in mice. *Investigative ophthalmology & visual science*. 55:1859-1866.
- Thomson, J.A., J. Itskovitz-Eldor, S.S. Shapiro, M.A. Waknitz, J.J. Swiergiel, V.S. Marshall, and J.M. Jones. 1998. Embryonic stem cell lines derived from human blastocysts. *Science*. 282:1145-1147.
- Tochitsky, I., A. Polosukhina, V.E. Degtyar, N. Gallerani, C.M. Smith, A. Friedman, R.N. Van Gelder, D. Trauner, D. Kaufer, and R.H. Kramer. 2014. Restoring visual function to blind mice with a photoswitch that exploits electrophysiological remodeling of retinal ganglion cells. *Neuron*. 81:800-813.
- Tochitsky, I., J. Trautman, N. Gallerani, J.G. Malis, and R.H. Kramer. 2017. Restoring visual function to the blind retina with a potent, safe and long-lasting photoswitch. *Scientific reports*. 7:45487.
- Toda, K., R.A. Bush, P. Humphries, and P.A. Sieving. 1999. The electroretinogram of the rhodopsin knockout mouse. *Visual neuroscience*. 16:391-398.
- Torikai, H., T. Mi, L. Gragert, M. Maiers, A. Najjar, S. Ang, S. Maiti, J. Dai, K.C. Switzer, H. Huls, G.P. Dulay, A. Reik, E.J. Rebar, M.C. Holmes, P.D. Gregory, R.E. Champlin, E.J. Shpall, and L.J. Cooper. 2016. Genetic editing of HLA expression in hematopoietic stem cells to broaden their human application. *Scientific reports*. 6:21757.
- Tucker, B.A., I.H. Park, S.D. Qi, H.J. Klassen, C. Jiang, J. Yao, S. Redenti, G.Q. Daley, and M.J. Young. 2011. Transplantation of adult mouse iPS cell-derived photoreceptor precursors restores retinal structure and function in degenerative mice. *PloS one*. 6:e18992.
- Tucker, B.A., S.M. Redenti, C. Jiang, J.S. Swift, H.J. Klassen, M.E. Smith, G.E. Wnek, and M.J. Young. 2010. The use of progenitor cell/biodegradable MMP2-PLGA polymer constructs to enhance cellular integration and retinal repopulation. *Biomaterials*. 31:9-19.
- Ueki, Y., M.S. Wilken, K.E. Cox, L. Chipman, N. Jorstad, K. Sternhagen, M. Simic, K. Ullom, M. Nakafuku, and T.A. Reh. 2015. Transgenic expression of the proneural transcription factor *Ascl1* in Muller glia stimulates retinal regeneration in young mice. *Proceedings of the National Academy of Sciences of the United States of America*. 112:13717-13722.
- Van Hooser, J.P., T.S. Aleman, Y.G. He, A.V. Cideciyan, V. Kuksa, S.J. Pittler, E.M. Stone, S.G. Jacobson, and K. Palczewski. 2000. Rapid restoration of visual pigment and function with oral retinoid in a mouse model of childhood blindness. *Proceedings of the National Academy of Sciences of the United States of America*. 97:8623-8628.
- van Wyk, M., J. Pielecka-Fortuna, S. Lowel, and S. Kleinlogel. 2015. Restoring the ON Switch in Blind Retinas: Opto-mGluR6, a Next-Generation, Cell-Tailored Optogenetic Tool. *PLoS biology*. 13:e1002143.
- Verbakel, S.K., R.A.C. van Huet, C.J.F. Boon, A.I. den Hollander, R.W.J. Collin, C.C.W. Klaver, C.B. Hoyng, R. Roepman, and B.J. Klevering. 2018. Non-syndromic retinitis pigmentosa. *Prog Retin Eye Res*. 66:157-186.
- Veske, A., S.E. Nilsson, K. Narfstrom, and A. Gal. 1999. Retinal dystrophy of Swedish briard/briard-beagle dogs is due to a 4-bp deletion in RPE65. *Genomics*. 57:57-61.
- Viczian, A., S. Sanyal, J. Toffenetti, G.J. Chader, and D.B. Farber. 1992. Photoreceptor-specific mRNAs in mice carrying different allelic combinations at the rd and rds loci. *Experimental eye research*. 54:853-860.
- Waldron, P.V., F. Di Marco, K. Kruczek, J. Ribeiro, A.B. Graca, C. Hippert, N.D. Aghaizu, A.A. Kalargyrou, A.C. Barber, G. Grimaldi, Y. Duran, S.J.I. Blackford, M. Kloc, D. Goh, E. Zabala Aldunate, R.D. Sampson, J.W.B. Bainbridge, A.J. Smith, A. Gonzalez-Cordero, J.C. Sowden,

- R.R. Ali, and R.A. Pearson. 2018. Transplanted Donor- or Stem Cell-Derived Cone Photoreceptors Can Both Integrate and Undergo Material Transfer in an Environment-Dependent Manner. *Stem cell reports*. 10:406-421.
- Wan, J., H. Zheng, Z.L. Chen, H.L. Xiao, Z.J. Shen, and G.M. Zhou. 2008. Preferential regeneration of photoreceptor from Muller glia after retinal degeneration in adult rat. *Vision research*. 48:223-234.
- Wang, J.S., and V.J. Kefalov. 2011. The cone-specific visual cycle. *Prog Retin Eye Res*. 30:115-128.
- Wang, W., S.J. Lee, P.A. Scott, X. Lu, D. Emery, Y. Liu, T. Ezashi, M.R. Roberts, J.W. Ross, H.J. Kaplan, and D.C. Dean. 2016. Two-Step Reactivation of Dormant Cones in Retinitis Pigmentosa. *Cell reports*. 15:372-385.
- Wassle, H. 2004. Parallel processing in the mammalian retina. *Nature reviews. Neuroscience*. 5:747-757.
- Weiland, J.D., S.T. Walston, and M.S. Humayun. 2016. Electrical Stimulation of the Retina to Produce Artificial Vision. *Annual review of vision science*. 2:273-294.
- Weisz, J.M., M.S. Humayun, E. De Juan, Jr., M. Del Cerro, J.S. Sunness, G. Dagnelie, M. Soyly, L. Rizzo, and R.B. Nussenblatt. 1999. Allogenic fetal retinal pigment epithelial cell transplant in a patient with geographic atrophy. *Retina*. 19:540-545.
- West, E.L., A. Gonzalez-Cordero, C. Hippert, F. Osakada, J.P. Martinez-Barbera, R.A. Pearson, J.C. Sowden, M. Takahashi, and R.R. Ali. 2012. Defining the integration capacity of embryonic stem cell-derived photoreceptor precursors. *Stem cells*. 30:1424-1435.
- West, E.L., R.A. Pearson, S.E. Barker, U.F. Luhmann, R.E. MacLaren, A.C. Barber, Y. Duran, A.J. Smith, J.C. Sowden, and R.R. Ali. 2010. Long-term survival of photoreceptors transplanted into the adult murine neural retina requires immune modulation. *Stem cells*. 28:1997-2007.
- West, E.L., R.A. Pearson, R.E. MacLaren, J.C. Sowden, and R.R. Ali. 2009. Cell transplantation strategies for retinal repair. *Progress in brain research*. 175:3-21.
- West, E.L., R.A. Pearson, M. Tschernutter, J.C. Sowden, R.E. MacLaren, and R.R. Ali. 2008. Pharmacological disruption of the outer limiting membrane leads to increased retinal integration of transplanted photoreceptor precursors. *Experimental eye research*. 86:601-611.
- Wiley, L.A., E.R. Burnight, A.P. DeLuca, K.R. Anfinson, C.M. Cranston, E.E. Kaalberg, J.A. Penticoff, L.M. Affatigato, R.F. Mullins, E.M. Stone, and B.A. Tucker. 2016. cGMP production of patient-specific iPSCs and photoreceptor precursor cells to treat retinal degenerative blindness. *Scientific reports*. 6:30742.
- Wong, K.Y., F.A. Dunn, D.M. Graham, and D.M. Berson. 2007. Synaptic influences on rat ganglion-cell photoreceptors. *The Journal of physiology*. 582:279-296.
- Wright, A.F., C.F. Chakarova, M.M. Abd El-Aziz, and S.S. Bhattacharya. 2010. Photoreceptor degeneration: genetic and mechanistic dissection of a complex trait. *Nature reviews. Genetics*. 11:273-284.
- Wright, L.S., M.J. Phillips, I. Pinilla, D. Hej, and D.M. Gamm. 2014. Induced pluripotent stem cells as custom therapeutics for retinal repair: progress and rationale. *Experimental eye research*. 123:161-172.
- Xue, Y., S. Sato, D. Razafsky, B. Sahu, S.Q. Shen, C. Potter, L.L. Sandell, J.C. Corbo, K. Palczewski, A. Maeda, D. Hodzic, and V.J. Kefalov. 2017. The role of retinol dehydrogenase 10 in the cone visual cycle. *Scientific reports*. 7:2390.
- Yang, Y., S. Mohand-Said, A. Danan, M. Simonutti, V. Fontaine, E. Clerin, S. Picaud, T. Leveillard, and J.A. Sahel. 2009. Functional cone rescue by RdCVF protein in a dominant model of retinitis pigmentosa. *Molecular therapy : the journal of the American Society of Gene Therapy*. 17:787-795.
- Yao, J., C.W. Ko, P.Y. Baranov, C.V. Regatieri, S. Redenti, B.A. Tucker, J. Mighty, S.L. Tao, and M.J. Young. 2015. Enhanced differentiation and delivery of mouse retinal progenitor cells using a

- micropatterned biodegradable thin-film polycaprolactone scaffold. *Tissue engineering. Part A*. 21:1247-1260.
- Yao, J., B.A. Tucker, X. Zhang, P. Checa-Casalengua, R. Herrero-Vanrell, and M.J. Young. 2011. Robust cell integration from co-transplantation of biodegradable MMP2-PLGA microspheres with retinal progenitor cells. *Biomaterials*. 32:1041-1050.
- Yao, K., S. Qiu, Y.V. Wang, S.J.H. Park, E.J. Mohns, B. Mehta, X. Liu, B. Chang, D. Zenisek, M.C. Crair, J.B. Demb, and B. Chen. 2018. Restoration of vision after de novo genesis of rod photoreceptors in mammalian retinas. *Nature*. 560:484-488.
- Young, M.J., J. Ray, S.J. Whiteley, H. Klassen, and F.H. Gage. 2000. Neuronal differentiation and morphological integration of hippocampal progenitor cells transplanted to the retina of immature and mature dystrophic rats. *Molecular and cellular neurosciences*. 16:197-205.
- Yu, H., T.H. Vu, K.S. Cho, C. Guo, and D.F. Chen. 2014. Mobilizing endogenous stem cells for retinal repair. *Translational research : the journal of laboratory and clinical medicine*. 163:387-398.
- Yu, W., S. Mookherjee, V. Chaitankar, S. Hiriyanna, J.W. Kim, M. Brooks, Y. Ataeijannati, X. Sun, L. Dong, T. Li, A. Swaroop, and Z. Wu. 2017. Nr1 knockdown by AAV-delivered CRISPR/Cas9 prevents retinal degeneration in mice. *Nature communications*. 8:14716.
- Yu, W., and Z. Wu. 2018. In Vivo Applications of CRISPR-Based Genome Editing in the Retina. *Frontiers in cell and developmental biology*. 6:53.
- Yue, L., J.D. Weiland, B. Roska, and M.S. Humayun. 2016. Retinal stimulation strategies to restore vision: Fundamentals and systems. *Prog Retin Eye Res*. 53:21-47.
- Zeng, H., and J.R. Sanes. 2017. Neuronal cell-type classification: challenges, opportunities and the path forward. *Nature reviews. Neuroscience*. 18:530-546.
- Zhang, F., L.P. Wang, M. Brauner, J.F. Liewald, K. Kay, N. Watzke, P.G. Wood, E. Bamberg, G. Nagel, A. Gottschalk, and K. Deisseroth. 2007. Multimodal fast optical interrogation of neural circuitry. *Nature*. 446:633-639.
- Zhang, Y., E. Ivanova, A. Bi, and Z.H. Pan. 2009. Ectopic expression of multiple microbial rhodopsins restores ON and OFF light responses in retinas with photoreceptor degeneration. *The Journal of neuroscience : the official journal of the Society for Neuroscience*. 29:9186-9196.
- Zhao, X., J. Liu, and I. Ahmad. 2002. Differentiation of embryonic stem cells into retinal neurons. *Biochemical and biophysical research communications*. 297:177-184.
- Zhong, X., C. Gutierrez, T. Xue, C. Hampton, M.N. Vergara, L.H. Cao, A. Peters, T.S. Park, E.T. Zambidis, J.S. Meyer, D.M. Gamm, K.W. Yau, and M.V. Canto-Soler. 2014. Generation of three-dimensional retinal tissue with functional photoreceptors from human iPSCs. *Nature communications*. 5:4047.
- Zhu, J., H. Cifuentes, J. Reynolds, and D.A. Lamba. 2017a. Immunosuppression via Loss of IL2rgamma Enhances Long-Term Functional Integration of hESC-Derived Photoreceptors in the Mouse Retina. *Cell stem cell*. 20:374-384 e375.
- Zhu, J., C. Ming, X. Fu, Y. Duan, D.A. Hoang, J. Rutgard, R. Zhang, W. Wang, R. Hou, D. Zhang, E. Zhang, C. Zhang, X. Hao, W. Xiong, and K. Zhang. 2017b. Gene and mutation independent therapy via CRISPR-Cas9 mediated cellular reprogramming in rod photoreceptors. *Cell research*. 27:830-833.